The Effects of Disorder and Interaction in Metallic Systems.

Thesis by
Chao-Jung Lee

In Partial Fulfillment of the Requirements for the
degree of
Doctor of Philosophy

Caltech

CALIFORNIA INSTITUTE OF TECHNOLOGY
Pasadena, California

2023
Defended May, 09, 2023

© 2023

Chao-Jung Lee
ORCID: 0000-0003-3339-1522

ACKNOWLEDGEMENTS

ABSTRACT

Metallic states in two-dimensional quantum matter have a long history and pose extremely challenging problems. A generic metallic state is described by a gapless system with a finite density of particles, along with disorders and interactions. Such correlated many-body systems are usually difficult to study, both analytically and numerically. In this thesis, we are dedicated to certain simplified cases which enable us to study via analytical approaches. Firstly, we study the effects of quenched disorder and a dissipative Coulomb interaction in the Dirac composite fermion theory describing the quantum phase transition of integer quantum Hall plateau and magnetic-field tuned 2D supercondutor The renormalization group study is presented, by considering the quantum effect of disorder and gauge fluctuation. Secondly, we present a study of integer quantum Hall plateau transition using a mean-field theory of composite fermions with a gyromagnetic ratio equal to two. We investigate the stability problem in terms of semi-classical approach and derive the corresponding nonlinear sigma model. Thirdly, we study a single 2D Dirac fermion at finite density, subjected to a quenched random magnetic field. The low-energy theory can be mapped onto an infinite collection of 1D chiral fermions coupled by a random vector potential matrix. The theory is exactly solvable, and the electrical response is computed non-perturbatively. Lastly, we shift our focus to a disorder-free system formed by a collection of 1D wires. We provide an example of an Ersatz Fermi liquid by deforming the chiral Wess-Zumino-Witten model with level k greater than unity.

PUBLISHED CONTENT AND CONTRIBUTIONS

[1] Chao-Jung Lee, Prashant Kumar, and Michael Mulligan. "Composite fermion nonlinear sigma models". In: *Phys. Rev. B* 104 (12 Sept. 2021), p. 125119. URL: https://link.aps.org/doi/10.1103/PhysRevB.104.125119.
C.-J. Lee participated in the conception of the project, performing the calculation, doing the analysis, and writing the manuscript.

[2] Chao-Jung Lee and Michael Mulligan. "Current algebra approach to two-dimensional interacting chiral metals". In: *Phys. Rev. B* 107 (20 May 2023), p. 205147. URL: https://link.aps.org/doi/10.1103/PhysRevB.107.205147.
C.-J. Lee participated in the conception of the project, performing the calculation, doing the analysis, and writing the manuscript.

[3] Chao-Jung Lee and Michael Mulligan. "Random magnetic field and the Dirac Fermi surface". In: *Phys. Rev. B* 107 (20 May 2023), p. 205145. URL: https://link.aps.org/doi/10.1103/PhysRevB.107.205145.
C.-J. Lee participated in the conception of the project, performing the calculation, doing the analysis, and writing the manuscript.

[4] Chao-Jung Lee and Michael Mulligan. "Scaling and diffusion of Dirac composite fermions". In: *Phys. Rev. Res.* 2 (2 June 2020), p. 023303. URL: https://link.aps.org/doi/10.1103/PhysRevResearch.2.023303.
C.-J. Lee participated in the conception of the project, performing the calculation, doing the analysis, and writing the manuscript.

TABLE OF CONTENTS

LIST OF ILLUSTRATIONS

LIST OF TABLES

C h a p t e r   1

INTRODUCTION

The metallic state of matter is defined as the system with a large number of particles forming a Fermi sea, and there is no energy gap between its ground state and the excitation states. From the electrical transport point of view, the metal is the state with a finite value of electrical conductivity at general temperature and frequency. To have finite conductivity, the system should contain mobile charge carriers, which would be neither localized nor ballistic. Therefore the presence of disorder and/or interaction are usually very crucial. In this chapter, we will give an overview of the physics of disorder electrons and some phenomenological evidences about certain anomalous metal occur in various systems exhibiting universal behaviors, which are poorly understood so far. The goal of this thesis is trying to address, or at least have a preliminary understanding of the relevant topics.

1.1   The definition of disorder and treating strategy

The term disorder we refer to in this thesis is the quenched randomness that has a statistical distribution. The term "quenched" implies that the disorder is frozen or fixed, meaning it does not change with time or temperature. This is in contrast to "annealed disorder," where the disorder can fluctuate or re-arrange over time. The statistical distribution means that the configuration of the disorder potential $V(x)$ is not a fixed function, but behaves like a random variable such that many of the possible configurations would result in a certain distribution function, such as normal distribution, e.g. the probability distribution of random potential $V(x)$ with kernel K^{-1} is defined as

$$P[V] \propto e^{-\frac{1}{2} \int dx dx' V(x) K^{-1}(x,x') V(x')},$$

(1.1)

To handle the disorder effect for free theory, the most straightforward way is to construct many different configurations of the disorder such that they obey the desired statistical distribution form. For a specific configuration, we can then perform exact diagonalization of the Hamiltonian to obtain the wave function. Using the wave function as an input allows us to compute certain physical observable. By Repeating this procedure for various disorder

configurations we can obtain various results for this physical observable. The desired observable is then obtained by averaging all of them.

The above numerical method is the exact way of treating the disorder non-perturbatively, which allows us to probe the strong disorder regime. However, this procedure is easy only for non-interacting theory. Once the interactions are included, the task would be extremely difficult, even if we treat the interaction as perturbation. Therefore, analytical approach to treat disorder is desirable.

As mentioned above, the physical observable $\mathcal{O}$ in disorder system is defined as [2]

$$\langle \mathcal{O} \rangle_{\text{dis,fun}} \equiv \int DV \, P[V] \, \langle \mathcal{O}(V) \rangle_{\text{fun}}, \tag{1.2}$$

$$\langle \mathcal{O}(V) \rangle_{\text{fun}} \equiv \frac{\int Df \, \mathcal{O}(V) e^{-S[V,f]}}{\int Df \, e^{-S[V,f]}}, \tag{1.3}$$

where the functional average is defined in the usual way, with generic fields operator f. To write in terms of partition function Z, we can imagine that the observable couple to certain source term $\mathcal{I}$, $S[V,f] \rightarrow S[V,f] - \int_{xt} \mathcal{O}\mathcal{I}$, therefore,

$$\langle \mathcal{O} \rangle_{\text{dis,fun}} = \int DV \, P[V] \, \frac{1}{Z[V,\mathcal{I}=0]} \frac{\delta}{\delta \mathcal{I}} Z[V,\mathcal{I}] \Big|_{\mathcal{I}=0} = \int DV \, P[V] \, \frac{\delta}{\delta \mathcal{I}} \ln Z[V,\mathcal{I}] \Big|_{\mathcal{I}=0} \tag{1.4}$$

The obstacle of performing the disorder average is the denominator $Z[V,\mathcal{I}=0]$ which contains the dependence of V. To resolve this issue, the most common way is resorting to the replica trick, which is

$$\ln Z = \lim_{R\to 0} \frac{e^{R \ln Z} - 1}{R} = \lim_{R\to 0} \frac{Z^R - 1}{R} \rightarrow \lim_{R\to 0} \frac{Z^R}{R} \tag{1.5}$$

The unity term can be dropped out since it's been eliminated by variation of $\mathcal{I}$. Therefore, to compute any physical observable, we can deform the theory into a new action defined as R copies of the original action. Once we obtain the result computed from this deformed theory, which is a function of R, we then take $R \to 0$ in the end. The step of zero replica limit is not always trivial, especially for some cases in 1D physics. Aside from this replica trick, there are also other methods such as supersymmetry or Keldysh approach. All of these methods are aiming at the denominator, making it not depend on randomness source.

1.2   The scaling theory of disordered electron gas

The presence of the disorder are almost ubiquitous in the actual materials. The earliest studies about the effect of disorder is in 1950s by Philip Anderson. He realized that the impurity would induce the quantum mechanical inferences making the electron possibly localized. Later on, Abrahams, Anderson, Licciardello, and Ramakrishnan proposed an one-parameter scaling theory [1] to explain how the conductivity flow under RG in $d = 1, 2, 3$ spatial dimension. They predict that for $d \leq 2$ there is no metallic state. For $d = 3$, there is a critical value g_c, when the conductivity g go across g_c, it undergoes a metal-insulator transition.
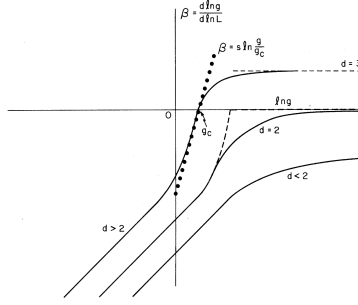
Figure 1.1: The conductivity evolution via scaling theory, figure is taken from the original paper[1]

To go beyond the phenomenological scaling theory, the renormalization behavior of the conductance can be understood by considering the quantum correction of the Cooperon and Diffuson four-fermion interaction kernel, the leading order quantum correction of the conductivity turns out to be

$$\sigma = \sigma_0 + \Delta\sigma, \tag{1.6}$$

where σ_0 is the lowest order and $\Delta\sigma$ is the quantum correction including the effect of disorder-induced four-fermion interaction, which are

$$\Delta\sigma \sim \frac{-e^2}{(2\pi)^2}\left(\frac{1}{L_{\mathrm{UV}}} - \frac{1}{L_{\mathrm{IR}}}\right) \qquad (3D) \tag{1.7}$$

$$\Delta\sigma \sim \frac{-e^2}{2\pi^2}\log\left(\frac{L_{\mathrm{IR}}}{L_{\mathrm{UV}}}\right) \qquad (2D) \tag{1.8}$$

$$\Delta\sigma \sim \frac{-e^2}{2\pi}L_{\mathrm{IR}} \qquad (1D) \tag{1.9}$$

where $L_{\mathrm{IR}} \gg L_{\mathrm{UV}}$ is the length scale of UV and IR. One can see that, as the system size increase, i.e. $L_{\mathrm{IR}} \to \infty$, the correction $\Delta\sigma$ is getting larger for

$d \leq 2$, thereby the total conductivity gradually decrease to zero. This is the well-known weak-localization.

1.3 Nonlinear sigma model for disordered non-interacting electron gas

A more general and systematic approach to study the quantum fluctuation of disorder can be formulated as a nonlinear sigma model (NLSM) field theory description with conductivity as its Lagrangian parameters, the localization behaviour can be examined by expanding around the saddle point of the Goldstone boson.

To sketch the idea, we can start from considering the functional integral of the retarded and advanced Greens function,

$$G^R_\epsilon(r_a, r_b) = \langle r_a| \frac{1}{\epsilon - \hat{H} + i\delta}|r_b\rangle = \int d\Phi^\dagger_R d\Phi_R \; \Phi^\dagger_{\alpha R}(r_a) \; \Phi_{\alpha R}(r_b) e^{\Phi^\dagger_R \left[\epsilon - \hat{H} + i\delta\right]\Phi_R} \tag{1.10}$$

$$G^A_\epsilon(r_a, r_b) = \langle r_a| \frac{1}{\epsilon - \hat{H} - i\delta}|r_b\rangle = \int d\Phi^\dagger_A d\Phi_A \; \Phi^\dagger_{\beta A}(r_a) \; \Phi_{\beta A}(r_b) e^{\Phi^\dagger_A \left[\epsilon - \hat{H} - i\delta\right]\Phi_A} \tag{1.11}$$

Examining the Kubo formula, the functional we construct should include the product of retarded-retarded, retarded-advanced, and advanced-advanced Greens function, with the energy dependency ϵ and $\epsilon - \omega$. The index α, β are a specific replica index.

Hence, the free action S_0 is motivated to choose as

$$S_0 = S^R(\epsilon) + S^A(\epsilon - \omega) = \Psi^\dagger \left[(\epsilon - \frac{\omega}{2} - \hat{H}) + \frac{\omega}{2}\Lambda + i\delta\Lambda \right]_{RA} \Psi, \quad \Psi \equiv \begin{pmatrix} \Phi_R \\ \Phi_A \end{pmatrix} \tag{1.12}$$

$$S_{\text{dis}} = \frac{-g_0}{2} \int_r (\Psi^\dagger\Psi)_r (\Psi^\dagger\Psi)_r \tag{1.13}$$

where the disorder action is taken to be Gaussian short-range kernel, as illustration purpose

Then we can apply Hubbard–Stratonovich transformation to rewrite the four-fermion interaction as the fermion coupled to boson Q action. And then we integrate out the fermion, perform gradient expansion around the saddle point of $\langle Q \rangle$, take $d = 2$ as an example, it reads

$$S[Q] = \int d^2x \, \frac{\sigma^{(0)}_{xx}}{8} \text{Tr}[(\nabla Q)^2], \tag{1.14}$$

where the superscript stands for the bare value.

To further examine the quantum fluctuation that leads to the localization behavior, we can expand the boson Q around its saddle point, we parametrize the fluctuation of Q as

$$Q = (1 - \frac{W}{2}) \Lambda (1 - \frac{W}{2})^{-1} = \Lambda(\mathbf{1} + W + \frac{1}{2}W^2 + \frac{W^3}{4} + \frac{W^4}{8} + ...) \quad (1.15)$$

Once we include the correction from W, the weak-localization effect would agree with eq. 1.7-1.9.

1.4 Nonlinear sigma model for Integer Quantum Hall transition

The formalism of NLSM describing disorder non-interacting electron can also be generalized to the system with strong magnetic field. The effective action of integer quantum Hall plateaus and their transitions can be described as

$$S[Q] = \int d^2x \frac{\sigma_{xx}^{(0)}}{8} \mathrm{Tr}[(\nabla Q)^2] - \frac{\sigma_{xy}^{(0)}}{8} \mathrm{Tr}[Q\epsilon_{ij}\partial_i Q\partial_j Q] \quad (1.16)$$
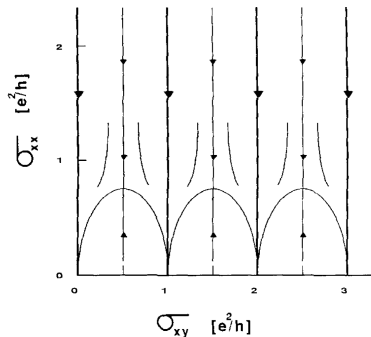
Figure 1.2: The NLSM RG flow for integer quantum Hall effect; figure is taken from the original paper [4].

The renormalization effect of the parameter $(\sigma_{xx}, \sigma_{xy})$ in this integer quantum Hall case is more involved. The first study of the RG effect is done by Pruisken [4]. He found that when Hall conductivity σ_{xy} is half-integer, the longitudinal conductivity σ_{xx} would be finite, otherwise it flows to zero, corresponding to an insulator state.

We know that the integer quantum Hall plateau is an insulator in the bulk because the states are localized. When one tune the chemical potential near the regime of transition between two plateaus, the extended states would then

contribute to the longitudinal conductance. If one takes the middle point between two plateaus as the integer quantum Hall transition critical point, then the prediction from Pruisken's RG analysis seem to be consistent with the truth of the metallic nature of the critical point.

However, Pruisken's NLSM study cannot provide any quantitative predictions. Firstly, the RG flow does not have any IR stable fixed point, the RG flow would run to insulating phases when Hall conductivity slightly deviate away from half-integer. Secondly, the construction of NLSM is in the regime of $\sigma_{xx} \gg 1$, the weak disorder regime. Near the critical point of IQHT with σ_{xx} of order unity correspond to the strong-disorder regime. Thirdly, the NLSM itself does not contain any information of critical exponent. Indeed, numerous numerical and experimental pieces of evidence suggest that while the integer quantum Hall plateau can be explained by non-interacting theory, the presence of interacting effects becomes crucial in the vicinity of the critical point. Therefore, it is necessary to go beyond the NLSM description to fully understand the IQHT.

Before ending up the NLSM discussion, it worth mention that the extension of the NLSM to more general free theory cases is possible. The above discussion about NLSM only consider simplest case with spinless fermion. If Hilbert space is larger, say including the spin or other possible quantum numbers, one can use the ten-fold symmetry classification for different type of NLSM. The fundamental transformations contain time-reversal and particle-hole, or can combining together into chiral transform. It can be figured out that there are only ten possibility of the Hamiltonian [3]. In each case, the target manifold that the sigma model field live in would be different. It was shown that, nine out of ten classes exhibit either topological term or Wess-Zumino Witten term can prevent from localization and thus lead to metallic state at criticality.

1.5 Some phenomenon of metallic states in 2D thin tuned by magnetic field

The scaling theory conclude at $T = 0$ there is no metallic ground state in two dimensions, which is generally not correct based on many of experimental evidences and theoretical studies. The reason is that the scaling theory does not include the interaction within the fermion nor other possible experimental-control sources, such as background magnetic field or gate voltage. The IQHT

example mentioned above in terms of NLSM is one typical example of metallic state, which occurs near quantum critical point. Aside from IQHT, there are also other metallic states in magnetic field-tuned systems. We will focus on the two dimensional system throughout the remaining of the discussion. In the following, we would introduce the bosonic and fermionic examples of magnetic fined-tuned metal.

For the bosoinc system, the superconductor-insulator transition (SIT) is one of the typical example. SIT is a phenomenon that occurs in certain materials when they are subjected to a magnetic field. When we adjust the magnetic field from zero to a certain critical value, there is a transition between the superconducting phase and the insulating phase. At or near the critical point, the state would be metallic with finite resistivity. It's been aware that near the critical point of SIT, the conductivity tensor is proportional to the vortex-resistivity tensor, which leads to the famous semi-circle law at the self-dual point,

$$\sigma_{xx}^2 + \sigma_{xy}^2 = (\frac{4e^2}{h})^2 \tag{1.17}$$

The particle-vortex duality can only determine the sum of their squares. However, experimental measurement near $T \to 0$ found that $\sigma_{xy} = 0$ and $\sigma_{xx} = \frac{4e^2}{h}$. How to explain this universal value of conductivity so far is still an open question from the theoretical side.

For the fermionic system, the intriguing metallic states are the quantum Hall transition criticalities, which are the intervening states between two plateaus, either integer or fractional. It is widely believe that the integer quantum Hall states can be understood in terms of free fermion, while the interaction is crucial for fractional quantum Hall states because the interaction effects are responsible for the emergence of the energy gap and collective behavior of fractional excitation. However, many evidences indicate that, for either the integer quantum Hall transition critical points, or the fractional quantum Hall plateau critical points, the effects of interactions are both important and not negligible. More surprisingly, these critical points share the same critical exponents $\nu \approx \frac{7}{3}$ and $z \approx 1$. The exponent ν is the one that characterizes the divergence of the correlation length near the critical point, and the dynamical exponent z is the one that quantifies how time or frequency scales with respect to length scales near the critical point, namely $\omega \to \lambda^z \omega$ if one defined the

momentum scaled as $p \to \lambda p$. This fact that the critical behavior near these phase transitions exhibits universal properties that are independent of the microscopic details of the system is refereed as superuniversality. How to explain this class of superuniversal metallic states with order unity conductivity is a mysterious question that still poorly understood.

1.6   Fermi surface and non-Fermi liquid

Another motivation of studying metallic state of matter is to have a better understanding of the non-Fermi liquid (NFL). For the regular Fermi liquid, the low-energy excitations near the Fermi surface can be described by well-defined quasi-particles with definite properties, such as charge, spin, and energy. However, in NFL metallic states, the notion of quasi-particles breaks down, and the low-energy excitations display unconventional or exotic behavior. From the spectrum function point of view, the existence of quasi-particle means that there is a well-defined localized peak when the dispersion relation is near the on-shell regime. On the other hand, in a NFL state, the spectrum function does not exhibit well-defined quasi-particle peaks; instead, the spectrum usually displays broad or continuum distribution features. Mathematically, the quasi-particle corresponds to simple-pole structure of the Greens function, while the NFL state Greens function usually have branch-point or other exotic analytical structure.

Though NFL does not have to originate from the quantum critical points, many theoretical examples suggest that the finite Fermi surface couple to gapless boson (usually an order parameter field variables) system, within certain kinetic regime, can form NFL state.

As for the experimental signature of NFL, the linear temperature-dependent resistivity is one of the key features. To be specific, the electrical conductivity (focus on the real part)

$$\rho_{xx}^{-1} \sim \sigma_{xx}(\omega, T) = \text{Drude} + \frac{1}{T^\xi}\Big(c_0 + c_1(\frac{\omega}{T})^1 + c_2(\frac{\omega}{T})^2 + ...\Big), \qquad (1.18)$$

where the Drude part is the temperature independent part. The famous linear in T behavior occur when $\xi = 1$ and $c_0 \neq 0$

The other suggestive signature is the violation of the Wiedemann-Franz Law. The Wiedemann-Franz law is a relationship between the electrical conductivity and the thermal conductivity of a metal. The statement is that the ratio of

thermal conductivity and electrical conductivity is equal to a constant over temperature. The law suggests that metals with high electrical conductivity also have high thermal conductivity, and vice versa. This is because both electrical and thermal conductivities are related to the ability of electrons to move through the material. This interpretation already assumes the existence of a well-defined quasi-particle. By directly examining the Kubo formula, one can prove that the thermal conductivity is related to the electrical one in terms of single particle Greens function convolutions. Therefore the deviation from the Wiedemann-Franz law is the evidence of the break-down of quasi-particle. [1]

1.7 Organization of this thesis

In fact, for finite density systems, even in the cases that only interaction or only disorder are present, we usually don't have a simple analytically controllable perturbation theory to tackle the problems. The finite Fermi surface couple to gapless fluctuating boson mediating the interaction usually requires artificial double parameters expansion to make it controllable. The non-interacting Fermi surface in the presence of disorder generally flows to strong-disorder fixed points if the system does not have particular symmetry constraints. Thus there is very limited quantitative prediction can we make.

Though we're unable to resolve the generic strong-correlated disordered metallic systems, we can alternatively step back to investigate relevant but simplified models, which is the primary goal of this thesis.

In Chapter 2, we study the renormalization group flow of Dirac composite fermion model at zero density perturbed by gauge fluctuation and various disorders.

In Chapter 3, we consider a theory of fermion with gyromagnetic ratio $g = 2$ with emergent particle-hole symmetry with the assistant of disorder. We study the stability problems at leading order when more than one disorder is present simultaneously.

In Chapter 4, we study Dirac fermion at finite density with random magnetic flux. The low energy projection allows us to treat the disorder non-

---

[1]Nevertheless, the violation of Wiedemann-Franz law is only an indirect evidence of NFL state. In fact, there are examples of NFL state in one dimension that still satisfy the Wiedemann-Franz law.

perturbatively. We compute diffusive observables directly by evaluating the statistical average of the products of exponential of random matrix.

In Chapter 5, we consider a clean Fermi liquid theory constructed from the multiple chiral fermion wires. Turning on the hopping operator within the wires allows it to form 2D gapless states. Then we generalize to the case with interaction effect is included.

In Chapter 6, we highlight the result of each chapter and make a brief summary of this thesis.

BIBLIOGRAPHY

[1]   E. Abrahams et al. "Scaling Theory of Localization: Absence of Quantum Diffusion in Two Dimensions". In: *Phys. Rev. Lett.* 42 (10 Mar. 1979), pp. 673–676. URL: https : / / link . aps . org / doi / 10 . 1103 / PhysRevLett.42.673.

[2]   Alexander Altland and Ben D. Simons. *Condensed Matter Field Theory.* 2nd ed. Cambridge University Press, 2010.

[3]   Alexander Altland and Martin R. Zirnbauer. "Nonstandard symmetry classes in mesoscopic normal-superconducting hybrid structures". In: *Phys. Rev. B* 55 (2 Jan. 1997), pp. 1142–1161. URL: https://link.aps.org/doi/10.1103/PhysRevB.55.1142.

[4]   Adrianus M.M. Pruisken. "Quasiparticles in the theory of the integral quantum Hall effect (I)". In: *Nuclear Physics B* 285 (1987), pp. 719–759. ISSN: 0550-3213. URL: https : / / www . sciencedirect . com / science / article/pii/0550321387903634.

C h a p t e r 2

SCALING AND DIFFUSION OF DIRAC COMPOSITE FERMIONS

2.1   Introduction

Delocalization transitions determine the phase diagrams of various electronic systems [48, 7, 46]. In three spatial dimensions, such transitions can occur between a diffusive metal and a localized insulator. In two dimensions (and fewer), localization generally relegates $T = 0$ metallic states to isolated critical points. The integer quantum Hall transition (IQHT) and the superconductor-insulator transition (SIT) are prototypical examples of such two-dimensional diffusive quantum critical points, having been well characterized by extensive experimental and numerical work over the past 30 years (see [72, 50, 51, 49] and references therein). Nevertheless, our understanding of these quantum states remains incomplete.

Theories of noninteracting electrons have provided valuable insight to the IQHT [36]. As the critical point is approached by tuning the external magnetic field or electron density to criticality $\delta \to 0$, the localization length is found to diverge as $|\delta|^{-\nu}$ with $\nu = 2.593(5)$ [69], while $\nu_{expt} \approx 2.38$ experimentally [50, 51]. On the other hand, a diverging timescale $\xi_t \sim \xi^{-\nu z}$ is also expected near the quantum critical point. Theories of noninteracting electrons yield a dynamical critical exponent $z = 2$ [36, 11, 38]; $z_{expt} \approx 1$ [72, 51] (although see [65]).[1] The challenge is to develop a framework that combines the effects of electron interactions with those of disorder [37].

Duality is a powerful tool for understanding the behavior of strongly interacting systems. Recent work has uncovered a duality web that relates various (2+1)d relativistic quantum field theories (see [67] and references therein). Included in this set are simple, toy models for integer quantum Hall and superconductor-insulator transitions. In this paper, we study the combined effects of quenched disorder and a dissipative Coulomb interaction on the critical properties of two such models. The hope is to abstract lessons that may be

---

[1] For the magnetic field-tuned SIT, $\nu_{expt} \approx 4/3$ or $\nu_{expt} \approx 7/3$ and $z_{expt} \approx 1$ experimentally [53].

valid more generally. As we discuss, these theories have a rich set of random critical behaviors.

For the first member of the duality web, consider a system of spinless electrons hopping on a square lattice with a half-unit of magnetic flux penetrating each plaquette [52] ([30] may alternatively be considered). An IQHT obtains as the ratio of the (staggered) chemical potential to next-neighbor hopping is varied. The critical properties of the transition are controlled by a free Dirac fermion Ψ with Lagrangian,[2]

$$\mathcal{L}_{\mathrm{D}irac} = \overline{\Psi} i \slashed{D}_A \Psi - M \overline{\Psi} \Psi + \frac{1}{2} \frac{1}{4\pi} A dA, \tag{2.1}$$

where A_μ is a non-dynamical $U(1)$ gauge field and the Chern-Simons term $AdA = \epsilon^{\mu\nu\rho} A_\mu \partial_\nu A_\rho$. The mass M vanishes at criticality. In the presence of an external magnetic field, (2.1) describes the particle-hole symmetric limit of the half-filled zeroth/lowest Landau level of Dirac/nonrelativistic electrons [71]. In this paper, we consider vanishing magnetic field. A dual effective theory to (2.1) consists of a Dirac fermion ψ coupled to a dynamical (emergent) $U(1)$ gauge field a_μ,

$$\mathcal{L}_{\mathrm{F}} = \overline{\psi} i \slashed{D}_a \psi - m \overline{\psi} \psi - \frac{1}{2} \frac{1}{2\pi} a dA + \frac{1}{2} \frac{1}{4\pi} A dA - \frac{1}{4} f_{\mu\nu}^2, \tag{2.2}$$

where the mass $m \propto M$ and the field strength $f_{\mu\nu} = \partial_\mu a_\nu - \partial_\nu a_\mu$.[3] (2.2) was first introduced as a dual description of the half-filled Landau level [71] or the gapless surface state of a time-reversal invariant topological insulator [76, 56] (when the AdA term is absent) with ψ being the Dirac composite fermion; its inclusion in the duality web was explained in [66, 45, 60]. When the external magnetic field is zero, the Dirac composite fermion chemical potential sits at the Dirac point.

For the second member of the duality web, consider a collection of repulsive bosons in a periodic potential [23]. For commensurate filling, the system exhibits a superfluid to Mott insulator transition with a charge-conjugation symmetry as the ratio of the boson hopping strength to repulsion is tuned. The long wavelength critical properties are described by the 3d XY model,

$$\mathcal{L}_{\mathrm{XY}} = |D_A \Phi|^2 - M|\Phi|^2 - |\Phi|^4. \tag{2.3}$$

---

[2]Additional details for the Lagrangians appearing in this section are given in §3.2.

[3]We use "condensed matter" notation when writing these Lagrangians; see [66] for a precise explanation of the meaning of, e.g., Chern-Simons terms with half-integer levels.

(Broken charge-conjugation symmetry generally results in a term proportional to $\Phi^* i\partial_t \Phi$.) In mean-field theory, the $M < 0$ region is a superfluid, while the $M > 0$ region is an insulator; we'll view (2.3) as describing a SIT. A dual effective theory [13, 6, 58] to (2.3) is

$$\mathcal{L}_{\mathrm{B}} = \overline{\psi} i \slashed{D}_a \psi - m\overline{\psi}\psi + \frac{1}{2}\frac{1}{4\pi}ada - \frac{1}{2\pi}adA + \frac{1}{4\pi}AdA - \frac{1}{4}f_{\mu\nu}^2. \qquad (2.4)$$

The statistics of the particles that (2.2) and (2.4) describe is controlled by the coefficient of the ada term.

Quenched disorder can have a profound effect on the nature of the above critical points and lead to new universality classes. Ref. [52] considered the effects of quenched randomness on the free Dirac fermion fixed point in (2.1). While for generic disorder the theory flows to strong coupling, if only a random vector potential $\mathbf{A}(\mathbf{x})$ is present the theory features a line of diffusive fixed points characterized by a continuously variable dynamical exponent z; the clean fixed point is stable to random mass disorder $M(\mathbf{x})$. Sachdev and Ye [82, 81] generalized this study to fractional quantum Hall transitions in the presence of an unscreened Coulomb interaction using a model closely related to (2.4). Recently, Goswami, Goldman, and Raghu [28] and Thomson and Sachdev [73] considered the effects of randomness on (2.2) with $2N_f$ fermion flavors. We use the large N_f expansion and the dimensional reduction renormalization group (RG) scheme[4] to reexamine these works and extend them to include the effects of "topological disorder" (§2.2) and a dissipative Coulomb interaction, generally finding agreement with this prior work that found interacting, diffusive fixed points. Related work studying the effects of quenched randomness on theories of Dirac fermions coupled to a fluctuating boson include [24, 83].

In contrast to the fermion models, only random mass disorder $M(\mathbf{x})$ has resulted in accessible diffusive fixed points of the XY model. Early work [20, 9, 47, 78] studying the $O(2N_f)$ generalization of (2.3) used a double-ϵ expansion to find an interacting, finite disorder fixed point. However, the nature of the renormalization group flow in the vicinity of the fixed point is peculiar, exhibiting an anomalously long "time" to achieve criticality. Recently, this problem was reexamined within a large N_f expansion by Goldman, Thomson, Nie, and Bi [27], where it was argued that the anomalous renormalization group trajectories [20, 9, 47, 78] are a relic of the double-ϵ expansion. Furthermore, [27]

---

[4]This scheme is valid for theories with or without Chern-Simons terms and is closely related to the approach in [82, 81, 73].

find remarkable agreement with the critical exponents of the dirty XY model calculated by numerical simulation [63, 61, 55, 75]. We consider this analysis from the perspective of the "fermionic dual" of the XY model in 2.4, providing qualitative confirmation of the renormalization group flow found in [27]. To $\mathcal{O}(1/N_f)$, we find a finite-disorder fixed point with critical exponents,

$$\nu^{-1} = 1 \quad \text{and} \quad z = 1 + \frac{1.411}{N_f}; \tag{2.5}$$

$\nu = 1$ and $z = 1 + .54/N_f$ is reported in [27]. We also consider other types of disorder that is sourced by the random gauge field $A_\mu(\mathbf{x})$.

The important influence of a Coulomb interaction on the critical properties of the above transitions was stressed long ago [22], where it was argued that an unscreened Coulomb interaction generically results in a dynamical critical exponent $z = 1$. In addition, the observed IQHT and SIT appear to be sensitive to the precise nature of the Coulomb interaction ([43, 77] and references therein). For example, a capacitively-coupled screening plane has been found to affect the metallic behavior in thin films [54], lifting an anomalous low-temperature metallic regime that intervenes a direct magnetic field-tuned SIT. To investigate such effects, we consider a Coulomb interaction that is screened by a diffusive two-dimensional Fermi gas [74]. The dissipative Coulomb interaction that results allows for two types of fixed points: those with a finite, nonzero Coulomb coupling and $z = 1$ and those with an effectively infinite Coulomb interaction and $z \neq 1$ [70]. For the "fermionic dual" of the XY model with random mass disorder, we find critical exponents,

$$\nu^{-1} = 1 \quad \text{and} \quad 1 \leq z < 2, \tag{2.6}$$

with z saturating the lower bound for the unscreened Coulomb interaction and varying continuously with an effective dissipation parameter for $z > 1$. In our approach, we're unable to access the "infinite z" fixed point found in the study of the dissipative XY model in [3]. Our result differs from that of Vishwanath, Moore, and Senthil [74] who studied the effects a dissipative Coulomb interaction on the dirty XY model using the double-ϵ expansion and found a line of fixed points with $z = 1$ and continuously varying ν. We also consider the effects of other types of disorder on the theories in (2.4) (and (2.2)) when a dissipative Coulomb interaction is present.

2.2 Setup

In this section, we introduce the effective model that realizes an IQHT/SIT and whose critical properties we'll analyze in §2.3.

Consider the $(2+1)$d theory of N_f Dirac fermions ψ_I coupled to a $U(1)$ Chern-Simons gauge field a_μ at level $(\theta - 1/2)$[5]

$$\mathcal{L}^{(1)} = \sum_{I=1}^{N_f} \overline{\psi}_I(i\slashed{D}_a - m)\psi_I - \frac{1}{2}\frac{1}{4\pi}ada + \frac{\theta}{4\pi}(a - A)d(a - A) - \frac{1}{4}f_{\mu\nu}^2. \quad (2.7)$$

When $N_f = 2\theta = 1$, we recover (2.2), the dual of a free Dirac fermion; when $N_f = \theta = 1$, we find the dual (2.4) to the 3d XY model. Reminiscent of conventional flux attachment [41, 25], θ^{-1} quantifies the number of attached flux quanta; for general θ, $\mathcal{L}^{(1)}$ is the model for an anyon gas introduced by Chen, Fisher, and Wu [13]. We refer to ψ_I as a Dirac composite fermion. A_μ is a nondynamical $U(1)$ gauge field that we identify with electromagnetism.[6]

In §2.2 and §5.27, where we discuss the phase diagram and symmetry of (2.7), we take $N_f = 1$. Otherwise, N_f is an arbitrary parameter that allows for analytic control as $N_f \to \infty$.

Mean-Field Phase Diagram at $N_f = 1$

For a given θ, the mean-field phase diagram of (2.7) at $N_f = 1$ is parameterized by the Dirac composite fermion mass m. At energies less than $|m|$, we may integrate out[7] the Dirac composite fermion to obtain the effective Lagrangian,

$$\mathcal{L}_{\mathrm{eff}} = \frac{sign(m) - 1 + 2\theta}{2}\frac{1}{4\pi}ada - \frac{\theta}{2\pi}adA + \frac{\theta}{4\pi}AdA - \frac{1}{4}f_{\mu\nu}^2. \quad (2.8)$$

Higher-order terms in a_μ can be ignored as $|m| \to \infty$. The Maxwell term $f_{\mu\nu}^2$ can also be dropped in this long wavelength analysis.

---

[5]The notation in (2.7) is as follows: $\bar{\psi} = \psi^\dagger\gamma^0$; $\slashed{D}_a = (\partial_\mu - ia_\mu)\gamma^\mu$ with $\mu \in \{0, 1, 2\} = \{t, x, y\}$; and a Chern-Simons term $AdA = \epsilon^{\mu\nu\rho}A_\mu\partial_\nu A_\rho$. For the purpose of discussing the symmetries of (2.7) later in this section, we choose Minkowski signature $\eta^{\mu\nu} = \mathrm{d}iag(+1, -1, -1)$ and γ-matrices $(\gamma^0, \gamma^1, \gamma^2) = (\sigma^3, i\sigma^1, i\sigma^2)$ where σ^j are the Pauli σ-matrices; in the renormalization group analysis in §2.3, we'll work in Euclidean signature.

[6]In §2.2 we give A_0 dynamics to discuss the Coulomb interaction.

[7]By "integrate out," we refer to path integral relations of the form: $\int \mathcal{D}\phi \, e^{i\int(\frac{1}{2}\phi K\phi + \phi J)} \propto e^{i\int(-\frac{1}{2}JK^{-1}J)}$, where ϕ and J are real fields and K is some kernel, e.g., a kinetic term for ϕ. Thus, we equate the Lagrangians $\frac{1}{2}\phi K\phi + \phi J = -\frac{1}{2}JK^{-1}J$ upon integrating out ϕ. Such identities follow directly from the ϕ equation of motion when ϕ appears quadratically in the Lagrangian.

$\theta = 1/2$

Setting $\theta = 1/2$, there are two phases. For $m > 0$ we find the effective Lagrangian for an insulator at zero temperature,

$$\mathcal{L}_{\mathrm{INS}} = \frac{1}{2}\left(\frac{1}{4\pi}ada - \frac{1}{2\pi}adA + \frac{1}{4\pi}AdA\right) = 0, \tag{2.9}$$

where the second equality follows from integrating out a_μ. For $m < 0$ we find the long wavelength Lagrangian for an integer Hall state,

$$\mathcal{L}_{\mathrm{IQH}} = \frac{1}{2}\left(-\frac{1}{4\pi}ada - \frac{1}{2\pi}adA + \frac{1}{4\pi}AdA\right) = \frac{1}{4\pi}AdA. \tag{2.10}$$

$\theta = 1$

Next set $\theta = 1$. We again find the insulator when $m > 0$,

$$\mathcal{L}_{\mathrm{INS}} = \frac{1}{4\pi}ada - \frac{1}{2\pi}adA + \frac{1}{4\pi}AdA = 0. \tag{2.11}$$

To identify the $m < 0$ phase, it's helpful to include the charge $e_* = q$ (measured in units of the electric charge e) carried by the boson Φ in (2.3) by substituting $A_\mu \to qA_\mu$:

$$\mathcal{L}_{\mathrm{SC}} = -\frac{q}{2\pi}adA + \frac{q^2}{4\pi}AdA. \tag{2.12}$$

(2.12) describes a $\mathbb{Z}/q$ gauge theory, the long wavelength description of a superconductor with charge-q condensate [32, 44].

Discrete Symmetry at $N_f = 1$

The types of randomness that can be added to (2.7) are characterized by charge-conjugation $\mathcal{C}$ and time-reversal $\mathcal{T}$ symmetries. (Parity, i.e., spatial reflection, is necessarily broken in the presence of quenched disorder.) These symmetries are defined with respect to the electron and boson Lagrangians in Eqs (2.1) and (2.3). We discuss their implementation [71, 66, 57, 34, 12] in the dual Lagrangian (2.7) at $N_f = 1$ at criticality $m = 0$.

$\theta = 1/2$

The free Dirac Lagrangian in (2.1) is invariant under charge-conjugation $\mathcal{C}$,

$$\Psi \mapsto \sigma^1 \Psi^*, \quad A_\mu \mapsto -A_\mu. \tag{2.13}$$

The presence of the Chern-Simons term for A_μ reflects the violation of time-reversal $\mathcal{T}$:

$$t \mapsto -t, \quad \Psi \mapsto -i\sigma^2 \Psi, \quad (A_0, A_i) \mapsto (A_0, -A_i), \tag{2.14}$$

which is anti-unitary ($i \mapsto -i$). On the surface of a time-reversal invariant topological insulator, this Chern-Simons term is absent and so $\mathcal{T}$ can be preserved.

The dual Lagrangian (2.7) at $\theta = 1/2$ is also invariant under $\mathcal{C}$:

$$\psi \mapsto \sigma^1 \psi, \quad a_\mu \mapsto -a_\mu, \quad A_\mu \mapsto -A_\mu. \tag{2.15}$$

Identifying the electromagnetic currents across the duality between (2.1) and (2.7), $\frac{\delta \mathcal{L}_{\text{Dirac}}}{\delta A_\mu} = \frac{\delta \mathcal{L}^{(1)}}{\delta A_\mu}$, we equate

$$\bar{\Psi} \gamma^\mu \Psi = \frac{1}{4\pi} \epsilon^{\mu\nu\rho} \partial_\nu a_\rho. \tag{2.16}$$

Similarly, the a_0 equation of motion relates

$$\frac{1}{4\pi} \epsilon^{\mu\nu\rho} \partial_\nu A_\rho = \bar{\psi} \gamma^\mu \psi. \tag{2.17}$$

Eqs. (2.16) and (2.17) imply that in (2.7), $\mathcal{C}T$:

$$t \mapsto -t, \quad \psi \mapsto -i\sigma^2 \psi^*, \quad (a_0, a_i) \mapsto (a_0, -a_i), \quad (A_0, A_i) \mapsto (-A_0, A_i). \tag{2.18}$$

Thus, $\mathcal{T}$ and $\mathcal{C}T$ are exchanged across the duality: the $\mathcal{T}$ transformations on Ψ and A_μ is identical to the $\mathcal{C}T$ transformations on ψ and a_μ, and vice versa. In the absence of the Chern-Simons term for A_μ, (2.7) is time-reversal invariant.

While the dual Lagrangians in (2.1) and (2.7) violate time-reversal invariance as (2+1)d theories, they do preserve a "non-local" particle-hole (PH) transformation. To define this, consider the following transformations of a general Lagrangian $L(A)$ which has a $U(1)$ symmetry current that is coupled to a non-dynamical field A_μ [80]:

$$\mathbf{T} : L(A) \mapsto L(A) + \frac{1}{4\pi} A dA; \tag{2.19}$$

$$\mathbf{S} : L(A) \mapsto L(c) + \frac{1}{2\pi} c dA. \tag{2.20}$$

$\mathbf{T}$ shifts the Hall conductivity by a unit; $\mathbf{S}$ converts A_μ into a dynamical $U(1)$ gauge field c_μ and adds a BF term, which couples the field strength dc to a

new external field A_μ. (2.19) and (2.20) implement modular transformations on the conductivity tensor of the $U(1)$ symmetry current coupling to A_μ. The PH transformation is defined as $\mathcal{T}$ followed by the modular **T** transformation (2.19). Notice that the Dirac masses $\bar{\Psi}\Psi$ and $\bar{\psi}\psi$ are odd under PH symmetry and even under $\mathcal{C}$. The **S** transformation will play a role in our discussion of the SIT theory.

$\theta = 1$

The XY model in (2.3) is invariant under charge-conjugation $\mathcal{C}$,

$$\Phi \mapsto \Phi^*, \quad A_\mu \mapsto -A_\mu, \tag{2.21}$$

and time-reversal $\mathcal{T}$,

$$t \mapsto -t, \quad \Phi \mapsto \Phi, \quad (A_0, A_i) \mapsto (A_0, -A_i). \tag{2.22}$$

The dual Lagrangian in (2.7) at $\theta = 1$ is only invariant under $\mathcal{C}$ defined in (2.15); it isn't invariant under $\mathcal{T}$,

$$t \mapsto -t, \quad \psi \mapsto -\sigma^3 \psi^*, \quad (a_0, a_i) \mapsto (-a_0, a_i), \quad (A_0, A_i) \mapsto (A_0, -A_i), \tag{2.23}$$

with $i \mapsto -i$. Instead, time-reversal is an emergent symmetry of the long wavelength physics [66, 57]. In addition, (2.7) is invariant under a "non-local" particle-vortex (PV) transformation:

$$t \mapsto -t, \quad \psi \mapsto -i\sigma^2 \psi, \quad (a_0, a_i) \mapsto (a_0, -a_i), \quad (A_0, A_i) \mapsto (-A_0, A_i), \tag{2.24}$$

followed by the modular **S** transformation (2.20). The PV transformation is analogous to the PH transformation of the previous section [59]; it maps the 3d XY model to its scalar quantum electrodynamics dual [62, 19], and vice versa.

Duality maps $|\Phi|^2 \leftrightarrow \bar{\psi}\psi$. While it's clear that the Dirac mass is even under $\mathcal{C}$, it's less obvious that perturbation by $\bar{\psi}\psi$ is time-reversal invariant. This can be understood in the following sense: Perturbation of (2.7) by $\bar{\psi}\psi$ and its time-reversal, obtained using (2.23), by $-\bar{\psi}\psi$ result in identical phases.

Symmetry Assignment Summary

Table 2.1 summarizes the transformations of the operators that appear in (2.7) under charge-conjugation $\mathcal{C}$ and time-reversal $\mathcal{T}$ symmetries. We use these transformation assignments to characterize the types of randomness that may be added to $\mathcal{L}^{(1)}$ for general N_f.

	$\mathcal{C}$	$\mathcal{T}$
$\bar{\psi}\psi$	+	-
$\bar{\psi}\gamma_0\psi$	-	-
$\bar{\psi}\gamma_j\psi$	-	+
a_0	-	-
a_j	-	+
$b = \partial_x a_y - \partial_y a_x$	-	+
$e_j = \partial_0 a_j - \partial_j a_0$	-	-

Table 2.1: Charge-conjugation $\mathcal{C}$ and time-reversal $\mathcal{T}$ symmetry assignments of various operators.

Dissipative Coulomb Interaction

Dualizing the Coulomb Interaction

The Coulomb interaction between fermions/bosons carrying charge e_* arises from the exchange of a dynamical $(3+1)d$ electromagnetic scalar potential A_0. In Fourier space, we consider the action that couples a $(2+1)$d charge density $J_0(k_0, k)$ to the scalar potential $A_0(k_0, \vec{k})$:

$$-\frac{1}{2e_*^2}\int d^4k \; A_0(k_0, \vec{k})\left(\vec{k}^2\right)A_0(-k_0, -\vec{k}) - \int d^3k J_0(k_0, k)\int dk_3 A_0(-k_0, -\vec{k}),$$

$$(2.25)$$

where $k = (k_1, k_2)$ and $\vec{k} = (k_1, k_2, k_3)$. $J_0(k_0, k)$ is the Fourier transform of $\bar{\Psi}\gamma^0\Psi(x)$ for the free Dirac fermion (2.1) or $i\Phi^*\partial_0\Phi(x) - i(\partial_0\Phi^*)\Phi(x)$ for the XY model (2.3). The absence of an $A_0 k_0^2 A_0$ term means that A_0 mediates an instantaneous interaction for particles moving at speeds much less than the photon velocity. Integrating out the A_0 field we find the unscreened Coulomb interaction,

$$S_{\text{unscreened}} = -\frac{\pi}{2}\int d^3k \; J_0(k_0, k)\frac{e_*^2}{|k|}J_0(-k_0, -k), \qquad (2.26)$$

between $(2+1)d$ particles. It's convenient to interpret $S_{\text{unscreened}}$ as arising from the exchange of a purely $(2+1)$d gauge field $\tilde{A}_0$ with kinetic term and coupling to J_0 as

$$S_{\tilde{A}_0} = -\int d^3k \ \left(\tilde{A}_0(k_0, k)\frac{|k|}{\pi e_*^2}\tilde{A}_0(-k_0, -k) + J_0(k_0, k)\tilde{A}_0(-k_0, -k) \right). \quad (2.27)$$

The electromagnetic charge density $J_0(x)$ dualizes in (2.7) according to

$$J_0(x) = \frac{\delta\mathcal{L}^{(1)}}{\delta A_0} = -\frac{\theta}{2\pi}\epsilon_{ij}\partial_i a_j, \quad (2.28)$$

for vanishing A_j. Decomposing the gauge field $a_i(k_0, k) = i\frac{k_i}{|k|}a_L(k_0, k) - i\frac{k_j}{|k|}\epsilon_{ji}a_T(k_0, k)$ in terms of its longitudinal and transverse components, the (unscreened) Coulomb interaction becomes a kinetic term for a_T [42]:

$$S_{\text{unscreened}} = -\frac{e_*^2\theta^2}{8\pi}\int d^3k \ a_T(k_0, k)|k|a_T(-k_0, -k). \quad (2.29)$$

A similar transformation of the Coulomb interaction occurs in nonrelativistic composite fermion theories [31]. Notice that the unscreened Coulomb interaction results in a kinetic term that dominates a possible Maxwell coupling for a_μ at long wavelengths.

Dissipation

To model dissipation following [74], we consider an auxiliary system consisting of a parallel two-dimensional electron gas (2DEG) that is coupled to (2.7) through the Coulomb interaction, specifically, through $\tilde{A}_0$. The spatial separation between the system (2.7) and electron gas is assumed negligible. The electron Green's function is assumed to take a diffusive form,

$$G_{2D}^{-1}(ik_0, k) = ik_0 - (\frac{k^2}{2m} - \epsilon_F) + \frac{i}{2\tau}sign(k_0). \quad (2.30)$$

The dissipative effects arising from the coupling to the two-dimensional electron gas are encoded in a correction to the $\tilde{A}_0$ kinetic term in $S_{\tilde{A}_0}$ [4, 16],

$$\delta S_{\tilde{A}_0} = \int d^3k \ \tilde{A}_0(k_0, k)\frac{\sigma_e k^2}{|k_0| + D_e k^2}\tilde{A}_0(-k_0, -k), \quad (2.31)$$

where the Drude conductivity $\tilde{\sigma}_e = q_e^2 N D_e$ with N the density of states at Fermi energy ϵ_F of the two-dimensional electron gas and D_e its diffusivity. Higher-order corrections due to the two-dimensional electron gas will be

ignored. Including $\delta S_{\tilde{A}_0}$ we obtain the dissipation-corrected density-density (2.28) interaction upon integrating out $\tilde{A}_0$:

$$S^{(2)} = -\frac{e_*^2\theta^2}{8\pi} \int d^3k \; a_T(k_0, k)\Big(\frac{k^2}{|k| + f(k_0, k)}\Big)a_T(-k_0, -k), \qquad (2.32)$$

where

$$f(k_0, k) = \frac{\sigma_e k^2}{|k_0| + D_e k^2}, \quad \sigma_e = e_*^2\tilde{\sigma}_e. \qquad (2.33)$$

We recover the dual of an unscreened Coulomb interaction when $q_e = 0$, as expected, or as $|k|/|k_0| \to 0$. The Coulomb interaction is shortranged as $D_e \to \infty$ at finite density of states N or when $|k_0|/|k| \to 0$; in either of these limits, we find a Maxwell-like kinetic term for a_T (albeit with inverted charge $1/e_*$).

Quenched Randomness

We consider the effects of quenched disorder that's induced by random $A_\mu(\mathbf{x})$ and $M(\mathbf{x})$. In this discussion, we assume the Coulomb interaction has been included via (2.32) and $A_\mu(\mathbf{x})$ is a non-dynamical quenched random variable. Since $m(\mathbf{x}) \propto M(\mathbf{x})$, these perturbations readily map across the duality to

$$\delta\mathcal{L} = -m(\mathbf{x})\overline{\psi}\psi(x) - \frac{\theta}{2\pi}A(\mathbf{x})da(x), \qquad (2.34)$$

where $\mathbf{x} = (x_1, x_2)$ and $x = (x_0, x_1, x_2)$. The second term in Eq. (2.34) is "topological disorder," i.e., a random source to the field strength or "topological" current da. We have dropped a possible term proportional to $\epsilon_{ij}A_0(\mathbf{x})\partial_i A_j(\mathbf{x})$ arising from the Chern-Simons term for A in (2.7).

Interactions generate additional operators with random couplings, consistent with the symmetries of $A_\mu(\mathbf{x})$ and $m(\mathbf{x})$. The Harris criterion [33] (for Gaussian-correlated randomness) implies the relevant terms at low energies correspond to operators with scaling dimensions $\Delta \leq z + 1$. At large N_f [8, 15, 13] the most generic random terms to include are [73]

$$\mathcal{L}_{\mathrm{dis}} = m(\mathbf{x})\bar{\psi}\psi(x) + i\tilde{a}_0(\mathbf{x})\bar{\psi}\gamma^0\psi(x) + i\tilde{a}_j(\mathbf{x})\bar{\psi}\gamma^j\psi(x) - A_0(\mathbf{x})b(x) + \epsilon_{jk}A_j(\mathbf{x})e_k(x),$$
$$(2.35)$$

where $b = \epsilon_{ij}\partial_i a_j$ and $e_k = \partial_0 a_k - \partial_k a_0$. The random couplings are assumed to be *independent* Gaussian-correlated quenched random variables with zero

mean:

$$\langle m(\mathbf{x})m(\mathbf{x}')\rangle_{\mathrm{dis}} = g_m\delta^{(2)}(\mathbf{x}-\mathbf{x}'),$$
$$\langle \tilde{a}_0(\mathbf{x})\tilde{a}_0(\mathbf{x}')\rangle_{\mathrm{dis}} = g_0\delta^{(2)}(\mathbf{x}-\mathbf{x}'),$$
$$\langle \tilde{a}_k(\mathbf{x})\tilde{a}_k(\mathbf{x}')\rangle_{\mathrm{dis}} = g_j\delta^{(2)}(\mathbf{x}-\mathbf{x}'), \quad k\in\{x,y\},$$
$$\langle A_0(\mathbf{x})A_0(\mathbf{x}')\rangle_{\mathrm{dis}} = \Delta_0\delta^{(2)}(\mathbf{x}-\mathbf{x}'),$$
$$\langle A_k(\mathbf{x})A_k(\mathbf{x}')\rangle_{\mathrm{dis}} = \Delta_j\delta^{(2)}(\mathbf{x}-\mathbf{x}'), \quad k\in\{x,y\}, \tag{2.36}$$

where $\langle\,\cdot\,\rangle_{\mathrm{dis}}$ indicates a disorder average and there is no sum over k. The disorder variances $g_m, g_0, g_j, \Delta_0, \Delta_j$ are positive constants.

We study the effects of the randomness in (2.35) using the replica trick, which enables the calculation of the disorder-averaged free energy and all observables that derive from it. To this end, we introduce n_r replicas $\psi_{I,\ell}$ and $a_{\mu,\ell}$ with $\ell\in\{1,\ldots,n_r\}$ and consider the replicated partition function,

$$Z^{n_r} = \prod_\ell\left(\int\mathcal{D}\psi_\ell\mathcal{D}\bar{\psi}_\ell\mathcal{D}a_\ell\right)e^{i\sum_\ell\left(S^{(1)}[\psi_\ell,a_\ell]+S^{(2)}[a_\ell]+S_{\mathrm{dis}}[\psi_\ell,a_\ell]\right)}, \tag{2.37}$$

where $S^{(1)}[\psi_\ell,a_\ell] = \int d^3x\mathcal{L}^{(1)}(\psi_\ell,a_\ell)$ with $\mathcal{L}^{(1)}$ given in (2.7), $S^{(2)}[a_\ell]$ is given in (2.32), and $S_{\mathrm{dis}}[\psi_\ell,a_\ell] = \int d^3x\mathcal{L}_{\mathrm{dis}}(\psi_\ell,a_\ell)$ with $\mathcal{L}_{\mathrm{dis}}$ given in (2.35). Using the identity,

$$\log Z = \lim_{n_r\to 0}\frac{Z^{n_r}-1}{n_r}, \tag{2.38}$$

the disorder-averaged free energy, proportional to $\langle\log Z\rangle_{\mathrm{dis}}$, is found upon disorder-averaging. Using (2.36):

$$\langle Z^{n_r}\rangle_{\mathrm{dis}} = \prod_\ell\left(\int\mathcal{D}\psi_\ell\mathcal{D}\bar{\psi}_\ell\mathcal{D}a_\ell\right)e^{i\sum_\ell\left(S^{(1)}[\psi_\ell,a_\ell]+S^{(2)}[a_\ell]+iS^{(3)}[\psi_\ell,a_\ell]\right)}, \tag{2.39}$$

where

$$S^{(3)}[\psi_\ell,a_\ell] = -\frac{1}{2}\sum_k\int dt\,dt'\,d^2x\Big[g_m\Big(\bar{\psi}_\ell\psi_\ell\Big)(t)\Big(\bar{\psi}_k\psi_k\Big)(t') + g_0\Big(\bar{\psi}_\ell\gamma^0\psi_\ell\Big)(t)\Big(\bar{\psi}_k\gamma^0\psi_k\Big)(t')$$
$$+ g_j\Big(\bar{\psi}_\ell\gamma^j\psi_\ell\Big)(t)\Big(\bar{\psi}_k\gamma^j\psi_k\Big)(t') + \Delta_0 b_\ell(t)b_k(t') + \Delta_j\mathbf{e}_\ell(t)\cdot\mathbf{e}_k(t')\Big],$$

$$\tag{2.40}$$

$\Big(\bar{\psi}_\ell^{(I)}\psi_\ell^{(I)}\Big)(t)\Big(\bar{\psi}_k^{(J)}\psi_k^{(J)}\Big)(t') \equiv \bar{\psi}_\ell^{(I)}(x,t)\psi_\ell^{(I)}(x,t)\bar{\psi}_k^{(J)}(x,t')\psi_k^{(J)}(x,t')$ and similarly for the other terms appearing in $S_E^{(3)}$.

2.3 Renormalization Group Analysis

We now study the critical properties of the model introduced in §3.2. Details of our calculations are presented in Appendix 2.A.

Large N_f Expansion and Renormalization Group Scheme

The Euclidean effective action in $D + 1$ dimensions is

$$S_E = S_E^{(1)} + S_E^{(2)} + S_E^{(3)} \tag{2.41}$$

where[8]:

$$S_E^{(1)} = \int d\tau d^D x \Big[\bar{\psi}_\ell^{(I)} \Big(\gamma_\tau (\partial_\tau + i \frac{g}{\sqrt{N_f}} a_{\tau,\ell}) + v\gamma_j (\partial_j + i \frac{g}{\sqrt{N_f}} a_{j,\ell}) \Big) \psi_\ell^{(I)} + m \bar{\psi}_\ell^{(I)} \psi_\ell^{(I)}$$
$$+ \frac{i\kappa}{2} a_\ell da_\ell \Big], \tag{2.42}$$

$$S_E^{(2)} = \int d\omega d^D k \, \frac{w_x}{2} a_{\ell,T}(\omega, k) \frac{k^2}{|k| + f(\omega, k)} a_{T,\ell}(-\omega, -k), \tag{2.43}$$

$$S_E^{(3)} = -\frac{1}{2} \int d\tau d\tau' d^D x \Big[g_m \Big(\bar{\psi}_\ell^{(I)} \psi_\ell^{(I)} \Big)(\tau) \Big(\bar{\psi}_k^{(J)} \psi_k^{(J)} \Big)(\tau') + g_0 \Big(\bar{\psi}_\ell^{(I)} \gamma^0 \psi_\ell^{(I)} \Big)(\tau) \Big(\bar{\psi}_k^{(J)} \gamma^0 \psi_k^{(J)} \Big)(\tau')$$
$$+ g_j \Big(\bar{\psi}_\ell^{(I)} \gamma^j \psi_\ell^{(I)} \Big)(\tau) \Big(\bar{\psi}_k^{(J)} \gamma^j \psi_k^{(J)} \Big)(\tau') + \Delta_0 b_\ell(\tau) b_k(\tau') + \Delta_j \mathbf{e}_\ell(\tau) \cdot \mathbf{e}_k(\tau') \Big] \tag{2.44}$$

We've set the longitudinal component of a_i to zero (Coulomb gauge): $a_i(\omega, k) = i\frac{k_j}{|k|}\epsilon_{ji} a_T(\omega, k)$. The gauge coupling is $g/\sqrt{N_f}$ with g fixed and $N_f \to \infty$ [17], v is the Dirac composite fermion velocity, and the Dirac mass m vanishes at criticality. The disorder variances $g_m, g_0, g_j, \Delta_0, \Delta_j$ are assumed to scale as $1/N_f$. The Chern-Simons level is controlled by $\kappa = \frac{2\theta-1}{4\pi}$: $\kappa = 0$ gives an IQHT and $\kappa = 1/4\pi$ gives a SIT. $w_x = \frac{e_*^2}{4\pi}$ parameterizes the strength of the dissipative Coulomb interaction and $f(\omega, k) = \frac{\sigma_e k^2}{|\omega| + D_e k^2}$. The non-dynamical (electromagnetic) field $A_\mu = 0$. In the remainder, we'll often leave replica and flavor indices, as well as the spacetime dependence of fields implicit.

We regularize UV divergent integrals that appear in our renormalization group analysis of S_E using *dimensional reduction* [68, 14, 13]. This is the standard approach (e.g., [5, 14, 13, 26, 2] and references therein) used in the study of theories of Chern-Simons gauge fields coupled to matter and, in contrast to dimensional regularization, has been shown to preserve gauge invariance

---

[8]Replica indices $\ell, k \in \{1, \ldots, n_r\}$ and flavor indices $I, J \in \{1, \ldots, N_f\}$ with repeated indices summed. In Euclidean signature $(+, +, +)$, the coordinates $(\tau, x_j) = (it, x_j)$, Fourier space variables $(\omega, k_j) = (-ik_0, k_j)$, and the γ-matrices $(\gamma_0, \gamma_1, \gamma_2) = (\sigma^3, \sigma^1, \sigma^2)$.

at least to 2-loop order in the perturbative analysis of $S_E^{(1)}$ [14]. We assume without proof that this regularization procedure maintains gauge invariance in our large N_f study of S_E, which involves 3-loop integrals. We consider a slight variation of the conventional dimensional reduction approach. First, all vector, tensor, and spinor algebra is performed in 3d; in particular, the antisymmetric symbol $\epsilon^{\mu\nu\rho}$ obeys the usual 3d identities. Second, loop integrals are analytically continued to general (Euclidean) spatial dimension $D \leq 2$:

$$\int \frac{d\omega d^2 k}{(2\pi)^3} \rightarrow \mu^\epsilon \int \frac{d\omega d^D k}{(2\pi)^{D+1}}, \tag{2.45}$$

where $\epsilon = 2 - D$ and μ is the renormalization group scale.[9] Simple poles proportional to $2/\epsilon$ are identified with logarithmic divergences proportional to $\log(\Lambda^2/\mu^2)$ in a theory with momentum cutoff Λ; power-law divergences are set to zero.
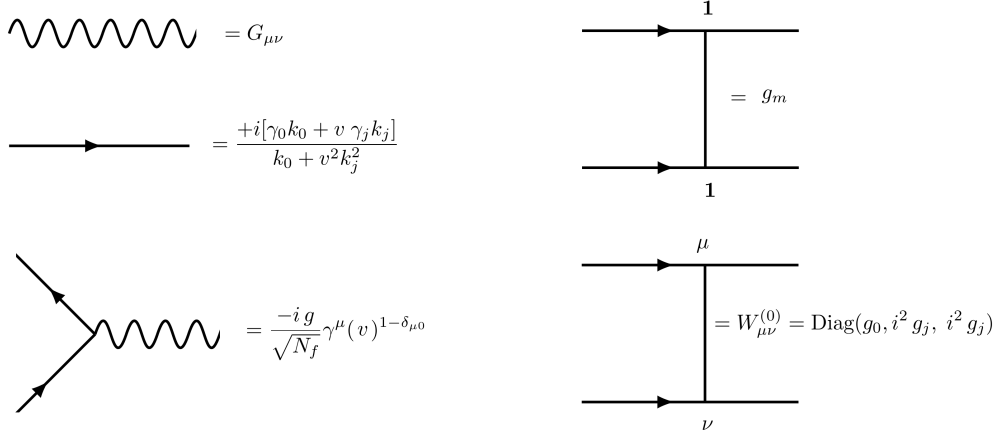
Figure 2.1: Feynman rules of S_E. The wavy line denotes the effective gauge field propagator and the directed solid line indicates the fermion propagator with $m = 0$. Disorder is represented by a solid line without an arrow and specified by its disorder variance (g_m, g_0, g_j). Screening of the disorder (g_0, g_j) and topological disorder (Δ_0, Δ_j) are discussed in the Appendix 2.C.

The large N_f Feynman rules that derive from S_E at $m = 0$ are given in Fig. 2.1. We've summed once and for all the geometric series of fermion bubble diagrams in Fig. 2.2 and replaced the bare gauge field propagator by the

---

[9]Typically in dimensional reduction the spacetime dimension is analytically continued.

effective propagator,

$$G_{mn} = \begin{pmatrix} \frac{g^2}{16} \frac{k^2}{\sqrt{\omega^2 + v^2 k^2}} & i\kappa|k| \\ i\kappa|k| & w_x \frac{k^2}{|k| + f(\omega,k)} + \frac{g^2}{16}\sqrt{\omega^2 + v^2 k^2} \end{pmatrix}^{-1}_{mn}, \qquad (2.46)$$

where $m, n \in \{0, T\}$ correspond to the zeroth and transverse components of a_μ. At large N_f this resummation is equivalent to the random phase approx-
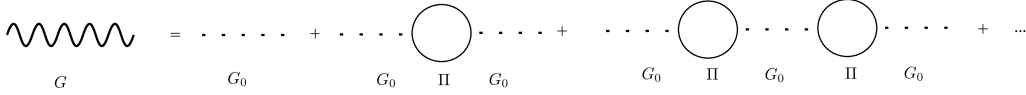
Figure 2.2: The effective gauge field propagator G. The dotted line G_0 represents the bare gauge field propagator and $\Pi_{\mu\nu}$ is the 1-loop gauge field self-energy. Each term in this geometric series of diagrams produces an $\mathcal{O}(N_f^0)$ correction to the gauge field propagator, since each fermion loop contributes a factor of N_f and the two vertices associated to each loop contribute an additional factor of g^2/N_f.

imation. The same effect also leads to a screening of the g_0 and g_j disorders (see Appendix 2.C) [81, 28]. Aside from a few exceptions that we'll discuss, we've found disorder screening to be a subleading effect in our analysis.

We use minimal subtraction [1, 79] to renormalize S_E. In this scheme, simple poles in ϵ appear in counterterms $b_{\lambda_a}(\vec{\lambda}^R)/\epsilon$ that relate bare (B) and renormalized (R) couplings:

$$\lambda_a^B \mu^{-\Delta_a(\epsilon)} = \lambda_a^R(\mu, \epsilon) + \frac{b_{\lambda_a}(\vec{\lambda}^R(\mu, \epsilon))}{\epsilon}, \qquad (2.47)$$

where the vector of coupling constants (either B or R)

$$\vec{\lambda} = \left(\frac{g^2}{N_f}, v, m, \kappa, w_x, \sigma_e, D_e, g_m, g_0, g_j, \Delta_0, \Delta_j\right)^T. \qquad (2.48)$$

The renormalized couplings $\lambda_a^R(\mu, \epsilon)$ and residues $b_{\lambda_a}(\vec{\lambda}^R(\mu, \epsilon))$ are analytic in ϵ. The higher-order poles that generally occur on the right-hand side of Eq. (2.47) can be set to zero. The bare couplings λ_a^B have engineering dimensions equal to $\Delta_{\lambda_a}(\epsilon)$ while the renormalized couplings are dimensionless. Appendix 2.A details the calculation of the counterterms $b_{\lambda_a}(\vec{\lambda}^R)/\epsilon$.

The engineering dimensions $\Delta_{\lambda_a}(\epsilon)$ of the bare couplings are given in Table 2.2. These dimensions are determined as follows. Each term in $S_E^{(1)}$ is dimensionless

λ_a	$\Delta_{\lambda_a}(\epsilon)$	$\bar{\Delta}_{\lambda_a}$	ρ_{λ_a}
$\frac{g^2}{N_f}$	ϵ	0	1
$\{v, w_x, \sigma_e\}$	$z-1$	$z-1$	0
m	z	z	0
$\{\kappa, \Delta_j\}$	0	0	0
D_e	$z-2$	$z-2$	0
$\{g_m, g_0, g_j\}$	$2z-D$	$2z-2$	1
Δ_0	$2z-2$	$2z-2$	0

Table 2.2: Engineering dimension $\Delta_{\lambda_a}(\epsilon) = \bar{\Delta}_{\lambda_a} + \rho_{\lambda_a}\epsilon$ of bare coupling λ_a^B (B superscript omitted in the table), where $\bar{\Delta}_{\lambda_a}$ is independent of $\epsilon = 2 - D$ and ρ_{λ_a} is the constant coefficient of ϵ.

with the assignments:

$$\Delta_\tau = -\Delta_\omega = -z, \quad \Delta_x = -\Delta_k = -1, \tag{2.49}$$

$$\Delta_{\psi(\tau,x)} = \frac{1}{2} - \frac{\epsilon}{2}, \quad \Delta_{a_0^E(\tau,x)} = z - \eta\epsilon, \quad \Delta_{a_j^E(\tau,x)} = 1 - \eta\epsilon, \tag{2.50}$$

and

$$\Delta_{g^2/N_f} = 2\eta\epsilon, \quad \Delta_v = z - 1, \quad \Delta_m = z, \quad \Delta_\kappa = (2\eta - 1)\epsilon, \tag{2.51}$$

where η is an arbitrary constant. We've introduced the dynamical critical exponent z with a value to be determined later; in the absence of $S_E^{(2)}$ and $S_E^{(3)}$, relativistic symmetry requires that v be dimensionless and $z = 1$. In the large N_f expansion, g is fixed and we formally take $\Delta_{N_f} = -2\eta\epsilon$. The effective gauge field propagator is consistent with the engineering dimensions $\Delta_{a_0^E(\omega,k)} = -D - \eta\epsilon$ and $\Delta_{a_j^E(\omega,k)} = (1-z) - D - \eta\epsilon$ if $\eta = 1/2$. The dimensions of the remaining couplings ensure the terms in $S_E^{(2)}$ and $S_E^{(3)}$ are dimensionless.

The beta functions β_{λ_a} at $\epsilon = 0$ are read off from the residues $b_{\lambda_a}(\vec{\lambda}^R)$ using

$$\beta_{\lambda_a}(\vec{\lambda}^R) \equiv -\mu\frac{\partial\lambda_a^R}{\partial\mu} = \bar{\Delta}_{\lambda_a}\lambda_a^R + \rho_{\lambda_a}b_{\lambda_a}(\vec{\lambda}^R) - \sum_c \rho_{\lambda_c}\lambda_c^R\frac{\partial b_{\lambda_a}(\vec{\lambda}^R)}{\partial\lambda_c^R}. \tag{2.52}$$

There is no sum over a in Eq. (2.52). The minus sign in front of $\mu\frac{\partial\lambda_a^R}{\partial\mu}$ means that a relevant/irrelevant coupling has a positive/negative beta function. Notice that only g^2/N_f and the variances g_m, g_0, g_j can contribute to the derivative term on the right-hand side of Eq. (2.52).

We characterize any fixed points $\beta_{\lambda_a}(\vec{\lambda}^R) = 0$ by the dynamical critical exponent z and correlation length exponent ν, evaluated at the fixed point. The dynamical critical exponent enters the beta functions (2.52) via $\bar{\Delta}_{\lambda_a}$ (see Table 2.2) and we determine its value by the condition of vanishing velocity beta function $\beta_v(\vec{\lambda}^R) = 0$[10]:

$$z = 1 + \frac{1}{v^R} \sum_c \rho_{\lambda_c} \lambda_c^R \frac{\partial b_v(\vec{\lambda}^R)}{\partial \lambda_c^R}. \tag{2.53}$$

Since the transitions we consider in this paper are tuned by the Dirac mass, we define the correlation length ξ as the inverse momentum scale μ_0^{-1} at which $v^R(\mu_0)/m^R(\mu_0) = 1$.[11] We write the mass beta function as

$$\beta_m(\vec{\lambda}^R) = \left(z - \gamma_{\bar{\psi}\psi}(\vec{\lambda}^R) \right) m^R, \tag{2.54}$$

where the anomalous dimension $\gamma_{\bar{\psi}\psi}$ controls the asymptotic scaling of the correlation function $\langle \bar{\psi}\psi(\tau, x)\bar{\psi}\psi(0) \rangle \sim |v^2\tau^2 + x^2|^{-(D+\gamma_{\bar{\psi}\psi})}$. Using Eqs. (2.52) - (2.54), we find

$$\xi = \Lambda^{-1} \left(\frac{m_\Lambda/v_\Lambda}{\Lambda} \right)^{-\nu} \tag{2.55}$$

where Λ is an arbitrary momentum cutoff defining the "initial conditions," $m^R(\Lambda) = m_\Lambda/\Lambda^z$ and $v^R(\Lambda) = v_\Lambda/\Lambda^{z-1}$, and the inverse correlation length exponent

$$\nu^{-1} = z - \gamma_{\bar{\psi}\psi}. \tag{2.56}$$

Note that m^R does not enter the residues $b_{\lambda_a}(\vec{\lambda}^R)$ with $\lambda_a^R \neq m^R$ and only appears linearly in $b_m(\vec{\lambda}^R)$.

In the remainder of the main text, we drop the B and R superscripts for notional clarity.

---

[10]Nonzero β_v implies a quantum correction to the tree-level dynamical exponent, i.e., the engineering dimension $-\Delta_\tau$. This follows from the fermion dispersion relation $|\omega| = v|k|$ (see, e.g., [70]). We've chosen to introduce an arbitrary z in Table 3 with a value to be determined by vanishing renormalization of the velocity. An equivalent choice is to take engineering dimensions consistent with conformal invariance and infer any correction to the tree-level dynamical scaling from a nonzero velocity beta function.

[11]The factor of $v^R(\mu_0)$ accounts for possible running of the velocity in the equivalent approach where $z = 1$ is chosen in Table 2.2 and the nonzero velocity beta function determines the correction $z - 1$ to dynamical scaling.

General Analysis

We now present the results of our renormalization group calculation, which is valid to order $1/N_f$ in the large N_f expansion. See Appendix 2.A for details.

Vanishing velocity beta function determines the dynamical critical exponent to be

$$z = 1 + \overline{g_m} + \overline{g_0} + 2\overline{g_j} - F_w(\overline{w_x}, \kappa, \overline{\sigma_e}), \qquad (2.57)$$

where $g_1 = g^2/16$, the rescaled couplings are

$$\overline{m} = \frac{m}{v}, \overline{w_x} = \frac{w_x}{v}, \overline{\sigma_e} = \frac{\sigma_e}{v}, \overline{g_m} = \frac{g_m}{2\pi v^2}, \overline{g_0} = \frac{g_0}{2\pi v^2}, \overline{g_j} = \frac{g_j}{2\pi v^2}, \overline{\Delta_0} = \Delta_0, \overline{\Delta_j} = \Delta_j \, v^2, \qquad (2.58)$$

and

$$F_w(\overline{w_x}, \kappa, \overline{\sigma_e}) = \frac{1}{4\pi^2 N_f} \int_{-\infty}^{\infty} dy \, \frac{g_1(-1 + 2y^2)(\sigma_e + |y|) + \overline{w_x}|y|\sqrt{1 + y^2}}{(1 + y^2)^2 \left(\sqrt{1 + y^2}(g_1^2 + \kappa^2)(\overline{\sigma_e} + |y|) + g_1 \, \overline{w_x} \, |y| \right)} \qquad (2.59)$$

The beta functions $\beta_{\lambda_a} = -\mu \frac{\partial \lambda_a}{\partial \mu}$ for the remaining couplings take the form:

$$\beta_{\overline{w_x}} = \overline{w_x}\big(z - 1\big), \qquad (2.60)$$

$$\beta_{\overline{\sigma_e}} = \overline{\sigma_e}\big(z - 1\big), \qquad (2.61)$$

$$\beta_{D_e} = D_e\big(z - 2\big), \qquad (2.62)$$

$$\beta_{\overline{m}} = \overline{m}\big(z - \gamma_{\bar{\psi}\psi}\big), \qquad (2.63)$$

$$\beta_{\overline{g_m}} = 2\overline{g_m}\Big(z - 1 + \frac{2\overline{g_0}\,\overline{g_j}}{\overline{g_m}} - \gamma_{\bar{\psi}\psi}\Big), \qquad (2.64)$$

$$\beta_{\overline{g_0}} = 2\overline{g_0}\Big(z - 1 + \frac{2\overline{g_j}\,\overline{g_m}}{\overline{g_0}}\Big), \qquad (2.65)$$

$$\beta_{\overline{g_j}} = 2\overline{g_j}\Big(z - 1 + \frac{\overline{g_m}\,\overline{g_0}}{\overline{g_j}} - \overline{g_m} - \overline{g_0} - 2\overline{g_j} + F_w(\overline{w_x}, \kappa, \overline{\sigma_e})\Big), \qquad (2.66)$$

$$\beta_{\overline{\Delta_0}} = \overline{\Delta_0}(2z - 2) + \frac{\overline{g_m}\big(\overline{\Delta_j}(g_1 + \overline{w_x})^2 + \overline{\Delta_0}\kappa^2\big)}{64\big(g_1(g_1 + \overline{w_x})\big)^2} + \frac{\overline{g_0}\,\overline{g_m}\,N_f\,\pi\,v^2}{32}, \qquad (2.67)$$

$$\beta_{\overline{\Delta_j}} = \frac{\overline{g_m}\,(g_1^2\,\overline{\Delta_0} + \kappa^2\,\overline{\Delta_j})}{128\big(g_1(g_1 + \overline{w_x}) + \kappa^2\big)^2} + \frac{\overline{g_j}\,\overline{g_m}N_f\pi v^4}{64}, \qquad (2.68)$$

where z is given in Eq. (2.57), the mass anomalous dimension

$$\gamma_{\bar{\psi}\psi} = 2\overline{g_m} + 2\overline{g_0} - \frac{\overline{g_0}g_1 - \overline{g_j}(g_1 + \overline{w_x})}{g_1^2 + g_1\overline{w_x} + \kappa^2} + F_m(\overline{w_x}, \kappa, \overline{\sigma_e}) - F_w(\overline{w_x}, \kappa, \overline{\sigma_e}), \qquad (2.69)$$

and

$$F_m(\overline{w_x}, \kappa, \overline{\sigma_e}) = \frac{1}{4\pi^2 N_f} \int_{-\infty}^{\infty} dy \Bigg[\frac{g_1(\overline{\sigma_e} + |y|)(-2y^2 - 3) - \overline{w_x}\sqrt{1+y^2}|y|}{(1+y^2)^2 \left[\sqrt{1+y^2}(g_1^2 + \kappa^2)(\overline{\sigma_e} + |y|) + g_1\,\overline{w_x}\,|y| \right]}$$

$$+ \frac{(\overline{\sigma_e} + |y|)\left(\sqrt{1+y^2}(g_1^2 - \kappa^2)(\overline{\sigma_e} + |y|) + g_1\overline{w_x}|y| \right)}{2(1+y^2)\left[\sqrt{1+y^2}(g_1^2 + \kappa^2)(\overline{\sigma_e} + |y|) + g_1\overline{w_x}|y| \right]^2} \Bigg].$$

$$(2.70)$$

To simplify the above expressions, we have ignored terms that arise from the screening of the g_0, g_j disorders (see Appendix 2.C); our detailed analysis below includes such effects whenever relevant. The gauge coupling $g/\sqrt{N_f}$ is marginal once the large N_f effective gauge field propagator in Fig. 2.2 is adopted and so its beta function is not included.

Let's make a few additional comments about these expressions.

1. In general, the above beta functions don't have an IR stable solution at $\overline{m} = 0$, even when disorder screening is included. In the remaining sections, we analyze cases for which we have found fixed points when a symmetry is present.

2. We've taken the variances to scale as $1/N_f$ for $N_f \to \infty$. The beta functions have terms that scale as $1/N_f$ and $1/N_f^2$. The "classical" contributions to the beta functions arising from the engineering dimensions of couplings scale as $1/N_f$; the "quantum" corrections generally scale as $1/N_f^2$. The exception to the latter appears in the third term in $\beta_{\overline{\Delta_0}}$ and the second term in $\beta_{\overline{\Delta_j}}$.

3. The first three beta functions $\beta_{\overline{w_x}}, \beta_{\overline{\sigma_e}}, \beta_{D_e}$ characterize the dissipative Coulomb interaction. In our analysis, we consider $z < 2$ and so the diffusion constant D_e is an irrelevant parameter that will be set to zero. A nonzero Coulomb interaction allows for two classes of fixed points: (1) a *f*inite Coulomb interaction either with $\overline{w_x}, \overline{\sigma_e} \neq 0$ and $z = 1$ or with $\overline{w_x} = \overline{\sigma_e} = 0$ and z determined by Eq. (2.57); (2) an *in*finite Coulomb interaction with $\overline{w_x} \to \infty, \overline{\sigma_e} \to \infty$, and $1 < z < 2$ that is controlled by the dissipation parameter $\overline{\sigma_e}/\overline{w_x}$.

4. Whenever two of the three disorder variances g_m, g_0, g_j are considered, the third variance is radiatively generated. When all three variances

g_m, g_0, g_j are present, both types of topological disorder Δ_0, Δ_j are generated. This is consistent with the symmetry assignments in Table 2.1.

Finite Coulomb Interaction

No Disorder

In the absence of any disorder, the only nontrivial beta functions are associated to the Coulomb interaction,

$$\beta_{\overline{w_x}} = -\overline{w_x}\, F_w(\overline{w_x}, \kappa, \overline{\sigma_e}). \tag{2.71}$$

Since $\frac{1}{\overline{\sigma_e}}\beta_{\overline{\sigma_e}} = \frac{1}{\overline{w_x}}\beta_{\overline{w_x}}$, it's sufficient to consider the behavior of $\overline{w_x}$ when studying a finite Coulomb interaction. The integral that defines F_w in Eq. (2.59) can only be evaluated numerically for general $\overline{\sigma_e}$. We've found that F_w is positive for any κ when $\overline{w_x} \neq 0$. Consequently, the clean fixed point with $\overline{w_x} = \overline{\sigma_e} = 0$ is perturbatively stable to the addition of a Coulomb interaction and $z = 1$. Two examples for the behavior of $\beta_{\overline{w_x}}$ are displayed in Fig. 2.3.
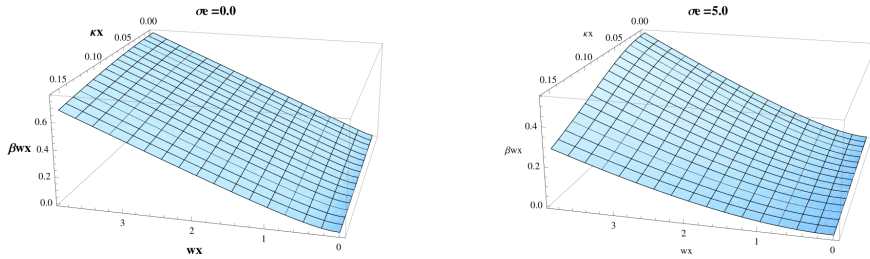
Figure 2.3: $\beta_{\overline{w_x}}$ as a function of $\overline{w_x}$ and κ

In particular, in the limit of $\overline{\sigma_e} = 0$ the beta function for $\overline{w_x}$ is always negative for any Chern-Simons coupling κ. This result should be contrasted with earlier work [82] where a critical value of $|\kappa|$ was reported above which the Coulomb interaction was found to be relevant.[12] As a check on our calculation, we find the mass anomalous dimension is given by

$$\gamma_{\bar\psi\psi} = \frac{128}{3\pi^2 N_f}\frac{1 - 512\kappa^2}{(1 + 256\kappa^2)^2} \tag{2.72}$$

in agreement with [13, 64, 15, 40] for general κ. For the IQHT ($\kappa = 0$), $\nu^{-1} \approx 1 - 4.3/N_f$; for the SIT ($\kappa = 1/4\pi$), $\nu^{-1} \approx 1 + 1.4/N_f$.

---

[12]The discrepancy seems to arise from assigning the Chern-Simons coupling κ an engineering dimension proportional to $\epsilon = 2 - D$. This choice, which appears to be inconsistent with the scaling of the effective gauge field propagator in the large N_f expansion, results in additional derivatives with respect to κ in the beta function in (2.52).

$\mathcal{C}$ Symmetry

According to Table 2.1, the Coulomb couplings and random mass disorder (g_m) are allowed when there is charge-conjugation symmetry. The beta functions are

$$\beta_{\overline{w_x}} = \overline{w_x}\left(\overline{g_m} - F_w(\overline{w_x}, \kappa, \overline{\sigma_e})\right), \tag{2.73}$$

$$\beta_{\overline{g_m}} = -2\overline{g_m}\left(\overline{g_m} + F_m(\overline{w_x}, \kappa, \overline{\sigma_e})\right), \tag{2.74}$$

where F_w and F_m are defined in Eqs. (2.59) and (2.70). The flow of the random mass is controlled by the mass anomalous dimension $\gamma_{\bar{\psi}\psi} = 2\overline{g_m} - F_w(\overline{w_x}, \kappa, \overline{\sigma_e}) + F_m(\overline{w_x}, \kappa, \overline{\sigma_e})$. Within the large N_f approximation, random mass disorder is only a relevant perturbation to the clean fixed point of the previous section $(\overline{w_x} = \overline{\sigma_e} = 0)$ when $\gamma_{\bar{\psi}\psi} < 0$, i.e., when $1 < 512\kappa^2$ (see Eq. (2.72)), in agreement with [73]. The presence of a Coulomb interaction does not appear to alter this conclusion within our analysis. For $\kappa = 1/4\pi$ (or any $\kappa^2 > 1/512$), there exists a line of fixed points with finite disorder and Coulomb interaction parameterized by $\overline{\sigma_e}$. Fig. 2.4 shows a few examples of this behavior. Since $\beta_{\overline{w_x}} \propto z - 1$ and $\beta_{\overline{g_m}} \propto -\gamma_{\bar{\psi}\psi}$ when $z = 1$, any fixed point
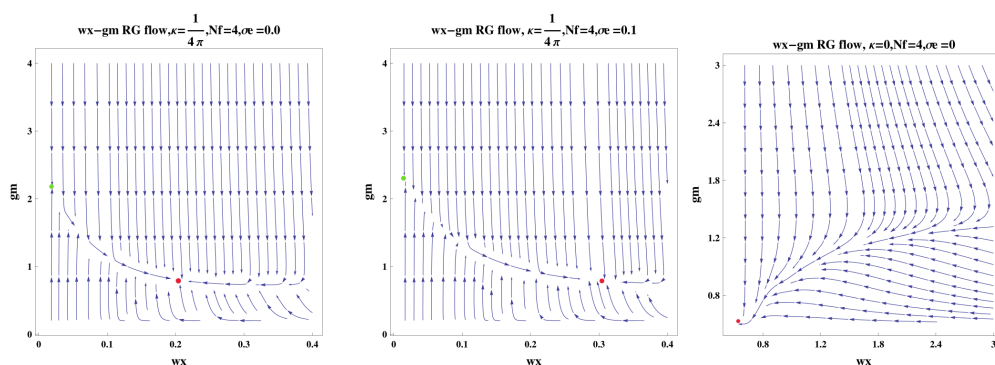
Figure 2.4: RG flow of w_x vs. g_m.

with finite disorder and Coulomb interaction has

$$\nu^{-1} = z = 1. \tag{2.75}$$

At the (generally unstable) fixed point with nonzero random mass disorder and vanishing Coulomb interaction,

$$\nu^{-1} = 1 \quad \text{and} \quad z = 1 - \frac{128}{3\pi^2 N_f}\frac{1 - 512\kappa^2}{(1 + 256\kappa^2)^2}, \tag{2.76}$$

where $\kappa^2 > 1/512$. For $\kappa = 1/4\pi$, $z \approx 1 + 1.4/N_f$.

It's interesting to compare our results for the critical exponents with recent analytic and numerical studies of the dirty XY model. In a large N_f expansion [27] report $\nu = 1$ and $z = 1 + .5/N_f$; numerics [75] directly probes $N_f = 1$ with the result $\nu = 1.16(5)$ and $z = 1.52(3)$. In [28], a finite disorder fixed point of quantum electrodynamics without Chern-Simons term was found using an ϵ expansion about $(3+1)$d. Since our approximation schemes are different, there is no contradiction with our conclusion that random mass disorder is irrelevant when $\kappa = 0$. Nevertheless, it would be interesting to consider this issue further.

$\mathcal{CT}$ Symmetry

According to Table 2.1, the Coulomb coupling, random scalar potential g_0, and topological disorder Δ_j are allowed by $\mathcal{CT}$ symmetry. Because a nonzero Chern-Simons term is odd under time-reversal symmetry, we only consider $\kappa = 0$ in the next two subsections that study $\mathcal{CT}$ and $\mathcal{T}$ preserving disorder. The beta functions are

$$\beta_{\overline{w_x}} = \overline{w_x}\left(\overline{g_0}(1 - \phi_1) - F_w(\overline{w_x}, \kappa = 0, \overline{\sigma_e})\right), \tag{2.77}$$

$$\beta_{\overline{g_0}} = \frac{2\overline{g_0}}{\overline{w_x}}\beta_{\overline{w_x}}, \tag{2.78}$$

$$\beta_{\overline{\Delta_j}} = 0, \tag{2.79}$$

where ϕ_1 isolates any terms that arise from the screening of the disorder: $\phi_1 = 0$ means disorder screening is ignored; $\phi_1 = 1$ means that disorder screening is included. While we're unaware of a general reason to exclude disorder screening, we'll discuss the behavior of the above beta functions both with and without screening to illustrate its effect.

As mentioned previously, F_w in Eq. (2.59) is positive for any κ when $\overline{w_x}$ is nonzero; in particular when $\overline{\sigma_e} = 0$, $F_w(\overline{w_x}, 0, 0)$ is a monotonically increasing function that approaches $\frac{8}{N_f\pi^2}$ for $\overline{w_x} \to \infty$. When disorder screening is ignored ($\phi_1 = 0$), there is a fixed surface defined by $\overline{g_0} = F_w$, which is parameterized by $(\overline{w_x}, \overline{g_0}, \overline{\Delta_j})$, in agreement with [73]. This fixed surface is unstable, e.g., consider perturbation to $\overline{g_0}$ at fixed $\overline{w_x}$ and $\overline{\Delta_j}$. When disorder screening is included ($\phi_1 = 1$), there is a line of stable fixed points parameterized by $(\overline{w_x}, \overline{g_0}, \overline{\Delta_j}) = (0, 0, \overline{\Delta_j})$. This result is consistent with [28]. This behavior

is illustrated in Fig. 2.5. The corresponding critical exponents at the stable
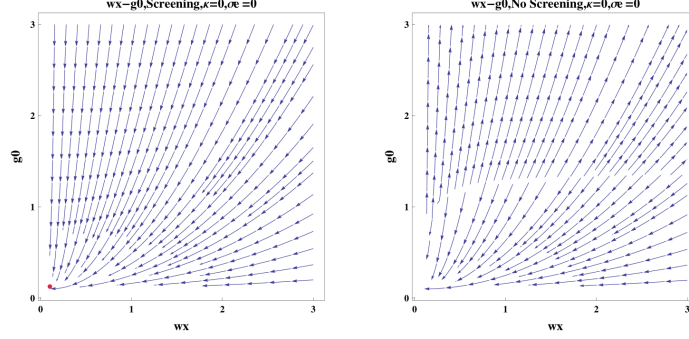
Figure 2.5: RG flow of $\overline{w_x}$ vs. $\overline{g_0}$.

fixed point ($\phi_1 = 1$) reduce to those of the clean theory without Coulomb interactions. Recall that g_0 and Δ_j disorders are generated by random electrical vector potential $A_j(\mathbf{x})$ in the free Dirac fermion dual at $N_f = 1$ for which a line of diffusive fixed points was found in [52]. It's unclear to what extent the line of fixed points parameterized by Δ_j is related.

If $\mathcal{C}T$ and $\mathcal{T}$ are emergent symmetries of the SIT theory we consider, then the beta functions should only have fixed point solutions respecting these symmetries at $\kappa = 1/4\pi$. Unfortunately, the leading terms in the large N_f beta functions don't produce any such nontrivial fixed points. Even if $\overline{g_m}$ is initially tuned to zero, the random mass beta function receives a positive correction from disorder screening equal to

$$\delta\beta_{\overline{g_m}} = \frac{8\overline{g_0}^2 g_1^2 \kappa^4}{(g_1^2 + g_1\overline{w_x} + \kappa^2)^4}. \tag{2.80}$$

Nonzero $\overline{g_0}$ and $\overline{g_m}$ then results in the generation of all couplings, for which we find runaway flow.

$\mathcal{T}$ Symmetry

According to Table 2.1, the Coulomb coupling, random vector potential g_j, and topological disorder Δ_0 are allowed by $\mathcal{T}$ symmetry. The beta functions are

$$\beta_{\overline{w_x}} = \overline{w_x}\left(2\overline{g_j}\left(1 - \phi_1\frac{g_1(g_1 + 2\overline{w_x})}{(g_1 + \overline{w_x})^2}\right) - F_w(\overline{w_x}, \kappa = 0, \overline{\sigma_e})\right), \tag{2.81}$$

$$\beta_{\overline{g_j}} = 0, \tag{2.82}$$

$$\beta_{\overline{\Delta_0}} = \frac{2\overline{\Delta_0}}{\overline{w_x}}\beta_{\overline{w_x}}, \tag{2.83}$$

where we continue to use ϕ_1 to isolate terms that arise from the screening of the disorder.

If screening is ignored ($\phi_1 = 0$), there is a surface of fixed points defined by $2\overline{g_j} = F_w(\overline{w_x}, 0, \overline{\sigma_e})$ and parameterized by $(\overline{w_x}, \overline{g_j}, \overline{\Delta_0})$ with $\overline{g_j} < 4/N_f\pi^2$ and non-negative $\overline{\Delta_0}$. On this surface $z = 1$ and $\nu^{-1} = 1 + 2\overline{g_j} - \frac{\overline{g_j}}{g_1} - F_m(\overline{w_x}, 0, \overline{\sigma_e})$; F_m is a monotonically decreasing function of $\overline{w_x}$ when $\kappa = \overline{\sigma_e} = 0$: $\frac{128}{3\pi^2 N_f} \geq F_m(\overline{w_x}) \geq -\frac{8}{\pi^2 N_f}$. For fixed $\overline{g_j}$, this surface is stable to small deformation by $\overline{w_x}$ since F_w is an increasing function of $\overline{w_x}$. For $\overline{g_j} > 4/N_f\pi^2$, we find runaway flows. This behavior is shown in Fig. 2.6. If screening is included ($\phi_1 = 1$),
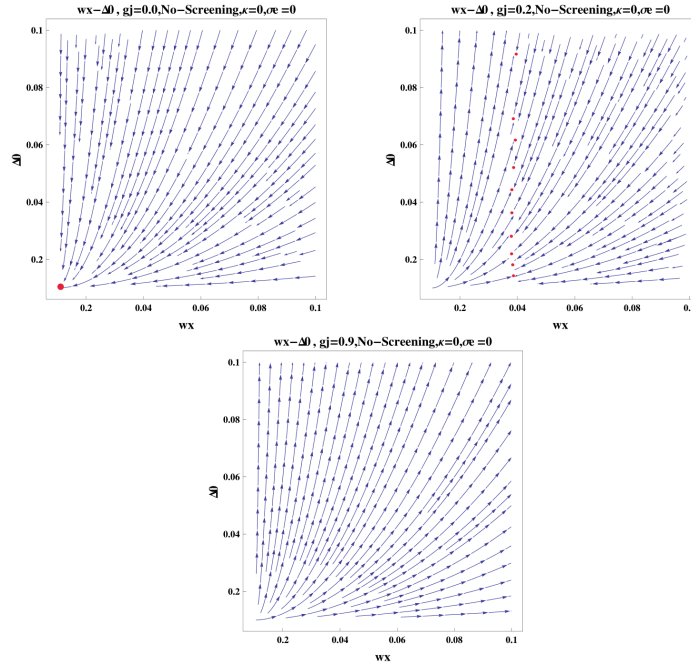
Figure 2.6: RG flow of $\overline{w_x}$ vs. $\overline{\Delta_0}$.

the fixed points are determined by the equation,

$$\overline{g_j}^* = \frac{F_w(\overline{w_x})}{2[1 - \phi_1 \frac{g_1(g_1 + 2\overline{w_x})}{(g_1 + \overline{w_x})^2}]} \equiv f_s(\overline{w_x}) \tag{2.84}$$

where $f_s(\overline{w_x})$ monotonically decreases from $f_s(\overline{w_x} = 0) = \infty$ to $f_s(\overline{w_x} \to \infty) = \frac{4}{N_f\pi^2}$. If $\overline{g_j}$ is chosen to be smaller than $\frac{4}{N_f\pi^2}$, then the RG flows to $(\overline{w_x}^*, \overline{\Delta_0}^*) = (0,0)$ because $\beta_{\overline{w_x}}$ is nonnegative and only vanishes when $\overline{w_x} = 0$. If $\overline{g_j} > \frac{4}{N_f\pi^2}$, then there exists a finite value of $\overline{w_x}$ for which the beta function vanishes, however, the resulting fixed point is IR unstable.

Infinite Coulomb Interaction

Dissipation has played only a minor role in the above analysis. We'll now discuss how dissipation allows for fixed points with $z \neq 1$ in the presence of a nonzero Coulomb interaction [70].

The runnings of the Coulomb interaction parameters $\overline{w_x}$ and $\overline{\sigma_e}$ are determined by their engineering dimensions, which are both equal to $z - 1$ (see Eqs. (2.60) and (2.61)), in the large N_f expansion. Any situation with nonzero Coulomb interaction and $z > 1$ necessarily requires $\overline{w_x}$ and $\overline{\sigma_e}$ individually flowing to strong coupling. Note, however, that it is their dimensionless ratio $\overline{\sigma_e}/\overline{w_x}$ that appears in the action S_E in the limit $\overline{w_x}, \overline{\sigma_e} \to \infty$. Consequently, we can parameterize this infinite Coulomb interaction limit with the marginal parameter $\alpha = \overline{\sigma_e}/\overline{w_x}$. We refer to α as the dissipation strength. $z > 1$ is required for any fixed point with infinite Coulomb interaction to be IR attractive; treating α as a tuning parameter, we'll view any infinite Coulomb interaction fixed point with $0 < z < 1$ as an IR unstable fixed point.

For $\overline{w_x} \to \infty$, F_w in (2.59) reduces to

$$F_\infty(\kappa, \alpha) \equiv \int_{-\infty}^{\infty} dy \frac{g_1 \sqrt{1+y^2}(-1+2y^2)\alpha + (1+y^2)|y|}{4\pi^2 N_f (1+y^2)^{\frac{5}{2}} \left(\sqrt{1+y^2}(g_1^2 + \kappa^2)\alpha + g_1 |y| \right)} \quad (2.85)$$

For any κ and $\alpha \geq 0$, $0 \leq F_\infty(\kappa, \alpha) \leq \frac{8}{N_f \pi^2}$. In this limit, the dynamical critical exponent at infinite Coulomb coupling is

$$z_\infty = 1 + \overline{g_m} + \overline{g_0} + 2\overline{g_j} - \phi_1 \overline{g_0} - F_\infty(\kappa, \alpha), \quad (2.86)$$

where we've explicitly indicated how screening appears in z_∞.

$\mathcal{C}$ Symmetry

At infinite Coulomb coupling and in the presence of charge-conjugation symmetry, there exist nontrivial fixed points for any κ. These occur at small values of $\overline{g_m}$ and are found by solving $\beta_{\overline{g_m}} = 0$ from (2.64) using Eq. (2.86):

$$\begin{aligned}
\overline{g_m}^*(\alpha) &= F_m(\alpha, \kappa) \\
&\equiv \int_{-\infty}^{\infty} dy \frac{\sqrt{1+y^2}\,|y| + g_1 \alpha\,(3 + 2y^2)}{4N_f \pi^2 (1+y^2)^2 \left[g_1|y| + \alpha \sqrt{1+y^2}(g_1^2 + \kappa^2) \right]} \\
&\quad - \frac{\alpha \left[g_1 \sqrt{1+y^2}\,|y| + (1+y^2)(g_1^2 - \kappa^2)\,\alpha \right]}{8N_f \pi^2 (1+y^2)^{\frac{3}{2}} \left[g_1|y| + \alpha \sqrt{1+y^2}(g_1^2 + \kappa^2) \right]^2}.
\end{aligned} \quad (2.87)$$
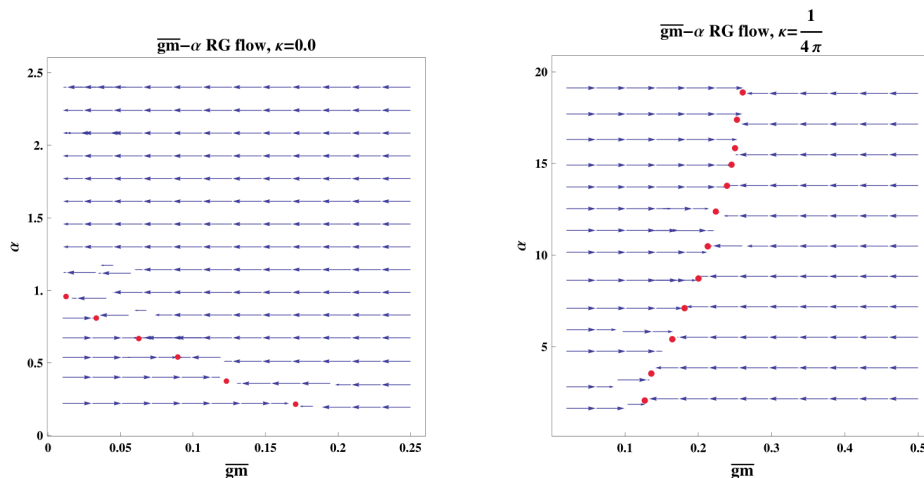
Figure 2.7: RG flow of α vs. $\overline{g_m}$. The dissipation parameter α is exactly marginal, so it's a free parameter that can be tuned.

Fig. (2.7) shows the behavior of the renormalization group flows for $\kappa = 0$ and $\kappa = 1/4\pi$.

Note that the beta functions for $\overline{w_x} \to \infty$ are different from the case of finite $\overline{w_x}$, even when $\alpha = 0$: nontrivial fixed points exist for any value of κ. The correlation length exponent $\nu^{-1} = 1$ because the fixed points are solved from $\beta_{\overline{g_m}} = 0$ (see Eq. (2.69)). The dynamical critical expoennt z_∞ is found using (2.86):

$$z_\infty(\alpha) = \overline{g_m}^*(\alpha) - F_\infty(\kappa, \alpha). \tag{2.88}$$

To guarantee the irrelevancy of the diffusion constant D_e of the 2DEG bath, $z_\infty < 2$ is required. Fortunately, z_∞ does not exceed two for the values of α we've considered—see Fig. (2.8).

$\mathcal{CT}$ Symmetry

As with finite Coulomb coupling, we focus on $\kappa = 0$ in this and the next subsection because the Chern-Simons term is odd under $\mathcal{CT}$ and $\mathcal{T}$.

In the $\overline{w_x} \to \infty$ limit, only $\beta_{\overline{g_0}} = 0$ is nontrivial:

$$2\overline{g_0}^2(-1 + \phi_1) + 2\,\overline{g_0}\,F_\infty(\kappa = 0, \alpha) = 0 \tag{2.89}$$

Including disorder screening ($\phi_1 = 1$), $\overline{g_0}$ is marginally irrelevant. If disorder screening is ignored, an unstable fixed point lies at $\overline{g_0}^* = F_\infty(\kappa = 0, \alpha)$.
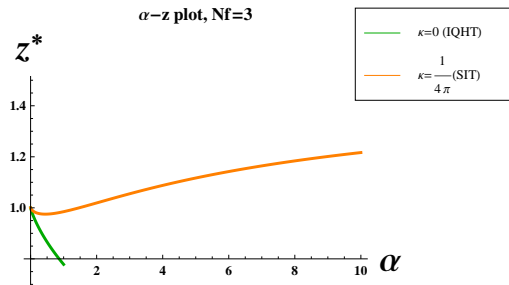
Figure 2.8: Dynamical critical exponent z_∞ versus effective dissipation strength α evaluated on the fixed points when $N_f = 3$. The green line corresponds to a $z_\infty < 1$, which is an unstable $\overline{w_x} \to \infty$ fixed point. When $\kappa = 1/4\pi$, $1 < z_\infty < 2$ for $\alpha \geq 1.47$.

Perturbation by $\overline{g_0}$ about this fixed point results either in flow (along the $\overline{g_0}$ direction) towards strong coupling or towards the infinite Coulomb interaction clean fixed point with critical exponents:

$$z_\infty(\alpha) = 1 - F_\infty(\kappa = 0, \alpha) < 1, \tag{2.90}$$

$$\nu^{-1} = 1 - F_m(\alpha, \kappa = 0). \tag{2.91}$$

Since $z_\infty < 1$, these infinite Coulomb coupling fixed points are IR unstable. This renormalization group flow is shown in Fig. 2.9.
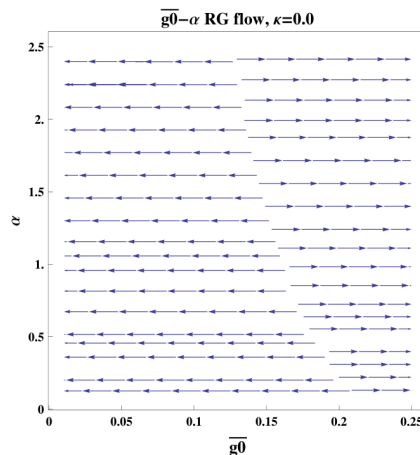
Figure 2.9: The RG flow of $\overline{g_0}$ with respect to α.

$\mathcal{T}$ Symmetry

When time-reversal symmetry is preserved and $\kappa = 0$, the only nontrivial beta function is $\beta_{\overline{\Delta_0}}$. In the limit of strong Coulomb coupling, the disorder

screening terms vanish. Solving $\beta_{\overline{\Delta_0}} = 0$ gives the condition

$$\overline{g_j}^* = \frac{1}{2}F_\infty(\alpha, \kappa = 0) \tag{2.92}$$

on the marginal couplings $\overline{g_j}$ and α. The resulting fixed point is IR unstable along the $\overline{\Delta_0}$ direction and, depending on the values of $\overline{g_j}$ and α, flows either to strong coupling or to zero when perturbed about this fixed point. This is shown in Fig. 2.10. Using Eq. (2.86), we see that $z_\infty = 1$ at the fixed
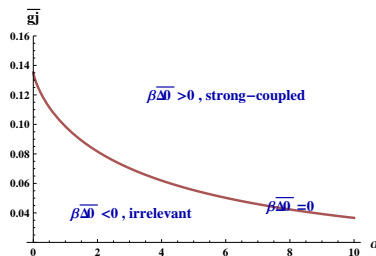
Figure 2.10: In the case of $\overline{w_x} \to \infty$, the fixed point solution for $\overline{\Delta_0}$ is obtained by tuning $\overline{g_j}$ and α so as to sit on the curve above.

point defined by $\beta_{\overline{\Delta_0}} = 0$. The correlation length exponent is given by $\nu^{-1} = 1 + 2\overline{g_j} - F_m(\alpha, \kappa = 0) - \frac{\overline{g_j}}{g_1} = 1 - 7F_\infty(\alpha, \kappa = 0) - F_m(\alpha, \kappa = 0)$, where the second equality is obtained after evaluating on the fixed point defined by Eq. (2.92).

2.4 Discussion

In this paper, we studied the influence of quenched disorder and a dissipative Coulomb interaction on two different quantum phase transitions: an integer quantum Hall transition (IQHT) and a superconductor-insulator transition (SIT). We considered both transitions using effective theories that consist of a Dirac fermion coupled to a $U(1)$ Chern-Simons gauge field at level $(\theta - 1/2)$: $\theta = 1/2$ corresponds to the IQHT, while $\theta = 1$ corresponds to the SIT. We performed a renormalization group analysis using a large N_f expansion in which the number fermion flavors $N_f \to \infty$ to study the critical properties of these theories. We found both theories to be stable to the addition of a Coulomb interaction. The IQHT was stable to $\mathcal{C}$ preserving disorder and exhibited a line of diffusive fixed points with $\mathcal{C}T$ disorder. ($\mathcal{C}$ is charge-conjugation symmetry and $\mathcal{T}$ is time-reversal symmetry.) The SIT exhibited a line of fixed points parameterized by the Coulomb coupling when $\mathcal{C}$ is preserved. Other cases resulted in runaway flow.

Without disorder, the free Dirac fermion in (2.1) has a correlation length exponent $\nu_{\mathrm{Dirac}}^{-1} = 1$, while the 3d XY model in (2.3) has a correlation length exponent $\nu_{\mathrm{Bose}}^{-1} \approx 3/2$. In the large N_f expansion, we find $\nu^{-1}(\theta = 1/2) \approx 1 - 4.3/N_f$ and $\nu^{-1}(\theta = 1) \approx 1 + 1.4/N_f$, in agreement with [13, 64, 15, 40]. Evidently the leading order term in the large N_f expansion provides a poor approximation to the critical exponents of the clean fixed points [13]. Comparing our results ($\nu^{-1} = 1, z = 1 + 1.4/N_f$) for the correlation length and dynamical critical exponents with recent numerical ($\nu \approx 1.2, z \approx 1.5$) [63, 61, 55, 75] and analytic ($\nu = 1, z \approx 1 + .5/N_f$) [27] studies (without a Coulomb interaction) suggests this may also be the case for the dirty 3d XY model. Higher-order $\mathcal{O}(1/N_f^2)$ terms may improve the comparison. Interestingly, the free Dirac fermion and 3d XY model admit duals involving a Dirac fermion coupled to a *n*on-Abelian $U(N)$ Chern-Simons gauge field for any $N > 1$ [35, 39]. Such formulations suggest alternative approximation schemes. For instance, without disorder, these theories have a correlation length exponent equal to unity at 2-loop order in the planar limit [26]. Might the planar limit furnish better approximations to such theories, compared with the large N_f expansion?

There are a variety of other observables and generalizations to consider. For example, scaling dimensions of the lowest dimension monopole operators in the Chern-Simons theories we studied should correspond to the η exponents of the Dirac and XY models. In $(2+1)$d, the dc $T \to 0$ conductivity tensor can be universal [22, 18]; it would be interesting to calculate and compare across the duality [29]. Perhaps considering the effects of finite density is most pressing, given that the electronic systems inspiring this work have a finite density of states.

One of the motivations of the current work was to better understand the emergent symmetries that are found at IQHTs and SITs via electrical transport experiments. For concreteness, consider the magnetic field-tuned SIT at which a "self-duality"[13] with dc $\sigma_{xx} \approx (2e)^2/h$ and $\sigma_{xy} \approx 0$ is found at low temperatures [10]. It was argued in [58] that PV symmetry (see §5.27) of the "fermionic dual" to the XY model in 2.7 results in self-dual transport. How this symmetry might be preserved quantum mechanically is unclear [34]. This question is related to the emergent time-reversal symmetry of this "fermionic

---

[13]"Self-duality" requires that the electrical conductivity tensor of the 3d XY model satisfy: $\sigma_{xx}^2 + \sigma_{xy}^2 = (e_*^2/h)^2$, where e_* is the electromagnetic charge of the bosons [21].

dual" at zero Dirac composite fermion density. Perhaps unsurprisingly, the leading order large N_f beta functions that we studied do not appear to respect the emergent time-reversal symmetry; at least, we haven't found nontrivial solutions with an emergent time-reversal invariance at $\kappa = 1/4\pi$. It would be interesting to further understand this apparent shortcoming.

APPENDIX

2.A Calculation Overview

In this appendix we derive the residues $b_{\lambda_a}(\vec{\lambda}^R(\mu,\epsilon))$ in Eq. (2.47),

$$\lambda_a^B \mu^{-\Delta_a(\epsilon)} = \lambda_a^R(\mu,\epsilon) + \frac{b_{\lambda_a}(\vec{\lambda}^R(\mu,\epsilon))}{\epsilon}, \tag{2.93}$$

that determine the beta functions at $\epsilon = 0$ via Eq. (2.52):

$$\beta_{\lambda_a}(\vec{\lambda}^R) \equiv -\mu \frac{\partial \lambda_a^R}{\partial \mu} = \bar{\Delta}_{\lambda_a} \lambda_a^R + \rho_{\lambda_a} b_{\lambda_a}(\vec{\lambda}^R) - \sum_c \rho_{\lambda_c} \lambda_c^R \frac{\partial b_{\lambda_a}(\vec{\lambda}^R)}{\partial \lambda_c^R}. \tag{2.94}$$

After establishing notation, we'll list the main results used in the main text. Later sections provide algebraic details.

Setup

Identify S_E in Eqs. (2.42) - (2.44) with the bare action S_B by endowing all fields and couplings with bare (B) subscripts/superscripts. To simplify notation, we'll leave replica and flavor indices implicit. Define renormalized (R) fields and couplings,

$$\psi_B = Z_f^{1/2} \psi_R, \quad a_B^0 = Z_{a,0}^{1/2} a_R^0, \quad a_B^j = Z_{a,j}^{1/2} a_R^j, \quad \lambda_c^B = Z_c^{-1/2} \lambda_c^R \tag{2.95}$$

where the vector of couplings (either B or R)

$$\vec{\lambda} = \left(\frac{g^2}{N_f}, v, m, \kappa, w_x, \sigma_e, D_e, g_m, g_0, g_j, \Delta_0, \Delta_j \right)^T. \tag{2.96}$$

Separate S_B into physical and counterterm actions:

$$S_B = S_{\text{phys}}^{(1)} + S_{\text{phys}}^{(2)} + S_{\text{phys}}^{(3)} + S_{\text{CT}}^{(1)} + S_{\text{CT}}^{(2)} + S_{\text{CT}}^{(3)} \tag{2.97}$$

with

$$S_{\text{phys}}^{(1)} = \int d\tau d^D x \Big[\bar{\psi}_R \Big(\gamma_\tau (\partial^\tau + i \frac{g_R \mu^{\epsilon/2}}{\sqrt{N_f}} a_R^\tau) + v_R \mu^{z-1} \gamma_j (\partial^j + i \frac{g_R \mu^{\epsilon/2}}{\sqrt{N_f}} a_R^j) \Big) \psi_R$$

$$+ \mu^z m_R \bar{\psi}_R \psi_R + \frac{i \kappa_R}{2} a_R d a_R \Big], \tag{2.98}$$

$$S_{\text{phys}}^{(2)} = \int d\omega d^D k \, \frac{w_R \mu^{z-1}}{2} a_R^T(-\omega,-k) \frac{k^2}{|k| + f_R(\omega,k)} a_R^T(\omega,k), \tag{2.99}$$

$$S_{\text{phys}}^{(3)} = -\frac{1}{2} \int d\tau d\tau' d^D x \Big[(g_m)_R \mu^{2z-D} (\bar{\psi}_R \psi_R)(\bar{\psi}_R \psi_R) + (g_0)_R \mu^{2z-D} (\bar{\psi}_R \gamma^0 \psi_R)(\bar{\psi}_R \gamma^0 \psi_R)$$

$$+ (g_j)_R \mu^{2z-D} (\bar{\psi}_R \gamma^j \psi_R)(\bar{\psi}_R \gamma^j \psi_R) + (\Delta_0)_R \mu^{2z-2} b_R b_R + (\Delta_j)_R \mathbf{e}_R \cdot \mathbf{e}_R \Big] \tag{2.100}$$

$$S_{\mathrm{CT}}^{(1)} = \int d\tau d^D x \Big[\bar{\psi}_R \Big(\gamma_\tau (\partial^\tau + i \frac{g_R \mu^{\epsilon/2}}{\sqrt{N_f}} a_R^\tau) \delta_1 + v_R \mu^{z-1} \gamma_j (\partial^j + i \frac{g_R \mu^{\epsilon/2}}{\sqrt{N_f}} a_R^j) \delta_2 \Big) \psi_R$$
$$+ \mu^z m_R \bar{\psi}_R \psi_R \delta_m + \frac{i\kappa_R}{2} a_R d a_R \delta_\kappa \Big],$$

$$(2.101)$$

$$S_{\mathrm{CT}}^{(2)} = \int d\omega d^D k \; \frac{w_R \mu^{z-1} \delta_w}{2} a_R^T(-\omega, -k) \frac{k^2}{|k| + f_R(\omega, k)} a_R^T(\omega, k), \qquad (2.102)$$

$$S_{\mathrm{CT}}^{(3)} = -\frac{1}{2} \int d\tau d\tau' d^D x \Big[(g_m)_R \mu^{2z-D} \delta_{g_m} (\bar{\psi}_R \psi_R)(\bar{\psi}_R \psi_R) + (g_0)_R \mu^{2z-D} \delta_{g_0} (\bar{\psi}_R \gamma^0 \psi_R)(\bar{\psi}_R \gamma^0 \psi_R)$$
$$+ (g_j)_R \mu^{2z-D} \delta_{g_j} (\bar{\psi}_R \gamma^j \psi_R)(\bar{\psi}_R \gamma^j \psi_R) + (\Delta_0)_R \mu^{2z-2} \delta_{\Delta_0} b_R b_R + (\Delta_j)_R (2.103) e_R \Big],$$

$$f_R = \frac{e_*^2 (\sigma_e)_R \mu^{z-1}}{|\omega| + (D_e)_R \mu^{z-2} k^2}, \qquad (2.104)$$

and the renormalization group scale μ enters in accord with the engineering dimensions listed in Table 2.2. The counterterms δ_X have poles in ϵ with coefficients determined by the requirement that correlation functions of physical fields have no divergences as $\epsilon \to 0$. We focus exclusively on the terms in δ_X proportional to $1/\epsilon$. Using Eq. (2.95) to impose Eq. (2.97), we relate the bare and renormalized couplings:

$$v^B \mu^{1-z} = v^R (1 + \delta_2 - \delta_1), \qquad (2.105)$$

$$m^B \mu^{-z} = m^R (1 + \delta_m - \delta_1), \qquad (2.106)$$

$$\kappa^B = \kappa^R (1 + \delta_\kappa), \qquad (2.107)$$

$$w_x^B \mu^{1-z} = w_x^R (1 + \delta_w), \qquad (2.108)$$

$$g_X^B \mu^{D-2z} = g_X^R (1 - 2\delta_1 + \delta_{gX}), \quad g_X \in \{g_m, g_0, g_j\}, \qquad (2.109)$$

$$\Delta_0^B \mu^{2-2z} = \Delta_0^R (1 + \delta_{\Delta_0}), \qquad (2.110)$$

$$\Delta_j^B = \Delta_j^R (1 + \delta_{\Delta_j}), \qquad (2.111)$$

$$\sigma_e^B \mu^{1-z} = \sigma_e^R (1 + \delta_{\sigma_e}), \qquad (2.112)$$

$$D_e^B = D_e^R (1 + \delta_D). \qquad (2.113)$$

$$(2.114)$$

Thus, we can read off the residues:

$$b_v = v^R(\delta_2 - \delta_1)\epsilon \tag{2.115}$$

$$b_m = m^R(\delta_m - \delta_1)\epsilon \tag{2.116}$$

$$b_\kappa = \kappa^R \delta_\kappa \epsilon \tag{2.117}$$

$$b_w = w_x^R \delta_w \epsilon \tag{2.118}$$

$$b_{g_X} = -g_X^R(2\delta_1 - \delta_{g_X})\epsilon, \quad g_X \in \{g_m, g_0, g_j\}, \tag{2.119}$$

$$b_{\Delta_X} = \Delta_X^R \delta_{\Delta_X} \epsilon, \quad \Delta_X \in \{\Delta_0, \Delta_j\}, \tag{2.120}$$

$$b_{\sigma_e} = \sigma_e^R \delta_\sigma \epsilon, \tag{2.121}$$

$$b_{D_e} = D_e^R \delta_D \epsilon. \tag{2.122}$$

2.B   Counterterms

As discussed in the main text, we choose the dynamical critical exponent z in such a way that the fermion velocity v does not run, i.e., the velocity beta function is zero. In the expressions below, it's convenient to redefine couplings to absorb the velocity dependence as follows:

$$\overline{g_m} = \frac{g_m}{2\pi v^2} \ , \ \overline{g_0} = \frac{g_0}{2\pi v^2} \ , \ \overline{g_j} = \frac{g_j}{2\pi v^2} \ , \ \overline{\Delta_0} = \Delta_0 \ , \ \overline{\Delta_j} = \Delta_j v^2 \ ,$$

$$\overline{w_x} = \frac{w_x}{v} \ , \ \overline{\sigma_e} = \frac{\sigma_e}{v} \ , \ \int_{-\infty}^{\infty} dz F(z) = \int_{-\infty}^{\infty} v \, dy \, F(y = \frac{z}{v}), \tag{2.123}$$

where the function $F(z)$ is introduced below. We also define $g_1 = g/16$ and $\overline{m} = m/v$.

Let us make a few remarks about the expressions below.

- We use ϕ_1 to parameterize the screening of the disorder described in Appendix 2.C. $\phi_1 = 0$ means the screening is ignored; $\phi_1 = 1$ means the screening is included.

- Terms proportional to ξ are divergent. However, this is an unphysical divergence due to our gauge choice: This divergence does not appear in physical quantities such as critical exponents.

- The Ward identity guarantees the gauge field corrections to δ_1 and δg_0 cancel; the ones in δ_2 and δ_{g_j} likewise cancel. In the absence of the Coulomb interaction, the equality of the gauge corrections in δ_1 and δ_2 is a coincidence, which makes β_{g_0}, β_{g_j} independent of the gauge corrections.

When the Coulomb interaction is included, β_{g_0} receives corrections from the gauge field, while β_{g_j} does not.

δ_κ, δ_w, δ_σ, and δ_D Counterterms

Quantization of the Chern-Simons level and finiteness of the gauge field self-energy in 3d implies

$$\delta_\kappa = \delta_w = \delta_\sigma = \delta_D = 0. \tag{2.124}$$

Consequently, renormalizations of κ, w_x, σ_e, and D_e are controlled by their engineering dimensions.

δ_1 Counterterm

The diagrams that contribute to δ_1 are given by taking the temporal component of Fig. 2.B.1:

$$\delta_1 \, \epsilon = -(\overline{g_m} + \overline{g_0} + 2\overline{g_j}) + \phi_1 \left[\frac{g_1^2 \overline{w_x} \, (g_1 \overline{g_j} - g_1 \overline{g_0} - \overline{g_0} \, \overline{w_x})}{(g_1^2 + g_1 \overline{w_x} + \kappa^2)^2} + \frac{g_1 \, (g_1 \overline{g_j} + g_1 \overline{g_0} + 2\overline{g_0} \, \overline{w_x})}{g_1^2 + g_1 \overline{w_x} + \kappa^2} \right]$$
$$+ \int_{-\infty}^{\infty} \frac{1}{4\pi^2 N_f} \frac{(1-y^2)(g_1 \, \overline{\sigma_e} \, y^2 + \overline{w_x} \sqrt{1+y^2} \, |y| \,) + g_1 \, |y| \, y^2 \, (1-y^2 \, \xi)}{(1+y^2)^2 \left[\sqrt{1+y^2} (g_1^2 + \kappa^2)(\overline{\sigma_e} + |y|) + g_1 \, \overline{w_x} \, |y| \right]}. \tag{2.125}$$

δ_2 Counterterm

The diagrams that contribute to δ_2 are given by taking the spatial component of Fig. 2.B.1:

$$\delta_2 \, \epsilon = -\phi_1 \frac{g_1^2 \left[g_1^2 \overline{g_j} + 2 g_1 \overline{g_j} \, \overline{w_x} - (\overline{g_0} - 2\overline{g_j}) \, \kappa^2 \right]}{(g_1^2 + g_1 \overline{w_x} + \kappa^2)^2}$$
$$+ \int_{-\infty}^{\infty} dy \, \frac{1}{4\pi^2 N_f} \frac{g_1 (1 - y^2 - y^4) \, \overline{\sigma_e} - (\overline{w_x} \, y^2 \sqrt{1+y^2}) \, |y| + g_1 (1 - y^2 - y^4 \xi) \, |y|}{(1+y^2)^2 \left[\sqrt{1+y^2} (g_1^2 + \kappa^2)(\overline{\sigma_e} + |y|) + g_1 \, \overline{w_x} \, |y| \right]}. \tag{2.126}$$
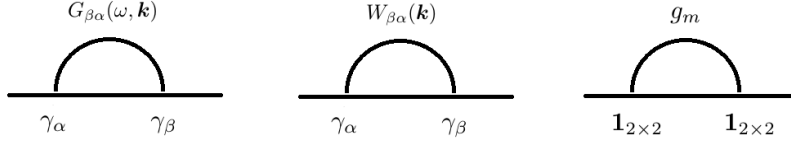
Figure 2.B.1: Diagrams contributing to δ_1, δ_2.
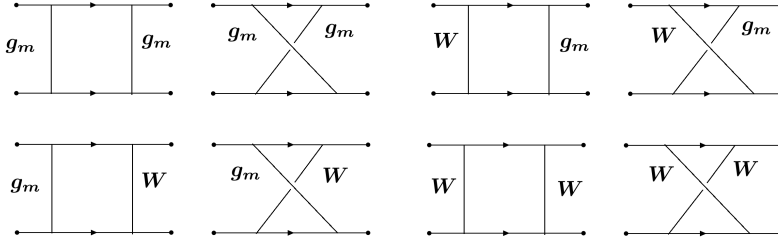
Figure 2.B.2: 2-PI diagrams contributing to $\delta_{g_m}, \delta_{g_0}, \delta_{g_j}$.

δ_{g_m} Counterterm

δ_{g_m} is extracted from the diagrams in Figs. 2.B.2 and 2.B.3:

$$\delta_{g_m}\epsilon = \left[\frac{2(\overline{g_0}+\overline{g_m})(\overline{g_m}-2\overline{g_j})}{\overline{g_m}} + 2\,\frac{g_1(\overline{g_j}-\overline{g_0})+\overline{g_j}\,\overline{w_x}}{g_1^2+g_1\,\overline{w_x}+\kappa^2}\right]$$

$$+\phi_1\left[4g_1\,\frac{g_1\kappa^2(-\overline{g_0}^2-\overline{g_j}^2)+\overline{g_j}\,\overline{g_0}\left[2g_1^3+4g_1^2\overline{w_x}+2\overline{w_x}\kappa^2+g_1(\overline{w_x}^2+4\kappa^2)\right]}{\overline{g_m}\left[g_1^2+g_1\,\overline{w_x}+\kappa^2\right]^2}\right]$$

$$+\phi_1\left[\frac{g_1^5(\overline{g_0}-\overline{g_j})+g_1^4\,\overline{w_x}\,(2\overline{g_0}-3\overline{g_j})+g_1^3\left(\overline{g_0}\,\overline{w_x}^2-2\overline{g_j}\,\overline{w_x}^2+3\overline{g_0}\,\kappa^2-3\overline{g_j}\,\kappa^2\right)}{\left[g_1^2+g_1\,\overline{w_x}+\kappa^2\right]^3}\right.$$

$$\left.+\frac{g_1^2\kappa^2(3\overline{g_0}\,\overline{w_x})+2g_1\kappa^4(\overline{g_j}-\overline{g_0})}{\left[g_1^2+g_1\,\overline{w_x}+\kappa^2\right]^3}\right]$$

$$+\phi_1\left[\frac{2g_1^4(\overline{g_j}-\overline{g_0})+4g_1^3\,\overline{w_x}(\overline{g_j}-\overline{g_0})+g_1^2(-2\overline{g_0}\,\overline{w_x}^2-6\overline{g_0}\kappa^2+6\overline{g_j}\,\kappa^2)-4g_1\,\overline{g_0}\,\overline{w_x}\,\kappa^2}{\left[g_1^2+g_1\,\overline{w_x}+\kappa^2\right]^2}\right]$$

$$+\phi_1^2\left[\frac{4g_1^2\overline{g_j}^2\kappa^2[g_1^2(g_1^2+2g_1\overline{w_x}-\overline{w_x}^2)+2g_1(g_1-\overline{w_x})\kappa^2-\kappa^4\,]}{\overline{g_m}[g_1^2+g_1\,\overline{w_x}+\kappa^2]^4}\right.$$

$$+\frac{4g_1^2\overline{g_0}^2\kappa^2[g_1^2(g_1^2+2g_1\overline{w_x}+\overline{w_x}^2)+2g_1(g_1+\overline{w_x})\kappa^2-\kappa^4]}{\overline{g_m}[g_1^2+g_1\,\overline{w_x}+\kappa^2]^4}$$

$$\left.+\frac{4\overline{g_0}\,\overline{g_j}g_1^2\left[-g_1^3(g_1+\overline{w_x})^2(g_1+2\overline{w_x})-2g_1^2(g_1+\overline{w_x})(2g_1+3\overline{w_x})\kappa^2-g_1(5g_1+2\overline{w_x})\kappa^4+2\kappa^6\right]}{\overline{g_m}[g_1^2+g_1\,\overline{w_x}+\kappa^2]^4}\right]$$

$$-\int_{-\infty}^{\infty}dy\,\frac{g_1(y^2+2)(1+y^2)\overline{\sigma_e}+\left(\overline{w_x}\,(1+y^2)\,\sqrt{1+y^2}+g_1(2+3y^2+y^4\xi)\right)|y|}{2\pi^2\,N_f\,(1+y^2)^2\left[\sqrt{1+y^2}(g_1^2+\kappa^2)(\overline{\sigma_e}+|y|)+g_1\,\overline{w_x}\,|y|\right]}$$

$$+\int_{-\infty}^{\infty}dy\,\frac{(\overline{\sigma_e}+|y|)\left((1+y^2)(g_1^2-\kappa^2)\,(\overline{\sigma_e}+|y|\,)+(g_1\,\overline{w_x}\,\sqrt{1+y^2})\,|y|\right)}{4\pi^2\,N_f\,(1+y^2)^{\frac{3}{2}}\left[\sqrt{1+y^2}(g_1^2+\kappa^2)(\overline{\sigma_e}+|y|)+g_1\,\overline{w_x}\,|y|\right]^2}\,. \tag{2.127}$$
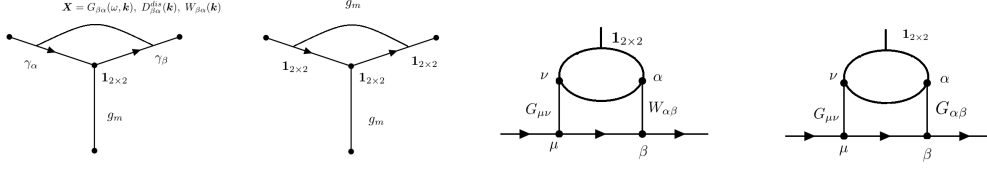
Figure 2.B.3: The mass vertex contributions to δ_{g_m}

δ_m Counterterm

δ_m is extracted from the diagrams in 2.B.3:

$$
\begin{aligned}
m\,\epsilon\,\delta_m ={}& \frac{1}{2} g_m\,\epsilon\left(\delta_{g_m} - [\text{2-PI boxes}]\right) \\
={}& \overline{g_0} - 2\overline{g_j} + \overline{g_m} - \frac{g_1(\overline{g_0} - \overline{g_j}) - \overline{g_j}\,\overline{w_x}}{2(g_1^2 + g_1\,\overline{w_x} + \kappa^2)} + \phi_1 \left(- \frac{g_1(\overline{g_0} - \overline{g_j}) + 3g_1(\overline{g_0} - \overline{g_j}) + 2\overline{g_0}\,\overline{w_x}}{g_1^2 + g_1\,\overline{w_x} + \kappa^2} \right. \\
& - g_1^2\,\frac{\overline{g_j}[4g_1^2 + 4\overline{w_x} + g_1(7 + 2\overline{w_x})\,] - \overline{g_0}[4g_1^2 + \overline{w_x}(7 + 2\overline{w_x}) + g_1(7 + 6\overline{w_x})]}{2(g_1^2 + g_1\,\overline{w_x} + \kappa^2)^2} \\
& - \left. \frac{-2g_1^3(g_1 + \overline{w_x})[-g_1\overline{g_j} + \overline{g_0}(g_1 + \overline{w_x})\,]}{(g_1^2 + g_1\,\overline{w_x} + \kappa^2)^3} \right) \\
& - \int_{-\infty}^{\infty} dy\, \frac{g_1(y^2 + 2)(1 + y^2)\,\overline{\sigma_e} + \left(\overline{w_x}\,(1 + y^2)\,\sqrt{1 + y^2} + g_1(2 + 3y^2 + y^4\xi)\right)|y|}{4\pi^2\,N_f\,(1 + y^2)^2\left[\sqrt{1 + y^2}(g_1^2 + \kappa^2)(\overline{\sigma_e} + |y|) + g_1\,\overline{w_x}\,|y|\right]} \\
& + \int_{-\infty}^{\infty} dy\, \frac{(\overline{\sigma_e} + |y|)\left((1 + y^2)(g_1^2 - \kappa^2)\,(\overline{\sigma_e} + |y|\,) + (g_1\,\overline{w_x}\,\sqrt{1 + y^2})\,|y|\right)}{8\pi^2\,N_f\,(1 + y^2)^{\frac{3}{2}}\left[\sqrt{1 + y^2}(g_1^2 + \kappa^2)(\overline{\sigma_e} + |y|) + g_1\,\overline{w_x}\,|y|\right]^2} ,
\end{aligned}
$$

$$(2.128)$$

where [2-PI boxes] refers to the contributions to δ_{g_m} from the diagrams in Fig. 2.B.2.

δ_{g_0} Counterterm

δ_{g_0} is extracted from the diagrams in Figs. 2.B.2 and 2.B.4:

$$\delta_{g_0}\epsilon = \frac{-2(\overline{g_0} + 2\overline{g_j})\,(\overline{g_0} + \overline{g_m})}{\overline{g_0}}$$

$$+\phi_1\Bigg[\frac{4g_1^2\,\overline{g_j}\,\overline{g_m}\,(g_1^2 + 2g_1\,\overline{w_x} + 2\kappa^2)}{\overline{g_0}\,[g_1^2 + g_1\,\overline{w_x} + \kappa^2]^2} + \frac{2g_1^2\big(g_1^2\overline{g_j} + 2g_1\overline{g_j}\,\overline{w_x} + (\overline{g_j} - 2\overline{g_m})\,\kappa^2\big)}{[g_1^2 + g_1\,\overline{w_x} + \kappa^2]^2}$$

$$+\frac{2\overline{g_0}g_1\,\big(g_1^3 + 2g_1^2\overline{w_x} + 2\kappa^2\,\overline{w_x} + g_1\overline{w_x}^2 + g_1\kappa^2\big)}{[g_1^2 + g_1\,\overline{w_x} + \kappa^2]^2}\Bigg]$$

$$+\int_{-\infty}^{\infty} dy\ \frac{g_1\,y^2(1 - y^2)\,\overline{\sigma_e} + g_1\,y^2(1 - y^2\,\xi)\,|y| + (1 - y^2)\,\overline{w_x}\sqrt{1 + y^2}\,|y|}{2\pi^2\,N_f\,(1 + y^2)^2\Big[\sqrt{1 + y^2}(g_1^2 + \kappa^2)(\overline{\sigma_e} + |y|) + g_1\,\overline{w_x}\,|y|\Big]}. \qquad (2.129)$$
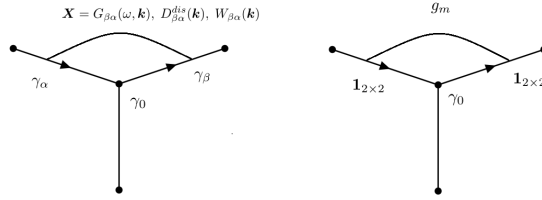
Figure 2.B.4: $\gamma_{\mu=0}$ vertex component contributions to δ_{g_0}
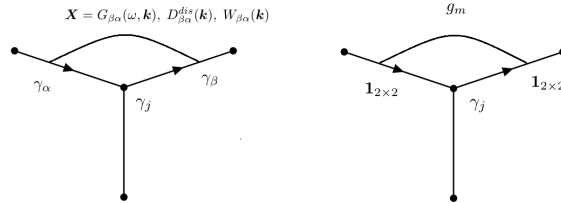
Figure 2.B.5: $\gamma_{\mu=j}$ vertex component contributions to δ_{g_j}

δ_{g_j} Counterterm

δ_{g_j} is extracted from the diagrams in Figs. 2.B.2 and 2.B.5:

$$\delta_{g_j}\epsilon = \frac{-2\overline{g_0}\,\overline{g_m}}{\overline{g_j}} + \phi_1\Bigg[\frac{2g_1^2(\overline{g_0} - \overline{g_m})\,\kappa^2}{[g_1^2 + g_1\,\overline{w_x} + \kappa^2]^2}\Bigg]$$

$$+\phi_1\Bigg[\frac{2g_1\,\overline{g_0}\,\overline{g_m}\Big(g_1^3 + 2g_1^2\,\overline{w_x} + 2\overline{w_x}\,\kappa^2 + g_1\overline{w_x}^2 + 2g_1\kappa^2\Big)}{[g_1^2 + g_1\,\overline{w_x} + \kappa^2]^2}\Bigg]$$

$$+\int_{-\infty}^{\infty} dy\,\frac{1}{2\pi^2 N_f}\frac{g_1(1 - y^2 - y^4)\,\overline{\sigma_e} - (\overline{w_x}\,y^2\sqrt{1 + y^2})\,|y| + g_1(1 - y^2 - y^4\xi)\,|y|}{(1 + y^2)^2\Big[\sqrt{1 + y^2}(g_1^2 + \kappa^2)(\overline{\sigma_e} + |y|) + g_1\,\overline{w_x}\,|y|\Big]} \qquad (2.130)$$
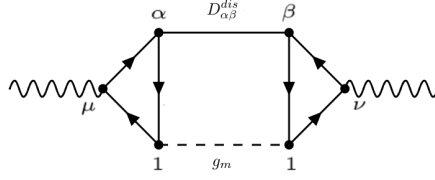
Figure 2.B.6: Diagrams contributing to $\delta_{\Delta_0}, \delta_{\Delta_j}$

δ_{Δ_0} Counterterm

δ_{Δ_0} is extracted from the diagram in Fig. 2.B.6:

$$\delta_{\Delta_0}\epsilon = \frac{-\overline{g_m}\,(g_1^2\,\overline{\Delta_j} + 2g_1\,\overline{w_x}\,\overline{\Delta_j} + \overline{w_x}^2\,\overline{\Delta_j} + \overline{\Delta_0}\,\kappa^2)}{64\overline{\Delta_0}\,(g_1^2 + g_1\,\overline{w_x} + \kappa^2)^2}$$
$$+\left[\frac{-\overline{g_0}\,\overline{g_m}N_f\,\pi\,v^2}{32\overline{\Delta_0}} + \phi_1\,\frac{g_1\overline{g_m}\,N_f\,\pi\,v^2[-g_1\overline{g_j}\kappa^2 + \overline{g_0}(g_1 + \overline{w_x})(g_1^2 + g_1\,\overline{w_x} + 2\kappa^2)]}{32\overline{\Delta_0}\,(g_1^2 + g_1\,\overline{w_x} + \kappa^2)^2}\right] \tag{2.131}$$

δ_{Δ_j} Counterterm

δ_{Δ_j} is extracted from the diagram in Fig. 2.B.6:

$$\delta_{\Delta_j}\epsilon = \frac{-\overline{g_m}(g_1^2\overline{\Delta_0} + \overline{\Delta_j}\,\kappa^2)}{128\overline{\Delta_j}\,(g_1^2 + g_1\,\overline{w_x} + \kappa^2)^2}$$
$$+\left[\frac{-\overline{g_j}\,\overline{g_m}\,N_f\,\pi v^2}{64\,\overline{\Delta_j}} + \phi_1\,\frac{g_1^2\,\overline{g_m}\,N_f\,\pi v^2[g_1^2\,\overline{g_j} + 2g_1\,\overline{g_j}\,\overline{w_x} - (\overline{g_0} - 2\overline{g_j})\kappa^2]}{64\overline{\Delta_j}\,(g_1^2 + g_1\,\overline{w_x} + \kappa^2)^2}\right] \tag{2.132}$$

2.C   Feynman Rules for Disorder and Screening

Feynman Rules for Disorder Vertices

From the action (2.100), we can read the Feynman rules for the various types of disorder.

4-fermion mass vertex:

$$\frac{1}{2}(\bar\psi\psi)(\bar\psi\psi) \;\;\Rightarrow\;\; \boxed{+g_m\,2\pi\delta(\omega = 0)}. \tag{2.133}$$

4-fermion density vertex:

$$\frac{1}{2}(\bar\psi\gamma^0\psi)(\bar\psi\gamma^0\psi) \;\;\Rightarrow\;\; \boxed{(g_0)(\gamma^0)(\gamma^0)2\pi\delta(\omega = 0)}. \tag{2.134}$$

4-fermion current vertex along the k-direction, $k = x$ or y:

$$\frac{1}{2}(\bar\psi i\gamma^k\psi)(\bar\psi i\gamma^k\psi) \;\;\Rightarrow\;\; \boxed{(+g_j)(i\gamma^k)\,(i\gamma^k)2\pi\delta(\omega = 0)}. \tag{2.135}$$

$b(\tau)b(\tau')$ disordered 2-pt vertex rule:

$$\frac{1}{2}b_z\, b_z \quad \Rightarrow \quad \boxed{\Delta_0\, (\delta_{ij}\mathbf{k}^2 - k_i k_j)2\pi\delta(\omega)a_i(\mathbf{k})a_j(-\mathbf{k})}. \qquad (2.136)$$

$e_j(\tau)e_j(\tau')$ disordered 2-pt vertex:

$$\frac{1}{2}(e_x\, e_x + e_y\, e_y) \quad \Rightarrow \quad \boxed{(-\Delta_j\, c^2)\, (k_x^2 + k_y^2)\, 2\pi\delta(\omega)\, a_0(\mathbf{k})a_0(-\mathbf{k})}.(2.137)$$

The factor of $\frac{1}{2}$ factor is canceled by symmetry factor equal to two. The 2π factor always cancels with the $1/2\pi$ that accompanies any frequency integral $\int \frac{d\omega}{2\pi}$.

Gauge Propagator
Vacuum Polarization Tensor

$$\Pi_{\mu\nu}(k_0, \mathbf{k}) = (\frac{-ig}{\sqrt{N_f}})^2(\frac{v}{c})^{2-\delta_{\mu 0}-\delta_{\nu 0}} \times N_f \times (-1)\int \frac{d^2 p_E}{(2\pi)^3}Tr[\gamma_\mu S_F(k+p)\gamma_\nu S_F(p)] \quad (2.138)$$

$$= (+g^2)(-i)^2\, (\frac{v}{c})^{2-\delta_{\mu 0}-\delta_{\nu 0}}\frac{1}{v^2}\int \frac{d^2\bar{p}_E dp_0}{(2\pi)^3}\, Tr[\gamma_\mu\gamma_\alpha\gamma_\nu\gamma_\beta]\frac{(\bar{k}+\bar{p})_\alpha(\bar{p})_\beta}{[x(\bar{k}+\bar{p})^2 + (1-x)\bar{p}^2]^2}, \quad (2.139)$$

$$\Pi_{\mu\nu}(k_0, \mathbf{k}) = \frac{-1}{16}\frac{g^2}{v^2}(\frac{v}{c})^{2-\delta_{\mu 0}-\delta_{\nu 0}}\frac{1}{|\bar{k}|}[\delta_{\mu\nu}\bar{k}^2 - \bar{k}_\mu\bar{k}_\nu] \quad , \quad \bar{k} = (\omega, v\,\mathbf{k}) \quad , \quad |\bar{k}| = \sqrt{\omega^2 + v^2\mathbf{k}^2}. \quad (2.140)$$

The minus sign comes from the fermion loop. The ratio v/c can be set to v in future equations.

"1-μ "Vacuum Polarization Vector

$$\Pi_\mu(k_0, \mathbf{k}) = \sqrt{g_m}(\frac{-ig}{\sqrt{N_f}})(\frac{v}{c})^{1-\delta_{\mu 0}} \times N_f \times (-1)\int \frac{d^2 p_E}{(2\pi)^3}Tr[\gamma_\mu S_F(k+p)\, \mathbf{1}\, S_F(p)] \qquad (2.141)$$

$$= \sqrt{g_m}\, (+ig)(-i)^2\, (\frac{v}{c})^{1-\delta_{\mu 0}}\frac{1}{v^2}\int \frac{d^2\bar{p}_E dp_0}{(2\pi)^3}\, Tr[\gamma_\mu\gamma_\alpha\, \gamma_\beta]\frac{(\bar{k}+\bar{p})_\alpha(\bar{p})_\beta}{[x(\bar{k}+\bar{p})^2 + (1-x)\bar{p}^2]^2} = 0. \quad (2.142)$$

The momentum part is proportional to $\delta_{\alpha\beta}\, p^2$, while the trace is proportional to the $\epsilon_{\mu\alpha\beta}$ tensor, and so it vanishes.

"1-1"Vacuum polarization scalar

$$\Pi_m(k_0, \mathbf{k}) = (\sqrt{g_m})^2 N_f \times (-1) \int \frac{d^2 p_E}{(2\pi)^3} Tr[\ \mathbf{1}\ S_F(k+p)\ \mathbf{1}\ S_F(p)] \quad (2.143)$$

$$= g_m \frac{1}{v^2} \int \frac{d^2\bar{p}_E dp_0}{(2\pi)^3}\ Tr[\ \gamma_\alpha\ \gamma_\beta]\frac{(\bar{k}+\bar{p})_\alpha(\bar{p})_\beta}{[x(\bar{k}+\bar{p})^2 + (1-x)\bar{p}^2]^2} = \frac{-|k|\ g_m}{8v^2} \quad (2.144)$$

Although nonzero, when connecting external fermion lines, the resulting diagram would be proportional to the number of replicas n_R and vanish in the $n_r \to 0$ limit.

Effective Gauge Propagator

In Coulomb gauge (longitundal component $a_L = 0$), the kinetic term for the gauge field is

$$S_{gauge} = \frac{1}{2} \int dk^2 d\omega\ \begin{pmatrix} a_0 & a_T \end{pmatrix} \begin{pmatrix} \frac{g^2}{16}\frac{k^2}{\sqrt{\omega^2+v^2k^2}} & i\kappa|k| \\ i\kappa|k| & w_x\frac{k^2}{|k|+f(\omega,k)} + \frac{g^2}{16}\sqrt{\omega^2+v^2k^2} \end{pmatrix} \begin{pmatrix} a_0 \\ a_T \end{pmatrix}, \quad (2.145)$$

where $(k^2 \equiv |\mathbf{k}|^2)$. Recall that $g_1 \equiv \frac{g^2}{16} = \frac{1}{16}$, the effective coulomb coupling $w_x \equiv \frac{+e^2}{4\pi^2}$, and $f(k,\omega) \equiv \frac{\sigma_e \mathbf{k}^2}{|\omega|+D_e \mathbf{k}^2}$. The transverse component of the gauge field is $a_T(k,\omega) \equiv i\hat{k}_x a_y(k,\omega) - i\hat{k}_y a_x(k,\omega)$, where $\hat{k}_j = k_j/|k|$.

When dealing with the gamma matrix contraction in Feynman diagram calculations, we have to write the effective gauge propagator obtained from S_{gauge} in the a_0, a_x, a_y basis $(i,j = x, y)$:

$$G_{00} = \frac{1}{\mathbf{k}^2}\ \frac{g_1\ \sqrt{\omega^2+v^2\mathbf{k}^2} + F(k,\omega)}{g_1^2 + \kappa^2 + \frac{g_1\ F(k,\omega)}{\sqrt{\omega^2+v^2\mathbf{k}^2}}} \quad (2.146)$$

$$G_{0i} = \frac{\kappa}{\mathbf{k}^2}\frac{-\epsilon_{ij}k_j}{g_1^2 + \kappa^2 + \frac{g_1\ F(k,\omega)}{\sqrt{\omega^2+v^2\mathbf{k}^2}}} \quad , \qquad G_{i0} = -G_{0i} = \frac{\kappa}{\mathbf{k}^2}\frac{+\epsilon_{ij}k_j}{g_1^2 + \kappa^2 + \frac{g_1\ F(k,\omega)}{\sqrt{\omega^2+v^2\mathbf{k}^2}}} \quad (2.147)$$

$$G_{ij} = (\delta_{ij} - \frac{k_i k_j}{\mathbf{k}^2})\frac{\frac{g_1}{\sqrt{\omega^2+v^2\mathbf{k}^2}}}{\left[g_1^2 + \kappa^2 + \frac{g_1\ F(k,\omega)}{\sqrt{\omega^2+v^2\mathbf{k}^2}}\right]} \quad (2.148)$$

where $\quad F(k,\omega) \equiv \frac{+e^2}{4\pi^2}\frac{|\mathbf{k}|^2}{|\mathbf{k}| + f(k,\omega)} = \frac{+e^2}{4\pi^2}\frac{|\mathbf{k}|^2}{|\mathbf{k}| + \frac{\sigma_e \mathbf{k}^2}{|\omega|+D_e\mathbf{k}^2}} \xrightarrow{\text{critical limit}, D_e=0} \frac{+e^2}{4\pi^2}\frac{|\mathbf{k}|^2}{|\mathbf{k}| + \frac{\sigma_e \mathbf{k}^2}{|\omega|}} \quad (2.149)$

Screened Disorder $W_{\mu\nu}$

The disorders g_0, g_j are screened by the fermion polarization. The Feynman rules in (2.134)-(2.135) have to be adjusted to account for this screening:

$$W_{\mu\nu} = W_{\mu\nu}^{(0)} + \phi_1 W_{\mu\nu}^{(sc)}, \quad (2.150)$$

where $W_{\mu\nu}^{(0)} = \mathrm{Diag}\,(g_0, i^2 g_j, i^2 g_j)$ is the bare part in (2.134),(2.135) and $W_{\mu\nu}^{(sc)}$ is the screening part from the summation of fermion bubbles.

The prefactor ϕ_1 isolates the screened and un-screened contributions: $\phi_1 = 0$ means that disorder screening is ignored; $\phi_1 = 1$ means that disorder screening is included. When disorder connects with the gauge propagator, we should set $\sigma_e = 0$ before setting $\omega = 0$ (due to the presence of the $\delta(\omega)$) factor. Otherwise, there is no disorder screening. Note that the vertex factors are included in $W_{\mu\nu}$, so when applying the Feynman rules, we only need to multiply by γ_μ without any constant or velocity factor.

We separate the screening part into symmetric and antisymmetric components:

$$W^{(sc)} = W^{\mathrm{sym}} + W^{\mathrm{as}}, \tag{2.151}$$

$$W_{00}^{\mathrm{sym}} = g_1 \frac{-g_1 g_j \kappa^2 + g_0(g_1 + \overline{w_x})\,(g_1^2 + g_1 \overline{w_x} + 2\kappa^2)}{(g_1^2 + g_1 \overline{w_x} + \kappa^2)^2}, \tag{2.152}$$

$$W_{ij}^{\mathrm{sym}} = \frac{g_1^2(g_1^2 g_j + 2 g_1 g_j \overline{w_x} - (g_0 - 2g_j)\kappa^2)}{(g_1^2 + g_1 \overline{w_x} + \kappa^2)^2}\,\frac{1}{k^2}(k^2 \delta_{ij} - k_i k_j), \tag{2.153}$$

$$W_{0i}^{\mathrm{as}} = \frac{g_1 \kappa\,(g_1 g_j \overline{w_x} + (-g_0 + g_j)\kappa^2)}{[g_1^2 + g_1 \overline{w_x} + \kappa^2]^2}\,\frac{-\epsilon_{ij}k_j}{k}. \tag{2.154}$$

Other components of $W^{(sc)}$ not included above vanish.

Effective Gauge Disorder $D_{\mu\nu}^{dis}$

The expressions in (2.136) and (2.137) 2-point vertex rules: each side of the vertex connects with dressed propagator found in (2.146)-(2.148). The effective gauge disorder is defined by

$$D_{\mu\nu}^{dis} = G_{\mu\alpha}\,D_{\alpha\beta}^{0,dis}\,G_{\beta\nu}, \tag{2.155}$$

where $D_{00}^{0,dis} = -\Delta_j\,\boldsymbol{k}^2$ defined in (2.137), $D_{ij}^{0,dis} = \Delta_0\,(\delta_{ij}\boldsymbol{k}^2 - k_i k_j)$ defined in (2.136), and $D_{0i}^{0,dis} = D_{i0}^{0,dis} = 0$. We decompose $D_{\mu\nu}^{dis}$ into symmetric and

antisymmetric components:

$$D_{\mu\nu}^{dis} = D_{\mu\nu}^{\mathrm{S}} + D_{\mu\nu}^{\mathrm{AS}}, \tag{2.156}$$

$$D_{00}^{\mathrm{S}} = -\frac{g_1^2 v^2 \Delta_j + 2g_1 v^2 \overline{w_x} \Delta_j + v^2 \overline{w_x}^2 \Delta_j + \Delta_0 \kappa^2}{(g_1^2 + g_1 \overline{w_x} + \kappa^2)^2}, \tag{2.157}$$

$$D_{ij}^{\mathrm{S}} = \frac{(g1^2 \Delta_0 + v^2 \Delta_j \kappa^2)}{v^2 (g_1^2 + g_1 \overline{w_x} + \kappa^2)^2} \frac{k^2 \delta_{ij} - k_i k_j}{k^2}, \tag{2.158}$$

$$D_{0i}^{\mathrm{AS}} = \frac{\kappa \left(-g_1 \Delta_0 + g_1 v^2 \Delta_j + v^2 \overline{w_x} \Delta_j\right) \epsilon_{ij} k_j}{v \left(g_1^2 + g_1 \overline{w_x} + \kappa^2\right)^2} \frac{}{k}. \tag{2.159}$$

Components of D^{dis} not listed above are zero.

Since $G_{\mu\nu}$ is constructed by the RPA sum of fermion loops, $G_{\mu\nu}$ can no longer connect any more fermion loop. Consequently, $D_{\mu\nu}^{dis}$ does not include any fermion loops. Note that $D_{\mu\nu}^{dis}$ generates $\frac{\Delta_{0,j}}{N_f}$. This disorder renormalizes Δ_0, Δ_j at 3-loop order.

2.D Fermion Self-energy

Self-energy—Screened Disorder Correction $W_{\mu\nu}$

$$\Sigma_d(p_0, \boldsymbol{p}) = \int \frac{d^2 \boldsymbol{k}}{(2\pi)^2} (\mathbf{1}_{2\times 2}) \, S_F(p_0 - 0, \boldsymbol{p} - \boldsymbol{k}) (\mathbf{1}_{2\times 2}) g_m + \int \frac{d^2 \boldsymbol{k}}{(2\pi)^2} \gamma_\nu S_F(p_0 - 0, \boldsymbol{p} - \boldsymbol{k}) \gamma_\mu W_{\mu\nu}(\boldsymbol{k})$$

$$= \int \frac{d^2 \boldsymbol{k}}{(2\pi)^2} (\mathbf{1}_{2\times 2}) \, S_F(p_0 - 0, \boldsymbol{p} - \boldsymbol{k}) (\mathbf{1}_{2\times 2}) g_m + \int \frac{d^2 \boldsymbol{k}}{(2\pi)^2} \gamma_\nu \left[(+i) \frac{\gamma_0 p_0 + v(\boldsymbol{p} - \boldsymbol{k})_i \gamma_i}{p_0^2 + v^2(\boldsymbol{p} - \boldsymbol{k})^2}\right] \gamma_\mu \, W_{\mu\nu}(\boldsymbol{k})$$

$$= \frac{+i}{v^2} \frac{p_0 \gamma_0}{2\pi\epsilon} [g_m] + \int \frac{d^2 \boldsymbol{k}}{(2\pi)^2} \gamma_\nu \left[(+i) \frac{\gamma_0 p_0 + v(\boldsymbol{p} - \boldsymbol{k})_i \gamma_i}{p_0^2 + v^2(\boldsymbol{p} - \boldsymbol{k})^2}\right] \gamma_\mu \, W_{\mu\nu}(\boldsymbol{k}) \tag{2.160}$$

$$= \frac{+i p_0 \gamma_0}{2\pi\epsilon v^2} g_m + \frac{+i p_0 \gamma_0}{2\pi\epsilon v^2} (g_0 + 2g_j)$$

$$+ \phi_1 \left[\frac{g_1^2 \overline{w_x} \left(g_1 \overline{g_j} - g_1 \overline{g_0} - \overline{g_0} \, \overline{w_x}\right)}{(g_1^2 + g_1 \overline{w_x} + \kappa^2)^2} + \frac{g_1 \left(g_1 \overline{g_j} + g_1 \overline{g_0} + 2\overline{g_0} \, \overline{w_x}\right)}{g_1^2 + g_1 \overline{w_x} + \kappa^2}\right] \frac{-i}{\epsilon} p_0 \, \gamma_0$$

$$+ \phi_1 \frac{(-1)g_1^2 \left[g_1^2 \overline{g_j} + 2g_1 \overline{g_j} \, \overline{w_x} - \left(\overline{g_0} - 2\overline{g_j}\right) \kappa^2\right]}{(g_1^2 + g_1 \overline{w_x} + \kappa^2)^2} \frac{-i}{\epsilon} v p_j \, \gamma_j. \tag{2.161}$$

Self-energy—Gauge Correction

Only the symmetric part of the gauge propagator produces a divergence at $\mathcal{O}(\frac{1}{N_f})$.

$$\Sigma_g(p_0, \boldsymbol{p}) = \left(\frac{-ig}{\sqrt{N_f}}\right)^2 \left(\frac{v}{c}\right)^{2 - \delta_{\mu 0} - \delta_{\nu 0}} \int \frac{d^3 k}{(2\pi)^3} \gamma_\nu S_F(p - k) \gamma_\mu \, G_{\mu\nu}(k_0, \boldsymbol{k}) \tag{2.162}$$

$$= \frac{-g^2}{N_f} (+i) \left(\frac{v}{c}\right)^{2 - \delta_{\mu 0} - \delta_{\nu 0}} \frac{1}{v^2} \int \frac{d^2 \bar{k} \, dk_0}{(2\pi)^3} \left[\gamma_\nu \frac{(p_0 - k_0)\gamma_0 + (\bar{p} - \bar{k})_a \gamma_a}{(p_0 - k_0)^2 + (\bar{p} - \bar{k})^2} \gamma_\mu\right] G_{\mu\nu}(k_0, \bar{k}) \tag{2.163}$$

Carrying out the momentum integral and setting $c = 1$:

$$- \Sigma_g(p_0, \boldsymbol{p})$$

$$= \int_{-\infty}^{\infty} dz \frac{ig^2\left((v^2 - z^2)g_1\, z^2\sigma_e + \left[g_1 z^2 v^2 - g_1 z^4 \times \xi + w_x\sqrt{v^2 + z^2}(v^2 - z^2)\right]|z|\right)(p_0\gamma_0)}{4\,\epsilon\, N_f\, \pi^2\, (v^2 + z^2)^2 \left[\sqrt{v^2 + z^2}(g_1^2 + \kappa^2)\sigma_e + |z|\left((g_1^2 + \kappa^2)\sqrt{v^2 + z^2} + g_1\, w_x\right)\right]}$$

$$+ \int_{-\infty}^{\infty} dz \frac{ig^2\left(g_1(v^4 - v^2 z^2 - z^4)\sigma_e - \left[w_x z^2\sqrt{v^2 + z^2} + g_1(-v^4 + v^2 z^2 + z^4 \times \xi)\right]|z|\right)(vp_j\gamma_j)}{4\,\epsilon\, N_f\, \pi^2\, (v^2 + z^2)^2 \left[\sqrt{v^2 + z^2}(g_1^2 + \kappa^2)\sigma_e + |z|\left((g_1^2 + \kappa^2)\sqrt{v^2 + z^2} + g_1\, w_x\right)\right]}$$

$$(2.164)$$

To obtain the above expression, we first perform a gradient expansion of $\Sigma(p_0, \boldsymbol{p})$ around $p_0 = \boldsymbol{p} = 0$. Next, focus on the linear term in $p_0, \boldsymbol{p}$ and replace the frequency integral $k_0 \to z\,|\boldsymbol{k}|$. When the 2d spatial momentum integral is done, the result is the expression shown above. The above expression is integrable only at $\sigma_e = 0$. The ξ term is a divergent integral that arises from the choice of Coulomb gauge. Physical observables are free from any ξ dependence.

Self-Energy—Effective Gauge Disorder $D_{\mu\nu}^{dis}$, $\mathcal{O}(\frac{\Delta_X}{N_f})$

$$\Sigma_b(p_0, \boldsymbol{p}) = \left(\frac{-i\,g}{\sqrt{N_f}}\right)^2 \left(\frac{v}{c}\right)^{2 - \delta_{\mu 0} - \delta_{\nu 0}} \int \frac{d^2\boldsymbol{k}}{(2\pi)^2}\, \gamma_\nu S_F(p_0 - 0, \boldsymbol{p} - \boldsymbol{k})\gamma_\mu\, D_{\mu\nu}^{dis}(\boldsymbol{k}) \quad (2.165)$$

$$= \frac{+i(\Delta_0 + v^2\Delta_j)}{2N_f\pi v^2\epsilon(g_1^2 + \kappa^2)}\, \gamma_0 p_0 + \frac{-i\,(g_1^2\Delta_0 + \kappa^2 v^2\Delta_j)}{2N_f\pi v^2\epsilon(g_1^2 + \kappa^2)^2}\,(v\,\gamma_j p_j). \quad (2.166)$$

2.E   3-point Vertex $\bar{u}(q)\,\delta\Gamma^\mu\,u(p)$

$$X = G_{\beta\alpha}(\omega, \boldsymbol{k}),\ D_{\beta\alpha}^{dis}(\boldsymbol{k}),\ W_{\beta\alpha}(\boldsymbol{k})$$
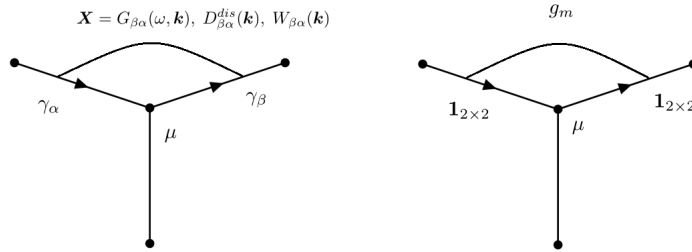
Γ^μ—**Gauge Correction**

$$\Gamma_1^\mu = \Big(\frac{-ig}{\sqrt{N_f}}\Big)^3 \Big(\frac{v}{c}\Big)^{3-\delta_{\alpha 0}-\delta_{\beta 0}-\delta_{\mu 0}} \int \frac{d^2\boldsymbol{k}d\omega}{(2\pi)^3}\, \gamma_\alpha S_F(q-k)\gamma_\mu S_F(p-k)\gamma_\beta G_{\beta\alpha}(k,\omega) \tag{2.167}$$

$$= \Big(\frac{-ig}{\sqrt{N_f}}\Big)^3 \Big(\frac{v}{c}\Big)^{3-\delta_{\alpha 0}-\delta_{\beta 0}-\delta_{\mu 0}} \frac{1}{v^2}$$

$$\times \int \frac{d^2\bar{\boldsymbol{k}}d\omega}{(2\pi)^3}\, \gamma_\alpha(+i)\frac{\gamma_0(q_0-k_0)+\gamma_c(\bar{q}-\bar{k})_c}{(q_0-k_0)^2+(\bar{q}-\bar{k})^2}\gamma_\mu(+i)\frac{\gamma_0(p_0-k_0)+\gamma_d(\bar{p}-\bar{k})_d}{(p_0-k_0)^2+(\bar{p}-\bar{k})^2}\gamma_\beta G_{\beta\alpha}(k,\omega) \tag{2.168}$$

To isolate the divergent part, one can set the external momentum $p = q = 0$.
Following the same steps we used in the self energy diagram evaluation, we
obtain

$$\Gamma_1^\mu = \frac{-ig}{\sqrt{N_f}}\frac{(-g^2)\Big((v^2-z^2)g_1\,z^2\sigma_e + \big[g_1 z^2 v^2 - g_1 z^4 \times \xi + w_x\sqrt{v^2+z^2}(v^2-z^2)\big]|z|\Big)}{4\,\epsilon\,N_f\,\pi^2\,(v^2+z^2)^2\Big[\sqrt{v^2+z^2}\big(g_1^2+\kappa^2\big)\sigma_e + |z|\Big((g_1^2+\kappa^2)\sqrt{v^2+z^2}+g_1\,w_x\Big)\Big]}(\gamma_0)$$

$$+\frac{-ig}{\sqrt{N_f}}\frac{v}{1}\frac{(-g^2)\Big(g_1(v^4-v^2z^2-z^4)\sigma_e - \big[w_x z^2\sqrt{v^2+z^2}+g_1(-v^4+v^2z^2+z^4\times\xi)\big]|z|\Big)}{4\,\epsilon\,N_f\,\pi^2\,(v^2+z^2)^2\Big[\sqrt{v^2+z^2}\big(g_1^2+\kappa^2\big)\sigma_e + |z|\Big((g_1^2+\kappa^2)\sqrt{v^2+z^2}+g_1\,w_x\Big)\Big]}(\gamma_j).$$

$$\tag{2.169}$$

As before, ξ labels the divergent part. Gauge invariance is easy to check by
comparing with Eq. (2.164): $\Gamma_1^t = \frac{-g}{\sqrt{N_f}}\frac{\partial\Sigma_g}{\partial p_0}$, $\Gamma_1^j = \frac{-g}{\sqrt{N_f}}\frac{\partial\Sigma_g}{\partial p_j}$.

Γ^μ—**Effective Gauge Disorder Correction**

$$\Gamma_2^\mu = \Big(\frac{-ig}{\sqrt{N_f}}\Big)^3 \Big(\frac{v}{c}\Big)^{3-\delta_{\alpha 0}-\delta_{\beta 0}-\delta_{\mu 0}} \int \frac{d^2\boldsymbol{k}}{(2\pi)^2}\, \gamma_\alpha S_F(q-k)\gamma_\mu S_F(p-k)\gamma_\beta D_{\beta\alpha}^{dis}(k) \tag{2.170}$$

$$= \frac{-i(\Delta_0+v^2\Delta_j)}{2N_f^{3/2}\pi v^2\epsilon(g_1^2+\kappa^2)}\,\gamma^0\; + \frac{i(g_1^2\Delta_0+v^2\kappa^2\Delta_j)}{2N_f^{3/2}\pi v\epsilon(g_1^2+\kappa^2)^2}\,\gamma^j. \tag{2.171}$$

Γ^μ—**Screened Disorder Correction** $W_{\mu\nu}$

$$\Gamma_3^\mu = \Big(\frac{-ig}{\sqrt{N_f}}\Big)\Big(\frac{v}{c}\Big)^{1-\delta_{\mu 0}} \times \int \frac{d^2\boldsymbol{k}}{(2\pi)^2}\gamma_\alpha S_F(q-k)\gamma_\mu S_F(p-k)\gamma_\beta W_{\beta\alpha} \tag{2.172}$$

$$= \frac{-ig}{\sqrt{N_f}}\frac{1}{\epsilon}\Bigg(\frac{g_0+2g_j}{2\pi v^2} + \phi_1\Big[\frac{g_1^2\overline{w_x}\,(-g_1\overline{g_j}+g_1\overline{g_0}+\overline{g_0}\,\overline{w_x})}{(g_1^2+g_1\overline{w_x}+\kappa^2)^2} - \frac{g_1\,(g_1\overline{g_j}+g_1\overline{g_0}+2\overline{g_0}\,\overline{w_x})}{g_1^2+g_1\overline{w_x}+\kappa^2}\Big]\Bigg)\gamma^0$$

$$+\frac{-ig}{\sqrt{N_f}}\,\phi_1\,\frac{1}{\epsilon}\,\Bigg(\frac{g_1^2\big[g_1^2\overline{g_j}+2g_1\overline{g_j}\,\overline{w_x}-(\overline{g_0}-2\overline{g_j})\,\kappa^2\big]}{(g_1^2+g_1\overline{w_x}+\kappa^2)^2}\Bigg)\gamma^j. \tag{2.173}$$

Γ^μ-**Random Mass Correction** g_m

$$\Gamma_4^\mu = (\frac{-ig}{\sqrt{N_f}})(\frac{v}{c})^{1-\delta_{\mu 0}} \times \int \frac{d^2\boldsymbol{k}}{(2\pi)^2}\mathbf{1}\, S_F(q-k)\gamma_\mu S_F(p-k)\,\mathbf{1}\, g_m = \frac{-ig}{\sqrt{N_f}}\frac{g_m}{2\pi v^2\epsilon}\gamma^0 + 0\,\gamma^j. \quad (2.174)$$

2.F   3-point Vertex $\bar{u}(q)\,1_{2\times 2}\,u(p)$

$\boldsymbol{X} = G_{\beta\alpha}(\omega,\boldsymbol{k}),\ D_{\beta\alpha}^{dis}(\boldsymbol{k}),\ W_{\beta\alpha}(\boldsymbol{k})$
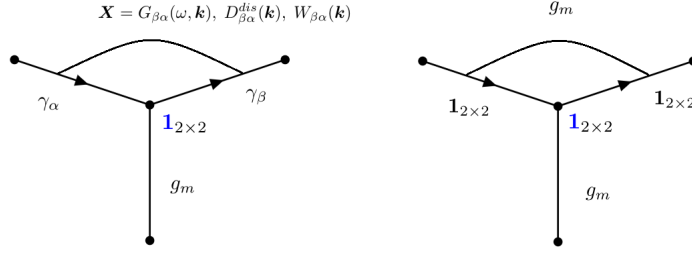
$1_{2\times 2}$—**Gauge Correction**

$$\Gamma_1^m = (\frac{-ig}{\sqrt{N_f}})^2(\frac{v}{c})^{2-\delta_{\alpha 0}-\delta_{\beta 0}}\,\frac{1}{v^2}(+i)^2$$

$$\times \int \frac{d^2\bar{k}d\omega}{(2\pi)^3}\gamma_\alpha\frac{\gamma_0(q_0-\omega) + \gamma_c(\bar{q}-\bar{k})_c}{(q_0-\omega)^2 + (\bar{q}-\bar{k})^2}\,\mathbf{1}\,\frac{\gamma_0(p_0-\omega) + \gamma_d(\bar{p}-\bar{k})_d}{(p_0-\omega)^2 + (\bar{p}-\bar{k})^2}\,\gamma_\beta\,G_{\alpha\beta} \quad (2.175)$$

$$\Gamma_1^m = \frac{(v^2+z^2)\,g^2\left[g_1(2v^2+z^2)\sigma_e + w_x\sqrt{v^2+z^2} + g_1(2v^2+z^2)\,|z|\right]}{4\,\epsilon\,N_f\,\pi^2\,(v^2+z^2)^2\left[\sqrt{v^2+z^2}(g_1^2+\kappa^2)\sigma_e + |z|\left((g_1^2+\kappa^2)\sqrt{v^2+z^2} + g_1\,w_x\right)\right]}\,\mathbf{1}_{2\times 2}$$

$$= \frac{g^2\left[g_1(2v^2+z^2)(v^2+z^2)\,\sigma_e + w_x(v^2+z^2)\sqrt{v^2+z^2} + g_1(2v^4+3z^2v^2+\xi\,z^4)\,|z|\right]}{4\,\epsilon\,N_f\,\pi^2\,(v^2+z^2)^2\left[\sqrt{v^2+z^2}(g_1^2+\kappa^2)\sigma_e + |z|\left((g_1^2+\kappa^2)\sqrt{v^2+z^2} + g_1\,w_x\right)\right]}\,\mathbf{1}_{2\times 2} \quad (2.176)$$

$1_{2\times 2}$—**Effective Gauge Disorder Correction**

$$\Gamma_2^m = (\frac{-ig}{\sqrt{N_f}})^2(\frac{v}{c})^{2-\delta_{\alpha 0}-\delta_{\beta 0}}\int \frac{d^2\boldsymbol{k}}{(2\pi)^2}\,\gamma_\alpha S_F(q-k)\,\mathbf{1}\,S_F(p-k)\gamma_\beta D_{\beta\alpha}^{dis}(\boldsymbol{k})$$

$$= \frac{(\Delta_0 - v^2\Delta_j)(g_1^2 - c^4\kappa^2)}{2\pi N_f v^2\epsilon(g_1^2 + c^4\kappa^2)^2}\,\mathbf{1}_{2\times 2}. \quad (2.177)$$

$1_{2\times 2}$—**Screened Disorder Correction** $W_{\mu\nu}$

$$\Gamma_3^m = \int \frac{d^2\boldsymbol{k}}{(2\pi)^2} \gamma_\alpha S_F(q-k)\mathbf{1}S_F(p-k)\gamma_\beta W_{\beta\alpha}$$
$$= \left[\frac{-g_0 + 2g_j}{2\pi v^2\epsilon} + \phi_1\frac{1}{\epsilon}\left(-\frac{g_1^2(2g_1 + \overline{w_x})(-g_1g_j + \overline{g_0}\,g_1 + \overline{g_0}\,\overline{w_x})}{(g_1^2 + g_1\overline{w_x} + \kappa^2)^2} + \frac{g_1(3\overline{g_0}\,g_1 - 3g_1\overline{g_j} + 2\overline{g_0}\,\overline{w_x})}{g_1^2 + g_1\overline{w_x} + \kappa^2}\right)\right]\mathbf{1}_{2\times 2}$$

$$(2.17)$$

$1_{2\times 2}$—**Random Mass Correction** g_m

$$\Gamma_4^m = \left(\frac{-ig}{\sqrt{N_f}}\right) \times \int \frac{d^2\boldsymbol{k}}{(2\pi)^2}\mathbf{1}\, S_F(q-k)\, \mathbf{1}\, S_F(p-k)\, \mathbf{1}\, g_m = \frac{-g_m}{2\pi v^2\epsilon}\, \mathbf{1}_{2\times 2} \quad (2.179)$$

2.G 4-point Fermion-Fermion Interaction

Define

$$H_{\mu\nu} \equiv D_{\mu\nu}^{dis}\left(\frac{-ig}{\sqrt{N_f}}\right)^2\left(\frac{v}{c}\right)^{2-\delta_{\mu 0}-\delta_{\nu 0}}. \quad (2.180)$$

Note that $W_{\mu\nu} \sim \mathcal{O}(\frac{1}{N_f^0})$ and $H_{\mu\nu} \sim \mathcal{O}(\frac{1}{N_f})$. Take the external three momenta to be p_1, p_2, p_3, p_4, where $p_i = (\omega_i, \boldsymbol{p_i})$. Schematically, the interaction has the form, $[\overline{\psi}(p_3)...\psi(p_1)]\,[\overline{\psi}(p_4)..\psi(p_2)]$. Define:

$$\Gamma_A \equiv (\gamma_7, \gamma_0, +\gamma_x, +\gamma_y)\ , \gamma_7 \equiv \mathbf{1}_{2\times 2}\ ,\ T^{A_1} = (\mathbf{1}\,g_m, W_{\mu\nu}, H_{\mu\nu})\ ,\ \tilde{T}^{A_1} = (\mathbf{1}\,g_m, W_{\mu\nu}^{(0)}, H_{\mu\nu}) \quad (2.181)$$
$$W_{\mu\nu}^{(0)} = Diag(g_0, i^2g_j, i^2g_j) \quad (2.182)$$

We use $A, B, C, D = \{1, 2, 3, 4\}$ indices to label $\mathbf{1}, \gamma_0, \gamma_x, \gamma_y$ and number subscripts, e.g., A_1, A_2, to label which interaction we choose: $A_1 = 1$ for the g_m interaction; $A_1 = 2$ for the $W_{\mu\nu}$ interaction; $A_1 = 3$ for the $H_{\mu\nu}$ interaction.

The diagrams below correspond to the following expressions:

$$B_1 = \int \frac{d^2k}{(2\pi)^2} \overline{\psi}(p_3)\Gamma_B S_F(p_1+k)\Gamma_A\psi(p_1) \ \overline{\psi}(p_4)\Gamma_D S_F(p_2-k)\Gamma_C\psi(p_2)$$

$$\times T_{CA}^{A_1}(\boldsymbol{k}, \omega=0) \ T_{BD}^{A_2}(p_1+k-p_3, \omega=0), \qquad (2.183)$$

$$B_2 = \int \frac{d^2k}{(2\pi)^2} \overline{\psi}(p_3)\Gamma_B S_F(p_1+k)\Gamma_A\psi(p_1) \ \overline{\psi}(p_4)\Gamma_C S_F(p_4+k)\Gamma_D\psi(p_2)$$

$$\times T_{CA}^{A_1}(\boldsymbol{k}, \omega=0) \ T_{BD}^{A_2}(p_1-p_3+k, \omega=0), \qquad (2.184)$$

$$B_3 = \int \frac{d^2k}{(2\pi)^2} \overline{\psi}(p_3)\Gamma_D S_F(p_3-k)\Gamma_A S_F(p_1-k)\Gamma_B\psi(p_1)$$

$$\times T_{BD}^{A_2}(\boldsymbol{k}, \omega=0), \quad \overline{\psi}(p_4)\Gamma_C\psi(p_2) \ \tilde{T}_{AC}^{A_1}(p_3-p_1, \omega=0), \qquad (2.185)$$

$$B_4 = \int \frac{d^2k}{(2\pi)^2} \overline{\psi}(p_3)\Gamma_A\psi(p_1) \ \tilde{T}_{AC}^{A_1}(p_3-p_1, \omega=0)$$

$$\times \overline{\psi}(p_4)\Gamma_D S_F(p_4-k) \ \Gamma_C S_F(p_2-k)\Gamma_B\psi(p_2) \ T_{BD}^{A_2}(k, \omega=0). \qquad (2.186)$$
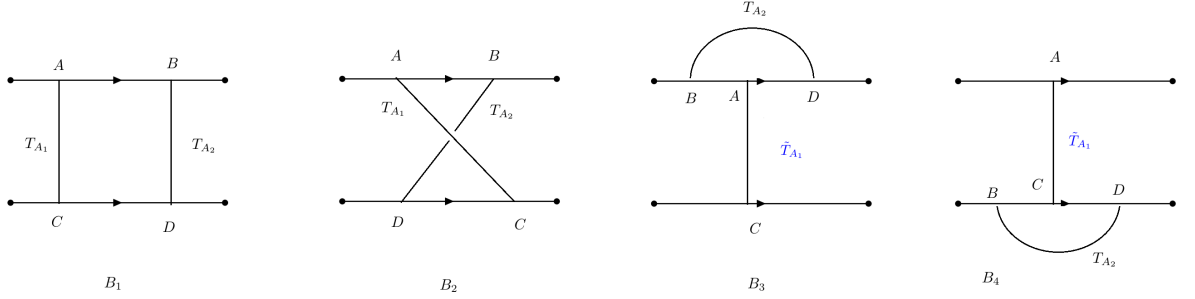
For diagrams B_3, B_4, the T_{A1} vertex is un-dressed, i.e., $W_{\mu\nu}^0$, which is directly related to the random coupling being renormalized.

4-point Interaction—Boxes B_3, B_4

Diagrams of type B_3, B_4 can be directly obtained from the 3-point vertex corrections in Appendices (2.E) and (2.F) with symmetry factor 2 (counting upper or lower vertices), so we don't have to recompute them at here. The terms in Γ^μ renormalize g_0, g_j and the terms in Γ^m renormalize g_m.

4-point Fermion Interaction—Boxes B_1, B_2

Diagrams for boxes B_1, B_2 are presented below.
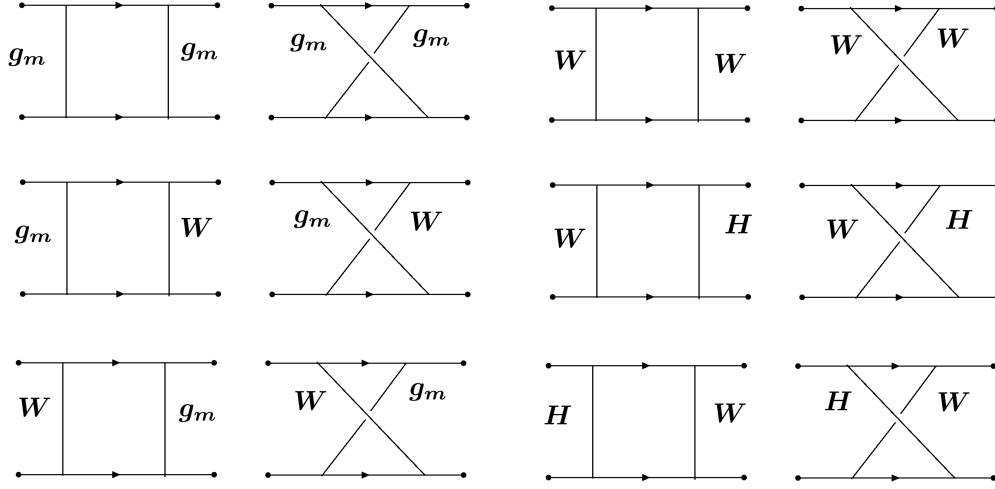
The W-H diagrams are $\mathcal{O}(\frac{\Delta_X\, g_X}{N_f})$. The H-H diagrams are $\mathcal{O}(\frac{\Delta_X^2}{N_f^2})$.

For each interaction, $(\bar{\psi}\psi)(\bar{\psi}\psi)$, $(\bar{\psi}\gamma_0\psi)(\bar{\psi}\gamma_0\psi)$, $(\bar{\psi}i\gamma_j\psi)(\bar{\psi}i\gamma_j\psi)$, we sum all these diagrams with the help of computer software to $\mathcal{O}(g_X^2, \frac{g_X}{N_f})$. The contribution from diagrams B_1, B_2 are the following.

$$
\mathrm{BOX}_{11} = \left[\frac{2g_0 g_j}{\pi v^2\,\epsilon\, g_m} + \phi_1(-4g_1)\frac{g_1\,\overline{g_0}\,\overline{g_j}(2g_1^2 + 4g_1\overline{w_x} + \overline{w_x}^2) - \kappa^2[\overline{g_0}^2 g_1 + g_1\overline{g_j}^2 - 2\overline{g_0}\,\overline{g_j}(2g_1 + \overline{w}}{\epsilon\,(g_1^2 + g_1\overline{w_x} + \kappa^2)^2} \right.
$$
$$
-\frac{\phi_1^2}{\epsilon}\left(\frac{4g_1^2\overline{g_j}^2\kappa^2[g_1^2(g_1^2 + 2g_1\overline{w_x} - \overline{w_x}^2) + 2g_1(g_1 - \overline{w_x})\kappa^2 - \kappa^4\,]}{\overline{g_m}[g_1^2 + g_1\,\overline{w_x} + \kappa^2]^4} \right.
$$
$$
+\frac{4g_1^2\overline{g_0}^2\kappa^2[g_1^2(g_1^2 + 2g_1\overline{w_x} + \overline{w_x}^2) + 2g_1(g_1 + \overline{w_x})\kappa^2 - \kappa^4]}{\overline{g_m}[g_1^2 + g_1\,\overline{w_x} + \kappa^2]^4}
$$
$$
\left.\left. +\frac{4\overline{g_0}\,\overline{g_j}g_1^2\big[-g_1^3(g_1 + \overline{w_x})^2(g_1 + 2\overline{w_x}) - 2g_1^2(g_1 + \overline{w_x})(2g_1 + 3\overline{w_x})\kappa^2 - g_1(5g_1 + 2\overline{w_x})\kappa^4 + 2\kappa^6\big]}{\overline{g_m}[g_1^2 + g_1\,\overline{w_x} + \kappa^2]^4} \right) \right]
$$
$$
\times(\bar{\psi}\mathbf{1}\psi)(\bar{\psi}\mathbf{1}\psi). \tag{2.18}
$$

$$
\mathrm{BOX}_{\gamma_0\gamma_0} = \left[\frac{2g_j g_m}{\pi v^2\,\epsilon\, g_0} - \phi_1\,\frac{4g_1^2\,\overline{g_m}[g_1^2\overline{g_j} + 2g_1\overline{g_j}\,\overline{w_x} - (\overline{g_0} - 2\overline{g_j})\kappa^2]}{\overline{g_0}\,\epsilon[g_1^2 + g_1\,\overline{w_x} + \kappa^2]^2} \right] (\bar{\psi}\gamma_0\psi)(\bar{\psi}\gamma_0\psi). \tag{2.188}
$$

$$
\mathrm{BOX}_{\gamma_j\gamma_j} = \left[\frac{2g_0 g_m}{\pi v^2\epsilon g_j} - \phi_1\frac{g_1\overline{g_m}[-g_1\overline{g_j}\kappa^2 + \overline{g_0}(g_1^3 + 2g_1^2\overline{w_x} + 2\overline{w_x}\kappa^2) + g_1(\overline{w_x}^2 + 2\kappa^2)\,]}{\overline{g_j}\epsilon[g_1^2 + g_1\overline{w_x} + \kappa^2]^2} \right] (\bar{\psi}i\gamma_j\psi)(\bar{\psi}i
$$
$$
\tag{2}
$$

As mentioned before, the index $j = x$ or y; there is no index sum here. And we assume the random current disorder variance $g_x = g_y \equiv g_j$ (isotropic).

2.H   2-loop Vertex Corrections

At leading order, the generic two-loop diagram has the form pictured below.
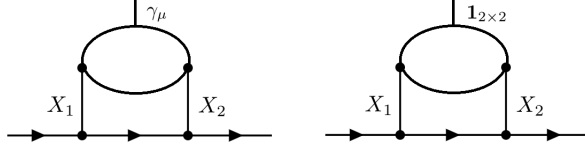
The interaction legs X_1 and X_2 can be chosen to be the gauge propagator $G_{\mu\nu}$ or disorder $E_{\mu\nu} \in \{W_{\mu\nu},\ g_m\}$. In principal there are four possible choice: $(X_1, X_2) = (G, G), (E, G), (G, E),$ or (E, E). In the replica limit $n_r \to 0$, the (E, E) diagram vanishes because the fermion bubble is proportional to n_R. Also, (E, G) and (G, E) are the same diagrams so we only need to compute one of them. The top vertex can be either γ^μ or $\mathbf{1}_{2\times2}$. However, we'll see below that diagrams using the γ^μ vertex are zero.

Mass Vertex $\overline{u}\,\mathbf{1}_{2\times2}\,u$—one leg gauge, one leg disorder
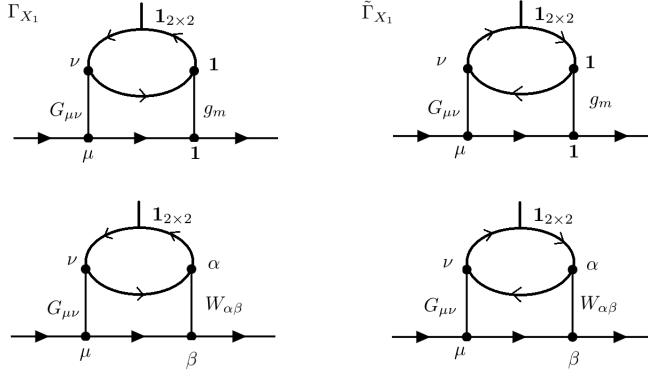
$$\Gamma_{X_1} = \frac{1}{v^2} \int \frac{d^2\bar{q}\,dq_0}{(2\pi)^3} \frac{1}{v^2} \int \frac{d^2\bar{k}}{(2\pi)^2}\ \overline{u}(p_3) \begin{pmatrix} 1 \\ \gamma_\beta \end{pmatrix} S_F(p_1 - k)[\frac{-ig}{\sqrt{N_f}}(\frac{v}{c})^{1-\delta_{\mu 0}}\gamma_\mu]\, u(p_1)\, G_{\mu\nu}(k)\, (-1) \times N_f$$

$$\times Tr\left[[\frac{-ig}{\sqrt{N_f}}(\frac{v}{c})^{1-\delta_{\nu 0}}\gamma_\nu]S_F(q - p_1 + p_3)\, \mathbf{1}\, S_F(q) \begin{pmatrix} 1 \\ \gamma_\alpha \end{pmatrix} S_F(k + q - p_1 + p_3)\right] \begin{pmatrix} g_m \\ W_{\alpha\beta}(k - p_1 + p_3) \end{pmatrix}.$$

$$(2.190)$$

$$\tilde{\Gamma}_{X_1} = \frac{1}{v^2} \int \frac{d^2\bar{q}\,dq_0}{(2\pi)^3} \frac{1}{v^2} \int \frac{d^2\bar{k}}{(2\pi)^2}\ \overline{u}(p_3) \begin{pmatrix} 1 \\ \gamma_\beta \end{pmatrix} S_F(p_1 - k)[\frac{-ig}{\sqrt{N_f}}(\frac{v}{c})^{1-\delta_{\mu 0}}\gamma_\mu]\, u(p_1)\, G_{\mu\nu}(k)\, (-1) \times N_f$$

$$\times Tr\left[[\frac{-ig}{\sqrt{N_f}}(\frac{v}{c})^{1-\delta_{\nu 0}}\gamma_\nu]S_F(q - k) \begin{pmatrix} 1 \\ \gamma_\alpha \end{pmatrix} S_F(q - p_1 + p_3)\, \mathbf{1}\, S_F(q)\right] \begin{pmatrix} g_m \\ W_{\alpha\beta}(k - p_1 + p_3) \end{pmatrix}.$$

$$(2.191)$$

The direction of the fermionic loop momenta is different in Γ and $\tilde{\Gamma}$. We use the upper/lower components to distinguish the diagrams that arise from either $g_m/W_{\mu\nu}$.

To extract the UV divergence, we can set $p_1 = p_3 = 0$. For g_m, the divergences in Γ_{X_1} and $\tilde{\Gamma}_{X_1}$ cancel (upon changing variables $q \to -q$ in $\tilde{\Gamma}_{X_1}$ and using basic properties of the trace). For $W_{\alpha\beta}$, Γ_{X_1} and $\tilde{\Gamma}_{X_1}$ have identical divergences.

$$\Gamma_{X_1} = \frac{-g^2}{1} \left(\frac{v}{c}\right)^{2-\delta_{\mu 0}-\delta_{\nu 0}} \int \frac{d^3k}{(2\pi)^3} \bar{u}(p_3) \left[\gamma_\beta \frac{k_0\gamma_0 + v\,k_c\gamma_c}{k_0^2 + v^2 k^2} \gamma_\mu\right] u(p_1)$$

$$\times\ G_{\mu\nu}(k)\ \times W_{\alpha\beta}(k) \times \int \frac{d^3q}{(2\pi)^3}\ Tr\left[\gamma_\nu \frac{q_0\gamma_0 + v\,q_d\gamma_d}{q_0^2 + v^2 q^2} \mathbf{1} \frac{q_0\gamma_0 + v\,q_e\gamma_e}{q_0^2 + v^2 q^2} \gamma_\alpha \frac{(k_0 + q_0)\gamma_0 + v\,(k_f + }{(k_0 + q_0)^2 + v^2(k + }\right.$$

Refer to the calculations in (2.204) to compute

$$\int \frac{d^3q}{(2\pi)^3} Tr\left[\gamma_\nu \frac{q_0\gamma_0 + v\,q_d\gamma_d}{q_0^2 + v^2 q^2} \frac{q_0\gamma_0 + v\,q_e\gamma_e}{q_0^2 + v^2 q^2} \gamma_\alpha \frac{(k_0 + q_0)\gamma_0 + v\,(k_f + q_f)\gamma_f}{(k_0 + q_0)^2 + v^2(k + q)^2}\right] = \frac{i\,\epsilon_{\nu\alpha\sigma}\,(k_0, v\,\boldsymbol{k})_\sigma}{8v^2\sqrt{k_0^2 + v^2\boldsymbol{k}^2}}. \quad (2$$

After setting $g = c = 1$,

$$\Gamma_{X_1} = \frac{-g^2}{1} \left(\frac{v}{c}\right)^{2-\delta_\mu-\delta_{\nu 0}} \int \frac{d^3k}{(2\pi)^3} \bar{u}(p_3) \left[\gamma_\beta \frac{k_0\gamma_0 + v\,k_c\gamma_c}{k_0^2 + v^2 k^2} \gamma_\mu\right] u(p_1) \times G_{\mu\nu}(k) \times W_{\alpha\beta}(k) \times \frac{i\,\epsilon_{\nu\alpha\sigma}\,(}{8v^2\sqrt{k}}$$

$$= \frac{(g_0\,g_1 - g_j g_1 - g_j\overline{w_x})}{4\pi v^2\epsilon(g_1^2 + g_1\overline{w_x} + \kappa^2)}$$

$$+\phi_1\left[\frac{2g_1^3(g_1 + \overline{w_x})(-g_1\,\overline{g_j} + g_1\overline{g_0} + \overline{g_0}\,\overline{w_x})}{\epsilon\,(g_1^2 + g_1\overline{w_x} + \kappa^2)^3} - \frac{g_1^2[7\overline{g_0}(g_1 + \overline{w_x}) - \overline{g_j}(7g_1 + 4\overline{w_x})]}{2\epsilon\,(g_1^2 + g_1\overline{w_x} + \kappa^2)^2} + \frac{g_1(\overline{g_0} - \overline{g_j})}{\epsilon\,(g_1^2 + g_1\overline{w_x} + }\right.$$

In total, we need to multiply by a factor of 4 to count the clockwise/counterclockwise fermion loops and the exchange of $W \leftrightarrow G$ in the diagrams.

$$\Gamma_{X_1} + \tilde{\Gamma}_{X_1} + \left(\Gamma_{X_1} + \tilde{\Gamma}_{X_1}\right)_{W \leftrightarrow G} = 4\Gamma_{X_1} \qquad (2.195)$$

Vector Vertex $\bar{u}\,\gamma^\rho\,u$—one leg gauge, one leg disorder

Replace the mass-vertex expressions $\mathbf{1}$ by γ_ρ
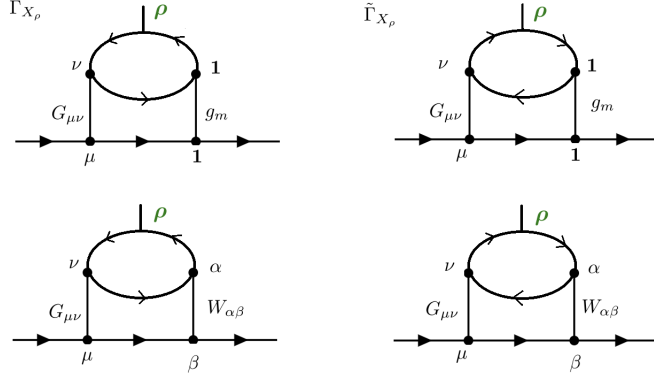
$$\Gamma_{X_\rho} = \frac{1}{v^2} \int \frac{d^2\bar{q}dq_0}{(2\pi)^3} \frac{1}{v^2} \int \frac{d^2\bar{k}}{(2\pi)^2} \; \bar{u}(p_3) \begin{pmatrix} 1 \\ \gamma_\beta \end{pmatrix} S_F(p_1 - k)[\frac{-ig}{\sqrt{N_f}}(\frac{v}{c})^{1-\delta_{\mu 0}}\gamma_\mu] \, u(p_1) \, G_{\mu\nu}(k) \, (-1) \times N_f$$

$$\times Tr\left[[\frac{-ig}{\sqrt{N_f}}(\frac{v}{c})^{1-\delta_{\nu 0}}\gamma_\nu] S_F(q - p_1 + p_3) \, \gamma_\rho \, S_F(q) \begin{pmatrix} 1 \\ \gamma_\alpha \end{pmatrix} S_F(k + q - p_1 + p_3) \right] \begin{pmatrix} g_m \\ W_{\alpha\beta}(k - p_1 + p_ \end{pmatrix}$$

$$(2.196)$$

$$\tilde{\Gamma}_{X_\rho} = \frac{1}{v^2} \int \frac{d^2\bar{q}dq_0}{(2\pi)^3} \frac{1}{v^2} \int \frac{d^2\bar{k}}{(2\pi)^2} \; \bar{u}(p_3) \begin{pmatrix} 1 \\ \gamma_\beta \end{pmatrix} S_F(p_1 - k)[\frac{-ig}{\sqrt{N_f}}(\frac{v}{c})^{1-\delta_{\mu 0}}\gamma_\mu] \, u(p_1) \, G_{\mu\nu}(k) \, (-1) \times N_f$$

$$\times Tr\left[[\frac{-ig}{\sqrt{N_f}}(\frac{v}{c})^{1-\delta_{\nu 0}}\gamma_\nu] S_F(q - k) \begin{pmatrix} 1 \\ \gamma_\alpha \end{pmatrix} S_F(q - p_1 + p_3) \, \gamma_\rho S_F(q) \right] \begin{pmatrix} g_m \\ W_{\alpha\beta}(k - p_1 + p_3) \end{pmatrix} .$$

$$(2.197)$$

By similar argument, the term with an even number of γ's in the trace would cancel between Γ and $\tilde{\Gamma}$, so in this case we only need to compute upper component (g_m). Set $p_1 = p_3 = 0$, straightforward calculation gives

$$\Gamma_{X_\rho} = (-N_f)(-i)^4(\frac{-ig}{\sqrt{N_f}})^2(\frac{v}{c})^{2-\delta_{\mu 0}-\delta_{\nu 0}}\frac{1}{v^2} \int \frac{d^3q}{(2\pi)^3} \frac{1}{v^2} \int \frac{d^2k}{(2\pi)^2}$$

$$\times \left[\bar{u}(p_3) \frac{(-k)^c}{k^2}\gamma_c\gamma_\mu \, u(p_1)\right] \, Tr[\gamma_\nu \slashed{q} \gamma_\rho \slashed{q}(\slashed{q} + \slashed{k})] \, \frac{1}{q^2 \, q^2(k + q)^2}G_{\mu\nu}(\boldsymbol{k}, \omega = 0) \, g_m$$

$$= 0. \qquad\qquad (2.198)$$

So there is no contribution from $\Gamma_{X_\rho}, \tilde{\Gamma}_{X_\rho}$

Mass Vertex $\bar{u}\,1_{2\times2}\,u$—both legs are gauge propagators
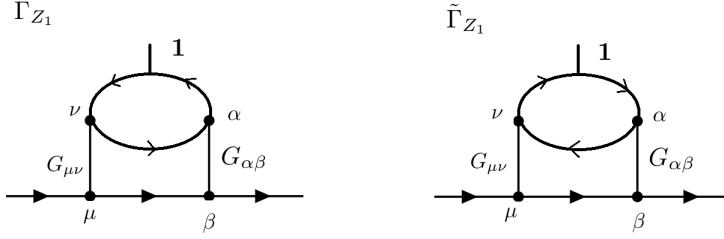
$$\Gamma_{Z_1} = (\frac{-ig}{\sqrt{N_f}})^4\,(\frac{v}{c})^{4-\delta_{\mu0}-\delta_{\nu0}-\delta_{\alpha0}-\delta_{\beta0}} \times (-1) \times (N_f) \int \frac{d^3k\,d^3q}{(2\pi)^3(2\pi)^3}\bar{u}(p_3)\,\gamma_\beta\,S_F(p_1-k)\,\gamma_\mu\,u(p_1)$$

$$\times\,G_{\mu\nu}(k)Tr\left[\gamma_\nu S_F(q-p_1+p_3)\,\mathbf{1}\,S_F(q)\,\gamma_\alpha\,S_F(k+q-p_1+p_3)\right]\,G_{\alpha\beta}(k-p_1+p_3).$$

$$(2.199)$$

$$\tilde{\Gamma}_{Z_1} = (\frac{-ig}{\sqrt{N_f}})^4\,(\frac{v}{c})^{4-\delta_{\mu0}-\delta_{\nu0}-\delta_{\alpha0}-\delta_{\beta0}} \times (-1) \times (N_f) \int \frac{d^3k\,d^3q}{(2\pi)^3(2\pi)^3}\bar{u}(p_3)\,\gamma_\beta\,S_F(p_1-k)\,\gamma_\mu\,u(p_1)$$

$$\times\,G_{\mu\nu}(k)Tr\left[\gamma_\nu S_F(-k+q+p_1-p_3)\,\gamma_\alpha\,S_F(q)\,\mathbf{1}\,S_F(q+p_1-p_3)\right]\,G_{\alpha\beta}(k-p_1+p_3).$$

$$(2.200)$$

Upon taking the external momenta to zero,

$$\Gamma_{Z_1} = \frac{g^4}{N_f}(\frac{v}{c})^{4-\delta_{\mu0}-\delta_{\nu0}-\delta_{\alpha0}-\delta_{\beta0}} \int \frac{d^3k}{(2\pi)^3}\bar{u}(p_3)\left[\gamma_\beta\,\frac{k_0\gamma_0+v\,k_c\gamma_c}{k_0^2+v^2k^2}\,\gamma_\mu\right]u(p_1)$$

$$\times G_{\mu\nu}(k)\,G_{\alpha\beta}(k) \times \int \frac{d^3q}{(2\pi)^3}\,Tr\left[\gamma_\nu\,\frac{q_0\gamma_0+v\,q_d\gamma_d}{q_0^2+v^2q^2}\,\mathbf{1}\,\frac{q_0\gamma_0+v\,q_e\gamma_e}{q_0^2+v^2q^2}\,\gamma_\alpha\,\frac{(k_0+q_0)\gamma_0+v\,(k_f+q_f)\gamma_f}{(k_0+q_0)^2+v^2(k+q)^2}\right]$$

$$(2.2$$

Perform the q integral first,

$$F_{\Gamma_z}(k) \equiv \int \frac{d^3q}{(2\pi)^3}Tr\left[\gamma_\nu\,\frac{q_0\gamma_0+v\,q_d\gamma_d}{q_0^2+v^2q^2}\,\frac{q_0\gamma_0+v\,q_e\gamma_e}{q_0^2+v^2q^2}\,\gamma_\alpha\,\frac{(k_0+q_0)\gamma_0+v\,(k_f+q_f)\gamma_f}{(k_0+q_0)^2+v^2(k+q)^2}\right] \quad (2.202)$$

$$= \frac{1}{v^2} \int \frac{d^3Q}{(2\pi)^3}Tr\left[\gamma_\nu\,\frac{Q_\lambda\gamma_\lambda}{Q^2}\,\frac{Q_\rho\gamma_\rho}{Q^2}\,\gamma_\alpha\,\frac{(K+Q)_\sigma\,\gamma_\sigma}{(K+Q)^2}\right]. \quad (2.203)$$

Here we define $Q \equiv (q_0, v\,\boldsymbol{q})$, $d^3Q \equiv dq_0 d^2(v\boldsymbol{q})$, $K \equiv (k_0, v\,\boldsymbol{k})$

Standard Feynman tricks give

$$F_{\Gamma_z}(k) = \frac{i\,\epsilon_{\nu\alpha\sigma}\,(k_0, v\,\boldsymbol{k})_\sigma}{8v^2\sqrt{k_0^2+v^2\boldsymbol{k}^2}}. \quad (2.204)$$

So we have $(k_0 = \omega)$

$$\Gamma_{Z_1} = \frac{g^4}{N_f}(\frac{v}{c})^{4-\delta_{\mu 0}-\delta_{\nu 0}-\delta_{\alpha 0}-\delta_{\beta 0}} \int \frac{d^3 k}{(2\pi)^3} \bar{u}(p_3) \left[\gamma_\beta \frac{k_0 \gamma_0 + v\, k_c \gamma_c}{k_0^2 + v^2 k^2}\, \gamma_\mu \right] u(p_1)$$

$$\times G_{\mu\nu}(k)\, G_{\alpha\beta}(k) \left(\frac{i\, \epsilon_{\nu\alpha\sigma}\,(k_0, v\, \boldsymbol{k})_\sigma}{8v^2 \sqrt{k_0^2 + v^2 \boldsymbol{k}^2}}\right)$$

$$= \bar{u}(p_3)\, \mathbf{1}_{2\times 2}\, u(p_1)$$

$$\times \int_{-\infty}^{\infty} dz\, \frac{-g^4 v^2(\sigma_e + |z|)\Big[(v^2 + z^2)(g_1^2 - \kappa^2)\,\sigma_e + |z|\left(g_1 w_x \sqrt{v^2 + z^2} + (g_1^2 - \kappa^2)\,(v^2 + z^2)\right)\Big]}{16\,\epsilon\, N_f\,\pi^2(v^2 + z^2)^{\frac{3}{2}}\Big[\sqrt{v^2 + z^2}(g_1^2 + \kappa^2)\,\sigma_e + |z|\left(g_1^2 \sqrt{v^2 + z^2} + (g_1\, w_x + \sqrt{v^2 + z^2}\,\kappa^2)\right)}$$

$$(2.2$$

The same manipulations are used in the computations of δ_1, δ_2. Note that unlike the case of δ_1, δ_2, this term renormalizes g_m without any divergent integration, labeled by ξ.

Taking the limit $\sigma_e = w_x = 0$, the expression reduces to

$$\Gamma_{Z_1}\Big|_{\sigma_e = w_x = 0} = \bar{u}(p_3)\, \mathbf{1}_{2\times 2}\, u(p_1) \times \frac{-g^4\,(g_1^2 - \kappa^2)}{8\,\epsilon\, N_f\,\pi^2 (g_1^2 + \kappa^2)^2}, \qquad (2.206)$$

which agrees with the result in [13] Unlike the case of Γ_{X_1}, the two legs are identical so the symmetry factor is 2:

$$\Gamma_{Z_1} + \tilde{\Gamma}_{Z_1} = 2\Gamma_{Z_1}. \qquad (2.207)$$

Vector Vertex $\bar{u}\,\gamma^\rho u$— both legs are gauge propagators

Replace $\mathbf{1}$ by γ_ρ to obtain the vector counterparts
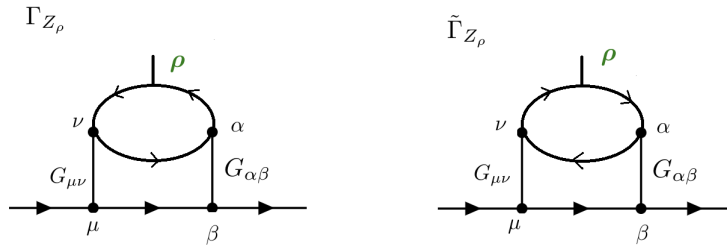
$$\Gamma_{Z_\rho} = (\frac{-ig}{\sqrt{N_f}})^4\,(\frac{v}{c})^{4-\delta_{\mu 0}-\delta_{\nu 0}-\delta_{\alpha 0}-\delta_{\beta 0}} \times (-1) \times (N_f) \int \frac{d^3 k d^3 q}{(2\pi)^3 (2\pi)^3} \bar{u}(p_3)\, \gamma_\beta\, S_F(p_1 - k)\, \gamma_\mu\, u(p_1)$$

$$\times G_{\mu\nu}(k) Tr\left[\gamma_\nu S_F(q - p_1 + p_3)\, \gamma_\rho\, S_F(q)\, \gamma_\alpha\, S_F(k + q - p_1 + p_3)\right]\, G_{\alpha\beta}(k - p_1 + p_3). \qquad (2.208)$$

$$\tilde{\Gamma}_{Z_\rho} = (\frac{-ig}{\sqrt{N_f}})^4 (\frac{v}{c})^{4-\delta_{\mu 0}-\delta_{\nu 0}-\delta_{\alpha 0}-\delta_{\beta 0}} \times (-1) \times (N_f) \int \frac{d^3k d^3q}{(2\pi)^3(2\pi)^3} \bar{u}(p_3) \gamma_\beta S_F(p_1 - k) \gamma_\mu u(p_1)$$

$$\times G_{\mu\nu}(k) Tr\left[\gamma_\nu S_F(-k+q+p_1-p_3) \gamma_\alpha S_F(q) \gamma_\rho S_F(q+p_1-p_3)\right] G_{\alpha\beta}(k-p_1+p_3).$$

$$(2.209)$$

By the same argument as before, there are six γ's in the trace, so Γ_{Z_ρ} and $\tilde{\Gamma}_{Z_\rho}$ cancel one another:

$$\Gamma_{Z_\rho} + \tilde{\Gamma}_{Z_\rho} = 0. \tag{2.210}$$

2.I   3-loop Corrections of Disorders Δ_0, Δ_j
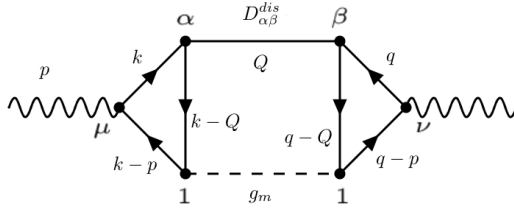
With $D_{\alpha\beta}^{dis}$ Propagator

$$\pi_1^{\mu\nu} = \int \frac{d^3k}{(2\pi)^3} \int \frac{d^3q}{(2\pi)^3} \int \frac{d^2Q dQ_0}{(2\pi)^2} (\frac{-ig}{\sqrt{N_f}})^4 (\frac{v}{c})^{4-\delta_{\mu 0}-\delta_{\nu 0}-\delta_{\alpha 0}-\delta_{\beta 0}} (-1)^2 (N_f)^2$$

$$\times Tr\left[\gamma_\mu S_F(k-p) \mathbf{1} S_F(k-Q)\gamma_\alpha S_F(k)\right]$$

$$\times g_m \delta(p_0 - Q_0)\delta(Q_0) D_{\alpha\beta}^{dis}(\mathbf{Q}, Q_0=0) \times Tr\left[\gamma_\nu S_F(q)\gamma_\beta S_F(q-Q) \mathbf{1} S_F(q-p)\right]$$

$$(2.211)$$

(flipping the signs for k and q variables)

$$= \int \frac{d^2Q}{(2\pi)^2} \left[\int \frac{d^3k}{(2\pi)^3} (\frac{v}{c})^{2-\delta_{\mu 0}-\delta_{\alpha 0}} Tr\left[\gamma_\mu S_F(k+p) \mathbf{1} S_F(k+Q)\gamma_\alpha S_F(k)\right]\right]$$

$$\times \left[\int \frac{d^3q}{(2\pi)^3} (\frac{v}{c})^{2-\delta_{\nu 0}-\delta_{\beta 0}} Tr\left[\gamma_\nu S_F(q)\gamma_\beta S_F(q+Q) \mathbf{1} S_F(q+p)\right]\right]$$

$$\times \left[g_m (\frac{-ig}{\sqrt{N_f}})^4 N_f^2 D_{\alpha\beta}^{dis}(\mathbf{Q}, Q_0=0) \delta(p_0=0)\right]. \tag{2.212}$$

Naively evaluating this diagram is problematic because the Feynman parameter integrals are not doable. To extract the divergence, we Taylor expand the

expression to second order in p. First, we define

$$T^{\mu\alpha}(Q,p) = \left[\int \frac{d^3k}{(2\pi)^3} \left(\frac{v}{c}\right)^{2-\delta_{\mu 0}-\delta_{\alpha 0}} \mathrm{Tr}\left[\gamma_\mu\, S_F(k+p)\, \mathbf{1}\, S_F(k+Q)\gamma_\alpha\, S_F(k)\right]\right] \tag{2.213}$$

By reversing the trace order , we have

$$\left[\int \frac{d^3q}{(2\pi)^3} \left(\frac{v}{c}\right)^{2-\delta_{\nu 0}-\delta_{\beta 0}} \mathrm{Tr}\left[\gamma_\nu S_F(q)\gamma_\beta S_F(q+Q)\, \mathbf{1}\, S_F(q+p)\right]\right] \tag{2.214}$$

$$= (-1)^5\left[\int \frac{d^3q}{(2\pi)^3} \left(\frac{v}{c}\right)^{2-\delta_{\nu 0}-\delta_{\beta 0}} \mathrm{Tr}\left[\gamma_\nu\, S_F(q+p)\, S(q+Q)\gamma_\beta S_F(q)\right]\right] = -T^{\nu\beta}(Q,p) \tag{2.215}$$

Let

$$\pi_1^{\mu\nu} = \int \frac{d^2Q}{(2\pi)^2}\ [T^{\mu\alpha}(Q,p)]\, [-T^{\nu\beta}(Q,p)] \times \left[g_m \left(\frac{-ig}{\sqrt{N_f}}\right)^4 N_f^2\, D_{\alpha\beta}^{dis}(\mathbf{Q},Q_0=0)\,\delta(p_0=0)\right] \tag{2.216}$$

and

$$T_2(Q,p) \equiv T^{\mu\alpha}T^{\nu\beta} \tag{2.217}$$

$$T_2(Q,p) = T_2(Q,0) + \frac{\partial T_2}{\partial p_x}p_x + \frac{\partial T_2}{\partial p_y}p_y + \frac{1}{2}\left[\frac{\partial^2 T_2}{\partial p_x^2}p_x^2 + \frac{\partial^2 T_2}{\partial p_y^2}p_y^2 + 2\frac{\partial^2 T_2}{\partial p_x p_y}p_x\, p_y\right] + \mathcal{O}(p^3). \tag{2.218}$$

$$= \left(\frac{\partial T^{\mu\alpha}}{\partial p_x}\frac{\partial T^{\nu\beta}}{\partial p_x}\right)\Bigg|_{\boldsymbol{p}=0} p_x^2 + \left(\frac{\partial T^{\mu\alpha}}{\partial p_y}\frac{\partial T^{\nu\beta}}{\partial p_y}\right)\Bigg|_{\boldsymbol{p}=0} p_y^2 + \left(\frac{\partial T^{\mu\alpha}}{\partial p_x}\frac{\partial T^{\nu\beta}}{\partial p_y} + \frac{\partial T^{\mu\alpha}}{\partial p_y}\frac{\partial T^{\nu\beta}}{\partial p_x}\right)\Bigg|_{\boldsymbol{p}=0} p_x\, p_y + \mathcal{O}(p^3) \tag{2.219}$$

Straightforward calculation gives

$$T^{\mu\alpha}(Q,p=0) = 0. \tag{2.220}$$

For first order derivatives, we can also obtain (after lengthy algebra)

$$\frac{\partial T^{\mu\alpha}}{\partial p_j} = \left(\frac{v}{c}\right)^{2-\delta_{\mu 0}-\delta_{\alpha 0}} \frac{1}{v^2}\frac{i(-i)^3}{32|\bar{Q}|}\left(\epsilon^{\mu\alpha j} + \frac{1}{\bar{Q}^2}\left[\epsilon^{\mu\alpha\tau}\bar{Q}_\tau\bar{Q}_j + \epsilon^{\alpha j\tau}\bar{Q}_\tau\bar{Q}_\mu - \epsilon^{j\mu\tau}\bar{Q}_\tau\bar{Q}_\alpha\right]\right) \tag{2.221}$$

Notice that this result is true in 3d with general temporal component Q_0

Plugging into Eq. (2.212) and taking the four diagrams into consideration (each triangle has either clockwise or counterclockwise flowing momenta), the total result is

$$\pi_{\mu\nu}^{tot} = 4\pi_{\mu\nu}, \tag{2.222}$$

where

$$\pi_{11} = (-1)\frac{g_m(g_1^2\Delta_0 + v^2\Delta_j\kappa^2)}{1024\pi v^4\epsilon(g_1^2 + g_1\frac{w_x}{v} + \kappa^2)^2}\, (\bar{p}_y^2 + \bar{p}_x^2), \tag{2.223}$$

$$\pi_{ij} = (+1)\frac{g_m(g_1^2 v^2\Delta_j + 2g_1 v\, w_x\Delta_j + w_x^2\Delta_j + \Delta_0\kappa^2)}{512\pi v^4\epsilon(g_1^2 + g_1\frac{w_x}{v} + \kappa^2)^2}\, (\delta_{ij}\bar{\boldsymbol{p}}^2 - \bar{p}_i\bar{p}_j) \tag{2.224}$$

and $\bar{p}_i = v\, p_i$. π_{11} renormalizes Δ_j and π_{ij} renormalizes Δ_0. This diagram scales as $1/N_f^2$ if g_m, Δ_0, Δ_j scale as $1/N_f$.

With $W_{\alpha\beta}$ Propagator
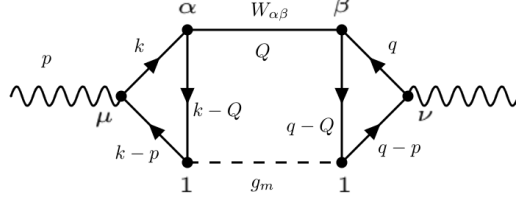
Replace the internal propagator with $W_{\alpha\beta}$, the remaining calculations are the same:

$$\tilde{\pi}_{\mu\nu}^{tot} = 4\tilde{\pi}_{\mu\nu}, \tag{2.225}$$

where

$$\tilde{\pi}_{11} = (-1)\,\frac{g_m\, g_j\, N_f}{1024\pi v^4 \epsilon}(\bar{p}_y^2 + \bar{p}_x^2) + \phi_1\,\frac{g_1^2 g_m N_f\, (g_1^2 g_j + 2g_1 g_j \frac{w_x}{v} + (2g_j - g_0)\kappa^2\,)}{1024\pi v^4\,\epsilon\,(g_1^2 + g_1\frac{w_x}{v} + \kappa^2)^2}(\bar{p}_y^2 + \bar{p}_x^2) \tag{2.226}$$

$$\tilde{\pi}_{ij} = (+1)\,\frac{g_0 g_m N_f}{512\pi v^4 \epsilon}\,(\delta_{ij}\bar{\boldsymbol{p}}^2 - \bar{p}_i \bar{p}_j)$$

$$+\phi_1\,\frac{g_1 g_m N_f\,\left[g_1 g_j \kappa^2 - g_0(g_1 + \frac{w_x}{v})\,(g_1^2 + g_1\frac{w_x}{v} + 2\kappa^2)\right]}{512\pi v^4\,\epsilon\,(g_1^2 + g_1\frac{w_x}{v} + \kappa^2)^2}\,(\delta_{ij}\bar{\boldsymbol{p}}^2 - \bar{p}_i \bar{p}_j)$$

$$\tag{2.227}$$

and $\bar{p}_i = v\, p_i$. $\tilde{\pi}_{11}$ renormalizes Δ_j, and $\tilde{\pi}_{ij}$ renormalizes Δ_0. This diagram scales as $1/N_f$ if g_m, g_j scale as $1/N_f$.

With Gauge Propagator $G_{\alpha\beta}$

By dimensional analysis, this term should be UV finite,

$$\sim \int d^2Q\, \frac{1}{Q}\frac{1}{Q}p^2\frac{1}{Q}\bigg|_{Q_0=p_0}.$$

2.J Summary

$$\bar{\delta}_1\, p_0\gamma^0 + \bar{\delta}_2\, v\, p_j \gamma^j = \Sigma_d + \Sigma_g + \Sigma_b \tag{2.228}$$

$$\bar{\delta}_{g_m}\,(\bar{\psi}\mathbf{1}\psi)\,(\bar{\psi}\mathbf{1}\psi) = \text{BOX}_{11} + 2\Big(\Gamma_1^m + \Gamma_3^m + \Gamma_4^m + 4\Gamma_{X_1} + 2\Gamma_{Z_1}\Big) + \tag{2.229}$$

$$\overline{\delta}_{g_0} \ (\bar{\psi}\gamma^0\psi) \ (\bar{\psi}\gamma^0\psi) = \text{BOX}_{\gamma_0\gamma_0} + 2\Big(\Gamma_1^\mu + \Gamma_3^\mu + \Gamma_4^\mu\Big)_{\mu=1} (\frac{-ig}{\sqrt{N_f}})^{-1} + 2\Gamma_2^{\mu=1}(\frac{-ig}{\sqrt{N_f}}) \tag{2.230}$$

$$\overline{\delta}_{g_j} \ (\bar{\psi}i\gamma^j\psi) \ (\bar{\psi}i\gamma^j\psi) = \text{BOX}_{\gamma_j\gamma_j} + 2\Big(\Gamma_1^\mu + \Gamma_3^\mu + \Gamma_4^\mu\Big)_{\mu=j} (\frac{-ig}{\sqrt{N_f}} \, v)^{-1} + 2\Gamma_2^{\mu=j} (\frac{-ig}{\sqrt{N_f}} \, v)^{-1} \tag{2.231}$$

where Σ_b, Γ_2^m, $\Gamma_2^{\mu=1}$, $\Gamma_2^{\mu=j}$ are the subleading order terms in the above expressions.

$$\overline{\delta}_{\Delta_0}(\delta_{ij}\boldsymbol{p}^2 - p_i p_j) = 4\pi_{ij} + 4\tilde{\pi}_{ij} \tag{2.232}$$

$$\overline{\delta}_{\Delta_j}(p_x^2 + p_y^2) = 4\pi_{11} + 4\tilde{\pi}_{11} \tag{2.233}$$

BIBLIOGRAPHY

[1] Gerard 't Hooft. "Dimensional regularization and the renormalization group". In: *Nucl. Phys.* B61 (1973), pp. 455–468.

[2] O. Aharony, G. Gur-Ari, and R. Yacoby. "d = 3 bosonic vector models coupled to Chern-Simons gauge theories". In: *Journal of High Energy Physics* 3, 37 (Mar. 2012), p. 37. arXiv: 1110.4382 [hep-th].

[3] Vivek Aji and C. M. Varma. "Quantum criticality in dissipative quantum two-dimensional XY and Ashkin-Teller models: Application to the cuprates". In: *Phys. Rev. B* 79 (18 May 2009), p. 184501. URL: https://link.aps.org/doi/10.1103/PhysRevB.79.184501.

[4] Alexander Altland and Ben Simons. *Condensed Matter Field Theory.* Cambridge University Press, 2010.

[5] L. V. Avdeev, G. V. Grigorev, and D. I. Kazakov. "Renormalizations in Abelian Chern-Simons field theories with matter". In: *Nucl. Phys.* B382 (1992), pp. 561–580.

[6] M. Barkeshli and J. McGreevy. "A continuous transition between fractional quantum Hall and superfluid states". In: *ArXiv e-prints* (Jan. 2012). arXiv: 1201.4393 [cond-mat.str-el].

[7] D. Belitz and T. R. Kirkpatrick. "The Anderson-Mott transition". In: *Rev. Mod. Phys.* 66 (2 Apr. 1994), pp. 261–380. URL: https://link.aps.org/doi/10.1103/RevModPhys.66.261.

[8] Vadim Borokhov, Anton Kapustin, and Xin-kai Wu. "Topological disorder operators in three-dimensional conformal field theory". In: *JHEP* 11 (2002), p. 049. arXiv: hep-th/0206054 [hep-th].

[9] Daniel Boyanovsky and John L. Cardy. "Critical behavior of m-component magnets with correlated impurities". In: *Phys. Rev. B* 26 (1 July 1982), pp. 154–170. URL: https://link.aps.org/doi/10.1103/PhysRevB.26.154.

[10] Nicholas P. Breznay et al. "Self-duality and a Hall-insulator phase near the superconductor-to-insulator transition in indium-oxide films". In: *Proceedings of the National Academy of Sciences* 113.2 (2016), p. 280.

[11] J. T. Chalker and G. J. Daniell. "Scaling, Diffusion, and the Integer Quantized Hall Effect". In: *Phys. Rev. Lett.* 61 (5 Aug. 1988), pp. 593–596. URL: https://link.aps.org/doi/10.1103/PhysRevLett.61.593.

[12] Jing-Yuan Chen et al. "Exact Boson-Fermion Duality on a 3D Euclidean Lattice". In: *Phys. Rev. Lett.* 120 (1 Jan. 2018), p. 016602. URL: https://link.aps.org/doi/10.1103/PhysRevLett.120.016602.

[13] Wei Chen, Matthew P. A. Fisher, and Yong-Shi Wu. "Mott transition in an anyon gas". In: *Phys. Rev. B* 48 (18 Nov. 1993), pp. 13749–13761. URL: http://link.aps.org/doi/10.1103/PhysRevB.48.13749.

[14] Wei Chen, Gordon W. Semenoff, and Yong-Shi Wu. "Two loop analysis of nonAbelian Chern-Simons theory". In: *Phys. Rev.* D46 (1992), pp. 5521–5539. arXiv: hep-th/9209005 [hep-th].

[15] Shai M. Chester and Silviu S. Pufu. "Anomalous dimensions of scalar operators in QED$_3$". In: *Journal of High Energy Physics* 2016.8, 69 (Aug. 2016), p. 69. arXiv: 1603.05582 [hep-th].

[16] Piers Coleman. *Introduction to Many-Body Physics*. Cambridge University Press, 2016.

[17] Sidney Coleman. *Aspects of Symmetry*. Cambridge: Cambridge University Press, 1985.

[18] Kedar Damle and Subir Sachdev. "Nonzero-temperature transport near quantum critical points". In: *Phys. Rev. B* 56 (14 Oct. 1997), pp. 8714–8733. URL: https://link.aps.org/doi/10.1103/PhysRevB.56.8714.

[19] C. Dasgupta and B. I. Halperin. "Phase Transition in a Lattice Model of Superconductivity". In: *Phys. Rev. Lett.* 47 (21 Nov. 1981), pp. 1556–1560.

[20] S.N. Dorogovtsev. "Critical exponents of magnets with lengthy defects". In: *Physics Letters A* 76.2 (1980), pp. 169–170. ISSN: 0375-9601. URL: http://www.sciencedirect.com/science/article/pii/0375960180906040.

[21] Matthew P. A. Fisher. "Quantum phase transitions in disordered two-dimensional superconductors". In: *Phys. Rev. Lett.* 65 (7 1990), p. 923. URL: http://link.aps.org/doi/10.1103/PhysRevLett.65.923.

[22] Matthew P. A. Fisher, G. Grinstein, and S. M. Girvin. "Presence of quantum diffusion in two dimensions: Universal resistance at the superconductor-insulator transition". In: *Phys. Rev. Lett.* 64 (5 1990), p. 587. URL: http://link.aps.org/doi/10.1103/PhysRevLett.64.587.

[23] Matthew P. A. Fisher et al. "Boson localization and the superfluid-insulator transition". In: *Phys. Rev. B* 40 (1 July 1989), pp. 546–570. URL: https://link.aps.org/doi/10.1103/PhysRevB.40.546.

[24] Matthew S. Foster and Andreas W. W. Ludwig. "Interaction effects on two-dimensional fermions with random hopping". In: *Phys. Rev. B* 73 (15 Apr. 2006), p. 155104. URL: https://link.aps.org/doi/10.1103/PhysRevB.73.155104.

[25] Eduardo Fradkin. *Field Theories of Condensed Matter Physics*. Cambridge University Press, 2013.

[26] S. Giombi et al. "Chern-Simons theory with vector fermion matter". In: *European Physical Journal C* 72, 2112 (Aug. 2012), p. 2112. arXiv: 1110.4386 [hep-th].

[27] Hart Goldman et al. "Collusion of Interactions and Disorder at the Superfluid-Insulator Transition: A Dirty 2d Quantum Critical Point". In: *arXiv e-prints*, arXiv:1909.09167 (Sept. 2019), arXiv:1909.09167. arXiv: 1909.09167 [cond-mat.str-el].

[28] Pallab Goswami, Hart Goldman, and S. Raghu. "Metallic phases from disordered $(2+1)$-dimensional quantum electrodynamics". In: *Phys. Rev. B* 95 (23 June 2017), p. 235145. URL: https://link.aps.org/doi/10.1103/PhysRevB.95.235145.

[29] G. Gur-Ari, S. Hartnoll, and R. Mahajan. "Transport in Chern-Simons-matter theories". In: *Journal of High Energy Physics* 7, 90 (July 2016), p. 90. arXiv: 1605.01122 [hep-th].

[30] F. D. M. Haldane. "Model for a Quantum Hall Effect without Landau Levels: Condensed-Matter Realization of the "Parity Anomaly"". In: *Phys. Rev. Lett.* 61 (18 Oct. 1988), pp. 2015–2018. URL: https://link.aps.org/doi/10.1103/PhysRevLett.61.2015.

[31] B. I. Halperin, Patrick A. Lee, and Nicholas Read. "Theory of the half-filled Landau level". In: *Phys. Rev. B* 47 (12 Mar. 1993), pp. 7312–7343. URL: http://link.aps.org/doi/10.1103/PhysRevB.47.7312.

[32] T. H. Hansson, Vadim Oganesyan, and S. L. Sondhi. "Superconductors are topologically ordered". In: *Annals of Physics* 313.2 (Oct. 2004), pp. 497–538. arXiv: cond-mat/0404327 [cond-mat.supr-con].

[33] A B Harris. "Effect of random defects on the critical behaviour of Ising models". In: *Journal of Physics C: Solid State Physics* 7.9 (May 1974), pp. 1671–1692. URL: https://doi.org/10.1088%2F0022-3719%2F7%2F9%2F009.

[34] Wei-Han Hsiao and Dam Thanh Son. "Self-Dual $\nu = 1$ Bosonic Quantum Hall State in Mixed Dimensional QED". In: *arXiv e-prints*, arXiv:1809.06886 (Sept. 2018), arXiv:1809.06886. arXiv: 1809.06886 [cond-mat.mes-hall].

[35] Po-Shen Hsin and Nathan Seiberg. "Level/rank Duality and Chern-Simons-Matter Theories". In: *JHEP* 09 (2016), p. 095. arXiv: 1607.07457 [hep-th].

[36] Bodo Huckestein. "Scaling theory of the integer quantum Hall effect". In: *Rev. Mod. Phys.* 67 (2 Apr. 1995), pp. 357–396. URL: https://link.aps.org/doi/10.1103/RevModPhys.67.357.

[37] Bodo Huckestein and Michael Backhaus. "Integer Quantum Hall Effect of Interacting Electrons: Dynamical Scaling and Critical Conductivity". In: *Phys. Rev. Lett.* 82 (25 June 1999), pp. 5100–5103. URL: https://link.aps.org/doi/10.1103/PhysRevLett.82.5100.

[38] Bodo Huckestein and Ludwig Schweitzer. "Relation between the correlation dimensions of multifractal wave functions and spectral measures in integer quantum Hall systems". In: *Phys. Rev. Lett.* 72 (5 Jan. 1994), pp. 713–716. URL: https://link.aps.org/doi/10.1103/PhysRevLett.72.713.

[39] Aaron Hui, Eun-Ah Kim, and Michael Mulligan. "Non-Abelian bosonization and modular transformation approach to superuniversality". In: *Phys. Rev. B* 99 (12 Mar. 2019), p. 125135. URL: https://link.aps.org/doi/10.1103/PhysRevB.99.125135.

[40] Aaron Hui, Michael Mulligan, and Eun-Ah Kim. "Non-Abelian fermionization and fractional quantum Hall transitions". In: *Phys. Rev. B* 97 (8 Feb. 2018), p. 085112. URL: https://link.aps.org/doi/10.1103/PhysRevB.97.085112.

[41] Jainendra K. Jain. *Composite Fermions*. Cambridge University Press, 2007.

[42] Shamit Kachru et al. "Mirror symmetry and the half-filled Landau level". In: *Phys. Rev. B* 92 (23 2015), p. 235105. URL: http://link.aps.org/doi/10.1103/PhysRevB.92.235105.

[43] Aharon Kapitulnik et al. "Effects of dissipation on quantum phase transitions". In: *Phys. Rev. B* 63 (12 2001), p. 125322. URL: http://link.aps.org/doi/10.1103/PhysRevB.63.125322.

[44] Anton Kapustin and Nathan Seiberg. "Coupling a QFT to a TQFT and Duality". In: *JHEP* 04 (2014), p. 001. arXiv: 1401.0740 [hep-th].

[45] Andreas Karch and David Tong. "Particle-Vortex Duality from 3D Bosonization". In: *Phys. Rev. X* 6 (3 Sept. 2016), p. 031043. URL: https://link.aps.org/doi/10.1103/PhysRevX.6.031043.

[46] Ad Lagendijk, Bart Van Tiggelen, and Diederik S Wiersma. "Fifty years of Anderson localization". In: *Phys. Today* 62.8 (2009), pp. 24–29.

[47] I D Lawrie and V V Prudnikov. "Static and dynamic properties of systems with extended defects: two-loop approximation". In: *Journal of Physics C: Solid State Physics* 17.10 (Apr. 1984), pp. 1655–1668. URL: https://doi.org/10.1088%2F0022-3719%2F17%2F10%2F007.

[48] Patrick A. Lee and T. V. Ramakrishnan. "Disordered electronic systems". In: *Rev. Mod. Phys.* 57 (2 Apr. 1985), pp. 287–337. URL: https://link.aps.org/doi/10.1103/RevModPhys.57.287.

[49] Wanli Li et al. "Crossover from the nonuniversal scaling regime to the universal scaling regime in quantum Hall plateau transitions". In: *Phys. Rev. B* 81 (3 Jan. 2010), p. 033305. URL: https://link.aps.org/doi/10.1103/PhysRevB.81.033305.

[50] Wanli Li et al. "Scaling and Universality of Integer Quantum Hall Plateau-to-Plateau Transitions". In: *Phys. Rev. Lett.* 94 (20 May 2005), p. 206807. URL: https://link.aps.org/doi/10.1103/PhysRevLett.94.206807.

[51] Wanli Li et al. "Scaling in Plateau-to-Plateau Transition: A Direct Connection of Quantum Hall Systems with the Anderson Localization Model". In: *Phys. Rev. Lett.* 102 (21 May 2009), p. 216801. URL: https://link.aps.org/doi/10.1103/PhysRevLett.102.216801.

[52] Andreas W. W. Ludwig et al. "Integer quantum Hall transition: An alternative approach and exact results". In: *Phys. Rev. B* 50 (11 Sept. 1994), pp. 7526–7552. URL: https://link.aps.org/doi/10.1103/PhysRevB.50.7526.

[53] Nadya Mason. "Superconductor-Metal-Insulator Transitions in Two Dimensions". PhD thesis. Stanford University, 2001.

[54] Nadya Mason and Aharon Kapitulnik. "Superconductor-insulator transition in a capacitively coupled dissipative environment". In: *Phys. Rev. B* 65 (22 May 2002), p. 220505. URL: https://link.aps.org/doi/10.1103/PhysRevB.65.220505.

[55] Hannes Meier and Mats Wallin. "Quantum Critical Dynamics Simulation of Dirty Boson Systems". In: *Phys. Rev. Lett.* 108 (5 Jan. 2012), p. 055701. URL: https://link.aps.org/doi/10.1103/PhysRevLett.108.055701.

[56] M. A. Metlitski and A. Vishwanath. "Particle-vortex duality of two-dimensional Dirac fermion from electric-magnetic duality of three-dimensional topological insulators". In: *Phys. Rev. B* 93.24, 245151 (June 2016), p. 245151. arXiv: 1505.05142 [cond-mat.str-el].

[57] David F. Mross, Jason Alicea, and Olexei I. Motrunich. "Symmetry and Duality in Bosonization of Two-Dimensional Dirac Fermions". In: *Phys. Rev. X* 7 (4 Oct. 2017), p. 041016. URL: https://link.aps.org/doi/10.1103/PhysRevX.7.041016.

[58] Michael Mulligan. "Particle-vortex symmetric liquid". In: *Phys. Rev. B* 95 (4 Jan. 2017), p. 045118. URL: https://link.aps.org/doi/10.1103/PhysRevB.95.045118.

[59] Michael Mulligan and S. Raghu. "Composite fermions and the field-tuned superconductor-insulator transition". In: *Phys. Rev. B* 93 (20 2016), p. 205116. URL: http://link.aps.org/doi/10.1103/PhysRevB.93.205116.

[60] Jeff Murugan and Horatiu Nastase. "Particle-vortex duality in topological insulators and superconductors". In: *Journal of High Energy Physics* 2017.5, 159 (May 2017), p. 159. arXiv: 1606.01912 [hep-th].

[61] Ray Ng and Erik S. Sørensen. "Quantum Critical Scaling of Dirty Bosons in Two Dimensions". In: *Phys. Rev. Lett.* 114 (25 June 2015), p. 255701. URL: https://link.aps.org/doi/10.1103/PhysRevLett.114.255701.

[62] Michael E. Peskin. "Mandelstam 't Hooft Duality in Abelian Lattice Models". In: *Annals Phys.* 113 (1978), p. 122.

[63] Nikolay Prokof'ev and Boris Svistunov. "Superfluid-Insulator Transition in Commensurate Disordered Bosonic Systems: Large-Scale Worm Algorithm Simulations". In: *Phys. Rev. Lett.* 92 (1 Jan. 2004), p. 015703. URL: https://link.aps.org/doi/10.1103/PhysRevLett.92.015703.

[64] Walter Rantner and Xiao-Gang Wen. "Spin correlations in the algebraic spin liquid: Implications for high-T_c superconductors". In: *Phys. Rev. B* 66 (14 Oct. 2002), p. 144501. URL: https://link.aps.org/doi/10.1103/PhysRevB.66.144501.

[65] Maryam Salehi et al. "Quantum-Hall to Insulator Transition in Ultralow-carrier-density Topological Insulator Films and a Hidden Phase of the Zeroth Landau Level". In: *arXiv e-prints*, arXiv:1903.00489 (Mar. 2019), arXiv:1903.00489. arXiv: 1903.00489 [cond-mat.mtrl-sci].

[66] N. Seiberg et al. "A duality web in 2 + 1 dimensions and condensed matter physics". In: *Annals of Physics* 374 (Nov. 2016), pp. 395–433. arXiv: 1606.01989 [hep-th].

[67] T. Senthil et al. "Duality between $(2+1)d$ Quantum Critical Points". In: *ArXiv e-prints*, arXiv:1810.05174 (Oct. 2018), arXiv:1810.05174. arXiv: 1810.05174 [cond-mat.str-el].

[68] Warren Siegel. "Supersymmetric dimensional regularization via dimensional reduction". In: *Physics Letters B* 84.2 (1979), pp. 193–196. ISSN: 0370-2693. URL: http://www.sciencedirect.com/science/article/pii/037026937990282X.

[69] Keith Slevin and Tomi Ohtsuki. "Critical exponent for the quantum Hall transition". In: *Phys. Rev. B* 80 (4 July 2009), p. 041304. URL: https://link.aps.org/doi/10.1103/PhysRevB.80.041304.

[70] D. T. Son. "Quantum critical point in graphene approached in the limit of infinitely strong Coulomb interaction". In: *Phys. Rev. B* 75 (23 June 2007), p. 235423. URL: https://link.aps.org/doi/10.1103/PhysRevB.75.235423.

[71] Dam Thanh Son. "Is the Composite Fermion a Dirac Particle?" In: *Phys. Rev. X* 5 (3 2015), p. 031027.

[72] S. L. Sondhi et al. "Continuous quantum phase transitions". In: *Rev. Mod. Phys.* 69 (1 1997), p. 315. URL: http://link.aps.org/doi/10.1103/RevModPhys.69.315.

[73] Alex Thomson and Subir Sachdev. "Quantum electrodynamics in 2+1 dimensions with quenched disorder: Quantum critical states with interactions and disorder". In: *Phys. Rev. B* 95 (23 June 2017), p. 235146. URL: https://link.aps.org/doi/10.1103/PhysRevB.95.235146.

[74] Ashvin Vishwanath, Joel E. Moore, and T. Senthil. "Screening and dissipation at the superconductor-insulator transition induced by a metallic ground plane". In: *Phys. Rev. B* 69 (5 Feb. 2004), p. 054507. URL: https://link.aps.org/doi/10.1103/PhysRevB.69.054507.

[75] Thomas Vojta et al. "Quantum critical behavior of the superfluid-Mott glass transition". In: *Phys. Rev. B* 94 (13 Oct. 2016), p. 134501. URL: https://link.aps.org/doi/10.1103/PhysRevB.94.134501.

[76] Chong Wang and T. Senthil. "Dual Dirac Liquid on the Surface of the Electron Topological Insulator". In: *Phys. Rev. X* 5 (4 2015), p. 041031.

[77] Y. Wang et al. "Absence of Cyclotron Resonance in the Anomalous Metallic Phase in InO_x". In: *Physical Review Letters* 120.16, 167002 (Apr. 2018), p. 167002. arXiv: 1708.01908 [cond-mat.supr-con].

[78] Peter B. Weichman and Ranjan Mukhopadhyay. "Particle-hole symmetry and the dirty boson problem". In: *Phys. Rev. B* 77 (21 June 2008), p. 214516. URL: https://link.aps.org/doi/10.1103/PhysRevB.77.214516.

[79] Steven Weinberg. *The quantum theory of fields. Vol. 2: Modern applications.* Cambridge University Press, 2013. ISBN: 9781139632478, 9780521670548, 9780521550024.

[80] E. Witten. "SL(2,Z) Action On Three-Dimensional Conformal Field Theories With Abelian Symmetry". In: *ArXiv High Energy Physics - Theory e-prints* (July 2003). eprint: hep-th/0307041.

[81] Jinwu Ye. "Effects of weak disorders on quantum Hall critical points". In: *Phys. Rev. B* 60 (11 Sept. 1999), pp. 8290–8303. URL: https://link.aps.org/doi/10.1103/PhysRevB.60.8290.

[82] Jinwu Ye and Subir Sachdev. "Coulomb Interactions at Quantum Hall Critical Points of Systems in a Periodic Potential". In: *Phys. Rev. Lett.* 80 (24 June 1998), pp. 5409–5412. URL: https://link.aps.org/doi/10.1103/PhysRevLett.80.5409.

[83] Hennadii Yerzhakov and Joseph Maciejko. "Disordered fermionic quantum critical points". In: *Phys. Rev. B* 98 (19 Nov. 2018), p. 195142. URL: https://link.aps.org/doi/10.1103/PhysRevB.98.195142.

Chapter 3

COMPOSITE FERMION NONLINEAR SIGMA MODELS

3.1 Introduction

Composite fermions [8, 17] provide a powerful alternative perspective of the quantum Hall effect, one in which the integer and fractional effects are realized as integer quantum Hall mean-field states. Over the last few years the possible relevance of composite fermion mean-field theory to the entire phase diagram and, in particular, quantum Hall plateau transitions has been emphasized. Although mean-field theory is inadequate to fully account for the effects of electron interactions, semiclassical reasoning [45] and numerical calculations [48, 24, 13] indicate that composite fermion mean-field theory has several advantages over the noninteracting electron approach [14] (see, e.g., [49, 26, 37] for some recent work): (1) integer and fractional quantum Hall transitions [41] are united within a single composite fermion framework (e.g., [39, 15]); (2) composite fermion mean-field theory produces finite, *n*onzero quantum critical conductivity without recourse to residual electron interactions [47]; (3) composite fermion theories can manifestly preserve [40, 38, 23] possible emergent reflection symmetries of the electron system [32].

There has been significant progress towards an analytical description of this quantum criticality [22, 25]. Specifically in [22] it was shown that the nonlinear sigma model (NLSM) for composite fermion diffusion,

$$S_{\text{NLSM}} = \int d^2x \, \text{Tr}\Big(\frac{1}{2g}(\partial_j Q)^2 + i\frac{\theta}{16\pi}\epsilon_{ij}Q\partial_i Q\partial_j Q\Big), \qquad (3.1)$$

contains a topological $\theta = \pi$ term. Here, $Q \in U(2n)/U(n) \times U(n)$ parameterizes composite fermion charge density fluctuations and the replica $n \to 0$ limit is understood. This result holds for both the Halperin, Lee, and Read (HLR) [12] and Dirac [40, 46, 28] composite fermion theories; it assumes a quenched disorder ensemble that preserves particle-hole symmetry (see below Eq. (3.6)). In (3.1) $g \propto 1/\sigma_{xx}^{\text{cf}}$ is a marginally-relevant coupling [6] that characterizes the evolution from the ballistic to the diffusive regime of finite (impurity-averaged) conductivity σ_{ij}^{cf}, measured in units of e^2/h. The topo-

logical θ term [1]—familiar from the seminal work of Pruisken et al. [35, 27] on the integer quantum Hall transition and from theoretical studies of disordered Dirac fermions in graphene and related systems [2, 43, 30, 31, 1]—is believed to prevent localization and thereby provide an explanation for the diffusive quantum criticality of the transition. $\theta = \pi$ indicates particle-hole symmetric dc electrical transport [20, 40]: For the nonrelativistic (HLR) composite fermion, $\theta = 2\pi\sigma_{xy}^{cf} \,(\mathrm{mod}\, 2\pi)$ [35]; for the Dirac composite fermion, $\theta = \pi + 2\pi\sigma_{xy}^{cf} \,(\mathrm{mod}\, 2\pi)$ [22, 30].

In this paper we consider the stability of this result to certain particle-hole symmetry violating perturbations. Consider the mean-field composite fermion Lagrangians for HLR ($\eta = 1$) and Dirac ($\eta = 0$) composite fermion theories (see Appendix 3.A for a review), expressed in a standard Dirac notation,

$$\mathcal{L} = \bar{\Psi}\big(i\slashed{\partial} + \slashed{a}\big)\Psi - \eta\Psi^{\dagger}P_2\big(i\partial_0 + a_0\big)\Psi + m_1\Psi^{\dagger}\Psi + m_2\bar{\Psi}\Psi. \qquad (3.2)$$

Above, a_0 and a_j for $j \in \{1, 2\}$ are uncorrelated quenched scalar and vector potential disorders; P_2 projects onto the second component of Ψ; m_1 is a chemical potential determined by the composite fermion density; and m_2 is a mass that is odd under particle-hole symmetry. We generalize the study in [22] to include uniform m_2 and random a_0. We show the $\theta = \pi$ term to be stable to the addition of nonzero m_2. This represents an emergent particle-hole symmetry of the diffusive quantum critical point. When a_0 is included, we find that the topological θ term varies continuously with the strength of this particle-hole symmetry violating disorder. We are unable to determine within this NLSM approach (valid for $\sigma_{xx}^{cf} \gg 1$) whether the ultimate low temperature fixed point of the sigma model with $\theta \neq \pi$ is an insulator or a quantum critical metal with varying Hall conductivity.

The remainder of this paper is organized as follows. We start with a description of the generating functional for disorder-averaged products of retarded and advanced composite fermion Green's functions. Encoded in this generating functional are observables such as the composite fermion density of states and conductivity. We then derive the NLSM for composite fermion mean-field theory, focusing on the topological θ term. We separately consider the effects of particle-hole symmetry preserving and particle-hole breaking quenched disorder. We conclude with a discussion of the HLR and Dirac composite fermion

---

[1]The θ angle is well defined modulo 2π because $\frac{1}{16\pi}\int \epsilon_{ij}\mathrm{Tr}(Q\partial_i Q\partial_j Q)$ is integrally quantized for smooth configurations of Q.

NLSMs and of possibilities for future work. HLR and Dirac composite fermion mean-field theories are defined in Appendix 3.A. Additional appendices supplement arguments in the main text. Unless stated otherwise we take $e^2 = \hbar = 1$.

3.2 Green's Function Generating Functional

We begin with the generating functional of composite fermion Green's functions. For a suitable choice of parameters this generating functional applies to both the HLR and Dirac composite fermion theories. We discuss both, in turn, before focusing for definiteness on the HLR theory in the next section.

Setup

HLR

Composite fermion mean-field states are described by a 2d field theory. Within the replica approach (see, e.g., [29, 3]), disorder-averaged retarded and advanced HLR composite fermion Green's functions obtain from the disorder average of the path integral,

$$Z = \int \mathcal{D}[\psi]\mathcal{D}[\psi^\dagger]e^{-S} \tag{3.3}$$

with action

$$S = -\int d^2x \ \psi^\dagger \Big(\frac{1}{2m}D_j^2 + V + E_F + (\omega + i\epsilon)\tau^3\Big)\psi. \tag{3.4}$$

Here $\psi^\dagger = \psi_I^\dagger(\mathbf{x})$ creates an HLR composite fermion of energy $E_F + \omega$ at $\mathbf{x} = (x_1, x_2)$; $I \in \{1, \ldots, n\}$ refer to retarded fermions and $I \in \{n+1, \ldots, 2n\}$ refer to advanced fermions; $D_j = \partial_j - ia_j$ is a covariant derivative with respect to possible quenched vector potential disorder $a_j(\mathbf{x})$; $\epsilon > 0$ is an infinitesimal; and the diagonal matrix $\tau_{IJ}^3 = \delta_{IJ}$ for $I, J \in \{1, \ldots, n\}$ and $\tau_{IJ}^3 = -\delta_{IJ}$ for $I, J \in \{n+1, \ldots, 2n\}$. This last term reduces the symmetry of S to $U_R(n) \times U_A(n) \subset U(2n)$, thereby distinguishing retarded and advanced fermions. The replica limit $n \to 0$ is understood to be taken after disorder averaging any correlation function obtained from Z.

Within this mean-field approach $E_F > 0$ is the Fermi energy and m/E_F is a finite nonzero parameter. In particular, we don't constrain the composite fermion mass m by Kohn's theorem [21]. See Appendix 3.A for additional details about HLR mean-field theory.

As a consequence of flux attachment, HLR mean-field theory realizes weak, quenched electron scalar potential disorder $V(\mathbf{x})$ as anticorrelated vector and scalar potential randomness [19, 45]:

$$\epsilon_{ij}\partial_i a_j(\mathbf{x}) = -2mV(\mathbf{x}). \tag{3.5}$$

We take the vector potential to be a transverse Gaussian random variable with zero mean and variance $W > 0$:

$$\overline{a_i(\mathbf{x})} = 0, \quad \overline{a_i(\mathbf{x})a_j(\mathbf{x}')} = W\delta_{ij}\delta(\mathbf{x} - \mathbf{x}'). \tag{3.6}$$

Particle-hole symmetric disorder ensembles have vanishing odd moments $\overline{V(\mathbf{x}_1)\cdots V(\mathbf{x}_{2p+1})} = 0$. Delta-function correlated vector potentials (3.6) arise from power-law correlated scalar potentials $\overline{V(\mathbf{x})V(\mathbf{x}')} \propto |\mathbf{x}-\mathbf{x}'|^{-4}$ [11]. (Nonrelativistic fermions coupled to power-law correlated vector potential disorder (without scalar potential disorder) obtain singular single-particle properties; two-particle properties remain regular and appear to coincide with delta-function correlated vector potential disorder [4, 18, 5].)

Following [22] we relate Z to a Euclidean 2d Dirac theory. First we factorize the derivative terms in S,

$$S = \int d^2x \left(\psi^\dagger iv(D_1 + iD_2)\chi + \chi^\dagger iv(D_1 - iD_2)\psi - \psi^\dagger\left(E_F + (\omega + i\epsilon)\tau^3\right)\psi - 2mv^2\chi^\dagger\chi \right), \tag{3.7}$$

using Eq. (3.5) and the auxiliary fermion [40]:

$$\chi = \frac{i}{2mv}(D_1 - iD_2)\psi, \quad \chi^\dagger = -\frac{i}{2mv}(D_1^* + iD_2^*)\psi^\dagger \tag{3.8}$$

where the arbitrary velocity $v > 0$ can be set to unity upon a rescaling of the coordinates and vector potential disorder. Next we define the Euclidean spinors [44],

$$\Psi = \begin{pmatrix} \psi \\ \chi \end{pmatrix}, \quad \Psi^\dagger = \begin{pmatrix} \psi^\dagger & \chi^\dagger \end{pmatrix}, \tag{3.9}$$

and choose gamma matrices,

$$\gamma^1 = \begin{pmatrix} 0 & -i \\ i & 0 \end{pmatrix}, \quad \gamma^2 = \begin{pmatrix} 0 & 1 \\ 1 & 0 \end{pmatrix}, \quad \gamma^5 = \begin{pmatrix} -1 & 0 \\ 0 & 1 \end{pmatrix}. \tag{3.10}$$

S becomes the Euclidean 2d Dirac action:

$$S = \int d^2x \; \Psi^\dagger \Big(\gamma^5 \gamma^j D_j - M_1 - M_2 \gamma^5 \Big) \Psi, \tag{3.11}$$

where the mass matrices are

$$M_1 = \Big(m + \frac{E_F}{2} \Big) \tau^0 + \frac{\omega + i\epsilon}{2} \tau^3, \quad M_2 = \Big(m - \frac{E_F}{2} \Big) \tau^0 + \frac{\omega + i\epsilon}{2} \tau^3, \tag{3.12}$$

where τ^0 is the $2n \times 2n$ identity matrix. We choose a regularization preserving the $U(2n)$ symmetry (present at $\omega = \epsilon = 0$) that identically rotates the spinor components $\psi = \frac{1}{2}(1 - \gamma^5)\Psi$ and $\chi = \frac{1}{2}(1 + \gamma^5)\Psi$.

Dirac

The corresponding action that appears in the generating functional of Dirac composite fermion retarded and advanced Green's functions has precisely the same form as (3.11) with the replacement of the mass matrices by

$$M_1^D = E_F \tau^0 + \big(\omega + i\epsilon \big) \tau^3, \quad M_2^D = m_D \tau^0. \tag{3.13}$$

See Appendix 3.A for additional details. At $\omega = \epsilon = 0$, the 2d actions governing HLR and Dirac Green's functions are identical upon the replacements $m + E_F/2 \leftrightarrow E_F$ and $m - E_F/2 \leftrightarrow m_D$. Consequently, it's sufficient to consider the HLR generating functional for dc quantities and rename parameters as appropriate to find the corresponding result for Dirac composite fermion theory.

Euclidean Discrete Symmetries

Hermitian conjugation complex conjugates the masses and leaves the remaining terms unchanged:

$$S^\dagger = \int d^2x \; \Psi^\dagger \Big(\gamma^5 \gamma^j D_j - M_1^* - M_2^* \gamma^5 \Big) \Psi. \tag{3.14}$$

The retarded and advanced parts of S are Hermitian conjugates at $\omega = 0$ for particle-hole symmetric disorder a_j. We take charge conjugation to act as

$$\mathcal{C} \Psi \mathcal{C} = \gamma^2 \Psi^*. \tag{3.15}$$

Since $\Psi^\dagger \gamma^5 \gamma^j \Psi$ and $\Psi^\dagger \Psi$ are odd under charge conjugation,

$$\mathcal{C} S \mathcal{C} = \int d^2x \; \Psi^\dagger \Big(\gamma^5 \gamma^j D_j^* + M_1 - M_2 \gamma^5 \Big) \Psi. \tag{3.16}$$

This is consistent with the usual definition of charge conjugation (e.g., [33]) and the identifications of iM_1 and M_2 as "γ_5-type" and "conventional" Dirac masses in the Minkowski signature version of this Euclidean action—see Appendix 3.B. Because Hermitian conjugation and Wick rotation don't commute, we use the Minkowski action (3.57) to determine that Ψ and $\Psi^\dagger$ transform under a $U(1)$ chiral rotation as

$$\Psi \to e^{i\alpha\gamma^5}\Psi, \quad \Psi^\dagger \to \Psi^\dagger e^{i\alpha\gamma^5}. \tag{3.17}$$

The derivative terms in S are invariant under continuous chiral transformations; the mass terms only preserve chiral transformations with $\alpha \in \pi\mathbb{Z}$.

The Dirac composite fermion mass m_D changes sign under a particle-hole transformation of the $(2+1)$d theory [40]. Notice that M_1 is invariant under the combination of charge-conjugation and a chiral rotation with $\alpha = \pi/2$, while M_2 changes sign under this operation. Consequently, we identify this transformation as the realization of electron particle-hole symmetry in the 2d Euclidean theory. Consistent with this interpretation, we'll find that nonzero M_2 is associated to particle-hole symmetry violating Hall response.

3.3 Effective Action for Charge Diffusion

In this section we derive the NLSM (3.1) for HLR composite fermion mean-field theory dc charge diffusion. This derivation holds for the Dirac composite fermion theory with the replacements: $m + E_F/2 \to E_F$ and $m - E_F/2 \to m_D$ (see (3.12), (3.13) and Appendix 3.A). We focus on the θ angle and its physical interpretation; the derivation of the leading non-topological term in the NLSM and further details on the calculation of the topological term can be found in Appendix 3.D.

Particle-hole Symmetric Disorder

In the dc zero-temperature limit we set the frequency $\omega = 0$ and use Eq. (3.6) to replace the action in (3.11) with its disorder average:

$$\overline{S} = \overline{S}^{(1)} + \overline{S}^{(2)}, \tag{3.18}$$

where

$$\overline{S}^{(1)} = \int d^2x \ \Psi^\dagger \left(\gamma^5 \gamma^j \partial_j - M_1 - M_2\gamma^5 \right) \Psi, \tag{3.19}$$

$$\overline{S}^{(2)} = \frac{W}{2} \int d^2x \ \left(\Psi_I^\dagger \gamma^5 \gamma^j \Psi_I \right) \left(\Psi_J^\dagger \gamma^5 \gamma^j \Psi_J \right), \tag{3.20}$$

and the parentheses around fermion bilinears indicate gamma matrix index contraction, e.g., $\left(\Psi_I^\dagger \gamma^5 \gamma^j \Psi_I\right) \equiv \Psi_{a,I}^\dagger \gamma_{ab}^5 \gamma_{bc}^j \Psi_{c,I}$ for $a, b, c \in \{1, 2\}$. To understand the effects of the interaction $\overline{S}^{(2)}$, we rewrite it as

$$\overline{S}^{(2)} = \frac{W}{2} \int d^2 x \left(\left(\Psi_I^\dagger \Psi_J\right)\left(\Psi_J^\dagger \Psi_I\right) - \left(\Psi_I^\dagger \gamma^5 \Psi_J\right)\left(\Psi_J^\dagger \gamma^5 \Psi_I\right) \right) \tag{3.21}$$

and decouple the resulting 4-fermion terms using the Hubbard-Stratonovich fields X_{IJ} and Y_{IJ},

$$e^{-\overline{S}^{(2)}} = \int \mathcal{D}[X]\mathcal{D}[Y] e^{-\int d^2 x \left(\frac{1}{2W} \mathrm{Tr} X^2 + \frac{1}{2W} \mathrm{Tr} Y^2 - i X_{IJ} \Psi_J^\dagger \Psi_I - Y_{IJ} \Psi_J^\dagger \gamma^5 \Psi_I \right)}, \tag{3.22}$$

where $\mathrm{Tr} X^2 \equiv X_{JI} X_{IJ}$ and $\mathrm{Tr} Y^2 \equiv Y_{JI} Y_{IJ}$. X_{IJ} and Y_{IJ} each transform in the adjoint rep of $U(2n)$.

The saddle-point equations that determine $\langle X_{IJ} \rangle$ and $\langle Y_{IJ} \rangle$ have the form:

$$X = \frac{W}{2} \mathrm{Tr}_\gamma \left(\int \frac{d^2 k}{(2\pi)^2} \frac{i}{i\gamma^5 \gamma^j k_j - (M_1 + iX) - (M_2 + Y)\gamma^5} \right), \tag{3.23}$$

$$Y = \frac{W}{2} \mathrm{Tr}_\gamma \left(\int \frac{d^2 k}{(2\pi)^2} \frac{\gamma^5}{i\gamma^5 \gamma^j k_j - (M_1 + iX) - (M_2 + Y)\gamma^5} \right), \tag{3.24}$$

where the trace Tr_γ is only taken over the gamma matrix indices. We consider an ansatz for X_{IJ} and Y_{IJ} that preserves the $U_R(n) \times U_A(n)$ symmetry:

$$\langle X \rangle = \Gamma \tau^3 + i\Sigma \tau^0, \quad \langle Y \rangle = Y_0 \tau^0, \tag{3.25}$$

where Γ, Σ, Y_0 are real. We've ignored here and below a possible addition to the $\langle Y \rangle$ ansatz proportional to τ^3 that appears to result in broken $U_R(n) \times U_A(n)$ symmetry. Σ is a logarithmic divergence that we absorb into a redefinition of the Fermi energy and composite fermion mass. For general renormalized M_2 there's no solution to (3.24) consistent with our ansatz; however when $M_2 = 0$ we find a nontrivial solution (at $\epsilon = 0$) indicative of composite fermion diffusion. This solution produces the finite scattering rate $\Gamma \propto W E_F$ for both spinor components of Ψ. This is different from the replacement of ϵ by Γ, which would instead only affect $\frac{1-\gamma^5}{2}\Psi$. Eq. (3.24) is solved at finite Γ by taking $Y_0 = 0$; thus, Y_{IJ} is massive and can be ignored at sufficiently low energies.

The saddle-point solution requires vanishing particle-hole symmetry violating mass (recall §3.2). Our interpretation is that even if initial conditions are chosen such that $M_2 \neq 0$, the saddle-point requires such particle-hole violating

perturbations to renormalize to zero. This implies the irrelevance of the m_D mass in Dirac composite fermion mean-field theory near the diffusive integer quantum Hall transition; it represents an emergent particle-hole symmetry in the HLR theory.

The saddle-point solution spontaneously breaks $U(2n) \to U_R(n) \times U_A(n)$. The Goldstone fluctuations of X_{IJ} about this saddle-point are parameterized by writing $Q(\mathbf{x}) \equiv X(\mathbf{x})/\Gamma = U^\dagger(\mathbf{x})\tau^3 U(\mathbf{x})$ where $U(\mathbf{x}) \in U(2n)$. This parameterization ensures that $Q(\mathbf{x})$ satisfies $Q^2(\mathbf{x}) = 1$. Since $Q(\mathbf{x}) = \tau^3$ for $U(\mathbf{x}) \in U_R(n) \times U_A(n)$, the target manifold of $Q(\mathbf{x})$ is $U(2n)/U_R(n) \times U_A(n)$. The NLSM for Q obtains by integrating out the fermions,

$$e^{-S_{\mathrm{NLSM}}} = \int \mathcal{D}\Psi\mathcal{D}\Psi^\dagger e^{-\int d^2x \ \Psi^\dagger\left(\gamma^5\gamma^j\partial_j - (M_1 + i\Gamma Q) - M_2\gamma^5\right)\Psi}. \tag{3.26}$$

Since M_2 vanishes ($\epsilon = 0$ in the remainder) in the saddle-point solution, the derivation of S_{NLSM} from Eq. (3.26) is identical to that in [22]. In particular, S_{NLSM} contains a topological term (3.1) with $\theta = \pi$. (This is confirmed by the complementary analysis presented in the next section.) The saddle-point solution that we found indicates that $\theta = \pi$ is stable against perturbation by particle-hole violating M_2. This result holds for both the HLR and Dirac composite fermion theories

Particle-hole Breaking Disorder

Semiclassical reasoning and numerics [45, 26] suggest that HLR composite fermions exhibit a Hall conductivity in violation of particle-hole symmetry (which for HLR composite fermions requires [20] $\sigma_{xy}^{cf} = -\frac{1}{2}$ at $\sigma_{xx}^{cf} < \infty$) if (3.5) isn't satisfied. Here we explore the effects of this broken particle-hole symmetry within the NLSM approach. (An alternative route to broken particle-hole symmetry that we don't pursue here is to consider a disorder ensemble with nonvanishing odd moments, in contrast to (3.6).)

To this end, we include additional scalar potential randomness $V_0(\mathbf{x})$ coupling to $\psi^\dagger\psi$ in (3.4)—independent of the anticorrelated vector and scalar potential disorders in (3.5)—that has zero mean and variance W_0. (Such a chiral coupling manifestly violates particle-hole symmetry in the Dirac composite fermion theory.) The contribution of $V_0(\mathbf{x})$ to the disorder-averaged action

$\overline{S} = \overline{S}^{(1)} + \overline{S}^{(2)} + \overline{S}^{(3)}$ is

$$\overline{S}^{(3)} = -\frac{W_0}{2} \int d^2x \left(\Psi_I^\dagger \frac{1 - \gamma^5}{2} \Psi_I \right) \left(\Psi_J^\dagger \frac{1 - \gamma^5}{2} \Psi_J \right), \tag{3.27}$$

where $\overline{S}^{(1)}$ and $\overline{S}^{(2)}$ are given in Eqs. (5.2) and (3.20). In parallel with our treatment of $\overline{S}^{(2)}$ discussed in the previous section, we decouple the "chiral disorder" in $\overline{S}^{(3)}$ with an additional Hubbard-Stratonovich field $Z_{IJ} \propto \Psi_I^\dagger \frac{1-\gamma^5}{2} \Psi_J$ and look for a saddle-point solution to the equations determining $\langle X_{IJ} \rangle$, $\langle Y_{IJ} \rangle$, and $\langle Z_{IJ} \rangle$:

$$X = \frac{W}{2} \text{Tr}_\gamma \left(\int \frac{d^2k}{(2\pi)^2} \frac{i}{i\gamma^5\gamma^j k_j - (M_1 + iX + i\frac{Z}{2}) - (M_2 + Y - i\frac{Z}{2})\gamma^5} \right), \tag{3.28}$$

$$Y = \frac{W}{2} \text{Tr}_\gamma \left(\int \frac{d^2k}{(2\pi)^2} \frac{\gamma^5}{i\gamma^5\gamma^j k_j - (M_1 + iX + i\frac{Z}{2}) - (M_2 + Y - i\frac{Z}{2})\gamma^5} \right), \tag{3.29}$$

$$Z = \frac{W_0}{4} \text{Tr}_\gamma \left(\int \frac{d^2k}{(2\pi)^2} \frac{1 - \gamma^5}{i\gamma^5\gamma^j k_j - (M_1 + iX + i\frac{Z}{2}) - (M_2 + Y - i\frac{Z}{2})\gamma^5} \right). \tag{3.30}$$

As detailed in Appendix 3.C, we find a $U_R(n) \times U_A(n)$ preserving solution to these equations with the ansatz:

$$\langle X \rangle = \Gamma_2 \tau^3 + iX_0 \tau^0, \tag{3.31}$$

$$\langle Y \rangle = Y_0 \tau^0, \tag{3.32}$$

$$\langle Z \rangle = (\Gamma_1 - \Gamma_2)\tau^3 + iZ_0\tau^0, \tag{3.33}$$

where $\Gamma_{1,2} > 0$ and we've again ignored a possible term in the $\langle Y \rangle$ ansatz proportional to τ^3. We absorb the logarithmically divergent real constants X_0 and Z_0 into a renormalization of m and E_F. Y_0 is a finite real constant that allows for nonzero (renormalized) $M_2 = m - E_F/2 \propto W_0$. The renormalized saddle-point mass matrix is therefore

$$\begin{pmatrix} E_F\tau^0 + i\Gamma_1\tau^3 & 0 \\ 0 & 2m\tau^0 + i\Gamma_2\tau^3 \end{pmatrix}. \tag{3.34}$$

Nonzero W_0 has produced unequal diffusion constants Γ_1 and Γ_2 for $\frac{1-\gamma^5}{2}\Psi$ and $\frac{1+\gamma^5}{2}\Psi$.

Similar to before, the saddle-point solution (3.31) - (3.33) spontaneously breaks the $U(2n)$ symmetry to $U(n)_R \times U(n)_A$. We consider the fluctuations about

this saddle-point by writing $Q_1(\mathbf{x}) \equiv (X(\mathbf{x}) + Z(\mathbf{x}))/\Gamma_1 = U_1(\mathbf{x})\tau^3 U_1^\dagger(\mathbf{x})$ and $Q_2(\mathbf{x}) \equiv X(\mathbf{x})/\Gamma_2 = U_2(\mathbf{x})\tau^3 U_2^\dagger(\mathbf{x})$ where $U_1(\mathbf{x}), U_2(\mathbf{x}) \in U(2n)$. Since the action is only invariant under global "vector" $U(2n)$ rotations (under which $\frac{1-\gamma^5}{2}\Psi$ and $\frac{1+\gamma^5}{2}\Psi$ transform identically) when E_F or m is nonzero, the Goldstone bosons correspond to those fluctuations of Q_1 and Q_2 for which $U_1 = U_2$; the "axial" fluctuations $Q_1 \neq Q_2$ are massive (see Appendix 3.D for an explicit demonstration) and can be neglected at low energies [2]. Thus we have a single light matrix boson $Q = Q_1 = Q_2 \in U(2n)/U_R(n) \times U_A(n)$ that we parameterize as $Q(\mathbf{x}) = U(\mathbf{x})\tau^3 U^\dagger(\mathbf{x})$ with $U(\mathbf{x}) \in U(2n)$.

The NLSM for Q obtains by integrating out the fermions. The real part of S_{NLSM}, which describes the diagonal conductivity of the system $1/g \propto W \gg 1$, is calculated in Appendix 3.D. The imaginary part of S_{NLSM} is the topological θ term,

$$S_{\mathrm{top}} = i\frac{\theta}{16\pi} \int d^2x \; \mathrm{Tr}\Big(\epsilon_{ij} Q \partial_i Q \partial_j Q\Big). \tag{3.35}$$

This term weights Q configurations by the second homotopy group $\Pi_2\big(U(2n)/U_R(n) \times U_A(n)\big) = \mathbb{Z}$. Since this classification is independent of the replica index n, we set $n = 1$ and so $Q(\mathbf{x}) = U(\mathbf{x})\tau^3 U^\dagger(\mathbf{x}) \in U(2)/U_R(1) \times U_A(1) = SU(2)/U(1)$ with $U(\mathbf{x}) \in SU(2)$. To extract the topological term, it's convenient to perform the gauge transformation $\Psi \to U(\mathbf{x})\Psi$ before integrating out the fermions. This allows us to interpret the fluctuations of Q in terms of the $SU(2)$ gauge field,

$$A_j = iU^\dagger \partial_j U. \tag{3.36}$$

Introducing the background fields,

$$\varphi_1 = m_+\tau^0 + i\Gamma_+\tau^3, \quad \varphi_2 = m_-\tau^0 + i\Gamma_-\tau^3, \tag{3.37}$$

for $m_\pm = m \pm E_F/2$ and $\Gamma_\pm = \frac{\Gamma_2 \pm \Gamma_1}{2}$, we calculate S_{NLSM} to quadratic order in A_j,

$$e^{-S_{\mathrm{NLSM}}} = \int \mathcal{D}\Psi \mathcal{D}\Psi^\dagger e^{-\int d^2x \; \Psi^\dagger\Big(\gamma^5\gamma^j(\partial_j - iA_j) - \varphi_1 - \varphi_2\gamma^5\Big)\Psi}. \tag{3.38}$$

---

[2]The Goldstone phase of the $O(n)$ model perturbed by a $O(n-1)$ preserving field h is a useful analogy here: at $h = 0$ the Goldstone fluctuations are parameterized by $O(n)/O(n-1)$; at $h \neq 0$ the Goldstone fluctuations are parameterized by $O(n-1)/O(n-2)$ with the remaining degrees of freedom massive.

This is sufficient to obtain the topological term, which is cubic in Q. Using (3.36) to relate Q to A_j and the identity $\epsilon_{jk}\partial_j A_k = i\epsilon_{jk}A_j A_k$ for a pure gauge potential, the topological θ term,

$$S_{\text{top}} = \frac{1}{4\pi} \int d^2x \ \text{Tr}\Big(\tau^3 \epsilon_{jk}\big(\theta^I \partial_j A_k + i\theta^{II} A_j A_k\big)\Big) \tag{3.39}$$

and the θ angle,

$$\theta = \theta^I + \theta^{II}. \tag{3.40}$$

Given the relation $\theta = 2\pi\sigma_{xy}^{cf}$, θ^{II} and θ^I are associated to the "classical" and "quantum" contributions to the Hall conductivity of the system [42].

We now calculate each of these contributions to θ. Appendix 3.D contains additional details. For particle-hole symmetry breaking φ_2—generated by W_0—we are unable to use the chiral anomaly argument in [22] to determine θ [3]. Instead we combine a result of Goldstone and Wilczek [10], familiar from work on topological insulators [36], with a direct evaluation; a similar argument in this context can be found in [30].

Because θ^I in (3.39) is only sensitive to the Abelian subgroup of $SU(2)$ generated by τ^3, we can simplify its determination by focusing on the associated Abelian gauge field $\frac{1}{2}\text{Tr}(\tau^3 A_j)$ under which the retarded and advanced components of Ψ carry opposite charge. We'll furthermore treat φ_1 and φ_2 in (3.37) as smoothly varying complex fields that assume their fixed values at the end of this calculation. Writing $\varphi_{1,2}$ in terms of the complex fields $\chi_{1,2}^{R,A}$,

$$\varphi_1 + \varphi_2 = \begin{pmatrix} e^{i\chi_1^R} & 0 \\ 0 & e^{i\chi_1^A} \end{pmatrix}, \quad \varphi_1 - \varphi_2 = -\begin{pmatrix} e^{-i\chi_2^R} & 0 \\ 0 & e^{-i\chi_2^A} \end{pmatrix}, \tag{3.41}$$

the generalization of [10] to complex $\varphi_{1,2}$ gives the linear in A_j contribution to S_{top}:

$$S_{\text{top}}^I = \frac{1}{8\pi} \int d^2x \ \epsilon_{jk}\partial_j\big(\chi_1^R + \chi_2^R - \chi_1^A - \chi_2^A\big)\text{Tr}\Big(\tau^3 A_k\Big). \tag{3.42}$$

After an integration by parts, we identify

$$\theta^I = -\frac{1}{2}\Big(\chi_1^R + \chi_2^R - \chi_1^A - \chi_2^A\Big). \tag{3.43}$$

---

[3]The issue is that a non-unitary chiral rotation is required to relate the retarded and advanced fermion mass matrices. We are unaware how the gauge field effective action changes under such to transformations.

We now evaluate θ^I on the saddle-point solution in (3.37). To ensure that θ^I is well defined modulo an integer multiple of 2π, we constrain the real parts $\mathrm{Re}[\chi_{1,2}^{R,A}] \in [0, \pi)$. For general $\varphi_{1,2}$ it's necessary to perform some combination of a charge conjugation (3.16) and a chiral rotation with $\alpha = \pi/2$ (3.17) on each fermion species in order to solve for $\chi_{1,2}^{R,A}$. Note that a flip of the relative sign in $\chi_1^R + \chi_2^R - \chi_1^A - \chi_2^A$ accompanies a charge conjugation on an advanced or retarded fermion. Likewise any chiral rotation would generally include an additional contribution to the NLSM action due to the anomalous variation of the fermion measure [9] in Eq. (3.38). For the $\varphi_{1,2}$ under consideration, it's only necessary to perform a charge conjugation on the advanced fermions with the result (see Appendix 3.D):

$$\theta^I = \pi + \arctan\left(\frac{\Gamma_+ - \Gamma_-}{m_+ - m_-}\right) - \arctan\left(\frac{\Gamma_+ + \Gamma_-}{m_+ + m_-}\right). \qquad (3.44)$$

In the diffusive regime $0 < \Gamma_{1,2} \ll E_F$ with weak particle-hole symmetry violation $|\Gamma_1 - \Gamma_2| \propto W_0 \ll W$,

$$\theta^I = \pi + \mathcal{O}(W_0). \qquad (3.45)$$

Eq. (3.39) indicates that θ^{II} is sensitive to the non-Abelian nature of $SU(2)$. By direct evaluation of (3.38) of the quadratic in A_j contribution to $S_{\mathrm{t}op}$, we find (see Appendix 3.D)

$$\theta^{II} = \frac{m_+\Gamma_- - m_-\Gamma_+}{m_+\Gamma_+ - m_-\Gamma_-}\left(\arctan\left(\frac{\Gamma_+ - \Gamma_-}{m_+ - m_-}\right) + \arctan\left(\frac{\Gamma_+ + \Gamma_-}{m_+ + m_-}\right)\right). \qquad (3.46)$$

$\theta^{II} = 0$ when $W_0 = 0$. Thus only θ^I contributes to θ when the disorder has particle-hole symmetry.

3.4 Discussion

In this note we showed the nonlinear sigma model of dc charge diffusion in HLR and Dirac composite fermion mean-field theories coincide in the presence of particle-hole symmetry preserving quenched disorder. In particular, both the Dirac and HLR sigma models contain a $\theta = \pi$ term that is attractive with respect to a certain particle-hole violating perturbation (see Eq. (3.2)). This topological term alters the renormalization group flow of the sigma model—which in its absence flows to a massive phase—towards a gapless fixed point. Consequently, this topological term simultaneously serves to prevent localization and explain the diffusive quantum criticality of the integer Hall transition.

Our result shows how particle-hole symmetry can emerge in the HLR composite fermion theory and gives further evidence for the possible IR equivalence of the Dirac and HLR theories.

We have also showed how electron particle-hole breaking disorder can shift the θ angle away from π. Since $\theta = 2\pi\sigma_{xy}^{\mathrm{c}f}$ (mod 2π) for the HLR theory and $\theta = \pi + 2\pi\sigma_{xy}^{\mathrm{c}f}$ (mod 2π) for the Dirac theory, nonzero W_0 results in a violation of particle-hole symmetric electrical transport [20, 40]. Because the nonlinear sigma model description is only appropriate for longitudinal conductivities $\sigma_{xx}^{\mathrm{c}f} \gg 1$ (in units of $e^2/h = 1$), we aren't able to determine the identity of the state that obtains for $\sigma_{xx}^{\mathrm{c}f} \leq 1$ towards which the nonlinear sigma model evolves. (Recall that the longitudinal conductivity is a coupling in the nonlinear sigma model that runs towards zero.) It would be interesting to understand if particle-hole symmetry emerges for $\sigma_{xx} \sim 1$, as predicted in [34] and found in a numerical study of noninteracting electrons [16]. Alternatively, if particle-hole symmetry doesn't emerge, we expect either a gapped insulator or a diffusive metal (at least in the vicinity of the particle-hole symmetric limit at $\theta = \pi$). It would be interesting to connect our result with recent work [13] that found evidence for a line of extended states with continuously varying exponents as particle-hole symmetry is violated by varying the coefficient of electron scalar potential $V(\mathbf{x})$ in (3.5).

APPENDIX

3.A   Composite Fermion Mean-Field Theory

In this appendix we derive the composite fermion mean-field theory Lagrangian (3.2). For a suitable choice of parameters, this Lagrangian describes both the HLR and Dirac composite fermion theories and it forms the basis for our current study.

HLR Mean-Field Theory

The HLR Lagrangian is [12]

$$\mathcal{L}_{\mathrm{HLR}} = \psi^\dagger \Big(i\partial_0 + A_0 + a_0 - \frac{\big(i\partial_j + A_j + a_j\big)^2}{2m} \Big)\psi + \frac{\epsilon^{\mu\nu\rho}}{8\pi} a_\mu \partial_\nu a_\rho + \dots . \quad (3.47)$$

Here, $\psi^\dagger$ creates an HLR composite fermion; A_μ is the external electromagnetic field; a_μ is a dynamical (2+1)d Chern-Simons gauge field; m is an effective mass, $\epsilon^{\mu\nu\rho}$ with $\mu, \nu, \rho \in \{0, 1, 2\}$ is the antisymmetric symbol with $\epsilon^{012} = 1$; and the "..." include all other possible couplings and interactions, which we set to zero in the remainder of this appendix. Variation of $\mathcal{L}$ with respect to A_0 implies the electron and composite fermion densities are equal. A nonzero uniform magnetic field $\epsilon_{ij}\partial_i A_j = B > 0$ is assumed such that the electron filling fraction $\nu = 1/2$.

To write this Lagrangian in a Dirac form, we factorize the spatial derivative terms using the auxiliary fermion χ defined in (3.8):

$$\mathcal{L}_{\mathrm{HLR}} = \psi^\dagger \big(i\partial_0 + A_0 + a_0 \big)\psi - \psi^\dagger iv(D_1 + iD_2)\chi - \chi^\dagger iv(D_1 - iD_2)\psi + 2mv^2 \chi^\dagger \chi + \frac{\epsilon^{\mu\nu\rho}}{8\pi} a_\mu \partial_\nu a_\rho$$

$$(3.48)$$

where the arbitrary velocity $v > 0$. (In the main text we rescale the spatial coordinates and the vector field to set $v = 1$ in the 2d theory associated to $\mathcal{L}_{\mathrm{hlr}}$. The Fermi energy and frequency are then redefined to absorb v: $E_F/v^2 \to E_F$ and $\omega/v^2 \to \omega$.) Notice that the scalar potential $A_0 + a_0$ only couples to ψ.

The mean-field approximation consists of imposing the a_0 equation of motion (i.e., flux attachment),

$$\psi^\dagger \psi = -\frac{1}{4\pi} \epsilon^{ij} \partial_i a_j, \quad (3.49)$$

and then setting all dynamical fluctuations of a_μ to zero. Introducing $\Psi = \begin{pmatrix} \psi & \chi \end{pmatrix}^T$ and the gamma matrices $(\Gamma^0, \Gamma^1, \Gamma^2) = (\sigma^3, i\sigma^1, i\sigma^2)$ for the Pauli-σ matrices σ^j, the resulting mean-field Lagrangian is

$$\mathcal{L} = \bar{\Psi}\left(i\slashed{\partial} + \slashed{a}\right)\Psi - \Psi^\dagger P_2\left(i\partial_0 + a_0\right)\Psi + \left(mv^2 + \frac{E_F}{2}\right)\Psi^\dagger\Psi - \left(mv^2 - \frac{E_F}{2}\right)\bar{\Psi}\Psi,$$
(3.50)

where $\bar{\Psi} = \Psi^\dagger\Gamma^0$, $i\slashed{\partial} + \slashed{a} = i\Gamma^0(\partial_0 + a_0) + iv\Gamma^j(\partial_j + a_j)$, $P_2 = \begin{pmatrix} 0 & 0 \\ 0 & 1 \end{pmatrix}$ projects onto the second component of Ψ, we've replaced $A_\mu + a_\mu$ by a_μ, and the Fermi energy $E_F > 0$ fixes $\psi^\dagger\psi = B/4\pi$ on average.

Dirac Mean-Field Theory

The Dirac composite fermion Lagrangian is [40, 46, 28, 38]

$$\mathcal{L}_{\mathrm{D}} = \bar{\Psi}\left(i\slashed{\partial} + \slashed{a}\right)\Psi + m_D v^2 \bar{\Psi}\Psi - \frac{1}{4\pi}\epsilon^{\mu\nu\rho}A_\mu\partial_\nu a_\rho + \frac{1}{8\pi}\epsilon^{\mu\nu\rho}A_\mu\partial_\nu A_\rho, \quad (3.51)$$

where Ψ is a 2-component Dirac fermion; a_μ is a dynamical $(2+1)$d gauge field; A_μ is the external electromagnetic field; m_D is a $(2+1)$d Dirac mass; and the remaining terms are defined as below (3.50). A uniform magnetic field $\epsilon_{ij}\partial_i A_j = B > 0$ and an electron filling fraction $\nu = 1/2$ are assumed. In contrast to the HLR composite fermion theory, the scalar potential couples to both components of Ψ in the Dirac theory. Particle-hole symmetry is a manifest invariance of $\mathcal{L}_{\mathrm{D}}$ [40, 38] at $m_D = 0$.

Similar to before, the mean-field approximation consists of imposing the a_0 equation of motion,

$$\Psi^\dagger\Psi = \frac{B}{4\pi}, \quad (3.52)$$

and setting all dynamical fluctuations of a_μ to zero. The resulting mean-field Lagrangian is

$$\mathcal{L} = \bar{\Psi}\left(i\slashed{\partial} + \slashed{a}\right)\Psi + E_F\Psi^\dagger\Psi + m_D v^2\bar{\Psi}\Psi, \quad (3.53)$$

where $E_F > 0$ fixes (3.52) on average. Possible quenched randomness in A_0 sources random a_j through the $\frac{1}{4\pi}\epsilon^{ij}A_0\partial_i a_j$ coupling in $\mathcal{L}_D$.

3.B Minkowski Action

In this appendix we translate the 2d Euclidean action S in (3.11) into Minkowski signature. Introduce the Minkowski spinors [44],

$$\Psi_M = e^{\frac{\pi}{4}\gamma^2\gamma^5}\Psi, \quad \Psi_M^\dagger = \Psi^\dagger e^{\frac{\pi}{4}\gamma^2\gamma^5}, \quad (3.54)$$

(note the same transformation is used for Ψ_M and $\Psi_M^\dagger$) and gamma matrices,

$$\tilde{\gamma}^1 = \gamma^1, \quad \tilde{\gamma}^2 = -\gamma^5, \quad \tilde{\gamma}^5 = \gamma^2. \tag{3.55}$$

The action S becomes

$$-\int d^2x \; \Psi_M^\dagger \left(\tilde{\gamma}^2 \tilde{\gamma}^j D_j - M_1 \tilde{\gamma}^2 \tilde{\gamma}^5 - M_2 \tilde{\gamma}^2 \right) \Psi_M. \tag{3.56}$$

Next we Wick rotate to Minkowski signature $(+1, -1)$ by defining $x^0 = -ix^2, x^1 = x^1$ and $\gamma_M^0 = \tilde{\gamma}^2, \gamma_M^1 = i\tilde{\gamma}^1, \gamma_M^5 = i\tilde{\gamma}^5$. The resulting Minkowski-signature action is

$$S_M = i \int dx^0 dx^1 \bar{\Psi}_M \left(i\gamma_M^\mu D_\mu - M_1 \gamma_M^5 - M_2 \right) \Psi_M, \tag{3.57}$$

where $\mu \in \{0, 1\}$, $\bar{\Psi} = \Psi_M^\dagger \gamma_M^0$, $D_\mu = \partial_\mu - iA_\mu$, and $A^0 = ia^2, A^1 = a^1$. This action contains a γ_5-type Dirac mass (matrix) iM_1 and a conventional Dirac mass (matrix) M_2. The chiral transformation in Minkowski signature is

$$\Psi_M \to e^{i\alpha\gamma_M^5} \Psi_M, \quad \Psi_M^\dagger \to \Psi_M^\dagger e^{-i\alpha\gamma_M^5}. \tag{3.58}$$

3.C   XYZ Saddle-Point Analysis

In this appendix we detail our saddle-point solution for particle-hole breaking disorder; our analysis of particle-hole preserving disorder obtains by taking $W_0 = 0$. We begin with the saddle-point equations,

$$X = \frac{W}{2} \text{Tr}_\gamma \left(\int \frac{d^2k}{(2\pi)^2} \frac{i}{i\gamma^5\gamma^j k_j - (m_+ + iX + i\frac{Z}{2}) - (m_- + Y - i\frac{Z}{2})\gamma^5} \right), \tag{3.59}$$

$$Y = \frac{W}{2} \text{Tr}_\gamma \left(\int \frac{d^2k}{(2\pi)^2} \frac{\gamma^5}{i\gamma^5\gamma^j k_j - (m_+ + iX + i\frac{Z}{2}) - (m_- + Y - i\frac{Z}{2})\gamma^5} \right), \tag{3.60}$$

$$Z = \frac{W_0}{4} \text{Tr}_\gamma \left(\int \frac{d^2k}{(2\pi)^2} \frac{1 - \gamma^5}{i\gamma^5\gamma^j k_j - (m_+ + iX + i\frac{Z}{2}) - (m_- + Y - i\frac{Z}{2})\gamma^5} \right), \tag{3.61}$$

and the $U_R(n) \times U_A(n)$ ansatz,

$$\langle X \rangle = (\Gamma_+ + \Gamma_-)\tau^3 + iX_0\tau^0, \tag{3.62}$$

$$\langle Y \rangle = Y_0\tau^0, \tag{3.63}$$

$$\langle Z \rangle = -2\Gamma_-\tau^3 + iZ_0\tau^0, \tag{3.64}$$

where $m_\pm = m \pm E_F/2$ and $\Gamma_\pm = \frac{\Gamma_2 \pm \Gamma_1}{2}$.

We define the real parameters J_1 and J_2 by

$$iJ_1\tau^3 + J_2\tau^0 \equiv \int \frac{d^2k}{(2\pi)^2} \frac{1}{k^2 + (m_+ + iX + i\frac{Z}{2})^2 + (m_- + Y - i\frac{Z}{2})^2}, \quad (3.65)$$

where by direct evaluation we find

$$J_1 = \frac{sign(\Gamma_-\tilde{m}_- - \Gamma_+\tilde{m}_+)}{8\pi}\left(\pi - 2\arctan\left(\frac{\tilde{m}_-^2 - \tilde{m}_+^2 - \Gamma_-^2 + \Gamma_+^2}{2|\Gamma_-\tilde{m}_- - \Gamma_+\tilde{m}_+|}\right)\right), \quad (3.66)$$

$$J_2 = -\frac{1}{8\pi}\log\left(\frac{\Lambda^4}{\left((\Gamma_+ + \Gamma_-)^2 + (\tilde{m}_+ + \tilde{m}_-)^2\right)\left((\Gamma_+ - \Gamma_-)^2 + (\tilde{m}_+ - \tilde{m}_-)^2\right)}\right), \quad (3.67)$$

with shifted

$$\tilde{m}_+ = m_+ - X_0 - Z_0, \quad (3.68)$$

$$\tilde{m}_- = m_- - Y_0, \quad (3.69)$$

and UV cutoff Λ. Written in terms of these parameters the saddle-point equations Eqs. (3.59) - (3.61) become

$$2\Gamma_- = W_0\left(J_1(\tilde{m}_+ + \tilde{m}_-) + J_2(\Gamma_+ + \Gamma_-)\right), \quad (3.70)$$

$$Z_0 = -W_0\left(J_1(\Gamma_+ + \Gamma_-) - J_2(\tilde{m}_+ + \tilde{m}_-)\right), \quad (3.71)$$

$$\Gamma_+ + \Gamma_- = -W\left(J_1\tilde{m}_+ + J_2\Gamma_+\right), \quad (3.72)$$

$$X_0 = -W\left(J_1\Gamma_+ - J_2\tilde{m}_+\right), \quad (3.73)$$

$$0 = W\left(J_1\tilde{m}_- + J_2\,\Gamma_-\right), \quad (3.74)$$

$$Y_0 = -W\left(J_1\,\Gamma_- + J_2\tilde{m}_-\right). \quad (3.75)$$

We solve these equations for $X_0, Y_0, Z_0, \Gamma_\pm$, and m_-:

$$m_- = \frac{-m_+ W_0\left(J_2 + W(J_1^2 + J_2^2)\right)}{2 + J_2(3W_0 + 4W) + W(3W_0 + 2W)(J_1^2 + J_2^2)}, \quad (3.76)$$

$$Y_0 = \frac{-m_+ W_0 W(J_1^2 + J_2^2)}{2 + J_2(3W_0 + 4W) + W(3W_0 + 2W)(J_1^2 + J_2^2)}, \quad (3.77)$$

$$\Gamma_- = \frac{E_1 W_0 J_1}{2 + J_2(3W_0 + 4W) + W(3W_0 + 2W)(J_1^2 + J_2^2)}, \quad (3.78)$$

$$\Gamma_+ + \Gamma_- = \frac{-2m_+ W J_1}{2 + J_2(3W_0 + 4W) + W(3W_0 + 2W)(J_1^2 + J_2^2)}, \quad (3.79)$$

$$Z_0 = \frac{2m_+ W_0\left(J_2 + W(J_1^2 + J_2^2)\right)}{2 + J_2(3W_0 + 4W) + W(3W_0 + 2W)(J_1^2 + J_2^2)}, \quad (3.80)$$

$$X_0 = \frac{m_+ W\left(2J_2 + (W_0 + 2W)(J_1^2 + J_2^2)\right)}{2 + J_2(3W_0 + 4W) + W(3W_0 + 2W)(J_1^2 + J_2^2)}. \quad (3.81)$$

Notice that Y_0, Γ_-, Z_0, and m_- vanish as $W_0 \to 0$. We treat $m_- = m - E_F/2$ as a variable in order to avoid an overly constrained set of equations; our interpretation is that W_0 and W disorders cause m/E_F to renormalize to a value determined by the saddle-point equations. To ensure the scattering rates $\Gamma_+ \pm \Gamma_- > 0$ of $\frac{1 \pm \gamma^5}{2} \Psi$ are positive, we require

$$J_1 \left(2 + J_2(3W_0 + 4W) + W(3W_0 + 2W) \left(J_1^2 + J_2^2 \right) \right) < 0. \qquad (3.82)$$

.

The retarded/advanced 2d Euclidean fermion Green's function that obtains from this saddle-point solution,

$$\bar{g}_{R/A} = \langle \mathbf{x} | \frac{1}{i\sigma_1 \partial_1 - i\sigma_2 \partial_2 + \left(m_+ - X_0 - Z_0 + \omega \pm i\Gamma_+ \right) - \left(m_- - Y_0 - \omega \pm i\Gamma_- \right) \sigma_3} | \mathbf{x}' \rangle$$
$$(3.83)$$

where ω parameterizes deviations about the Fermi energy, suggests how to absorb the logarithmic divergence J_2 into renormalized parameters. We first introduce the renormalization factors,

$$Z_R \equiv \frac{2 + J_2(3W_0 + 4W) + W(3W_0 + 2W) \left(J_1^2 + J_2^2 \right)}{(2 + W_0 J_2 + 2W J_2)}, \qquad (3.84)$$

$$Z_L \equiv \frac{J_2 + W(J_1^2 + J_2^2)}{J_2}. \qquad (3.85)$$

Then the renormalized $m_\pm$ and $\Gamma_\pm$ are

$$m_+^R = \frac{m_+ - X_0 - Z_0}{Z_R}, \qquad (3.86)$$

$$m_-^R = \frac{m_- - Y_0}{Z_L}, \qquad (3.87)$$

$$\Gamma_-^R = W_0 \frac{m_-^R J_1}{2 + (W_0 + 2W)J_2}, \qquad (3.88)$$

$$\Gamma_+^R = -\left(2W + W_0 \right) \frac{m_-^R J_1}{2 + (W_0 + 2W)J_2}. \qquad (3.89)$$

The condition (3.82) ensures the renormalized $\Gamma_+^R \pm \Gamma_-^R$ are positive. We use these renormalized parameters (without the R superscript) in the main text to find the θ angle.

3.D   Detailed NLSM Derivation

In this Appendix we detail the calculation of the NLSM for Q that is sketched in §3.3.

Setup

Here we have found it convenient to employ a different convention than the one used in the main text. The "translation table" between the two conventions is given below.

$$\Gamma_1 = \frac{\alpha_2 + \alpha_1}{2} \tag{3.90}$$

$$\Gamma_2 = \frac{\alpha_2 - \alpha_1}{2} \tag{3.91}$$

$$\Gamma_+ = \frac{\Gamma_2 + \Gamma_1}{2} = \frac{\alpha_2}{2} \tag{3.92}$$

$$\Gamma_- = \frac{\Gamma_2 - \Gamma_1}{2} = \frac{-\alpha_1}{2} \tag{3.93}$$

$$\gamma_1 = \sigma_y, \quad \gamma_2 = \sigma_x, \quad \gamma_5 = -\sigma_z. \tag{3.94}$$

Above $(\sigma_x, \sigma_y, \sigma_z)$ are the usual Pauli sigma matrices. Furthermore, we reflect both coordinates $(x, y) \to (-x, -y)$ and reverse the overall signs of the fermion and NLSM actions in (3.38):

$$e^{S_{NLSM}} = \int \mathcal{D}\Psi \mathcal{D}\Psi^\dagger \; e^S, \tag{3.95}$$

with

$$S = \int d^2x \; \Psi^\dagger \left(i\sigma_x \partial_x - i\sigma_y \partial_y - m_- \sigma_z + m_+ \sigma_0 + i\frac{\alpha_1 \sigma_z + \alpha_2 \sigma_0}{2} Q \right) \Psi. \tag{3.96}$$

Here σ_0 is the 2×2 identity matrix. In the dc limit of interest, $m_\pm = m \pm E_F/2$. The matrix boson $Q(\mathbf{x}) = U(\mathbf{x})\tau^3 U^\dagger(\mathbf{x})$ for $U(\mathbf{x}) \in U(2n)$ where $\tau^3 = \sigma_z \otimes \sigma_0^n$. Since all terms except for Q are singlets with respect to the replica indices (i.e., the τ space), we (generally) leave implicit the $2n \times 2n$ identity matrix τ_0 in this subspace.

We partially follow [30] to separately derive the real and imaginary parts of S_{NLSM}. Before proceeding, we define the self-consistent Born approximation (SCBA) Green's functions,

$$g_\pm \equiv \frac{1}{m_+ \sigma_0 + i\sigma_x \partial_x - i\sigma_y \partial_y - m_- \sigma_z \pm i(\frac{\alpha_1 \sigma_z + \alpha_2 \sigma_0}{2})\tau^3}, \tag{3.97}$$

which are related to the retarded and advanced Green's functions $g_{R,A}$ as follows:

$$(g_+)^\dagger = g_- \,, \quad g_+ = \mathrm{Diag}(g_R, g_A)_\tau, \quad g_- = \mathrm{Diag}(g_A, g_R)_\tau \tag{3.98}$$

$$g_+ - g_- = (g_R - g_A)\,\tau^3, \quad g_+ + g_- = (g_R + g_A)\,\tau_0. \tag{3.99}$$

Note that the $\pm$ subscript of $g_\pm$ labels the sign of the imaginary part of the Green's function; it is unrelated to the $\pm$ subscript of the masses $m_\pm$.

Real Part of S_{NLSM}

To compute the real part of S_{NLSM} we directly compute the fermion determinant implied by (3.95):

$$\mathrm{Re}(S_{\mathrm{NLSM}}) + i\mathrm{Im}(S_{\mathrm{NLSM}}) = \mathrm{Tr}\ln\left((m_+\,\sigma_0 - m_-\,\sigma_z + i\sigma_x\partial_x - i\sigma_y\partial_y) + i\,\frac{\alpha_1\sigma_z + \alpha_2\sigma_0}{2}\,Q\right).$$

(3.100)

For any operator $\hat{X}$ with determinant $\det\hat{X} = Re^{i\theta}$, we seek $\ln R$. Let $i\hat{C} \equiv i\left(\frac{\alpha_1\sigma_z + \alpha_2\sigma_0}{2}\right)Q$, $\hat{B} \equiv m_+\,\sigma_0 - m_-\,\sigma_z + i\sigma\partial_x - i\sigma_y\partial_y$, we can decompose the operator in 2×2 σ-space using the identities:

$$\det[i\hat{C} + \hat{B}] = \det[i\,\hat{C}] + \det[\hat{B}] + i\,\det[\hat{C}]\mathrm{Tr}[\hat{C}^{-1}\,\hat{B}], \quad (3.101)$$

$$\det[(\hat{B} + i\hat{C})\,\hat{H}^{-1}\,(\hat{B} - i\hat{C})\,\hat{H}] = \left|\det[i\hat{C} + \hat{B}]\right|^2, \quad (3.102)$$

where $\hat{H}$ is any constant matrix in σ-space that satifies $[\hat{C}, \hat{H}] = 0$. We choose $\hat{H} = \left(\frac{\alpha_1\sigma_z + \alpha_2\sigma_0}{2}\right)$. Up to an unimportant constant that we drop, we find

$$\begin{aligned}
\mathrm{Re}(S_{\mathrm{NLSM}}) =\ & \frac{1}{2}\mathrm{Tr}\ln\left[(g_+^{-1} - i\,\hat{H}\tau^3 + i\,\hat{H}\,Q)\,(\hat{H})^{-1}\,(g_-^{-1} + i\,\hat{H}\,\tau^3 - i\,\hat{H}\,Q)\right] \\
=\ & \frac{1}{2}\mathrm{Tr}\left[\left(\frac{i}{2}(g_R - g_A)\,\not{\nabla}Q\right) - \frac{1}{2}\left(\frac{i}{2}(g_R - g_A)\,\not{\nabla}Q\right)\left(\frac{i}{2}(g_R - g_A)\,\not{\nabla}Q\right)\right] \\
=\ & \frac{1}{16}\mathrm{Tr}_\sigma\left[(g_R - g_A)\,\kappa_a\,(g_R - g_A)\,\kappa_b\right]\mathrm{Tr}[\nabla_a Q\,\nabla_b Q] \\
\equiv\ & \frac{-S_{jk}}{8}\,\mathrm{Tr}[\nabla_j Q\,\nabla_k Q]
\end{aligned}$$

(3.103)

where $\frac{\not{\nabla}}{i} \equiv \kappa_x\frac{\partial_x}{i} + \kappa_y\frac{\partial_y}{i}$, $\kappa_x = \sigma_x, \kappa_y = -\sigma_y$. We identify $S_{jk} = \sigma_{xx}^{\mathrm{cf}}\delta_{jk}$ as the dc longitudinal conductivity:

$$\begin{aligned}
\sigma_{xx}^{\mathrm{cf}} =\ & -\frac{1}{2}\mathrm{Tr}\left[(g_R - g_A)\,\sigma_x\,(g_R - g_A)\,\sigma_x\right] & (3.104) \\
=\ & 1 + \frac{(4m_+^2 - 4m_-^2 - \alpha_1^2 + \alpha_2^2)(\pi + 2\mathrm{arccot}[\frac{|m_+\alpha_2 + m_-\alpha_1|}{4m_+^2 - 4m_-^2 + \alpha_1^2 - \alpha_2^2}])}{8|m_+\alpha_2 + m_-\alpha_1|} \\
\approx\ & \frac{\pi(m_+^2 - m_-^2)}{|m_+\alpha_2 + m_-\alpha_1|} \gg 1. & (3.105)
\end{aligned}$$

The last expression uses the weak disorder limit, i.e., $\mathcal{O}(E_F) \approx \mathcal{O}(m) \gg \alpha_2, \alpha_1$.

Here and below we use the dc ($\omega \to 0$) limit of the Kubo formula:

$$\begin{aligned}
\sigma_{ij}^{\mathrm{cf}}(q \to 0, \omega + i\eta) =\ & -\int\frac{d^2\mathbf{r}'}{V}\int d^2\mathbf{r}\,\frac{1}{2\pi\omega}\int_{-\infty}^{\infty}dz \\
& \times\left(\int_{-\infty}^{\infty}dz\left([f(z) - f(z-\omega)]\,\mathrm{Tr}[\kappa_i G_z^R(r, r')\kappa_j\,G_{z-\omega}^A(r', r)]\right.\right. \\
& \left.+\ f(z)\,\mathrm{Tr}[\kappa_i G_{z+\omega}^R(r, r')\kappa_j\,G_z^R(r', r)]\right.
\end{aligned}$$

$$- f(z) \operatorname{Tr}[\kappa_i G_z^A(r,r')\kappa_j G_{z-\omega}^A(r',r)] \bigg). \tag{3.106}$$

For the Dirac theory, the SCBA Green's function is

$$G_D(\epsilon + E_F;\omega)_{R/A} = \frac{1}{(\epsilon + E_F + \omega)\sigma_0 - m_D\sigma_z + i\partial_x\sigma_x - i\partial_y\sigma_y \pm i\frac{\alpha_1\sigma_z+\alpha_2\sigma_0}{2}} \tag{3.107}$$

For the linearized HLR theory,

$$g(\epsilon + E_F;\omega)_{R/A} = \frac{1}{(\epsilon + E_F)\sigma_0 + \omega P_1 + 2m_- P_2 + i\partial_x\sigma_x - i\partial_y\sigma_y \pm i\frac{\alpha_1\sigma_z+\alpha_2\sigma_0}{2}} \tag{3.108}$$

where $P_1 = \frac{1+\sigma_z}{2}$, $P_2 = \frac{1-\sigma_z}{2}$. The frequency term should be thought as "mass" term in the Hamiltonian instead of the physical frequency appear in (3.106); otherwise it's unable to match the object defined in Kubo formula. Notice that since we've included the Fermi level in the above Greens function, we only need to perform the energy integral $\int dz f(z)$ up to zero. We comment that a direct calculation of the Hall conductivity using the above SCBA Green's functions agrees with the results below, up to the crucial additive term equal to $\frac{1}{2}$.

Goldstone Parameterization

In the main text we argued that the massless Goldstone modes correspond to $Q_1 = Q_2$ fluctuations, where the matrix bosons $Q_1, Q_2 \in U(2n)/U(n) \times U(n)$. The $Q_1 = Q_2$ fluctuations correspond to "vector" gauge transformations of Ψ. Here we show explicitly that "axial" gauge transformations corresponding to $Q_1 \neq Q_2$ fluctuations are massive.

Consider the two-field sigma model

$$S[Q_1,Q_2] \equiv \operatorname{Tr} ln\left[\left(m_+\sigma_0 - m_-\sigma_z + i\sigma_x\partial_x - i\sigma_y\partial_y\right) + \begin{pmatrix} i\Gamma_1 Q_1 & 0 \\ 0 & i\Gamma_2 Q_2 \end{pmatrix}_\sigma\right] \tag{3.109}$$

Using the same logic that produced (3.103) with $\hat{H} = (\frac{\alpha_1\sigma_z+\alpha_2\mathbf{1}_\sigma}{2}) = i\Gamma_1 P_1 + i\Gamma_2 P_2$, $P_1 = \frac{1+\sigma_z}{2}, P_2 = \frac{1-\sigma_z}{2}$, and including a test function f, we calculate

$$(g_+^{-1} - i\hat{H}\tau^3 + i\Gamma_1 Q_1 P_1 + i\Gamma_2 Q_2 P_2)(\hat{H})^{-1}(g_-^{-1} + i\hat{H}\tau^3 - i\Gamma_1 Q_1 P_1 - iQ_2 P_2)\, f$$
$$= g_+^{-1}\hat{H}^{-1} g_-^{-1} f + \not{\nabla}(Q_V\mathbf{1}_\sigma + Q_A\sigma_z)f + (\not{\nabla}f)(Q_V\mathbf{1}_\sigma + Q_A\sigma_z) - (Q_V\mathbf{1}_\sigma + Q_A\sigma_z)(\not{\nabla}f)$$
$$= g_+^{-1}\hat{H}^{-1} g_-^{-1} f + \not{\nabla}(Q_V\mathbf{1}_\sigma + Q_A\sigma_z)f - 2Q_A\sigma_z(\not{\nabla}f), \tag{3.110}$$

where we've used $Q_1^2 = Q_2^2 = \mathbf{1}$ and introduced "vector" $Q_V = \frac{1}{2}(Q_1 + Q_2)$ and "axial" $Q_A = \frac{1}{2}(Q_1 - Q_2)$. The crucial term that leads to a mass for Q_A

is $-2Q_A\,\sigma_z\,\slashed{V}$. We find

$$\mathrm{Re}[S[Q_1,Q_2]] = \frac{1}{2}\mathrm{Tr}\ln\left[(g_+^{-1}\hat{H}^{-1}g_-^{-1})\left(\mathbf{1}+(g_-\,\hat{H}\,g_+)\,(\slashed{V}Q_V+\slashed{V}Q_A\sigma_z-2Q_A\sigma_z\slashed{V}))\right]\right]$$

$$= \frac{1}{16}\mathrm{Tr}\left[(g_R-g_A)\left(\slashed{V}Q_V+\slashed{V}Q_A\sigma_z-2Q_A\sigma_z\slashed{V}\right)(g_R-g_A)\left(\slashed{V}Q_V+\slashed{V}Q_A\sigma_z-2Q_A\sigma_z\slashed{V}\right)$$

(3.111)

Consider the last term quadratic in $Q_A\slashed{V}$:

$$\frac{1}{4}\mathrm{Tr}\left[(g_R-g_A)\left(Q_A\sigma_z\slashed{V}\right)(g_R-g_A)\left(Q_A\sigma_z\slashed{V}\right)\right]$$ (3.112)

$$= \int_{x,x_1,x_2,x_3}\int_{k_1k_2k_3k_4}\frac{1}{4}\mathrm{Tr}\Big[\langle x|(g_R-g_A)|k_1\rangle\langle k_1|x_1\rangle\langle x_1|Q_A\sigma_z\slashed{V}|k_2\rangle\langle k_2|x_2\rangle$$

$$\langle x_2|(g_R-g_A)|k_3\rangle\langle k_3|x_3\rangle\langle x_3|Q_A\sigma_z\slashed{V}|k_4\rangle\langle k_4|x\rangle\Big]$$ (3.113)

$$= \frac{-1}{4}\int_{k_1,k_2}\mathrm{Tr}[(g_R-g_A)\big|_{k_1}Q_A(k_2-k_1)\sigma_z\slashed{k_2}(g_R-g_A)\big|_{k_2}Q_A(k_1-k_2)\sigma_z\slashed{k_1}]$$ (3.114)

$$= \frac{-1}{4}\int_p Q_A(p)Q_A(-p)\int_{k_1}\mathrm{Tr}[(g_R-g_A)\big|_{k_1}\sigma_z(\slashed{p}+\slashed{k_1})(g_R-g_A)\big|_{k_1+p}\sigma_z\slashed{k_1}]$$ (3.115)

$$\equiv \frac{-1}{4}\int_p Q_A(p)Q_A(-p)\,F(p)$$

$$= \frac{-1}{4}\int_p Q_A(p)Q_A(-p)\left(F(p=0)+\frac{\partial F}{\partial\slashed{p}}\Big|_{p=0}\slashed{p}+\frac{1}{2}\frac{\partial^2 F}{\partial\slashed{p}^2}\Big|_{p=0}\slashed{p}^2+...\right)$$ (3.116)

where we made the change of variables $k_2-k_1\equiv p$.

Next, examine the two crossing terms containing $Q_A\slashed{V}$ and $\slashed{V}Q_A$:

$$\frac{1}{16}\mathrm{Tr}\left[(g_R-g_A)(\slashed{V}Q_A\sigma_z)(g_R-g_A)(-2Q_A\sigma_z\slashed{V})+(g_R-g_A)(-2Q_A\sigma_z\slashed{V})(g_R-g_A)(\slashed{V}Q_A\sigma_z)\right]$$

$$= \frac{-1}{4}\mathrm{Tr}\left[(g_R-g_A)(\slashed{V}Q_A\sigma_z)(g_R-g_A)(Q_A\sigma_z\slashed{V})\right]$$ (3.117)

$$= \frac{-1}{4}\int_{dp}Q_A(p)\,Q_A(-p)\int_{dk_1}\mathrm{Tr}\left[(g_R-g_A)\big|_{k_1}\sigma_z\slashed{k_1}(g_R-g_A)\big|_{p+k_1}\sigma_z\slashed{k_1}\right]$$ (3.118)

Combining Eq. (3.116) and (3.118), the total mass term for Q_A is $\frac{-1}{2}\int_{dp_1}Q_A(p_1)Q_A(-p_1)F(0)$. The function $F(0)\neq 0$ generally: Q_A is only massless if it's tuned to criticality. This is in sharp contrast to Q_V, which is massless because it's a Goldstone boson. Thus, Q_A is generally massive and we neglect it at low energies.

Imaginary Part of S_{NLSM}

To calculate the imaginary part of S_{NLSM} in (3.95), we first set $n=1$ and perform the gauge transformation $\Psi(\mathbf{x})\to U(\mathbf{x})\Psi(\mathbf{x})$ to introduce the gauge field $A_j(\mathbf{x})=iU^\dagger(\mathbf{x})\partial_j U(\mathbf{x})=\sum_{b=1}^3 A_j^b\,\tau_b$ where (τ_1,τ_2,τ_3) are the Pauli matrices

in retarded-advanced space. We determine $\text{Im}\big(S_{\text{NLSM}}\big)$ from the imaginary part of the expectation value of the current (calculated to linear order in A_j):

$$i\frac{\delta\big(\text{Im}S_{\text{NLSM}}\big)}{\delta A_j^b} = \frac{\delta S_{\text{top}}^I}{\delta A_j^b} + \frac{\delta S_{\text{top}}^{II}}{\delta A_j^b}, \tag{3.119}$$

where S_{top}^I and S_{top}^{II} are the linear ("quantum") and quadratic ("classical") in A_j contributions to the imaginary part of S_{NLSM} [42].

S_{top}^{II}

We begin with the "classical" contribution S_{top}^{II}. By direct evaluation we find

$$
\begin{aligned}
S_{\text{top}}^{II} &= \frac{1}{2}\text{Tr}[\kappa_\mu\, A_\mu\, g_+\kappa_\nu\, A_\nu\, g_+ \ - \kappa_\mu\, A_\mu\, g_-\kappa_\nu\, A_\nu\, g_-] \\
&= \frac{1}{2}\text{Tr}[\kappa_\mu\, A_\mu(g_+ + g_-)\,\kappa_\nu\, A_\nu(g_+ - g_-)] \\
&= \frac{i}{2}\text{Tr}_\sigma[\kappa_\mu\,(g_R + g_A)\,\kappa_\nu\,(g_R - g_A)]\,\text{Tr}_\tau[A_\mu A_\nu\,\tau_3] \\
&= \frac{i}{4}\text{Tr}_\sigma[\kappa_x\,(g_R + g_A)\kappa_y\,(g_R - g_A)]\text{Tr}_\tau[Q(\partial_x Q)(\partial_y Q)] \\
&\equiv i\frac{\theta^{II}}{2\pi}\text{Tr}_\tau[Q(\partial_x Q)(\partial_y Q)] \tag{3.120}
\end{aligned}
$$

where we used $\text{Tr}_\tau[Q(\partial_x Q)(\partial_y Q)] = 4i(A_i^1 A_j^2 - A_i^2 A_j^1)\epsilon_{ij}$. $\frac{\theta^{II}}{2\pi}$ is the "classical" contribution σ_{xy}^I to the dc Hall conductivity $\sigma_{xy}^{\text{cf}} = \sigma_{xy}^I + \sigma_{xy}^{II}$:

$$
\begin{aligned}
\sigma_{xy}^I &= \frac{1}{2\pi}\left(\frac{2m(\alpha_1 + \alpha_2) - \mu_F(\alpha_2 - \alpha_1)}{2m(\alpha_1 + \alpha_2) + \mu_F(\alpha_2 - \alpha_1)}\right)\left(\tan^{-1}[\frac{4m}{\alpha_2 - \alpha_1}] + \tan^{-1}[\frac{2E_F}{\alpha_2 + \alpha_1}]\right) \\
&= \frac{-1}{2\pi}\left(\frac{m_-\Gamma_+ - m_+\Gamma_-}{m_+\Gamma_+ - m_-\Gamma_-}\right)\left(\arctan[\frac{2(\Gamma_+ + \Gamma_-)}{2(m_+ + m_-)}] + \arctan[\frac{2(\Gamma_+ - \Gamma_-)}{2(m_+ - m_-)}]\right) \tag{3.121}
\end{aligned}
$$

The "quantum" contribution σ_{xy}^{II} to the Hall conductivity equals $\frac{\theta^I}{2\pi}$ (modulo 1); it's calculated in the next section.

S_{top}^I

S_{top}^I obtains from a result first obtained by Goldstone and Wilczek [10]; below we follow the treatment in [7]. We first introduce the "mass field,"

$$\Phi_m(0) \equiv m_+\sigma_0 - m_-\sigma_z + i(\frac{\alpha_1\sigma_z + \alpha_2\sigma_0}{2})\,\tau_3. \tag{3.122}$$

For this calculation, we'll treat $\Phi_m(0)$ as a spatially-varying field $\Phi_m(\mathbf{x})$ that takes its fixed point value (3.122) at the end of the calculation. We parame-

terize the "mass field" as

$$\Phi_m(x) \equiv m_1(x)\sigma_z + m_2(x)\sigma_0$$
$$\equiv \big(m_{1a}(x)\,\tau_3 + m_{1b}(x)\,\tau_0\big)\,\sigma_z + \big(m_{2a}(x)\,\tau_3 + m_{2b}(x)\,\tau_0\big)\sigma_0. \quad (3.123)$$

The fixed point values of these masses in two theories are

$$\begin{cases} \text{(HLR)} \quad m_1 = -m_- + i\frac{\alpha_1}{2}\tau_z \ , \quad m_2 = m_+ + i\frac{\alpha_2}{2}\tau_z \\ \text{(Dirac)} \quad m_1 = -m_D + i\frac{\alpha_1}{2}\tau_z, \quad m_2 = E_F + i\frac{\alpha_2}{2}\tau_z \end{cases} \quad . \quad (3.124)$$

The real space Green's function is then expanded about uniform Φ_m as

$$\begin{aligned} S(\Phi_m) &= \int \frac{dp_1 dp_2}{(2\pi)^2} \frac{1}{i\kappa_\mu D_\mu + \Phi_m(x)} e^{i\boldsymbol{p}\cdot(x-y)} \\ &= S_0 + \Big(- S_0\big(x_\nu\partial_\nu\Phi_m(0)\big)\,S_0 \Big) + \dots, \quad (3.125) \end{aligned}$$

where we drop the "..." in what follows. S_0 is the Green's function for uniform Φ_m with $S_0\big|_{A_j=0} = g_+$, defined (3.97)

The "quantum" current $\frac{\delta S^I_{top}}{\delta A^b_j}$ is then computed as

$$\begin{aligned} \frac{\delta S^I_{top}}{\delta A^b_j} &= - \lim_{y\to x} \text{Tr}[\langle \kappa_j\,\tau_b\,S(x,y)\rangle] \\ &\approx \langle x|\text{Tr}[\kappa_j\,\tau_b\,S_0\,\partial_k\Phi_m(0)\,iS_0\,\kappa_k\,S_0\,]|x\rangle, \quad (3.126) \end{aligned}$$

where we use $\langle x'|S_0\,\hat{r}_k|x\rangle = \langle x'|iS_0\,\kappa_k\,S_0|x\rangle$. We set the gauge potential in the Green's function S_0 to zero to find

$$\begin{aligned} \frac{\delta S^I_{top}}{\delta A^b_j} &= \int \frac{dq_x dq_y}{(2\pi)^2} \text{Tr}[\kappa_j\,\tau_b \frac{1}{\slashed{q} + \Phi_m(0)}\partial_k\Phi_m(0)\frac{1}{\slashed{q} + \Phi_m(0)}i\,\kappa_k\frac{1}{\slashed{q} + \Phi_m(0)}] \\ &= \frac{-1}{2\pi}\epsilon_{jk}\,\delta_{b3}\Big[\frac{(m_{2a} + m_{2b})\,\partial_k(m_{1a} + m_{1b}) - (m_{1a} + m_{1b})\,\partial_k(m_{2a} + m_{2b})}{(m_{1a} + m_{1b})^2 - (m_{2a} + m_{2b})^2} \\ &\quad - \frac{(-m_{2a} + m_{2b})\,\partial_k(-m_{1a} + m_{1b}) - (-m_{1a} + m_{1b})\,\partial_k(-m_{2a} + m_{2b})}{(-m_{1a} + m_{1b})^2 - (-m_{2a} + m_{2b})^2} \Big] \end{aligned}$$
$$\equiv \frac{i}{2\pi}\delta_{b3}\epsilon_{jk}\partial_k\,\theta^I,$$

$$(3.127)$$

where $\slashed{q} \equiv \kappa_x p_x + \kappa_y p_y$. We now deduce S^I_{top} by coupling this current to A^b_j and then performing an integration by parts:

$$S^I_{top} = \int d^2x \sum_{b=1}^3 A^b_j \frac{\delta S^I_{top}}{\delta A^b_j}$$

$$= \frac{i}{2\pi} \int d^2x \; A_j^3 \; \epsilon_{jk}\partial_k\theta^I$$
$$= -\frac{1}{4\pi} \int d^2x \; \theta^I \epsilon_{jk}\mathrm{Tr}_\tau[\tau^3\partial_k \; A_j]. \tag{3.128}$$

We now explain in detail how to obtain the specific value of θ^I for the fixed point value $\Phi_m(0)$ (3.122). This complements the discussion in the main text. To translate to the notation in the main text, we replace $m_2 \to \varphi_1, m_1 \to -\varphi_2$, $\frac{\alpha_2+\alpha_1}{2} = \Gamma_1$, $\frac{\alpha_2-\alpha_1}{2} = \Gamma_2$. We also use subscript $s = R, A$ to label the retarded and advanced components in τ space.

In Eq. 3.127, we observe that the retarded and advanced contributions are fully separable, i.e., θ^I only couples to $\frac{1}{2}\mathrm{Tr}(\tau^3 A_j) = A_j^3$. This allows us to determine θ^I as the contribution from the $U(1)$ subgroup of $SU(2)$. We write

$$\Phi_m^s(x) = -\varphi_2^s(x)\sigma_z + \varphi_1^s(x)\sigma_0 \equiv \begin{pmatrix} -e^{-i\chi_2^s} & 0 \\ 0 & e^{i\chi_1^s} \end{pmatrix}. \tag{3.129}$$

Plugging into Eq. 3.127, we find

$$-\partial_k\theta^I = \partial_k \frac{\chi_1^R + \chi_2^R - \chi_1^A - \chi_2^A}{2}. \tag{3.130}$$

In the above parameterizations, χ_1, χ_2 are generally complex. We restrict that $\mathrm{Re}[\chi_{1,2}] \in [0, \pi)$. We use $\varphi_1 + \varphi_2 = e^{i\chi_1}$, $\varphi_1 - \varphi_2 = -e^{-i\chi_2}$ and (3.122) to find the equations:

$$2m + i\Gamma_2 = e^{i\chi_1^R}, \qquad E_F + i\Gamma_1 = -e^{-i\chi_2^R}, \tag{3.131}$$
$$2m - i\Gamma_2 = e^{i\chi_1^A}, \qquad E_F - i\Gamma_1 = -e^{-i\chi_2^A}. \tag{3.132}$$

For retarded field $\chi_{1,2}^R$, we find the solution:

$$\mathrm{Re}[\chi_1^R] = \arctan[\frac{\Gamma_2}{2m}], \;\; \mathrm{Im}[\chi_1^R] = \frac{-1}{2}\log[(2m)^2 + (\Gamma_2)^2], \tag{3.133}$$
$$\mathrm{Re}[\chi_2^R] = \pi - \arctan[\frac{\Gamma_1}{E_F}], \;\; \mathrm{Im}[\chi_2^R] = \frac{-1}{2}\log[(E_F)^2 + (\Gamma_1)^2]. \tag{3.134}$$

Due to the restriction $\mathrm{Re}[\chi_{1,2}] \in [0, \pi)$, we need to perform a charge conjugation on the advanced fermion part of the action $S_A \to \mathcal{C}S_A\mathcal{C}$ defined in Eq. 3.16. It is in this step that we use the fact that θ^I is only sensitive to the Abelian $\frac{1}{2}\mathrm{Tr}(\tau^3 A_j)$ component of A_j. Charge conjugation flips the sign of mass term involving σ_0 as well as the gauge coupling of the advanced fermion

to A_j^3:

$$S_A = \Psi_A^\dagger\Big(m_+\sigma_0 - m_-\sigma_z + i\sigma_x(\partial_x - iA_x^3) - i\sigma_y(\partial_y - iA_y^3) - i\frac{\alpha_1\sigma_z + \alpha_2\sigma_0}{2}\Big)\,\Psi_A, \quad (3.135)$$

$$\mathcal{C}S_A\mathcal{C} = \Psi_A^\dagger\Big(-m_+\sigma_0 - m_-\sigma_z + i\sigma_x(\partial_x + iA_x^3) - i\sigma_y(\partial_y + iA_y^3) - i\frac{\alpha_1\sigma_z - \alpha_2\sigma_0}{2}\Big)\Psi_A. \quad (3.136)$$

In this new basis, i.e., after the charge conjugation, we find the current $\frac{\delta S_{top}^I}{\delta A_j^b}$ equals

$$\frac{\delta S_{top}^I}{\delta A_j^b} = \frac{-1}{2\pi}\epsilon_{jk}\,\delta_{b3}\Big[\frac{(m_{2a}+m_{2b})\,\partial_k(m_{1a}+m_{1b}) - (m_{1a}+m_{1b})\,\partial_k(m_{2a}+m_{2b})}{(m_{1a}+m_{1b})^2 - (m_{2a}+m_{2b})^2}$$

$$+\frac{(-1)\,(-m_{2a}+m_{2b})\,\partial_k(-m_{1a}+m_{1b}) - (-m_{1a}+m_{1b})\,(-1)\partial_k(-m_{2a}+m_{2b})}{(-m_{1a}+m_{1b})^2 - (-m_{2a}+m_{2b})^2}\Big]$$

$$\equiv \frac{i}{2\pi}\delta_{b3}\epsilon_{jk}\partial_k\,\theta^I. \tag{3.137}$$

The retarded contribution to θ^I is unchanged. The advanced fermion mass becomes

$$\Phi_m^A(x) = -\varphi_2^A(x)\sigma_z + (-1)\varphi_1^A(x)\sigma_0 \equiv \begin{pmatrix} -e^{-i\tilde\chi_2^A} & 0 \\ 0 & e^{i\tilde\chi_1^A} \end{pmatrix} \tag{3.138}$$

where $\phi_2^A = -m_1^A = m_- + \frac{i\alpha_1}{2}$, $\varphi_1^A(x) = m_2^A = m_+ - \frac{i\alpha_2}{2}$. This results in the equations:

$$2m - \Gamma_2 = e^{i\tilde\chi_2^A}, \qquad -E_F + i\Gamma_1 = e^{i\tilde\chi_1^A}, \tag{3.139}$$

$$\mathrm{Re}[\tilde\chi_2^A] = \arctan[\frac{\Gamma_2}{2m}], \qquad \mathrm{Re}[\tilde\chi_1^A] = \pi - \arctan[\frac{\Gamma_1}{E_F}] \tag{3.140}$$

Since charge conjugation also flips relative sign between retarded and advanced contributions in Eq. 3.130, we have

$$\theta^I = -\frac{1}{2}\Big[(\mathrm{Re}[\chi_1^R] + \mathrm{Re}[\chi_2^R] + \mathrm{Re}[\tilde\chi_1^A] + \mathrm{Re}[\tilde\chi_2^A])\Big] \tag{3.141}$$

$$= \pi + \arctan[\frac{\Gamma_+ - \Gamma_-}{m_+ - m_-}] - \arctan[\frac{\Gamma_+ + \Gamma_-}{m_+ + m_-}]. \tag{3.142}$$

We have used $\theta^I = 0 \pmod{2\pi}$ to fix the coefficient of π to be unity.

BIBLIOGRAPHY

[1]   Alexander Altland. "Low-Energy Theory of Disordered Graphene". In: *Phys. Rev. Lett.* 97 (23 Dec. 2006), p. 236802. URL: https://link.aps.org/doi/10.1103/PhysRevLett.97.236802.

[2]   Alexander Altland, B.D. Simons, and M.R. Zirnbauer. "Theories of low-energy quasi-particle states in disordered d-wave superconductors". In: *Physics Reports* 359.4 (2002), pp. 283–354. ISSN: 0370-1573. URL: http://www.sciencedirect.com/science/article/pii/S0370157301000655.

[3]   Alexander Altland and Ben Simons. *Condensed Matter Field Theory*. Cambridge University Press, 2010.

[4]   B. L. Altshuler and L. B. Ioffe. "Motion of fast particles in strongly fluctuating magnetic fields". In: *Phys. Rev. Lett.* 69 (20 Nov. 1992), pp. 2979–2982. URL: https://link.aps.org/doi/10.1103/PhysRevLett.69.2979.

[5]   A. G. Aronov, A. D. Mirlin, and P. Wölfle. "Localization of charged quantum particles in a static random magnetic field". In: *Phys. Rev. B* 49 (23 June 1994), pp. 16609–16613. URL: https://link.aps.org/doi/10.1103/PhysRevB.49.16609.

[6]   E. Brezin, S. Hikami, and Jean Zinn-Justin. "Generalized Nonlinear Σ Models With Gauge Invariance". In: *Nucl. Phys. B* 165 (1980), pp. 528–544.

[7]   Claudio Chamon et al. "Electron fractionalization for two-dimensional Dirac fermions". In: *Phys. Rev. B* 77 (23 June 2008), p. 235431. URL: https://link.aps.org/doi/10.1103/PhysRevB.77.235431.

[8]   Eduardo Fradkin. *Field Theories of Condensed Matter Physics*. Cambridge University Press, 2013.

[9]   Kazuo Fujikawa. "Path integral for gauge theories with fermions". In: *Phys. Rev. D* 21 (10 May 1980), pp. 2848–2858. URL: https://link.aps.org/doi/10.1103/PhysRevD.21.2848.

[10]   Jeffrey Goldstone and Frank Wilczek. "Fractional Quantum Numbers on Solitons". In: *Phys. Rev. Lett.* 47 (14 Oct. 1981), pp. 986–989. URL: https://link.aps.org/doi/10.1103/PhysRevLett.47.986.

[11]   Pallab Goswami and Sudip Chakravarty. "Superuniversality of topological quantum phase transition and global phase diagram of dirty topological systems in three dimensions". In: *Phys. Rev. B* 95 (7 Feb. 2017), p. 075131. URL: https://link.aps.org/doi/10.1103/PhysRevB.95.075131.

[12] B. I. Halperin, Patrick A. Lee, and Nicholas Read. "Theory of the half-filled Landau level". In: *Phys. Rev. B* 47 (12 Mar. 1993), pp. 7312–7343. URL: http://link.aps.org/doi/10.1103/PhysRevB.47.7312.

[13] Kevin S. Huang, S. Raghu, and Prashant Kumar. "Numerical Study of a Dual Representation of the Integer Quantum Hall Transition". In: *Phys. Rev. Lett.* 126 (5 Feb. 2021), p. 056802. URL: https://link.aps.org/doi/10.1103/PhysRevLett.126.056802.

[14] Bodo Huckestein. "Scaling theory of the integer quantum Hall effect". In: *Rev. Mod. Phys.* 67 (2 Apr. 1995), pp. 357–396. URL: https://link.aps.org/doi/10.1103/RevModPhys.67.357.

[15] Aaron Hui, Eun-Ah Kim, and Michael Mulligan. "Non-Abelian bosonization and modular transformation approach to superuniversality". In: *Phys. Rev. B* 99 (12 Mar. 2019), p. 125135. URL: https://link.aps.org/doi/10.1103/PhysRevB.99.125135.

[16] Y. Huo, R. E. Hetzel, and R. N. Bhatt. "Universal conductance in the lowest Landau level". In: *Phys. Rev. Lett.* 70 (4 Jan. 1993), pp. 481–484. URL: https://link.aps.org/doi/10.1103/PhysRevLett.70.481.

[17] Jainendra K. Jain. *Composite Fermions*. Cambridge University Press, 2007.

[18] D. V. Khveshchenko and S. V. Meshkov. "Particle in a random magnetic field on a plane". In: *Phys. Rev. B* 47 (18 May 1993), pp. 12051–12058. URL: https://link.aps.org/doi/10.1103/PhysRevB.47.12051.

[19] Yong Baek Kim et al. "Gauge-invariant response functions of fermions coupled to a gauge field". In: *Phys. Rev. B* 50 (1994), p. 17917.

[20] S. A. Kivelson et al. "Composite-fermion Hall conductance at $\nu = 1/2$". In: *Phys. Rev. B* 55 (23 1997), p. 15552. URL: http://link.aps.org/doi/10.1103/PhysRevB.55.15552.

[21] Walter Kohn. "Cyclotron Resonance and de Haas-van Alphen Oscillations of an Interacting Electron Gas". In: *Phys. Rev.* 123 (4 Aug. 1961), pp. 1242–1244. URL: https://link.aps.org/doi/10.1103/PhysRev.123.1242.

[22] Prashant Kumar, Yong Baek Kim, and S. Raghu. "Self-duality of the integer quantum Hall to insulator transition: Composite fermion description". In: *Phys. Rev. B* 100 (23 Dec. 2019), p. 235124. URL: https://link.aps.org/doi/10.1103/PhysRevB.100.235124.

[23] Prashant Kumar, Michael Mulligan, and S. Raghu. "Emergent reflection symmetry from nonrelativistic composite fermions". In: *Phys. Rev. B* 99 (20 May 2019), p. 205151. URL: https://link.aps.org/doi/10.1103/PhysRevB.99.205151.

[24] Prashant Kumar, Michael Mulligan, and S. Raghu. "Topological phase transition underpinning particle-hole symmetry in the Halperin-Lee-Read theory". In: *Phys. Rev. B* 98 (11 Sept. 2018), p. 115105. URL: https://link.aps.org/doi/10.1103/PhysRevB.98.115105.

[25] Prashant Kumar, P. A. Nosov, and S. Raghu. "Interaction effects on quantum Hall transitions: dynamical scaling laws and superuniversality". In: *arXiv e-prints*, arXiv:2006.11862 (June 2020), arXiv:2006.11862. arXiv: 2006.11862 [cond-mat.str-el].

[26] Prashant Kumar, S. Raghu, and Michael Mulligan. "Composite fermion Hall conductivity and the half-filled Landau level". In: *Phys. Rev. B* 99 (23 June 2019), p. 235114. URL: https://link.aps.org/doi/10.1103/PhysRevB.99.235114.

[27] Herbert Levine, Stephen B. Libby, and Adrianus M. M. Pruisken. "Electron Delocalization by a Magnetic Field in Two Dimensions". In: *Phys. Rev. Lett.* 51 (20 Nov. 1983), pp. 1915–1918. URL: https://link.aps.org/doi/10.1103/PhysRevLett.51.1915.

[28] M. A. Metlitski and A. Vishwanath. "Particle-vortex duality of two-dimensional Dirac fermion from electric-magnetic duality of three-dimensional topological insulators". In: *Phys. Rev. B* 93.24, 245151 (June 2016), p. 245151. arXiv: 1505.05142 [cond-mat.str-el].

[29] Chetan Nayak. "Quantum Condensed Matter Physics - Lecture Notes".

[30] P. M. Ostrovsky, I. V. Gornyi, and A. D. Mirlin. "Quantum Criticality and Minimal Conductivity in Graphene with Long-Range Disorder". In: *Phys. Rev. Lett.* 98 (25 June 2007), p. 256801. URL: https://link.aps.org/doi/10.1103/PhysRevLett.98.256801.

[31] P. M. Ostrovsky, I. V. Gornyi, and A. D. Mirlin. "Theory of anomalous quantum Hall effects in graphene". In: *Phys. Rev. B* 77 (19 May 2008), p. 195430. URL: https://link.aps.org/doi/10.1103/PhysRevB.77.195430.

[32] W. Pan et al. "Particle-Hole Symmetry and the Fractional Quantum Hall Effect in the Lowest Landau Level". In: *Phys. Rev. Lett.* 124 (15 Apr. 2020), p. 156801. URL: https://link.aps.org/doi/10.1103/PhysRevLett.124.156801.

[33] Michael E. Peskin and Daniel V. Schroeder. *An Introduction to quantum field theory*. Reading, USA: Addison-Wesley, 1995. ISBN: 9780201503975, 0201503972. URL: http://www.slac.stanford.edu/~mpeskin/QFT.html.

[34] A. M. M. Pruisken. "Dilute instanton gas as the precursor to the integral quantum Hall effect". In: *Phys. Rev. B* 32 (4 Aug. 1985), pp. 2636–2639. URL: https://link.aps.org/doi/10.1103/PhysRevB.32.2636.

[35] A.M.M. Pruisken. "On localization in the theory of the quantized hall effect: A two-dimensional realization of the θ-vacuum". In: *Nuclear Physics B* 235.2 (1984), pp. 277–298. ISSN: 0550-3213. URL: http://www.sciencedirect.com/science/article/pii/0550321384901019.

[36] Xiao-Liang Qi, Taylor L. Hughes, and Shou-Cheng Zhang. "Topological field theory of time-reversal invariant insulators". In: *Phys. Rev. B* 78 (19 Nov. 2008), p. 195424.

[37] Björn Sbierski et al. "Criticality of two-dimensional disordered Dirac fermions in the unitary class and universality of the integer quantum Hall transition". In: *arXiv e-prints*, arXiv:2008.09025 (Aug. 2020), arXiv:2008.09025. arXiv: 2008.09025 [cond-mat.mes-hall].

[38] N. Seiberg et al. "A duality web in 2 + 1 dimensions and condensed matter physics". In: *Annals of Physics* 374 (Nov. 2016), pp. 395–433. arXiv: 1606.01989 [hep-th].

[39] E. Shimshoni, S. L. Sondhi, and D. Shahar. "Duality near quantum Hall transitions". In: *Phys. Rev. B* 55 (20 1997), p. 13730. URL: http://link.aps.org/doi/10.1103/PhysRevB.55.13730.

[40] Dam Thanh Son. "Is the Composite Fermion a Dirac Particle?" In: *Phys. Rev. X* 5 (3 2015), p. 031027.

[41] S. L. Sondhi et al. "Continuous quantum phase transitions". In: *Rev. Mod. Phys.* 69 (1 1997), p. 315. URL: http://link.aps.org/doi/10.1103/RevModPhys.69.315.

[42] P Streda. "Theory of quantised Hall conductivity in two dimensions". In: *Journal of Physics C: Solid State Physics* 15.22 (Aug. 1982), pp. L717–L721. URL: https://doi.org/10.1088/0022-3719/15/22/005.

[43] K. Takahashi and K. B. Efetov. "Effect of spin on electron motion in a random magnetic field". In: *Phys. Rev. B* 66 (16 Oct. 2002), p. 165304. URL: https://link.aps.org/doi/10.1103/PhysRevB.66.165304.

[44] Peter van Nieuwenhuizen and Andrew Waldron. "On Euclidean spinors and Wick rotations". In: *Physics Letters B* 389 (Feb. 1996), pp. 29–36. arXiv: hep-th/9608174 [hep-th].

[45] C. Wang et al. "Particle-Hole Symmetry in the Fermion-Chern-Simons and Dirac Descriptions of a Half-Filled Landau Level". In: *Physical Review X* 7.3, 031029 (July 2017), p. 031029. arXiv: 1701.00007 [cond-mat.str-el].

[46] Chong Wang and T. Senthil. "Dual Dirac Liquid on the Surface of the Electron Topological Insulator". In: *Phys. Rev. X* 5 (4 2015), p. 041031.

[47] Ziqiang Wang et al. "Short-range interactions and scaling near integer quantum Hall transitions". In: *Phys. Rev. B* 61 (12 Mar. 2000), pp. 8326–8333. URL: https://link.aps.org/doi/10.1103/PhysRevB.61.8326.

[48] Qiong Zhu et al. "Localization-length exponent in two models of quantum Hall plateau transitions". In: *Phys. Rev. B* 99.2, 024205 (Jan. 2019), p. 024205.

[49] Martin R. Zirnbauer. "The integer quantum Hall plateau transition is a current algebra after all". In: *Nuclear Physics B* 941 (2019), pp. 458–506. ISSN: 0550-3213. URL: http://www.sciencedirect.com/science/article/pii/S0550321319300458.

C h a p t e r 4

RANDOM MAGNETIC FIELD AND THE DIRAC FERMI SURFACE

4.1   Introduction

In this paper, we introduce and analyze a new effective theory for studying the influence of a quenched random magnetic field on a single Dirac fermion, moving in two spatial dimensions (2d) and placed at finite density. Applications of this theory include: graphene when restricted to a single valley [3] (where the vector potential disorder describes the effects of ripples in the graphene sheet [39, 40]) and the gapless surface states of a time-reversal invariant 3d topological insulator [50]; an integer quantum Hall plateau transition for spinless electrons in a periodic potential [14, 37]; and Dirac composite fermion mean-field descriptions of the half-filled Landau level and topological insulator surface state [62, 65, 38, 58], other even-denominator metallic states [17, 13, 66], and the superconductor-insulator transition [41]. In this last guise, the random vector potential arises from a random scalar potential perturbation to the dual electron system.

In contrast to a 2d nonrelativistic fermion [2, 28], a single Dirac cone enjoys a sort of topological protection against localization [43, 44, 5]: A free Dirac fermion cannot be gapped without breaking on average either time-reversal symmetry[1] or charge conservation; the random vector potential is unique (among random perturbations quadratic in the fermions) in that it respects a particle-hole symmetry [37]. The Dirac theory therefore gives rise to a delocalized, critical state for all values of the Fermi energy. The problem here is to find an effective theory for this metal.

The conventional analytical approach to this problem, due to Pruisken and others [34, 22, 48, 67, 33, 26] (see [11, 21] for reviews and [25, 24, 46, 23, 30, 31] for specific studies of a disordered Dirac fermion), coarse grains away the elemen-

---

[1]Here we are explicitly referring to the symmetry of the Lagrangian for a single Dirac fermion. This may be realized in a time-reversal invariant way as the surface state of time-reversal invariant topological insulator. In a purely 2d theory, the simplest model breaks time-reversal microscopically [42, 51, 14]; the resulting theory preserves a nonlocal particle-hole symmetry [62, 58], which we are here viewing as an effective time-reversal symmetry for the Dirac fermion sector of the theory.

tary fermionic excitations in favor of a nonlinear sigma model with topological term, in which renormalization group fixed points are parameterized by the (disorder-averaged) Dirac fermion conductivity tensor. Because the longitudinal resistivity $\sim 1/\sigma_{xx}$ plays the role of a coupling constant in this model, it is a challenge to quantitatively extend this description to the regime, $\sigma_{xx} \sim e^2/h$, relevant to experiment (e.g., [36, 35]). Tsvelik [64] has conjectured a $PSL(2|2)_8$ Wess-Zumino-Novikov-Witten theory for the $\sigma_{xx} \sim e^2/h$ regime, based on its consistency with various numerical studies of the Chalker-Coddington model [4, 15] for the integer quantum Hall transition. Unfortunately, there is as yet no consensus among the most recent numerical works (e.g., [49, 69, 16, 56, 9]): For instance, there are statistically significant deviations among the various predictions for the localization length exponent (see Fig. 1 of [9]). These deviations are understood to be the result of finite-size corrections to scaling [61, 45]; effects that are exacerbated by a leading irrelevant perturbation that is close to marginality. Motivated in part by the lack of numerical consensus, Zirnbauer [71, 70] has recently proposed a fixed point description in terms of a CFT with only marginal perturbations. Currently, this scenario appears to lack direct numerical support [9, 8]. An alternative study of the Dirac theory using (non-)Abelian bosonization by Ludwig et al. [37] makes use of an $SU(2)$ symmetry that is present only at zero density. The zero density theory exhibits a fixed line (as a function of the disorder variance), along which the dynamical critical exponent varies continuously while the longitudinal conductivity is constant and of order e^2/h. Perturbation by a chemical potential within this treatment leads to difficulty: The associated chemical potential deformation breaks the $SU(2)$ symmetry and causes a flow to strong coupling.[2]

Here we present a different approach to studying the finite density theory: We first take the limit of the theory that focuses on the low-energy fluctuations about the Dirac Fermi surface before incorporating disorder. Taking inspiration from [37], the idea is to try to study the effects of disorder on the scale-invariant effective theory of (a system with) a Fermi surface [47, 60], rather than the "microscopic" Dirac theory that includes both particle and antiparticle excitations. We show how this approach allows for an exact solution of the effective theory—a random fixed line—provided the quenched vector

---

[2]It may be surprising that the chemical potential perturbation—an operator quadratic in the fermions—leads to strong coupling. The bosonization used in [37] to treat the 2d disordered theory maps the chemical potential operator to a nonlinear cosine term in the corresponding boson field with imaginary coefficient.

potential is suitably long ranged and weak, and for direct calculations of the effects of disorder on various physical observables without the need for replicas, supersymmetry, or Keldysh formalisms. In contrast to the zero density theory [37], we find the longitudinal dc conductivity—calculated in the collisionless $\hbar\omega/k_B T \to \infty$ limit [54]—to vary continuously along this finite-density fixed line.

The remainder of the paper is organized as follows. In §4.2 we derive the effective theory of a Dirac Fermi surface in a random magnetic field. This theory takes the form of an infinite collection of 1d chiral fermions—one fermion for each point on the Fermi surface—coupled by the quenched vector potential disorder. The large emergent symmetry $U(N)$ with $N \to \infty$ of the clean theory allows for an exact solution of the disordered theory, for each disorder realization, in which the randomness is removed entirely from the effective action by a gauge transformation. Operators not invariant under the $U(N)$ symmetry, however, depend on the disorder. In §4.3 we use the exact solution to directly compute various disorder-averaged physical observables. We warm up by showing that the average fermion Green's function is short-ranged and that the system has a finite density of states. We then turn to a calculation of the longitudinal conductivity, finding the conductivity to vary continuously with the strength of the disorder. In §4.4 we summarize and discuss possible directions of future work. Appendices 4.A and 4.B contain relevant details of the calculations summarized in the main text.

4.2   Low-Energy Effective Theory

In this section, we derive the low-energy effective theory of a 2d Dirac fermion in a random magnetic field in terms of an infinite collection of 1d chiral fermions, coupled via a random vector potential.

Low-Energy Limit

Our starting point is the theory of a two-component Dirac fermion $\Psi(t, \mathbf{x})$ at finite density, coupled to a quenched random $U(1)$ vector potential $A_j(\mathbf{x})$:

$$S = S_0 + S_1, \tag{4.1}$$

where S_0 is the action of a free Dirac fermion in 2d,[3]

$$S_0 = \int dt d^2\mathbf{x} \ \Psi^\dagger(t, \mathbf{x})\left(i\sigma_a \partial_a + \mu\right)\Psi(t, \mathbf{x}), \qquad (4.2)$$

and S_1 is the coupling of the Dirac fermion to the vector potential disorder,

$$S_1 = \int dt d^2\mathbf{x} \ \Psi^\dagger(t, \mathbf{x})\sigma_j A_j(\mathbf{x})\Psi(t, \mathbf{x}). \qquad (4.3)$$

Above, $\mathbf{x} = (x_1, x_2)$; $a \in \{0, 1, 2\}$; σ_0 is the 2×2 identity matrix and σ_j for $j = 1, 2$ are standard Pauli matrices; repeated indices are summed over unless otherwise specified. The chemical potential μ is finite and nonzero, and we have set the velocity of the Dirac fermion to unity. The vector potential $A_j(\mathbf{x})$ is chosen to be a zero-mean Gaussian random variable. We specify its disorder ensemble in §4.2; for the present discussion, we require that $A_j(\mathbf{x})$ be of sufficiently long wavelength that its Fourier transform $A_j(\mathbf{q})$[4] is only nonzero for wave vectors $|\mathbf{q}| \ll 2|\mu|$. This condition on the vector potential restricts to small-angle impurity scattering between fermionic excitations about nearby Fermi points.

Following [19], we derive the low-energy limit of this theory, in which we first focus on the low-energy excitations near the Fermi surface, defined by (5.1), and then incorporate scattering between Fermi points mediated by A_j in (5.2). This order of limits assumes that the fluctuations of A_j are sufficiently weak compared with $|\mu|$.

In Fourier space, the equation of motion following from (5.1) is

$$\left((\omega + \mu)\sigma_0 - p_j\sigma_j\right)\Psi(\omega, \mathbf{p}) = 0, \qquad (4.4)$$

where $\Psi(\omega, \mathbf{p})$ is the Fourier transform of $\Psi(t, \mathbf{x})$ and $\mathbf{p} = (p_1, p_2)$. The equation of motion (4.4) implies that the particle/antiparticle excitations have the dispersion relation, $\omega + \mu = \pm p$ with $p = |\mathbf{p}| \geq 0$. As such, (4.4) can be rewritten as

$$P^{(\mp)}(\mathbf{p})\Psi(\omega, \mathbf{p}) = 0, \qquad (4.5)$$

---

[3]This form of the action corresponds to a relativistic one with γ matrices: $\left(\gamma^0, \gamma^1, \gamma^2\right) = \left(\sigma_3, i\sigma_2, -i\sigma_1\right)$.

[4]Our Fourier transform convention: $A_j(\mathbf{x}) = \int \frac{d^2\mathbf{p}}{(2\pi)} e^{i\mathbf{p}\cdot\mathbf{x}} A_j(\mathbf{p})$ and $\Psi(t, \mathbf{x}) = \int \frac{d\omega d^2\mathbf{p}}{(2\pi)^3} e^{-i\omega t + i\mathbf{p}\cdot\mathbf{x}}\Psi(\omega, \mathbf{p})$.

where the projection matrices,

$$P^{(\mp)}(\mathbf{p}) \equiv \frac{1}{2}\left(\sigma_0 \mp \frac{p_j \sigma_j}{p}\right). \tag{4.6}$$

Using the projection matrices, we may write (5.1) in Fourier space as

$$S_0 = \int \frac{d\omega d^2\mathbf{p}}{(2\pi)^3} \ \Psi^\dagger(\omega,\mathbf{p})\Big((\omega+\mu-p)P^{(+)}(\mathbf{p}) + (\omega+\mu+p)P^{(-)}(\mathbf{p})\Big)\Psi(\omega,\mathbf{p}) \tag{4.7}$$

For a spherical Fermi surface, we parameterize $\mathbf{p} = p\,\hat{r}_\theta \equiv p\,(\cos\theta, \sin\theta)$ with $\theta \in [0, 2\pi)$ labeling the points on the Fermi surface. The projection matrices become

$$P^{(\mp)}(\mathbf{p}) = \frac{1}{2}\begin{pmatrix} 1 & \mp e^{-i\theta} \\ \mp e^{+i\theta} & 1 \end{pmatrix} \tag{4.8}$$

and we may expand Ψ in terms of its particle (R) and antiparticle (L) excitations as

$$\Psi(t,\mathbf{x}) = \int \frac{d\omega d^2\mathbf{p}}{(2\pi)^3} \ e^{-i\omega t + i\mathbf{p}\cdot\mathbf{x}}\left(\frac{1}{\sqrt{2}}\begin{pmatrix} e^{-i\theta} \\ 1 \end{pmatrix} R_\theta(\omega,p) + \frac{1}{\sqrt{2}}\begin{pmatrix} -e^{-i\theta} \\ 1 \end{pmatrix} L_\theta(\omega,p)\right), \tag{4.9}$$

where

$$P^{(+)}(\mathbf{p})\Psi(\omega,\mathbf{p}) = \frac{1}{\sqrt{2}}\begin{pmatrix} e^{-i\theta} \\ 1 \end{pmatrix} R_\theta(\omega,p), \tag{4.10}$$

$$P^{(-)}(\mathbf{p})\Psi(\omega,\mathbf{p}) = \frac{1}{\sqrt{2}}\begin{pmatrix} -e^{-i\theta} \\ 1 \end{pmatrix} L_\theta(\omega,p). \tag{4.11}$$

Inserting this expansion (4.9) into (4.7), the free Dirac fermion action in Fourier space simplifies to

$$S_0 = \int \frac{d\omega d^2\mathbf{p}}{(2\pi)^3}\left(R_\theta^*(\omega,p)\big(\omega+\mu-p\big)R_\theta(\omega,p) + L_\theta^*(\omega,p)\big(\omega+\mu+p\big)L_\theta(\omega,p)\right). \tag{4.12}$$

For $\mu > 0$, particles (R) with momentum $p \sim k_F \equiv |\mu|$ are light and antiparticles (L) have energy $\omega \geq k_F$; for $\mu < 0$, the antiparticles are light and the particles are heavy. Therefore, depending on the sign of μ, the low-energy effective theory for excitations with $p \sim k_F$ only retains the particles or antiparticles. Expanding about the Fermi momentum k_F,

$$p = k_F + p_\perp, \quad |p_\perp| \ll k_F, \tag{4.13}$$

we have

$$d^2\mathbf{p} = pdpd\theta \approx k_F dp_\perp d\theta, \tag{4.14}$$

and, for $\mu > 0$, S_0 becomes

$$S_0 = \int \frac{d\omega dp_\perp d\theta}{(2\pi)^3} \, R_\theta^*(\omega, p_\perp)(\omega - p_\perp)R_\theta(\omega, p_\perp), \tag{4.15}$$

where we replaced $R_\theta(\omega, p) \to \frac{1}{\sqrt{k_F}}R_\theta(\omega, p_\perp)$. For $\mu < 0$, we substitute $R \to L$ and $\omega - p_\perp \to \omega + p_\perp$. Note that the deviation $p_\perp$ of the momentum about k_F can be positive or negative. Depending on the sign of μ, we may interpret S_0 (4.15) as an infinite collection of 1d chiral fermions $R_\theta(\omega, p_\perp)$. We will only consider a single species of fermions with $\mu > 0$ so the low-energy theory will only involve R fermions.

The vector field $A_j(\mathbf{x})$ couples the chiral fermions $R_\theta(\omega, p_\perp)$ to one another according to S_1 (5.2). To derive this coupling, we first decompose the Fourier transform of the vector potential $A_j(\mathbf{q})$ in terms of its longitudinal $A_L(\mathbf{q})$ and transverse $A_T(\mathbf{q})$ components:

$$A_j(\mathbf{q}) = i\frac{q_j}{q}A_L(\mathbf{q}) + i\epsilon_{jk}\frac{q_k}{q}A_T(\mathbf{q}). \tag{4.16}$$

The momentum transfer,

$$\mathbf{q} = \mathbf{p} - \mathbf{p}', \tag{4.17}$$

where $\mathbf{p} = (k_F + p_\perp)\hat{r}_\theta$ and $\mathbf{p}' = (k_F + p'_\perp)\hat{r}_{\theta'}$. Since $p \sim p' \approx k_F$, we take

$$\frac{q_j}{q} \approx \frac{\hat{r}_\theta - \hat{r}_{\theta'}}{|\hat{r}_\theta - \hat{r}_{\theta'}|}. \tag{4.18}$$

Plugging the resulting decomposition (4.16) and the expansion (4.9) into (5.2), we obtain the low-energy vector potential coupling for $\mu > 0$:

$$S_1 = i\int \frac{d\omega d^2\mathbf{p} d^2\mathbf{p}'}{(2\pi)^5} \, R_\theta^*(\omega, p)R_{\theta'}(\omega, p')sign(\theta - \theta')e^{\frac{i}{2}(\theta - \theta')}A_T(\mathbf{p} - \mathbf{p}'), \tag{4.19}$$

where $sign(X) = 1$ for $X \geq 0$ and $sign(X) = -1$ for $X < 0$. We have dropped a particle-antiparticle coupling between R and L fermions that is mediated by the longitudinal component A_L of the vector potential, since such a term has an energy cost $\sim 2k_F$. The longitudinal component is therefore absent from this low-energy vector potential coupling. For $\mu < 0$, (4.19) acquires an overall minus sign and we substitute $R \to L$.

In general, $A_T(\mathbf{q})$ couples $R_\theta(\omega, p)$ and $R_{\theta'}(\omega, p')$ for arbitrary θ and θ'. By assuming that $A_T(\mathbf{q})$ is only nonzero for $|\mathbf{q}| \ll 2k_F$ (see §4.2 for further discussion), we may further simplify the effective coupling (4.19). For $|\mathbf{q}| \ll 2k_F$, the momentum transfer $\mathbf{q} = \mathbf{p} - \mathbf{p}'$ can be approximated as

$$\mathbf{p} - \mathbf{p}' = (p_\perp - p'_\perp)\hat{r}_{\theta'} + k_F(\theta - \theta')\frac{d}{d\theta'}\hat{r}_{\theta'}, \qquad (4.20)$$

where $|p_\perp - p'_\perp| \ll 2k_F$ and $|\theta - \theta'| \ll 1$. Here, $\hat{r}_{\theta'} = (\cos\theta', \sin\theta')$ and $\frac{d}{d\theta'}\hat{r}_{\theta'} = (-\sin\theta', \cos\theta')$ are orthogonal unit vectors about the Fermi surface point θ'. Defining

$$V_{\theta\theta'}(p_\perp - p'_\perp) \equiv i\, k_F\, sign(\theta - \theta')\, e^{\frac{i}{2}(\theta - \theta')}\, A_T(\mathbf{p} - \mathbf{p}'), \qquad (4.21)$$

and given (4.20), the vector potential coupling (4.19) becomes

$$S_1 = \int \frac{d\omega dp_\perp d\theta dp'_\perp d\theta'}{(2\pi)^5}\; R_\theta^*(\omega, p_\perp)R_{\theta'}(\omega, p'_\perp)V_{\theta\theta'}(p_\perp - p'_\perp). \qquad (4.22)$$

(Recall the rescaling $R_\theta(\omega, p) \to \frac{1}{\sqrt{k_F}}R_\theta(\omega, p_\perp)$.) Note that the same $A_T(\mathbf{q})$ can enter different components of $V_{\theta\theta'}(p_\perp - p'_\perp)$ since a given $\mathbf{q}$ can correspond to the momentum transfer between distinct pairs of fermions.

We next perform the inverse Fourier transform[5] $(\omega, p_\perp) \to (t, z)$ on the fields appearing in the low-energy forms of S_0 (4.15) and S_1 (4.22). For $\mu > 0$, $S = S_0 + S_1$ becomes

$$S = \int \frac{dt dz d\theta}{2\pi}\; R_\theta^*(t, z)i(\partial_t + \partial_z)R_\theta(t, z) + \int \frac{dt dz d\theta d\theta'}{(2\pi)^2}\; R_\theta^*(t, z)V_{\theta\theta'}(z)R_{\theta'}(t, z). \qquad (4.23)$$

The first term describes an infinite collection of 1d chiral fermions, labeled by the Fermi point θ. The second term is a (quenched) random coupling $V_{\theta\theta'}(z)$ between fermions associated to the Fermi points θ and θ'.

Electrical Current

The electrical current (density) is

$$J_j(t, \mathbf{x}) = \Psi^\dagger(t, \mathbf{x})\sigma_j\Psi(t, \mathbf{x}). \qquad (4.24)$$

We are interested in the contribution to this current that arises from the low-energy excitations near the Fermi surface when $\mu > 0$. The simplest way

---

[5] We have $R_\theta(t, z) = \int \frac{d\omega dp_\perp}{(2\pi)^2}\, e^{-i\omega t + ip_\perp z}R_\theta(\omega, p_\perp)$ and $V_{\theta\theta'}(z) = \int \frac{dp_\perp}{2\pi}\, e^{ip_\perp z}V_{\theta\theta'}(p_\perp)$.

to obtain this low-energy current is to replace in (5.2) the quenched vector potential $A_j(\mathbf{x})$ by a slowly varying background vector field $\mathcal{A}_j(t, \mathbf{x})$ and to take the low-energy limit described in the previous section. ("Slowly varying" means $|q_0|, |\mathbf{q}| \ll k_F$.) This produces the coupling (compare with (4.19)),

$$S_2 = \int \frac{d\omega d^2\mathbf{p}d\omega'd^2\mathbf{p}'}{(2\pi)^6} \, R_\theta^*(\omega, p)R_{\theta'}(\omega', p')\Big(\frac{e^{i\theta} + e^{-i\theta'}}{2}\mathcal{A}_x(q_0, \mathbf{q}) + \frac{e^{i\theta} - e^{-i\theta'}}{2i}\mathcal{A}_y(q_0, \mathbf{q})\Big),$$

(4.25)

where $q_0 = \omega - \omega'$ and $\mathbf{q} = \mathbf{p} - \mathbf{p}'$. As before, $p = k_F + p_\perp$ and $p' = k_F + p_\perp'$. The variational derivative $J_j(-q_0, -\mathbf{q}) = (2\pi)^3 \frac{\delta S_2}{\delta \mathcal{A}_j(q_0, \mathbf{q})}$ gives the Fourier transform of the low-energy current:

$$J_x(-q_0, -\mathbf{q}) = \int \frac{d\omega d^2\mathbf{p}d^2\mathbf{p}'}{(2\pi)^3}\delta(\mathbf{q} - \mathbf{p} + \mathbf{p}')R_\theta^*(\omega, p)\Big(\frac{e^{i\theta} + e^{-i\theta'}}{2}\Big)R_{\theta'}(\omega - q_0, p'),$$

(4.26)

$$J_y(-q_0, -\mathbf{q}) = \int \frac{d\omega d^2\mathbf{p}d^2\mathbf{p}'}{(2\pi)^3}\delta(\mathbf{q} - \mathbf{p} + \mathbf{p}')R_\theta^*(\omega, p)\Big(\frac{e^{i\theta} - e^{-i\theta'}}{2i}\Big)R_{\theta'}(\omega - q_0, p').$$

(4.27)

In computing the electrical conductivity, we will use a mixed Fourier space representation of the $\mathbf{q} = 0$ component of these currents. Fourier transforming $J_j(-q_0, \mathbf{q} = 0)$ with respect to $q_0,$[6] we have

$$J_x(t) \equiv J_x(t, \mathbf{q} = 0) = \int \frac{dzd\theta}{2\pi} \, R_\theta^*(t, z)\cos(\theta)R_\theta(t, z), \qquad (4.28)$$

$$J_y(t) \equiv J_y(t, \mathbf{q} = 0) = \int \frac{dzd\theta}{2\pi} \, R_\theta^*(t, z)\sin(\theta)R_\theta(t, z). \qquad (4.29)$$

$J_j(t)$ is the sum over the Fermi surface of the fermion density, weighted by $\cos(\theta)$ or $\sin(\theta)$, according to the current component j.

Disorder Ensemble

We take the vector potential $A_j(\mathbf{q})$ to be a zero-mean Gaussian random variable with variance:

$$\overline{A_j(\mathbf{q})A_k(\mathbf{q}')} = g\delta_{ij}f(|\mathbf{q}|)\delta(\mathbf{q} + \mathbf{q}'). \qquad (4.30)$$

Here, g is a dimensionless constant that controls the overall scale of the fluctuations of the vector potential; $g\,f(|\mathbf{q}|)$ is a unit-normalized function with

---

[6]We use our previous convention for the Fourier transform of $R_\theta(t, z)$ and $J_j(t, \mathbf{q}) = \int \frac{dq_0}{2\pi}e^{-iq_0 t}J_j(q_0, \mathbf{q})$.

support $|\mathbf{q}| \ll k_F$. For definiteness, we choose $f(|\mathbf{q}|) = \exp(-|\mathbf{q}|/M)$, where $M \ll k_F$ provides a smooth cutoff on the momentum transfer $\mathbf{q}$ in a scattering process.

We would like to determine what (4.30) implies for the random matrix $V_{\theta\theta'}(z)$. We will argue that $V_{\theta\theta'}(z)$ gives rise to a local interaction in the effective 1d theory. To this end, we consider the disorder average:

$$\overline{V_{\theta_1\theta_2}(z)V_{\theta_3\theta_4}(z')} = -k_F^2 sign(\theta_1 - \theta_2)sign(\theta_3 - \theta_4)e^{\frac{i}{2}(\theta_1 - \theta_2)}e^{\frac{i}{2}(\theta_3 - \theta_4)}$$
$$\times \int \frac{dp_\perp dp'_\perp}{(2\pi)^2}e^{ip_\perp z}e^{ip'_\perp z'}\overline{A_T(\mathbf{q})A_T(\mathbf{q}')}, \tag{4.31}$$

where (using our conventions from (4.20))

$$\mathbf{q} = p_\perp \hat{r}_{\theta_2} + k_F(\theta_1 - \theta_2)\frac{d}{d\theta_2}\hat{r}_{\theta_2}, \tag{4.32}$$

$$\mathbf{q}' = p'_\perp \hat{r}_{\theta_4} + k_F(\theta_3 - \theta_4)\frac{d}{d\theta_4}\hat{r}_{\theta_4}. \tag{4.33}$$

We decompose $A_T(\mathbf{q})$ in terms of its Cartesian components by replacing

$$i\, sign(\theta_1 - \theta_2)e^{\frac{i}{2}(\theta_1 - \theta_2)}A_T(\mathbf{q}) = \frac{e^{i\theta_1} + e^{-i\theta_2}}{2}A_x(\mathbf{q}) + \frac{e^{i\theta_1} - e^{-i\theta_2}}{2i}A_y(\mathbf{q}),$$
$$\tag{4.34}$$

$$i\, sign(\theta_3 - \theta_4)e^{\frac{i}{2}(\theta_3 - \theta_4)}A_T(\mathbf{q}') = \frac{e^{i\theta_3} + e^{-i\theta_4}}{2}A_x(\mathbf{q}') + \frac{e^{i\theta_3} - e^{-i\theta_4}}{2i}A_y(\mathbf{q}'),$$
$$\tag{4.35}$$

and then use (4.30) to find

$$\overline{V_{\theta_1\theta_2}(z)V_{\theta_3\theta_4}(z')} = \frac{k_F^2}{2}\int \frac{dp_\perp dp'_\perp}{(2\pi)^2}e^{ip_\perp z}e^{ip'_\perp z'}f(|\mathbf{q}|)\delta(\mathbf{q} + \mathbf{q}')\left(e^{i(\theta_1 - \theta_4)} + e^{-i(\theta_2 - \theta_3)}\right).$$
$$\tag{4.36}$$

We will approximate (4.36) by

$$\overline{V_{\theta_1\theta_2}(z)V_{\theta_3\theta_4}(z')} = gk_F\delta(\theta_1 - \theta_4)\delta(\theta_2 - \theta_3)f(z - z'), \tag{4.37}$$

where

$$f(z) = \int \frac{dp_\perp}{2\pi}e^{ip_\perp z}f(p_\perp) \tag{4.38}$$

and it is to be understood that $|\theta_1 - \theta_2| \ll 1$ and $|\theta_3 - \theta_4| \ll 1$. The disorder (4.37) is local in z since it depends on the relative coordinate $z - z'$. We expect

(4.37) to be a good approximation to (4.36) at small momentum transfers and sufficiently low energies. More precisely, we require $M/k_F \ll 1$ and that the cutoff on $p_\perp \in (-\Lambda, \Lambda)$ satisfies $\Lambda/M \ll 1$.

A detailed explanation for the approximation (4.37) goes as follows. We begin by noting that for $M/k_F \ll 1$ and using $\delta(\mathbf{q}+\mathbf{q}')$, $f(\mathbf{q}) = f(\mathbf{q}')$ fixes $|\theta_1 - \theta_2| \ll 1$ and $|\theta_3 - \theta_4| \ll 1$. Next, we expect the dominant contributions to (4.36) to arise when the terms in the sum $\left(e^{i(\theta_1 - \theta_4)} + e^{-i(\theta_2 - \theta_3)}\right)$ are in-phase. This sets $\theta_1 = \theta_4 + \theta_3 - \theta_2 + 2\pi m$, for an arbitrary integer m. Using the earlier two conditions, the in-phase requirement implies $|\theta_1 - \theta_4 - \pi m| \ll 1$: This is modeled by $\delta(\theta_1 - \theta_4 - \pi|m|)$. Substituting $\theta_1 = \theta_4 + \pi m$ into $f(\mathbf{q})$ and $\theta_4 = \theta_1 - \pi m$ into $f(\mathbf{q}')$ fixes $|\theta_4 - \theta_2 + \pi m| \ll 1$ and $|\theta_3 - \theta_1 + \pi m| \ll 1$. Since $\theta_i \in [0, 2\pi)$, these two conditions allow either $m = 0$ or $|m| = 1, 2$. First consider $m = 0$. Since $\theta_2 \approx \theta_1$ and $\theta_4 \approx \theta_1$, $\mathbf{q} \approx p_\perp \hat{r}_{\theta_1} + k_F(\theta_1 - \theta_2)\frac{d}{d\theta_1}\hat{r}_{\theta_1}$ and $\mathbf{q}' \approx p'_\perp \hat{r}_{\theta_1} + k_F(\theta_3 - \theta_4)\frac{d}{d\theta_1}\hat{r}_{\theta_1}$. Because $\hat{r}_{\theta_1}$ and $\frac{d}{d\theta_1}\hat{r}_{\theta_1}$ are orthonormal, $\delta(\mathbf{q}+\mathbf{q}') = \delta(p_\perp + p'_\perp)\delta\left(k_F(\theta_1 - \theta_2 + \theta_3 - \theta_4)\right) = \frac{1}{k_F}\delta(p_\perp + p'_\perp)\delta(\theta_3 - \theta_2)$, using $\delta(\theta_1 - \theta_4 - \pi|m|)$. For Gaussian $f(|\mathbf{q}|)$, the dependence on $p_\perp$ and $\theta_1 - \theta_2$ factorizes. Absorbing into g the variation of this Gaussian on $|\theta_1 - \theta_2| \approx 0$, we perform the integral over $p'_\perp$ using $\delta(p_\perp + p'_\perp)$ to arrive at (4.37). Next consider $m = 1$; the $m = -1$ and $m = \pm 2$ cases work similarly and will not be discussed. Following the $m = 0$ logic, the replacement $\theta_4 = \theta_1 - \pi$ introduces a relative phase in the angular delta function, $\delta(\mathbf{q}+\mathbf{q}') = \frac{1}{k_F}\delta(p_\perp - p'_\perp)\delta\left(\theta_1 - \theta_2 - (\theta_3 - \theta_4)\right) = \frac{1}{k_F}\delta(p_\perp - p'_\perp)\delta\left(2\theta_1 - \theta_2 - \theta_3 - \pi\right) \approx \frac{1}{k_F}\delta(p_\perp - p'_\perp)\delta\left(\theta_1 - \theta_2\right)$, using $\theta_3 \approx \theta_1 - \pi$. The delta function has support when $\theta_1 = \theta_2$ (and similarly requires using the in-phase delta function $\delta(\theta_1 - \theta_4 - \pi)$ and $f(\mathbf{q}')$ that $\theta_3 = \theta_4$). For $\Lambda/M \ll 1$, scattering along the Fermi surface dominates and the relative contributions of $m \neq 0$ terms should be suppressed. We therefore ignore the $|m| = 1, 2$ terms in the remainder.

Before studying further the effect of the vector potential disorder, we'd like to make some remarks about other types of disorder: quenched scalar potential A_0 and mass m disorders. Applying the same logic that lead to the low-energy theory (4.23), these couplings take the form:

$$
\begin{aligned}
S^{A_0 + m} &= \int d^2x dt \; \Psi^\dagger(t, \mathbf{x})\Big(A_0(\mathbf{x})\sigma_0 + m(\mathbf{x})\sigma_3\Big)\Psi(t, \mathbf{x}) \\
&\approx \int \frac{dt dz d\theta d\theta'}{(2\pi)^2} \; R^*_\theta(t, z)\Big(V^{A_0}_{\theta\theta'}(z) + V^m_{\theta\theta'}(z)\Big)R_{\theta'}(t, z), \quad (4.39)
\end{aligned}
$$

where $V_{\theta\theta'}^{A_0}(z)$ and $V_{\theta\theta'}^{m}(z)$ are the Fourier transforms $(p_\perp \to z)$ of

$$V_{\theta\theta'}^{A_0}(p_\perp - p_\perp') \equiv \frac{1}{2}\big(e^{i(\theta-\theta')} + 1\big)A_0(\mathbf{p} - \mathbf{p}'), \qquad (4.40)$$

$$V_{\theta\theta'}^{m}(p_\perp - p_\perp') \equiv \frac{1}{2}\big(e^{i(\theta-\theta')} - 1\big)m(\mathbf{p} - \mathbf{p}'), \qquad (4.41)$$

with $A_0(\mathbf{q})$ and $m(\mathbf{q})$ the Fourier transforms of $A_0(\mathbf{x})$ and $m(\mathbf{x})$. Taking $A_0(\mathbf{q})$ and $m(\mathbf{q})$ to be zero-mean Gaussian random variables, we find the disorder averages:

$$\overline{V_{\theta_1\theta_2}^{A_0}(z)\, V_{\theta_3\theta_4}^{A_0}(z')} \propto \big(e^{i(\theta_1-\theta_2+\theta_3-\theta_4)} + e^{i(\theta_1-\theta_2)} + e^{i(\theta_3-\theta_4)} + 1\big), \ (4.42)$$

$$\overline{V_{\theta_1\theta_2}^{m}(z)\, V_{\theta_3\theta_4}^{m}(z')} \propto \big(e^{i(\theta_1-\theta_2+\theta_3-\theta_4)} - e^{i(\theta_1-\theta_2)} - e^{i(\theta_3-\theta_4)} + 1\big). \ (4.43)$$

Denote $\theta_1 - \theta_2 = \alpha$ and $\theta_3 - \theta_4 = \beta$. Under the same assumptions we used before, $|\alpha|, |\beta| \ll 1$, and excluding large-angle scattering, the most dominant in-phase (coherent) contribution to the random scalar potential average occurs when $\alpha = \beta = 0$. This turns out to make no contribution to disorder-averaged quantities in the large N limit considered in the next section, being suppressed by a factor of $1/N$, where N is the number of points on the Fermi surface. The random mass average vanishes when $\alpha = \beta = 0$. A subdominant contribution to the random mass average occurs when $\alpha = -\beta$. The right-hand side of (4.43) then becomes $2 - 2\cos\alpha \approx \frac{\alpha^2}{2}$. This is an order of magnitude smaller than the contribution of the random magnetic field that we focus on in the remainder of this paper.

Random Fixed Point and its Discrete Approximation

Under the renormalization group transformation[7] [47, 60] that leaves the S_0 part of (4.23) invariant, the leading flow equation [12] for the disorder variance g is

$$\frac{dg}{d\ell} = (3 - 2\Delta)g, \qquad (4.44)$$

where $\Delta = 1$ is the scaling dimension of $R_\theta^*(t, z)R_{\theta'}(t, z)$ and ℓ is the renormalization group length scale that increases as the energy is reduced. We have substituted $f(z - z') = \delta(z - z')$ in deriving (4.44). Randomness is therefore a relevant perturbation that drives the clean Dirac theory towards strong disorder.

---

[7]The scale transformation is the following: $z \to \lambda z, t \to \lambda t, \theta \to \theta, R_\theta(t, z) \to \lambda^{-1/2}R_\theta(t, z)$.

Because the randomness is $\mathcal{O}(1)$ relevant, perturbation theory about the clean fixed point cannot access the strong disorder regime. Luckily, the low-energy action (4.23) admits an exact solution for arbitrary g (such that the derivation in §4.2 holds), in which $V_{\theta\theta'}(z)$ is eliminated via the field redefinition [52, 20, 6]:

$$\tilde{R}_\theta(t, z) = \int \frac{d\theta'}{2\pi} U_{\theta\theta'}(z) R_{\theta'}(t, z), \tag{4.45}$$

where the unitary matrix,

$$U_{\theta\theta'}(z) \equiv \left(\mathcal{T}_z e^{-i \int_{z_0}^z dz' V(z')} \right)_{\theta\theta'}. \tag{4.46}$$

Here, $\mathcal{T}_z$ denotes path ordering along z and z_0 is an arbitrary base point. The resulting action simplifies to

$$S = \int \frac{dt dz d\theta}{2\pi} \tilde{R}_\theta^*(t, z) i (\partial_t + \partial_z) \tilde{R}_\theta(t, z). \tag{4.47}$$

The action (4.47) exactly describes the strong disorder regime of a Dirac fermion at finite density, subject to a random vector potential of sufficiently long wavelength. The random vector potential has been eliminated from the effective action using the infinite-dimensional symmetry of the Fermi surface [10, 7, 32].

The formal manipulations above are made concrete by discretizing the θ coordinate (say, by putting the system in a finite-size box). To this end, we take the Fermi surface to consist of N discrete points: $\theta \to \theta_I = 2\pi I/N$ with $I = 1, \ldots, N$. The fields and disorder are therefore replaced as

$$R_\theta(t, z) \to \sqrt{N} R_{\theta_I}(t, z) \equiv \sqrt{N} R_I(t, z) \tag{4.48}$$

$$V_{\theta\theta'}(z) \to V_{\theta_I \theta_J}(z) \equiv V_{IJ}(z). \tag{4.49}$$

(The scaling of $R_{\theta_I}(t, z)$ by $\sqrt{N}$ is for notational simplicity.) We are specifically interested in the limit $N \to \infty$. Substituting in the discrete form of the angular integration $\int \frac{d\theta}{2\pi} \to \frac{1}{N} \sum_I$, we have the (equivalent) discrete forms for the low-energy action,

$$S = \int dt dz \sum_{I=1}^N R_I^*(t, z) i (\partial_t + \partial_z) R_I(t, z) + \frac{1}{N} \int dt dz \sum_{I,J=1}^N R_I^*(t, z) V_{IJ}(z) R_J(t, z) \tag{4.50}$$

$$= \int dt dz \sum_{I=1}^N \tilde{R}_I^*(t, z) i (\partial_t + \partial_z) \tilde{R}_I(t, z), \tag{4.51}$$

where the rotated fermions, in discrete form, are

$$\tilde{R}_I(t,z) = \sum_{J=1}^{N} U_{IJ}(z) R_J(t,z), \quad U_{IJ}(z) = \left(\mathcal{T}_z e^{-\frac{i}{N} \int_{z_0}^{z} dz' V(z')} \right)_{IJ}. \qquad (4.52)$$

The discrete action has an emergent $U(N)$ symmetry. In discrete form, the low-energy currents (4.28) - (4.29) become

$$J_x(t) = \int dz \sum_I R_I^*(t,z) \cos(\theta_I) R_I(t,z), \qquad (4.53)$$

$$J_y(t) = \int dz \sum_I R_I^*(t,z) \sin(\theta_I) R_I(t,z). \qquad (4.54)$$

For discrete θ, the disorder variance (4.37) becomes

$$\overline{V_{IJ}(z) V_{KL}(z')} = g k_F N \delta_{IL} \delta_{JK} f(z - z'). \qquad (4.55)$$

The overall factor of N arises from the discrete form of $\delta(\mathbf{q} + \mathbf{q}')$ in (4.36) with $\theta_I = 2\pi I/N$. It is the discrete form of the action (4.51) that we will use in the next section.

4.3 Observables along the Fixed Line

In general, in the presence of quenched disorder V with unit-normalized distribution $P[V]$, the disorder-average of the correlation function of a physical observable $\mathcal{O}$ is defined as

$$\overline{\langle \mathcal{O} \rangle} \equiv \int DV P[V] \langle \mathcal{O} \rangle_V, \qquad (4.56)$$

where the correlation function $\langle \mathcal{O} \rangle_V$ in the disorder realization V is

$$\langle \mathcal{O} \rangle_V \equiv \frac{\int D\Phi \, \mathcal{O} \, e^{iS[\Phi,V]}}{\int D\Phi \, e^{iS[\Phi,V]}}. \qquad (4.57)$$

Here, we are momentarily denoting the dynamical fields of the theory by Φ and the action $S[\Phi, V]$ indicates a dependence upon both Φ and the disorder V. In most theories, the presence of V in the denominator of $\langle \mathcal{O} \rangle_V$ renders the direct analytic integration over all possible disorders in $\overline{\langle \mathcal{O} \rangle}$ difficult, if not impossible. As such, various ingenious tricks—such as replica, supersymmetric, and Keldysh formalisms—have been employed with various levels of success. In this paper, we instead make use of the exact solution of the low-energy effective theory presented in §4.2 to directly perform the disorder average.

To see how this works, consider the correlation function of a local observable $\mathcal{O}(R)$, which is a function of the unrotated $R_I(t, z)$ fermion:

$$\langle \mathcal{O}(R) \rangle_V = \frac{\int DR^\dagger DR \, \mathcal{O}(R) \, e^{iS[R,V]}}{\int DR^\dagger DR \, e^{iS[R,V]}} = \frac{\int D\tilde{R}^\dagger D\tilde{R} \, \mathcal{O}(U^\dagger \tilde{R}) \, e^{iS[\tilde{R}]}}{\int D\tilde{R}^\dagger D\tilde{R} \, e^{iS[\tilde{R}]}}. \quad (4.58)$$

In the first equality, $S[R, V]$ denotes the action (4.50); in the second equality, $S[\tilde{R}]$ denotes (4.51) with $\tilde{R}$ the rotated fermion (4.52) with rotation U a function of V. After the rotation, the denominator no longer depends on V and, in this case, yields the usual fermion determinant. The disorder V now only appears in the expression for the observable $\mathcal{O}(U^\dagger \tilde{R})$ and may, in principle, be averaged over.[8] A key point for us is that the local observables we consider separate into a sum of terms of the form,

$$\mathcal{O}(U^\dagger \tilde{R}) = \sum_{a,b} c_{ab} \mathcal{A}_a(\tilde{R}) \mathcal{B}_b(V), \quad (4.59)$$

for some constants c_{ab}, such that the disorder-averaged correlation function $\overline{\langle \mathcal{O}(R) \rangle}$ factorizes:

$$\begin{aligned}
\overline{\langle \mathcal{O}(R) \rangle} &= \sum_{a,b} c_{ab} \frac{\int D\tilde{R}^\dagger D\tilde{R} \, \mathcal{A}_a(\tilde{R}) \, e^{iS[\tilde{R}]}}{\int D\tilde{R}^\dagger D\tilde{R} \, e^{iS[\tilde{R}]}} \cdot \int dV P[V] \mathcal{B}_b(V) \\
&\equiv \sum_{a,b} c_{ab} \langle \mathcal{A}_a(\tilde{R}) \rangle \cdot \overline{\mathcal{B}_b(V)}.
\end{aligned} \quad (4.60)$$

Terms like $\langle \mathcal{A}_a(\tilde{R}) \rangle$ are calculated using the exact solution to the strong-disorder fixed point; terms like $\overline{\mathcal{B}_b(V)}$ are calculated with respect to the given disorder ensemble. We will show how this factorization can be used to compute the fermion Green's function and the longitudinal conductivity at the random fixed point (4.51).

Diffusive Green's Function and Density of States

We begin by calculating the disorder-averaged Green's function and density of states. We will find that the average Green's function is short-ranged and that the density of states is a positive constant. These calculations will introduce the technique we will later use to calculate the conductivity.

---

[8]Note that any possible quantum anomalies [52] associated with the unitary rotations (4.46) of the chiral fermion path integral measures, being a function of the disorder V only, mutually cancel between the numerator and denominator.

Using the low-energy action (4.51), the fermion two-point function averaged over the disorder is

$$\overline{\langle R_I(t,z)R_I^\dagger(0,0)\rangle} = \sum_{A,B}\langle \tilde{R}_A(t,z)\tilde{R}_B^\dagger(0,0)\rangle \cdot \overline{U_{IA}^\dagger(z)U_{BI}(0)}$$

$$= \sum_{A,B}\frac{i}{2\pi}\frac{\delta_{AB}}{(z-t)+i\alpha}\cdot \overline{U_{IA}^\dagger(z)U_{BI}(0)}, \qquad (4.61)$$

where $U(z)$ is defined in (4.52), α is a short-distance cutoff, and the index I is not summed over. Following [1], we compute the disorder average of U matrices by decomposing the interval $[0,z]$ into n steps $z_0 = 0, z_1 = \delta z, \ldots, z_n = n\delta z$ of length $\delta z = |z|/n$ such that

$$U(z) = e^{-\frac{i}{N}\int_{z_{n-1}}^{z_n} dz'V(z')}\cdots e^{-\frac{i}{N}\int_{z_1}^{z_2} dz'V(z')}e^{-\frac{i}{N}\int_{z_0}^{z_1} dz'V(z')}. \qquad (4.62)$$

We have chosen the arbitrary reference point $z_0 = 0$. For sufficiently large n with fixed $n\delta z = |z|$, the argument of each exponential can be approximated as

$$\frac{1}{N}\int_{z_{j-1}}^{z_j} dz'V(z') \approx \frac{1}{N}V(z_j)\delta z \equiv M_j. \qquad (4.63)$$

Using (4.55), M_j is a zero-mean Gaussian random variable with variance,

$$\overline{(M_i)_{IJ}(M_j)_{KL}} = \frac{gk_F}{N}\delta_{IL}\delta_{JK}f(z_i - z_j)\delta z^2, \qquad (4.64)$$

where $f(z_i - z_j)$ is given in (4.38). For discrete z, we take

$$f(z_i - z_j)\delta z = f_0\delta_{|i-j|,0} + f_1\delta_{|i-j|,1}. \qquad (4.65)$$

The dimensionless coefficients f_0 and f_1 approximate a Gaussian $f(z_i - z_j)$ of finite width.

Using this, the disorder average of the product of U matrices in (4.61) becomes

$$\sum_A \overline{U_{IA}^\dagger(z)U_{AI}(0)} = \sum_A \overline{\left(e^{iM_1}\cdots e^{iM_n}\right)_{IA}\times \mathbf{1}_{AI}}$$

$$= \overline{\left([1+iM_1 - \frac{M_1^2}{2}+\ldots]\cdots[1+iM_n-\frac{M_n^2}{2}+\ldots]\right)_{II}}$$

$$= \delta_{II} - gk_F[\frac{f_0}{2}n + f_1(n-1)]\delta z\,\delta_{II}$$

$$= e^{-gk_F\left(\frac{f_0}{2}+f_1\right)|z|}\delta_{II}. \qquad (4.66)$$

In the third equality, we have dropped higher-order terms in δz. In Appendix 4.A, we check that these higher-order terms exponentiate to the form given

in the fourth equality. Further details on such computations are given in Appendix 4.B. Defining

$$g_{\text{eff}} \equiv g\left(\frac{f_0}{2} + f_1\right), \tag{4.67}$$

we obtain the disorder-averaged Green's function,

$$\overline{\langle R_I(t,z) R_I^\dagger(0,0)\rangle} = \frac{i}{2\pi} \frac{e^{-g_{\text{eff}} k_F |z|}}{(z-t)+i\alpha}. \tag{4.68}$$

This Green's function has a spatial decay length $\lambda = 1/g_{\text{eff}} k_F$.

We now use the Green's function (4.68) to check that the density of states is finite. For this, we need the retarded Green's function averaged over the disorder:

$$\overline{G_{II}^R}(t,z;0,0) = -i\Theta(t)\overline{\langle\{R_I(t,z), R_I(0,0)\}\rangle} = -\Theta(t)\frac{i}{\pi}\frac{\alpha e^{-g_{\text{eff}} k_F |z|}}{(z-t)^2 + \alpha^2}, \tag{4.69}$$

where $\Theta(t)$ is the step function. Fourier transforming $\overline{G^R}(t,z;0,0)$ for $\alpha \to 0$, we obtain

$$\overline{G_{II}^R}(\omega, p_\perp) = \frac{1}{\omega - p_\perp + i g_{\text{eff}} k_F}. \tag{4.70}$$

From (4.70), we obtain the density of states per unit volume,

$$\rho(\omega) = -\frac{1}{\pi}\text{Im}\int \frac{dp_\perp}{2\pi}\frac{1}{\omega - p_\perp + i g_{\text{eff}} k_F} = \frac{1}{2\pi}. \tag{4.71}$$

Longitudinal Conductivity

We next turn to the disorder-averaged longitudinal conductivity $\sigma_{xx}(\omega)$. The Kubo formula reads:

$$\sigma_{xx}(\omega) = \frac{1}{i\omega_n}\frac{1}{L}\frac{k_F}{N}\int_0^\beta d\tau e^{i\omega_n \tau}\overline{\langle \mathcal{T}_\tau J_x(\tau) J_x(0)\rangle}\bigg|_{i\omega_n \to \omega + i0^+}, \tag{4.72}$$

where $\tau = it$, $\omega_n = (2n+1)\pi\beta$ is a positive Matsubara frequency at temperature $1/\beta$, and $L \cdot N/k_F$ is a spatial volume factor equal to $\lim_{\mathbf{q}\to 0}\delta(\mathbf{q}) = \lim_{p_\perp \to 0}\delta(p_\perp)\cdot\frac{1}{2\pi}\delta(k_F\theta_I)$ for some I.

Plugging in the expression for the current $J_x(\tau)$ (4.53) and using the unitary (4.52), the current two-point function is

$$
\langle \mathcal{T}_\tau J_x(\tau) J_x(0) \rangle = \int dz dz' \sum_{I,J,A,B,C,D} \langle \tilde{R}_A^\dagger(\tau,z) \tilde{R}_B(\tau,z) \tilde{R}_C^\dagger(0,z') \tilde{R}_D(0,z') \rangle
$$
$$
\cdot \overline{U_{AI}(z) \cos(\theta_I) U_{IB}^\dagger(z) U_{CJ}(z') \cos(\theta_J) U_{JD}^\dagger(z')}
$$
$$
= \int dz dz' \left(\frac{i}{2\beta \sinh \left(\frac{\pi(z-z'+i(\tau-\tau'))}{\beta} \right)} \right)^2 \cdot \mathrm{Tr} \, \overline{U(z) C U^\dagger(z) U(z') C U^\dagger(z')}.
$$

$$(4.73)$$

In the first equality, we introduced the diagonal matrix $C_{II'} = \cos\left(\frac{2\pi I}{N}\right)\delta_{II'}$; in the second equality, we used (4.51) to compute the finite-temperature fermion four-point function and expressed the product of U and C matrices using standard matrix notation. The disorder average of the product of U and C matrices is computed as in the previous section. To this end, we partition the interval $[0, z]$ into n segments and the interval $[0, z']$ into m segments, each of size $\delta z = z/n = z'/m$, and decompose each U matrix as in (4.62). We find

$$
\overline{\mathrm{Tr}\left(e^{-iM_n} \cdots e^{-iM_1}\right) C\left(e^{iM_1} \cdots e^{iM_n}\right)\left(e^{-iM_m} \cdots e^{-iM_1}\right) C\left(e^{iM_1} \cdots e^{iM_m}\right)}
$$
$$
= \sum_I \cos^2\left(\frac{2\pi I}{N}\right) e^{-2g_{eff}k_F|z-z'|}
$$
$$
= \frac{N}{2} e^{-2g_{eff}k_F|z-z'|},
$$

$$(4.74)$$

where g_{eff} is defined in (4.67). The details for the evaluation of the disorder average are given in Appendix 4.B. The sum over I in the second equality is performed for $N \to \infty$ using the continuum limit $\frac{1}{N}\sum_I \to \int \frac{d\theta}{2\pi}$.

Inserting (4.74) into the current two-point function (4.73), the conductivity (4.72) becomes

$$
\sigma_{xx}(\omega) = \frac{1}{i\omega_n} \frac{k_F}{2L} \int dz dz' d\tau \, e^{i\omega_n \tau} \left(\frac{i}{2\beta \sinh^2\left(\frac{\pi(z-z'+i(\tau-\tau'))}{\beta}\right)} \right)^2 e^{-2g_{eff}k_F|z-z'|} \Bigg|_{i\omega_n \to \omega + i0^+}.
$$

$$(4.75)$$

Shifting $z \to z + z'$ and $\tau \to \tau + \tau'$, the integral over z' produces a factor of L; we next calculate the integral over τ in the zero temperature limit $\beta \to \infty$.

The relevant term is

$$\int_0^\infty d\tau\, e^{i\omega_n \tau}\left(\frac{i}{2\pi}\frac{1}{(z+i\tau)}\right)^2 = -\frac{1}{4\pi}|\omega_n|\,e^{-\omega_n z}\Theta(\omega_n z). \qquad (4.76)$$

Performing the remaining integral over z, we obtain the conductivity

$$\sigma_{xx}(\omega) = \frac{1}{8}\cdot\frac{1}{g_{\text{eff}} - i\frac{\omega}{2vk_F}} \quad (\text{units of } e^2/h), \qquad (4.77)$$

where we have restored the fermion velocity v, previously set to one. This is the main result of this paper. The dc longitudinal conductivity varies as $1/g_{\text{eff}}$ along the random fixed line. An identical calculation with $\cos\left(\frac{2\pi I}{N}\right) \to \sin\left(\frac{2\pi I}{N}\right)$ produces $\sigma_{yy}(\omega) = \sigma_{xx}(\omega)$. The Hall conductivity $\sigma_{xy}(\omega)$ vanishes because there is no time-reversal symmetry breaking on average. This follows from an explicit computation similar to the above, in which $\sum_I \cos^2\left(\frac{2\pi I}{N}\right) \to \sum_I \cos\left(\frac{2\pi I}{N}\right)\sin\left(\frac{2\pi I}{N}\right) = 0$.

We may crudely estimate the regime of validity of (4.77) as follows. Recall from (4.30) that $g_{\text{eff}} \sim g$ characterizes the scale of the fluctuations of the random vector potential $\mathbf{A}(\mathbf{q})$, which in turn determines the random coupling $|V_{\theta\theta'}(p_\perp - p'_\perp)| \sim k_F|\mathbf{A}(\mathbf{q})| \sim k_F\sqrt{g_{\text{eff}}}$ in (4.22). General effective field theory considerations require $k_F\sqrt{g_{\text{eff}}} \leq \Lambda$, where $\Lambda \ll k_F$ is the cutoff on momenta transverse to the Fermi surface. Inserting this inequality into (4.77) at $\omega = 0$, we find

$$\sigma_{xx}(\omega = 0) \geq \frac{1}{8}\cdot\frac{k_F^2}{\Lambda^2}. \qquad (4.78)$$

$\Lambda \ll k_F$ (rather than $\Lambda \leq k_F$) ensures the scattering is primarily tangential to the Fermi surface, instead of perpendicular to it (see §4.2). A study of the effects of the various leading corrections to the effective theory (4.23) could potentially clarify the bound (4.78).

4.4 Discussion and Summary

We have studied the effects of a quenched random, transverse magnetic field on a 2d Dirac fermion placed at finite density. For weak disorder of sufficiently long wavelength, we showed how the effective theory reduces to an infinite collection of chiral fermions coupled by the vector potential. This simplification allows for an exact treatment of the effects of the disorder. We found a line of fixed points along which the longitudinal dc conductivity (4.77) varies continuously with the disorder variance.

The dc conductivity was calculated in the collisionless $\hbar\omega/k_B T \to \infty$ limit. It is important to extend our study to the opposite order of limits $\hbar\omega/k_B T \to 0$, the so-called incoherent regime [54], relevant to experiment. (See [53] for a study of distinct dc limits of the ac conductivity of a clean Dirac fermion at zero density.) This question is pertinent to the expected universality of the conductivity at a quantum phase transition [63]. Numerical studies[9] [18, 29, 57] of the integer quantum Hall transition appear to be roughly consistent with experiment (e.g., [59, 68]), giving a value for the dc longitudinal conductivity $\sigma_{xx} \sim (.54 - .60)\, e^2/h$.

We focused exclusively on the point where the Dirac fermion is massless. In the clean limit at finite density, a metal intervenes between integer quantum Hall states with $\sigma_{xy} = \pm\frac{1}{2}\frac{e^2}{h}$ as the mass m is tuned between $\pm\mu$, where μ is the chemical potential. Based on numerics (e.g., [56]), the metallic region is absent in the presence of disorder and a direct integer quantum Hall transition should obtain. It would be interesting to redo our analysis with a finite mass m to try to find the localization length exponent for this transition.

The disorder we studied was of sufficiently long wavelength that it mediated elastic scattering between nearby Fermi points only. The opposite regime, in which all Fermi points are coupled by the disorder, might be interesting to consider. The action of the theory at energy $\omega = 0$ takes the form:

$$S_{\omega=0} = \int dz \sum_{I,J=1}^{N} R_I^*(z)\Big(i\partial_z \delta_{IJ} + J_{IJ}\Big)R_J(z), \qquad (4.79)$$

with random J_{IJ} coupling all Fermi points I, J, subject to a given ensemble. Interpreting z as "time," this action is reminiscent of the quadratic Sachdev-Ye-Kitaev model [27, 55] with complex fermions.

The similarity of the effective theory (4.50) of the random Dirac Fermi surface to the theory of N chiral free fermions in 1d suggests a possible route towards a non-Fermi liquid generalization, in which disorder may be studied simultaneously. For example, we may consider two independent Dirac fermions—with chemical potentials that are of equal magnitude and opposite sign—in the presence of quenched vector potential disorder. The effective action is $S_R + S_L$,

---

[9]We are grateful to Prashant Kumar for discussions about this.

where

$$S_{\mathrm{R}} = \int dt dz \sum_{I,J=1}^{N} R_I^*(t,z)\Big(i\big(\partial_t + \partial_z\big)\delta_{IJ} + \frac{1}{N}V_{IJ}(z)\Big)R_J(t,z), \qquad (4.80)$$

$$S_{\mathrm{L}} = \int dt dz \sum_{I,J=1}^{N} (L_I^*(t,z)\Big(i\big(\partial_t - \partial_z\big)\delta_{IJ} - \frac{1}{N}V_{IJ}(z)\Big)L_J(t,z), \qquad (4.81)$$

and R_I (L_J) is the low-energy excitation about the Fermi surface defined by positive (negative) chemical potential. Couplings between right ($R_I^* R_I$) and left ($L_J^* L_J$) densities leads to Luttinger liquid-like behavior. So long as the couplings preserve a diagonal subgroup of the $U(N) \times U(N)$ symmetry of the Fermi surface, the interactions and disorder can be studied simultaneously. The implications and possible microscopic origin of such a theory are unclear.

APPENDIX

4.A   Disorder Average of Single particle Greens function

In this appendix, we check that the higher-order corrections to the third equality in (4.66) exponentiate. This ensures the disorder-averaged Green's function takes the short-range form (4.68). Beginning with (4.66), we write

$$\sum_A \overline{U_{IA}^\dagger(z)U_{AI}(0)} = \sum_A \overline{\left(e^{iM_1}...e^{iM_{n-1}}e^{iM_n}\right)}_{II} \tag{4.82}$$

$$= \overline{\left([1 + iM_1 - \frac{M_1^2}{2} + ..][1 + iM_2 - \frac{M_2^2}{2} + ..]...[1 + iM_n - \frac{M_n^2}{2} + ..]\right)}_{II}$$

$$\equiv \mathrm{Lin} + \mathrm{Quad} + \mathrm{Cubic} + ... \tag{4.83}$$

where Lin, Quad, and Cubic stand for terms with two, four, and six M-contractions. To simplify the presentation here, we set $f_0 = 0$ in (4.65), which leads to

$$\overline{(M_i)_{IJ}(M_j)_{KL}} = (\frac{g\,k_F}{N}f_1)\,\delta z\,\delta_{IL}\,\delta_{JK}\,\delta_{|i-j|,1}\,,\quad g_Y \equiv \frac{g\,k_F}{N}f_1. \tag{4.84}$$

First, we compute the linear term:

$$\mathrm{Lin} = \overline{\left((iM_1)(iM_2) + (iM_2)(iM_3) + ...(iM_{n-1})(iM_n)\right)}_{II}$$

$$= \sum_{j=1}^{n-1}\overline{[(iM_j)(iM_{j+1})]_{II}}$$

$$= i^2 g_Y\,N\delta_{II}\,(n-1)\,\delta z \tag{4.85}$$

Next we compute the quadratic term:

$$\mathrm{Quad} = \overline{\Big(\sum_{j=1}^{n-1}\frac{1}{4}(iM_j)^2(iM_{j+1})^2 + \sum_{j=1}^{n-2}\frac{1}{2}(iM_j)(iM_{j+1})^2(iM_{j+2}) + \sum_{j<k,j+1\neq k}(iM_j)(iM_{j+1})(iM_k)(iM}$$

$$= \frac{1}{4}i^4 g_Y^2\,N^2\,(n-1)\delta z^2 + \frac{1}{2}i^4 g_Y^2\,N^2\,(n-2)\delta z^2 + i^4 g_Y^2\,N^2\,\frac{(n-2)(n-3)}{2}\delta z^2$$

$$\to i^4 g_Y^2\,N^2\,\frac{z^2}{2}.$$

In the last line, we took the continuum limit $n\delta z \to z$, in which only the n^2 term survives; in this limit, all linear in n terms can be dropped. Finally, we

compute the cubic term. Given the computation of the quadratic term, we only retain the n^3 terms here:

$$
\begin{aligned}
\text{Cubic} &= \sum_{j,k,\ell,j<k<\ell,j+1\neq k,k+1\neq\ell} \overline{\left((iM_j)(iM_{j+1})(iM_k)(iM_{k+1})(iM_\ell)(iM_{\ell+1})\right)}_{II} \\
&= i^6\, g_Y^3\, N^3\, \frac{n^3 + (\text{subleading terms})}{6}\, \delta z^3 \\
&\to i^6\, g_Y^3\, N^3\, \frac{z^3}{6}.
\end{aligned}
$$

(4.88)

Examining Lin, Quad, and Cubic, in particular, the combinational factors $\frac{1}{2!}, \frac{1}{3!}$, we have confidence that the average $\sum_A \overline{U_{IA}^\dagger(z)U_{AI}(0)}$ indeed takes the exponential form:

$$
\sum_A \overline{U_{IA}^\dagger(z)U_{AI}(0)} = 1 + i^2 g_Y\, N\, z + i^4 g_Y^2 N^2\, \frac{z^2}{2} + i^6\, g_Y^3\, N^3\, \frac{z^3}{6} + \ldots = e^{-g_Y N z} = e^{-g k_F f_1 z}. \quad (4.89)
$$

4.B Disorder Average of Products of U and C Matrices

In this appendix, we detail the evaluation of the disorder average of products of U and C matrices, focusing on the product that appears in (4.73):

$$
Tr\, \overline{U(z)CU^\dagger(z)U(z')CU^\dagger(z')} \equiv \overline{U_{AI}(z)C_{II'}U_{I'B}^\dagger(z)U_{BJ}(z')C_{JJ'}U_{J'A}^\dagger(z')}, \quad (4.90)
$$

where $U_{IJ}(z)$ is defined in (4.52), $C_{II'} = \cos\left(\frac{2\pi I}{N}\right)\delta_{II'}$, and the sums over $A, I, I', B, J, J' = 1, \ldots, N$ are understood. The computation of (4.66) is similar and will not be discussed.

To calculate (4.90), we discretize the z direction into segments $[z_{k-1}, z_k]$ of length $\delta z > 0$, where $z_k = k\delta z$ for all integer k. We take $z = z_n$, $z' = z_m$, and consider the limit $n, m \to \infty$ with z_n and z_m fixed. $U(z)$ is decomposed as

$$
U(z) = e^{-\frac{i}{N}\int_{z_{n-1}}^{z_n} dz'\, V(z')} \cdots e^{-\frac{i}{N}\int_{z_1}^{z_2} dz'\, V(z')} e^{-\frac{i}{N}\int_{z_0}^{z_1} dz'\, V(z')} \quad (4.91)
$$

and similarly for $U(z')$. Since δz is infinitesimal, we approximate

$$
\frac{1}{N}\int_{z_{j-1}}^{z_j} dz'\, V(z') \approx \frac{1}{N}V(z_j)\delta z \equiv M_j. \quad (4.92)
$$

The decomposition of U becomes

$$
U(z) = e^{-i\, M_n} e^{-i M_{n-1}} \cdots e^{-i\, M_1}. \quad (4.93)
$$

From (4.55), M_j is a zero-mean Gaussian random variable with variance,

$$\overline{(M_i)_{IJ}(M_j)_{KL}} = \frac{gk_F}{N}\delta_{IL}\delta_{JK}f(z_i - z_j)\delta z^2, \tag{4.94}$$

where $f(z_i - z_j)$ is defined by

$$f(z_i - z_j)\delta z = f_0\delta_{|i-j|,0} + f_1\delta_{|i-j|,1} + f_2\delta_{|i-j|,2} + ... + f_k\delta_{|i-j|,k}. \tag{4.95}$$

We refer to f_0 as the on-site correlation coefficient, f_1 as the 1st neighbor correlation coefficient, f_2 as the 2nd neighbor correlation coefficient, etc. Using (4.95), we write the disorder average (4.90) as

$$\text{Tr}\,\overline{U(z)CU^\dagger(z)U(z')CU^\dagger(z')} = \text{Tr}[C\,C] + W_0 + W_1 + \ldots + W_k, \tag{4.96}$$

where W_j denotes the contribution from f_j. The first term $\text{Tr}[C\,C]$ is the constant term without any Wick contraction due to the disorder averaging.

1st-neighbor correlation: W_1

We begin with the 1st neighbor contribution W_1. We substitute (4.93) into (4.96) and expand the exponentials to obtain

$$\begin{aligned}
W_1 = \overline{\left(e^{-i\,M_n}\cdots e^{-i\,M_1}\right)_{AI} C_{II'}\left(e^{i\,M_1}\cdots e^{i\,M_n}\right)_{I'B}} \\
\times \left.\overline{\left(e^{-i\,M_m}\cdots e^{-i\,M_1}\right)_{BJ} C_{JJ'}\left(e^{i\,M_1}\cdots e^{i\,M_m}\right)_{J'A}}\right|_{f_1} \\
\approx \overline{\left((1-iM_n)\cdots(1-iM_1)\right)_{AI} C_{II'}\left((1+iM_1)\cdots(1+iM_n)\right)_{I'B}} \\
\times \left.\overline{\left((1-iM_m)\cdots(1-iM_1)\right)_{BJ} C_{JJ'}\left((1+iM_1)\cdots(1+iM_m)\right)_{J'A}}\right|_{f_1} \tag{4.97}
\end{aligned}$$

where $\left.\right|_{f_1}$ indicates that we only consider the contributions due to the 1st neighbor correlation f_1 in (4.95). Note that the disorder average in the first equality is being performed over the entire product, not separately over each term in the product. Assuming $n > m$, there are four possible contractions

involving M_n that we isolate by writing W_1 as

$$\overline{\left((-iM_n)(-iM_{n-1})\right)}_{AI}C_{II'}\delta_{I'B}\,\delta_{BJ}C_{JJ'}\delta_{J'A} + \overline{(-iM_n)_{AI}(iM_{n-1})_{I'B}}\,C_{II'}\delta_{BJ}C_{JJ'}\delta_{J'A}$$

$$+\overline{(-iM_{n-1})_{AI}(iM_n)_{I'B}}C_{II'}\,\delta_{BJ}C_{JJ'}\delta_{J'A} + \delta_{AI}C_{II'}\overline{\left((iM_{n-1})(iM_n)\right)}_{I'B}\,\delta_{BJ}C_{JJ'}\delta_{J'A}$$

$$+\overline{\left(e^{-iM_{n-1}}\cdots e^{-iM_1}\right)_{AI}C_{II'}\left(e^{iM_1}\cdots e^{iM_{n-1}}\right)_{I'B}\left(e^{-iM_m}\cdots e^{-iM_1}\right)_{BJ}C_{JJ'}\left(e^{iM_1}\cdots e^{iM_m}\right)_{J'A}}\Big|_{f_1}$$

$$= 2g\,f_1\,k_F\,\delta z\left(-\delta_{AI}\delta_{I'B} + \frac{1}{N}\delta_{II'}\delta_{AB}\right)\delta_{BJ}\hat{C}_{II'}\hat{C}_{JJ'}\delta_{J'A}$$

$$+\overline{\left(e^{-iM_{n-1}}\cdots e^{-iM_1}\right)_{AI}C_{II'}\left(e^{iM_1}\cdots e^{iM_{n-1}}\right)_{I'B}\left(e^{-iM_m}\cdots e^{-iM_1}\right)_{BJ}C_{JJ'}\left(e^{iM_1}\cdots e^{iM_m}\right)_{J'A}}\Big|_{f_1}.$$

$$(4.98)$$

The subleading term $\propto \frac{1}{N}$, which comes from "crossing-contractions," vanishes because $C_{II'}\delta_{II'} = \text{Tr}[C] = 0$.

We continue as above sequentially contracting 1st neighbor pairs involving $M_{n-1}, M_{n-2}, \ldots, M_{m+2}$ to arrive at

$$W_1 = -2g\,f_1\,k_F\text{Tr}[CC]\Big(n - (m+2) + 1\Big)\,\delta z + \Big(\text{Contractions of } M_{m+1}, \ldots, M_1\Big)$$

$$(4.99)$$

There are eight contractions that involve M_{m+1} and M_m in the second term in (4.99):

$$\Big[\overline{\left((-iM_{m+1})(-iM_m)\right)}_{AI}C_{II'}\delta_{I'B}\delta_{BJ}C_{JJ'}\delta_{J'A} + \overline{(-iM_{m+1})_{AI}(iM_m)_{I'B}}C_{II'}\delta_{BJ}C_{JJ'}\delta_{J'A}$$

$$+\overline{(-iM_{m+1})_{AI}(-iM_m)_{BJ}}C_{II'}\delta_{I'B}C_{JJ'}\delta_{J'A} + \overline{(-iM_{m+1})_{AI}(+iM_m)_{J'A}}C_{II'}\delta_{I'B}\delta_{BJ}C_{JJ'}\Big]$$

$$+\Big[\overline{(M_m)_{AI}(M_{m+1})_{I'B}}C_{II'}\delta_{BJ}C_{JJ'}\delta_{J'A} - \overline{(M_mM_{m+1})_{I'B}}\delta_{AI}C_{II'}\delta_{BJ}C_{JJ'}\delta_{J'A}$$

$$+\delta_{AI}C_{II'}\overline{(M_{m+1})_{I'B}(M_m)_{BJ}}C_{JJ'}\delta_{J'A} - \delta_{AI}C_{II'}\overline{(M_{m+1})_{I'B}(M_m)_{J'A}}\delta_{BJ}C_{JJ'}\Big]. \quad (4.100)$$

In the first $[\ldots]$, the first term cancels with the fourth and the second term cancels with the third; the same pairs mutually cancel in the second $[\ldots]$. Next we consider the contractions involving M_m and M_{m-1}, and we again obtain zero. These cancellations continue through to contractions involving M_1. This makes sense since we expect the result to only depend on the difference $(n-m)$. Summarizing, we have

$$W_1 = -\text{Tr}[CC]\Big(2g\,f_1\,k_F\,[n - (m+2) + 1]\delta z\Big). \quad (4.101)$$

2nd-neighbor correlation and beyond: $W_2, \ldots, W_k$

Following the logic used to compute the 1st neighbor correlations, we find

$$
\begin{aligned}
W_2 &= \overline{\left(e^{-i\,M_n} \cdots e^{-i\,M_1}\right)_{AI} C_{II'} \left(e^{i\,M_1} \cdots e^{i\,M_n}\right)_{I'B}} \\
&\quad \times \overline{\left(e^{-i\,M_m} \cdots e^{-i\,M_1}\right)_{BJ} C_{JJ'} \left(e^{i\,M_1} \cdots e^{i\,M_m}\right)_{J'A}}\Big|_{f_1} \\
&\approx \overline{\left((1-iM_n)\cdots(1-iM_1)\right)_{AI} C_{II'}\left((1+iM_1)\cdots(1+iM_n)\right)_{I'B}} \\
&\quad \times \overline{\left((1-iM_m)\cdots(1-iM_1)\right)_{BJ} C_{JJ'}\left((1+iM_1)\cdots(1+iM_m)\right)_{J'A}}\Big|_{f_2} \\
&= -\text{Tr}[CC]\Big(2g\,f_2\,k_F\,[n-(m+3)+1]\delta z\Big).
\end{aligned}
\tag{4.102}
$$

Generalizing to k^{th} neighbor correlations, we have

$$
W_k = -\text{Tr}[CC]\Big(2g\,f_k\,k_F\,[n-(m+k+1)+1]\delta z\Big).
\tag{4.103}
$$

On-site Correlation: W_0

Unlike the off-site correlations discussed above, we have to expand the exponentials to quadratic order to obtain the contribution from on-site correlations:

$$
\begin{aligned}
W_0 &= \overline{\left(e^{-i\,M_n} \cdots e^{-i\,M_1}\right)_{AI} C_{II'} \left(e^{i\,M_1} \cdots e^{i\,M_n}\right)_{I'B}} \\
&\quad \times \overline{\left(e^{-i\,M_m} \cdots e^{-i\,M_1}\right)_{BJ} C_{JJ'} \left(e^{i\,M_1} \cdots e^{i\,M_m}\right)_{J'A}}\Big|_{f_0} \\
&\approx \overline{\left((1-iM_n-\tfrac{M_n^2}{2})\cdots(1-iM_1-\tfrac{M_1^2}{2})\right)_{AI} \hat{C}_{II'}\left((1+iM_1-\tfrac{M_1^2}{2})\cdots(1+iM_n-\tfrac{M_n^2}{2})\right)_{I'B}} \\
&\quad \times \overline{\left((1+iM_m-\tfrac{M_m^2}{2})\cdots(1+iM_1-\tfrac{M_1^2}{2})\right)_{BJ} \hat{C}_{JJ'}\left((1+iM_1-\tfrac{M_1^2}{2})\cdots(1+iM_m-\tfrac{M_m^2}{2})\right)_{J'A}}\Big|_{f_0} \\
&= gf_0 k_F \delta z\Big(-\delta_{AI}\delta_{I'B} + \frac{2}{N}\delta_{II'}\delta_{AB}\Big)\delta_{BJ}\hat{C}_{II'}\hat{C}_{JJ'}\delta_{J'A} + \Big(\text{Contractions of } M_{n-1},\ldots,M_1\Big).
\end{aligned}
\tag{4.104}
$$

The crossing term $\propto \frac{1}{N}$ again vanishes. Continuing in this way we arrive at

$$
W_0 = -\text{Tr}[CC]\Big(g\,f_0\,k_F\,[n-(m+1)+1]\delta z\Big) + \Big(\text{Contractions of } M_m,\ldots,M_1\Big).
\tag{4.105}
$$

Similar to the cancellations that were discussed in the context of the 1st neighbor correlations, the remaining contractions of $M_m,\ldots,M_1$ equal zero. Thus, we have

$$
W_0 = -\text{Tr}[CC]\Big(g\,f_0\,k_F\,[n-(m+1)+1]\delta z\Big).
\tag{4.106}
$$

Final Result

Collecting all correlations $f_0, f_1, \ldots, f_k$ and replacing $\lim_{n\to\infty} n\delta z = z$ and $\lim_{m\to\infty} m\delta z = z'$, we have

$$\mathrm{Tr}\,\overline{U(z)CU^\dagger(z)U(z')CU^\dagger(z')} = \mathrm{Tr}[CC]\left(1 - 2gk_F\delta z\left(\frac{f_0}{2}(n-m) + \sum_{j=1}^{k} f_j[n-m-k]\right)\right)$$

$$= \mathrm{Tr}[CC]e^{-2gk_F|z-z'|\left(\frac{f_0}{2}+f_1+\ldots f_k\right)}.$$

$$(4.107)$$

Note that each term proportional to k in the sum vanishes at large n and m. This concludes our calculation of the disorder average in (4.74). In the main text, f_0 and f_1 are nonzero, and $f_{k\geq 2} = 0$. Since the calculation of this disorder average is essentially the same as that of the fermion two-point function, the demonstration in Appendix 4.A carries over and ensures that the exponential form above holds.

BIBLIOGRAPHY

[1]   Toshinao Akuzawa and Miki Wadati. "Exact Ensemble Average of the Random Perturbation to the Random Fixed Point". In: *Journal of the Physical Society of Japan* 66.8 (1997), pp. 2283–2287. eprint: https://doi.org/10.1143/JPSJ.66.2283. URL: https://doi.org/10.1143/JPSJ.66.2283.

[2]   Gerd Bergmann. "Weak localization in thin films". In: *Physics Reports* 107.1 (1984), pp. 1–58. ISSN: 0370-1573. URL: http://www.sciencedirect.com/science/article/pii/0370157384901030.

[3]   A. H. Castro Neto et al. "The electronic properties of graphene". In: *Rev. Mod. Phys.* 81 (2009), p. 109.

[4]   J T Chalker and P D Coddington. "Percolation, quantum tunnelling and the integer Hall effect". In: *Journal of Physics C: Solid State Physics* 21.14 (May 1988), pp. 2665–2679. URL: https://doi.org/10.1088/0022-3719/21/14/008.

[5]   Yang-Zhi Chou and Matthew S. Foster. "Chalker scaling, level repulsion, and conformal invariance in critically delocalized quantum matter: Disordered topological superconductors and artificial graphene". In: *Phys. Rev. B* 89 (16 Apr. 2014), p. 165136. URL: https://link.aps.org/doi/10.1103/PhysRevB.89.165136.

[6]   H. R. Christiansen and F. A. Schaposnik. "Fermion condensates of massless two-dimensional QED at finite density in nontrivial topological sectors". In: *Phys. Rev. D* 53 (6 Mar. 1996), pp. 3260–3265. URL: https://link.aps.org/doi/10.1103/PhysRevD.53.3260.

[7]   Luca V. Delacretaz et al. "Nonlinear Bosonization of Fermi Surfaces: The Method of Coadjoint Orbits". In: *arXiv e-prints*, arXiv:2203.05004 (Mar. 2022), arXiv:2203.05004. arXiv: 2203.05004 [cond-mat.str-el].

[8]   E. J. Dresselhaus, B. Sbierski, and I. A. Gruzberg. "Scaling collapse of longitudinal conductance near the integer quantum Hall transition". In: *arXiv e-prints*, arXiv:2112.09847 (Dec. 2021), arXiv:2112.09847. arXiv: 2112.09847 [cond-mat.mes-hall].

[9]   Elizabeth J. Dresselhaus, Björn Sbierski, and Ilya A. Gruzberg. "Numerical evidence for marginal scaling at the integer quantum Hall transition". In: *Annals of Physics* 431, 168560 (Aug. 2021), p. 168560. arXiv: 2101.01716 [cond-mat.dis-nn].

[10] Dominic V. Else, Ryan Thorngren, and T. Senthil. "Non-Fermi Liquids as Ersatz Fermi Liquids: General Constraints on Compressible Metals".

In: *Phys. Rev. X* 11 (2 Apr. 2021), p. 021005. URL: https://link.aps.org/doi/10.1103/PhysRevX.11.021005.

[11] Ferdinand Evers and Alexander D. Mirlin. "Anderson transitions". In: *Rev. Mod. Phys.* 80 (4 Oct. 2008), pp. 1355–1417. URL: https://link.aps.org/doi/10.1103/RevModPhys.80.1355.

[12] T. Giamarchi and H. J. Schulz. "Anderson localization and interactions in one-dimensional metals". In: *Phys. Rev. B* 37 (1 Jan. 1988), pp. 325–340. URL: https://link.aps.org/doi/10.1103/PhysRevB.37.325.

[13] Hart Goldman and Eduardo Fradkin. "Dirac composite fermions and emergent reflection symmetry about even-denominator filling fractions". In: *Phys. Rev. B* 98 (16 Oct. 2018), p. 165137. URL: https://link.aps.org/doi/10.1103/PhysRevB.98.165137.

[14] F. D. M. Haldane. "Model for a Quantum Hall Effect without Landau Levels: Condensed-Matter Realization of the "Parity Anomaly"". In: *Phys. Rev. Lett.* 61 (18 Oct. 1988), pp. 2015–2018. URL: https://link.aps.org/doi/10.1103/PhysRevLett.61.2015.

[15] C.-M. Ho and J. T. Chalker. "Models for the integer quantum Hall effect: The network model, the Dirac equation, and a tight-binding Hamiltonian". In: *Phys. Rev. B* 54 (12 Sept. 1996), pp. 8708–8713. URL: https://link.aps.org/doi/10.1103/PhysRevB.54.8708.

[16] Kevin S. Huang, S. Raghu, and Prashant Kumar. "Numerical Study of a Dual Representation of the Integer Quantum Hall Transition". In: *Phys. Rev. Lett.* 126 (5 Feb. 2021), p. 056802. URL: https://link.aps.org/doi/10.1103/PhysRevLett.126.056802.

[17] Aaron Hui, Eun-Ah Kim, and Michael Mulligan. "Non-Abelian bosonization and modular transformation approach to superuniversality". In: *Phys. Rev. B* 99 (12 Mar. 2019), p. 125135. URL: https://link.aps.org/doi/10.1103/PhysRevB.99.125135.

[18] Y. Huo, R. E. Hetzel, and R. N. Bhatt. "Universal conductance in the lowest Landau level". In: *Phys. Rev. Lett.* 70 (4 Jan. 1993), pp. 481–484. URL: https://link.aps.org/doi/10.1103/PhysRevLett.70.481.

[19] Shamit Kachru et al. "Mirror symmetry and the half-filled Landau level". In: *Phys. Rev. B* 92 (23 Dec. 2015), p. 235105. URL: https://link.aps.org/doi/10.1103/PhysRevB.92.235105.

[20] C. L. Kane and Matthew P. A. Fisher. "Impurity scattering and transport of fractional quantum Hall edge states". In: *Phys. Rev. B* 51 (19 May 1995), pp. 13449–13466. URL: https://link.aps.org/doi/10.1103/PhysRevB.51.13449.

[21] Jonas F. Karcher and Matthew S. Foster. "How spectrum-wide quantum criticality protects surface states of topological superconductors from Anderson localization: Quantum Hall plateau transitions (almost) all the way down". In: *Annals of Physics* 435, 168439 (Dec. 2021), p. 168439. arXiv: 2101.08799 [cond-mat.dis-nn].

[22] D. E. Khmel'Nitskiĭ. "Quantization of Hall conductivity". In: *Soviet Journal of Experimental and Theoretical Physics Letters* 38 (Nov. 1983), pp. 552–556.

[23] D. V. Khveshchenko. "Dirac fermions in a power-law–correlated random vector potential". In: *Europhysics Letters* 82.5 (May 2008), p. 57008. URL: https://dx.doi.org/10.1209/0295-5075/82/57008.

[24] D. V. Khveshchenko. "Electron Localization Properties in Graphene". In: *Phys. Rev. Lett.* 97 (3 July 2006), p. 036802. URL: https://link.aps.org/doi/10.1103/PhysRevLett.97.036802.

[25] D. V. Khveshchenko and A. G. Yashenkin. "Planar Dirac fermions in long-range-correlated random vector potential". In: *Physics Letters A* 309.5-6 (Mar. 2003), pp. 363–370. arXiv: cond-mat/0202173 [cond-mat].

[26] Yong Baek Kim, Akira Furusaki, and Derek K. K. Lee. "Network model of localization in a random magnetic field". In: *Phys. Rev. B* 52 (23 Dec. 1995), pp. 16646–16650. URL: https://link.aps.org/doi/10.1103/PhysRevB.52.16646.

[27] A. Kitaev. "A simple model of quantum holography". http://online.kitp.ucsb.edu/online/entan

[28] B Kramer and A MacKinnon. "Localization: theory and experiment". In: *Reports on Progress in Physics* 56.12 (1993), p. 1469. URL: http://stacks.iop.org/0034-4885/56/i=12/a=001.

[29] B. Kramer, T. Ohtsuki, and S. Kettemann. "Random network models and quantum phase transitions in two dimensions". In: *Physics Reports* 417.5 (2005), pp. 211–342. ISSN: 0370-1573. URL: https://www.sciencedirect.com/science/article/pii/S0370157305002851.

[30] Prashant Kumar, Yong Baek Kim, and S. Raghu. "Self-duality of the integer quantum Hall to insulator transition: Composite fermion description". In: *Phys. Rev. B* 100 (23 Dec. 2019), p. 235124. URL: https://link.aps.org/doi/10.1103/PhysRevB.100.235124.

[31] Chao-Jung Lee, Prashant Kumar, and Michael Mulligan. "Composite fermion nonlinear sigma models". In: *Phys. Rev. B* 104 (12 Sept. 2021), p. 125119. URL: https://link.aps.org/doi/10.1103/PhysRevB.104.125119.

[32] Chao-Jung Lee and Michael Mulligan. "Current Algebra Approach to 2d Chiral Metals". In: *arXiv e-prints*, arXiv:2204.05328 (Apr. 2022), arXiv:2204.05328. arXiv: 2204.05328 [cond-mat.str-el].

[33] Dung-Hai Lee. "Network models of quantum percolation and their field-theory representations". In: *Phys. Rev. B* 50 (15 Oct. 1994), pp. 10788–10791. URL: https://link.aps.org/doi/10.1103/PhysRevB.50.10788.

[34] Herbert Levine, Stephen B. Libby, and Adrianus M. M. Pruisken. "Electron Delocalization by a Magnetic Field in Two Dimensions". In: *Phys. Rev. Lett.* 51 (20 Nov. 1983), pp. 1915–1918. URL: https://link.aps.org/doi/10.1103/PhysRevLett.51.1915.

[35] Wanli Li et al. "Crossover from the nonuniversal scaling regime to the universal scaling regime in quantum Hall plateau transitions". In: *Phys. Rev. B* 81 (3 Jan. 2010), p. 033305. URL: https://link.aps.org/doi/10.1103/PhysRevB.81.033305.

[36] Wanli Li et al. "Scaling in Plateau-to-Plateau Transition: A Direct Connection of Quantum Hall Systems with the Anderson Localization Model". In: *Phys. Rev. Lett.* 102 (21 May 2009), p. 216801. URL: https://link.aps.org/doi/10.1103/PhysRevLett.102.216801.

[37] Andreas W. W. Ludwig et al. "Integer quantum Hall transition: An alternative approach and exact results". In: *Phys. Rev. B* 50 (11 Sept. 1994), pp. 7526–7552. URL: https://link.aps.org/doi/10.1103/PhysRevB.50.7526.

[38] Max A. Metlitski, Ashvin Vishwanath, and Cenke Xu. "Duality and bosonization of $(2+1)$-dimensional Majorana fermions". In: *Phys. Rev. B* 95 (20 May 2017), p. 205137. URL: https://link.aps.org/doi/10.1103/PhysRevB.95.205137.

[39] S. V. Morozov et al. "Strong Suppression of Weak Localization in Graphene". In: *Phys. Rev. Lett.* 97 (1 July 2006), p. 016801. URL: https://link.aps.org/doi/10.1103/PhysRevLett.97.016801.

[40] A. F. Morpurgo and F. Guinea. "Intervalley Scattering, Long-Range Disorder, and Effective Time-Reversal Symmetry Breaking in Graphene". In: *Phys. Rev. Lett.* 97 (19 Nov. 2006), p. 196804. URL: https://link.aps.org/doi/10.1103/PhysRevLett.97.196804.

[41] Michael Mulligan. "Particle-vortex symmetric liquid". In: *Phys. Rev. B* 95 (4 Jan. 2017), p. 045118. URL: https://link.aps.org/doi/10.1103/PhysRevB.95.045118.

[42] A.J. Niemi and G.W. Semenoff. "Axial Anomaly Induced Fermion Fractionization and Effective Gauge Theory Actions in Odd Dimensional Space-Times". In: *Phys. Rev. Lett.* 51 (1983), p. 2077.

[43] Kentaro Nomura, Mikito Koshino, and Shinsei Ryu. "Topological Delocalization of Two-Dimensional Massless Dirac Fermions". In: *Phys. Rev. Lett.* 99 (14 Oct. 2007), p. 146806. URL: https://link.aps.org/doi/10.1103/PhysRevLett.99.146806.

[44] Kentaro Nomura et al. "Quantum Hall Effect of Massless Dirac Fermions in a Vanishing Magnetic Field". In: *Phys. Rev. Lett.* 100 (24 June 2008), p. 246806. URL: https://link.aps.org/doi/10.1103/PhysRevLett.100.246806.

[45] Hideaki Obuse, Ilya A. Gruzberg, and Ferdinand Evers. "Finite-Size Effects and Irrelevant Corrections to Scaling Near the Integer Quantum Hall Transition". In: *Phys. Rev. Lett.* 109 (20 Nov. 2012), p. 206804. URL: https://link.aps.org/doi/10.1103/PhysRevLett.109.206804.

[46] P. M. Ostrovsky, I. V. Gornyi, and A. D. Mirlin. "Quantum Criticality and Minimal Conductivity in Graphene with Long-Range Disorder". In: *Phys. Rev. Lett.* 98 (25 June 2007), p. 256801. URL: https://link.aps.org/doi/10.1103/PhysRevLett.98.256801.

[47] Joseph Polchinski. "Effective field theory and the Fermi surface". In: *Theoretical Advanced Study Institute (TASI 92): From Black Holes and Strings to Particles*. June 1992, pp. 0235–276. arXiv: hep-th/9210046.

[48] Adrianus M.M. Pruisken. "Quasi particles in the theory of the integral quantum Hall effect: (II). Renormalization of the Hall conductance or instanton angle theta". In: *Nuclear Physics B* 290 (1987), pp. 61–86. ISSN: 0550-3213. URL: https://www.sciencedirect.com/science/article/pii/0550321387901787.

[49] Martin Puschmann et al. "Integer quantum Hall transition on a tight-binding lattice". In: *Phys. Rev. B* 99 (12 Mar. 2019), p. 121301. URL: https://link.aps.org/doi/10.1103/PhysRevB.99.121301.

[50] Xiao-Liang Qi, Taylor L. Hughes, and Shou-Cheng Zhang. "Topological field theory of time-reversal invariant insulators". In: *Phys. Rev. B* 78 (19 Nov. 2008), p. 195424.

[51] A. N. Redlich. "Gauge Noninvariance and Parity Violation of Three-Dimensional Fermions". In: *Phys. Rev. Lett.* 52 (1984), p. 18.

[52] Ralph Roskies and Fidel Schaposnik. "Comment on Fujikawa's analysis applied to the Schwinger model". In: *Phys. Rev. D* 23 (2 Jan. 1981), pp. 558–560. URL: https://link.aps.org/doi/10.1103/PhysRevD.23.558.

[53] S. Ryu et al. "Landauer conductance and twisted boundary conditions for Dirac fermions in two space dimensions". In: *Phys. Rev. B* 75 (20 May 2007), p. 205344. URL: https://link.aps.org/doi/10.1103/PhysRevB.75.205344.

[54] Subir Sachdev. "Nonzero-temperature transport near fractional quantum Hall critical points". In: *Phys. Rev. B* 57 (12 Mar. 1998), pp. 7157–7173. URL: https://link.aps.org/doi/10.1103/PhysRevB.57.7157.

[55]   Subir Sachdev and Jinwu Ye. "Gapless spin-fluid ground state in a random quantum Heisenberg magnet". In: *Phys. Rev. Lett.* 70 (21 May 1993), pp. 3339–3342. URL: https://link.aps.org/doi/10.1103/PhysRevLett.70.3339.

[56]   Björn Sbierski et al. "Criticality of Two-Dimensional Disordered Dirac Fermions in the Unitary Class and Universality of the Integer Quantum Hall Transition". In: *Phys. Rev. Lett.* 126 (7 Feb. 2021), p. 076801. URL: https://link.aps.org/doi/10.1103/PhysRevLett.126.076801.

[57]   L. Schweitzer and P. Marko š. "Universal Conductance and Conductivity at Critical Points in Integer Quantum Hall Systems". In: *Phys. Rev. Lett.* 95 (25 Dec. 2005), p. 256805. URL: https://link.aps.org/doi/10.1103/PhysRevLett.95.256805.

[58]   N. Seiberg et al. "A duality web in $2 + 1$ dimensions and condensed matter physics". In: *Annals of Physics* 374 (Nov. 2016), pp. 395–433. arXiv: 1606.01989 [hep-th].

[59]   D. Shahar et al. "Universal Conductivity at the Quantum Hall Liquid to Insulator Transition". In: *Phys. Rev. Lett.* 74 (22 1995), p. 4511. URL: http://link.aps.org/doi/10.1103/PhysRevLett.74.4511.

[60]   R. Shankar. "Renormalization-group approach to interacting fermions". In: *Rev. Mod. Phys.* 66 (1 Jan. 1994), pp. 129–192. URL: https://link.aps.org/doi/10.1103/RevModPhys.66.129.

[61]   Keith Slevin and Tomi Ohtsuki. "Finite Size Scaling of the Chalker-Coddington Model". In: *International Journal of Modern Physics Conference Series*. Vol. 11. International Journal of Modern Physics Conference Series. Jan. 2012, pp. 60–69. arXiv: 1203.1384 [cond-mat.mes-hall].

[62]   Dam Thanh Son. "Is the Composite Fermion a Dirac Particle?" In: *Phys. Rev. X* 5 (3 Sept. 2015), p. 031027. URL: https://link.aps.org/doi/10.1103/PhysRevX.5.031027.

[63]   S. L. Sondhi et al. "Continuous quantum phase transitions". In: *Rev. Mod. Phys.* 69 (1 1997), p. 315. URL: http://link.aps.org/doi/10.1103/RevModPhys.69.315.

[64]   A. M. Tsvelik. "Evidence for the PSL(2|2) Wess-Zumino-Novikov-Witten model as a model for the plateau transition in the quantum Hall effect: Evaluation of numerical simulations". In: *Phys. Rev. B* 75 (18 May 2007), p. 184201. URL: https://link.aps.org/doi/10.1103/PhysRevB.75.184201.

[65]   Chong Wang and T. Senthil. "Dual Dirac Liquid on the Surface of the Electron Topological Insulator". In: *Phys. Rev. X* 5 (4 2015), p. 041031.

[66] Jie Wang. "Dirac Fermion Hierarchy of Composite Fermi Liquids". In: *Phys. Rev. Lett.* 122 (25 June 2019), p. 257203. URL: https://link.aps.org/doi/10.1103/PhysRevLett.122.257203.

[67] Hans A. Weidenmüller. "Single electron in a random potential and a strong magnetic field". In: *Nuclear Physics B* 290 (1987), pp. 87–110. ISSN: 0550-3213. URL: https://www.sciencedirect.com/science/article/pii/0550321387901799.

[68] Kun Yang et al. "Study of universality at integer quantum Hall transitions". In: *Journal of Physics: Condensed Matter* 12.25 (June 2000), pp. 5343–5360. URL: https://doi.org/10.1088/0953-8984/12/25/301.

[69] Qiong Zhu et al. "Localization-length exponent in two models of quantum Hall plateau transitions". In: *Phys. Rev. B* 99.2, 024205 (Jan. 2019), p. 024205.

[70] Martin R. Zirnbauer. "Marginal CFT perturbations at the integer quantum Hall transition". In: *Annals of Physics* 431 (2021), p. 168559. ISSN: 0003-4916. URL: https://www.sciencedirect.com/science/article/pii/S0003491621001652.

[71] Martin R. Zirnbauer. "The integer quantum Hall plateau transition is a current algebra after all". In: *Nuclear Physics B* 941 (2019), pp. 458–506. ISSN: 0550-3213. URL: http://www.sciencedirect.com/science/article/pii/S0550321319300458.

C h a p t e r   5

CURRENT ALGEBRA APPROACH TO 2D INTERACTING CHIRAL METALS

5.1   Introduction

States of matter with a sharp Fermi surface—but whose low-energy excitations are not Landau quasiparticles—present a challenge for effective field theory. One approach to such states begins by coupling the free Fermi gas to a gapless bosonic degree of freedom (e.g., [38, 23, 35, 3, 56, 51, 9, 52, 45, 1, 46, 72, 37, 47, 62, 39, 43, 44, 48, 18, 17, 25, 31, 61, 12, 26, 27, 59, 40, 75, 53, 16, 24]). This boson may represent an order parameter fluctuation of the Fermi fluid in the vicinity of a quantum critical point or be an emergent gauge field in an effective description that is dual to the interacting electron one. If the coupling between the fermions and bosons is relevant, in the renormalization group (RG) sense, the resulting fermion + boson system generally flows towards a strongly interacting non-Fermi liquid fixed point. Another approach—piggybacking on the generic breakdown of the Fermi liquid in one spatial dimension—employs 2d (or higher) arrays of coupled Luttinger liquids [77, 15, 73, 64, 49, 54, 50]. The resulting anisotropic states generally have power-law instabilities with nonuniversal exponents.

Here we combine this second approach with a recent proposal by Else, Thorngren, and Senthil (ETS) [14]. The ETS proposal is based on the IR symmetry enhancement that occurs in the Fermi liquid. The IR symmetry is associated with the long-lived gapless quasiparticle excitations of the Fermi liquid. The enhancement is relative to the microscopic symmetries of a free Fermi gas, such as fermion number and translation invariance. From the effective field theory point of view [63, 55], the enhanced symmetry of the Fermi liquid is due to the special kinematics of the Fermi surface, which renders most quasiparticle interactions irrelevant. A similar IR symmetry enhancement occurs at the Luttinger liquid fixed point [19, 20], for which generically no quasiparticle picture applies, and in related systems [65, 36, 74, 42, 78, 29]. ETS suggested the Fermi liquid symmetry enhancement may characterize a class of non-Fermi liquid metals in $d > 1$, termed ersatz Fermi liquids, and showed how these IR

symmetries, if preserved, constrain the properties of such states.

The ETS proposal is similar to how current algebra constrains the low-energy scattering of pions in QCD [76]. This analogy motivates us to ask: Is there a corresponding nonlinear sigma model for an interacting Fermi system in which the enhanced IR symmetries of the Fermi liquid are manifest?

In this paper, we construct one such effective theory and argue that it produces an exactly solvable interacting Fermi system in two space dimensions. Specifically, we argue that the chiral Wess-Zumino-Witten (WZW) model [79, 58, 66, 67] with $U(N)$ symmetry at integer level $k > 1$ in two spacetime dimensions describes an interacting chiral metal in two spatial dimensions. At $k = 1$, the WZW model is equivalent to Balents and Fisher's free chiral metal [5] (see also [10, 6, 4, 69]), an anisotropic free Fermi gas with half of an open Fermi surface. We identify $U(N)$ with the enhanced IR symmetry of the chiral metal, with $N \to \infty$ equal to the number of points on the Fermi surface. The additional spatial dimension of the 2d chiral metal arises from the $U(N)$ flavor degrees of freedom of the WZW model. While we focus exclusively on 2d chiral metals, in which all excitations move in the same direction along one of the spatial dimensions, the construction appears to be generalizable non-chiral metals and/or higher dimensions.

Our construction is inspired by the seminal works of Luther [41], Haldane [22], Castro Neto and Fradkin [8], and Houghton and Marston [28] who studied the bosonization of interacting fermions in $d \geq 2$ (see also [34]). One difference between these earlier constructions and ours is that we use a real-space effective theory throughout. A seminclassical bosonization scheme for interacting Fermi systems has recently appeared in [13]. It would be interesting to understand the relation between this recent work and ours.

The remainder of this paper is organized as follows. In §5.2 we introduce the free 2d chiral metal [5]. This state arises from a 2d array of N coupled parallel quantum wires (a real-space analog of partitioning the Fermi surface into small nonoverlapping patches), each hosting a single chiral fermion. We point out that, in addition to $U(1)$ number conservation and continuous translation invariance along the wire, this theory has a nonlocal $SU(N)$ symmetry, which corresponds to transforming fermions on arbitrarily-separated wires into one another. (The $SU(N)$ symmetry is nonlocal in the sense that the associated conserved charge is not the integral of local density.) This observation allows

us to show in §5.3 that the free chiral metal is equivalent to a perturbed WZW theory with $U(N)$ symmetry at level $k = 1$. Single-fermion hopping between wires corresponds to perturbation by certain $SU(N)$ symmetry currents. The solvability of the perturbed WZW model at $k = 1$ (when the theory is equivalent to a free Fermi gas) extends to level $k > 1$. Since k is restricted to be an integer, deformation by $k > 1$ is nonperturbative. The resulting $k > 1$ theories are not equivalent to free fermions, however, they do maintain the same symmetries as the $k = 1$ theory. It is the deformation by $k > 1$ that distinguishes these models from the usual coupled Luttinger liquid constructions. We probe these models in §5.4 by calculating two-point correlation functions of single-fermion operator, the $U(1)$ density, and current operators for arbitrary level $k \geq 1$. In §5.5 we summarize our work and discussing possible directions of future research. There are two appendices: in the first, we derive the commutation algebra of density operators of the free chiral metal; in the second appendix, we show how the nonchiral $U(2)_1$ WZW theory decomposes in terms of chiral $U(2)_1$ WZW theories.

5.2 Nonlocal Symmetry of the Free Chiral Metal

In this section, we introduce the free 2d chiral metal and describe its nonlocal $SU(N)$ symmetry.

Free Chiral Metal

Consider a stack of N integer quantum Hall states, spaced a unit distance $\delta = 1$ apart from one another (Fig. 5.2.1 (a)). In the absence of any coupling between the quantum Hall layers, the low-energy excitations of the system consist of N free chiral fermion edge modes $\psi_I(x)$ with Hamiltonian,

$$H_0 = -iv \int dx \sum_{I=1}^{N} \psi_I^\dagger(x) \partial_x \psi_I(x), \tag{5.1}$$

where the velocity $v > 0$. The positive sign of v corresponds to right-moving excitations. The electron creation operator along the layer I edge is $e^{ip_F x} \psi_I^\dagger(x)$, where p_F^2 is proportional to the bulk 2d electron density in each layer [1]. The most relevant perturbation to H_0 consists of single-particle hopping between

---

[1] For instance, in a coupled wire construction of the integer Hall state, the 2d electron density is $p_F/\pi b$, where b is the wire separation.
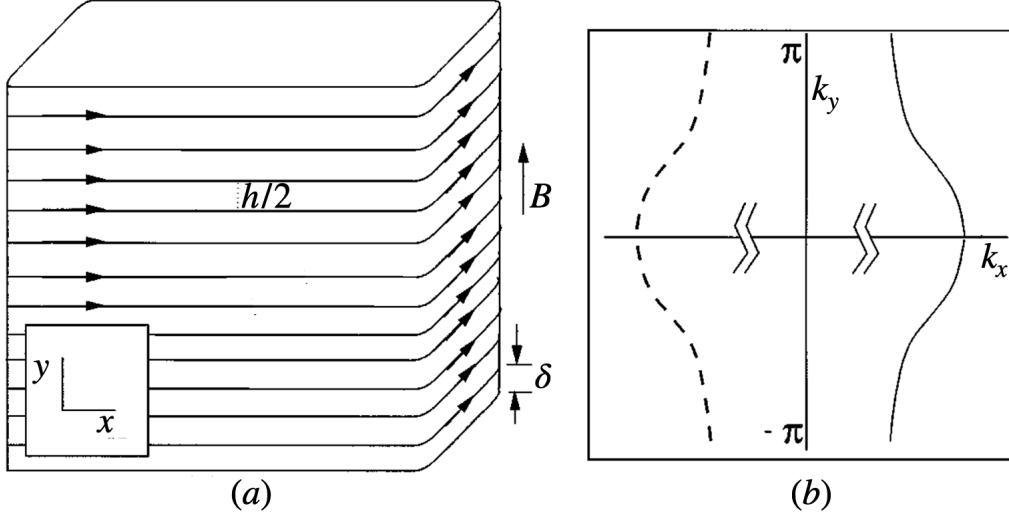
Figure 5.2.1: (a) Stack of 2d integer quantum Hall states with layer separation $\delta = 1$. $B > 0$ is the strength of the magnetic field; hopping between nearest-neighbor edge modes (each of whose chirality is indicated by the right-pointing arrow) proceeds with amplitude $h/2$. Periodic boundary conditions along the y direction are assumed. (b) Fermi surface of the free 2d chiral metal is indicated by the solid black line. The dashed line, which would be present in a conventional time-reversal invariant system with open Fermi surface, is absent. Both figures are slight adaptions of those in [5].

nearest-neighbor edges,

$$H_1 = \frac{h}{2} \int dx \sum_{I=1}^{N} \left(\psi_{I+1}^{\dagger}(x)\psi_I(x) + \psi_I^{\dagger}(x)\psi_{I+1}(x) \right). \tag{5.2}$$

We take the hopping amplitude $h > 0$; the overall factor of $1/2$ is for later convenience.

The total Hamiltonian $H = H_0 + H_1$ describes the free 2d chiral metal. Taking periodic boundary conditions, $\psi_I(x) = \psi_{I+N}(x)$, along the y direction and free boundary conditions along the x direction, the total Hamiltonian in momentum space $\mathbf{k} = (k_x, k_y)$ is

$$H = -\int d^2\mathbf{k} \left(vk_x - h\cos(k_y) \right) \psi^{\dagger}(\mathbf{k})\psi(\mathbf{k}), \tag{5.3}$$

where $\psi_I(x) = \int \frac{d^2\mathbf{k}}{2\pi} e^{-i\mathbf{k}\cdot\mathbf{r}}\psi(\mathbf{k}) \equiv \frac{1}{2\pi}\int_{-\infty}^{\infty} dk_x \int_{-\pi}^{\pi} dk_y\, e^{-i\mathbf{k}\cdot\mathbf{r}}\psi(\mathbf{k})$ and $\mathbf{r} = (x, I)$. The Fermi surface is half of a conventional open Fermi surface (Fig. 5.2.1 (b)):

Using (5.3), it consists of the N points $\mathbf{k}_F^{(m)} = (k_x^{(m)}, k_y^{(m)})$:

$$k_x^{(m)} = \frac{h}{v}\cos\left(k_y^{(m)}\right), \tag{5.4}$$

$$k_y^{(m)} = \frac{2\pi m}{N}, \tag{5.5}$$

for $m = -\frac{N}{2} + 1, \ldots, \frac{N}{2}$.

Nonlocal $SU(N)$ Symmetry

The free chiral metal has $U(1)$ number symmetry, continuous translation invariance along the x direction, and discrete translation invariance along the y direction. We will show in this section that the discrete translation invariance can be viewed as being part of a larger $SU(N)$ symmetry group. The $SU(N)$ symmetry is nonlocal in the sense that its associated conserved charges are not, in general, the spatial integrals of local densities. Including $SU(N)$, the full invariance of the chiral metal is then $U(N) \approx U(1) \times SU(N)$ symmetry and continuous translations along the x direction.

To demonstrate this symmetry enhancement, we reinterpret the free 2d chiral metal as a 1d system of N chiral fermions. Viewing the layer I label of ψ_I as a flavor index, the H_0 part of the total Hamiltonian (5.1) is invariant under the $U(N)$ transformations:

$$\psi_I \to \sum_{J=1}^{N} U_{IJ}\psi_J, \tag{5.6}$$

where $U_{IJ} \in U(N)$ is independent of x. From the 1d perspective, this transformation is simply a $U(N)$ global symmetry. From the 2d point of view, (5.6) is nonlocal since it generally relates fermions separated by an arbitrary distance $|I - J|$ modulo N along the y direction. We will refer to this transformation as a nonlocal symmetry. There is a local $U(1)^N$ subgroup consisting of the layer I phase rotations,

$$\psi_I \to e^{i\alpha_I}\psi_I, \quad I = 1, \ldots, N, \tag{5.7}$$

where α_I is an arbitrary constant phase. The hopping term H_1 (5.2) appears to reduce the $U(N)$ invariance to an overall $U(1)$ number symmetry. It turns out that the full nonlocal $U(N)$ symmetry is preserved for arbitrary hopping amplitude h [32].

To see this, we perform the gauge transformation,

$$\psi_I(x) = \sum_{J=1}^{N} M_{IJ}(x)\tilde{\psi}_J(x), \tag{5.8}$$

with unitary $SU(N)$ matrix,

$$M(x) = \exp\left(-i\frac{hx}{v}\sum_{m=1}^{N} X^{(m,m+1)}\right), \tag{5.9}$$

where the $SU(N)$ generators $X_{IJ}^{(m,n)} = \frac{1}{2}\left(\delta_{I,m}\delta_{J,n} + \delta_{I,n}\delta_{J,m}\right)$ with $m, n \in \{1, \ldots, N\}$ and $m \neq n$. As a result of the transformation (5.8), the hopping amplitude is gauged away and the total Hamiltonian becomes

$$H = -iv\int dx \sum_{I=1}^{N} \tilde{\psi}_I^\dagger(x)\partial_x\tilde{\psi}_I(x). \tag{5.10}$$

The nonlocal $U(N)$ symmetry of H is now manifest:

$$\tilde{\psi}_I = \sum_J U_{IJ}\tilde{\psi}_J \quad \leftrightarrow \quad \psi_I = \sum_{J,K,L} M_{IJ}U_{JK}M_{KL}^\dagger\psi_L. \tag{5.11}$$

Locality in the layer I direction is obscured in the diagonalized Hamiltonian (5.10) because the fermions $\tilde{\psi}_I(x)$ in (5.8) are linear combinations of $\psi_I(x)$ over all I. Note also that the gauge transformation alters the boundary conditions when the x direction is compact. For example, periodic boundary conditions on a circle of length L become "twisted" by multiplication of the fermions by $M(L)$.

The charges of the nonlocal $U(N)$ symmetry are

$$Q^a = \int dx \sum_{I,J} \tilde{\psi}_I^\dagger T_{IJ}^a \tilde{\psi}_J = \int dx \sum_{I,J,K,L} \psi_I^\dagger M_{IK} T_{KL}^a M_{LJ}^\dagger \psi_J, \tag{5.12}$$

where $T_{IJ}^0 = \delta_{IJ}$ and T_{IJ}^a for $a \in \{1, \ldots, N^2 - 1\}$ are Hermitian $SU(N)$ generators satisfying

$$\text{Tr}\left(T^a T^b\right) = \frac{1}{2}\delta^{ab}, \quad \left[T^a, T^b\right] = if^{abc}T^c, \tag{5.13}$$

with f^{abc} being $SU(N)$ structure constants. The gauge transformation by $M_{IJ}(x)$ in (5.8) effects a position-dependent similarity transformation of the $U(N)$ generators,

$$T_{IJ}^a \rightarrow \mathcal{T}_{IJ}^a(x) = \sum_{K,L} M_{IK}(x)T_{KL}^a M_{LJ}^\dagger(x), \tag{5.14}$$

under which the normalization and algebra in (5.13) are preserved. The real-space densities defining the Q^a are generally nonlocal with respect to the layer I direction.

The conserved momentum-space densities $n(\mathbf{k}) = \psi^\dagger(\mathbf{k})\psi(\mathbf{k})$ are associated with particular linear combinations of charges Q^a. To identify them, we introduce the linear combination of $SU(N)$ generators:

$$A_1 = \sum_{m=1}^{N} X^{(m,m+1)}, \quad A_2 = \sum_{m=1}^{N} X^{(m,m+2)}, \quad \cdots \quad , \quad A_{N/2} = \sum_{m=1}^{N} X^{(m,m+N/2)},$$

$$(5.15)$$

$$B_1 = \sum_{m=1}^{N} Y^{(m,m+1)}, \quad B_2 = \sum_{m=1}^{N} Y^{(m,m+2)}, \quad \cdots \quad , \quad B_{N/2} = \sum_{m=1}^{N} Y^{(m,m+N/2)},$$

$$(5.16)$$

with $X^{(m,n)}$ given below (5.9) and $Y_{IJ}^{(m,n)} = \frac{1}{2i}\left(\delta_{I,m}\delta_{J,n} - \delta_{I,n}\delta_{J,m}\right)$ $(m \neq n)$. The A_j $(B_{j'})$ matrices define nearest-neighbor, next nearest-neighbor, etc. hopping terms of the form:

$$Q^{A_j} = \int dx \sum_{I,J} \psi_I^\dagger (A_j)_{IJ} \psi_J, \tag{5.17}$$

$$Q^{B_{j'}} = \int dx \sum_{I,J} \psi_I^\dagger (B_{j'})_{IJ} \psi_J. \tag{5.18}$$

Fermions hopping via the $Q^{B_{j'}}$ set of operators acquire a $\pi/2$ phase. Because the A_j and $B_{j'}$ matrices commute with one another, the hopping terms take the same form when expressed in terms of the gauge-transformed fermions in (5.8). As such, these terms simply correspond to particular linear combinations of the charges Q^a in (5.12), the particular linear combination determined by the $SU(N)$ generators appearing in A_j $(B_{j'})$. In momentum space, these charges become

$$Q^{A_j} = \int d^2\mathbf{k} \, 2\cos(jk_y)n(\mathbf{k}), \tag{5.19}$$

$$Q^{B_{j'}} = \int d^2\mathbf{k} \, 2\sin(j'k_y)n(\mathbf{k}) \tag{5.20}$$

for $j, j' = 1, \ldots, N/2$.

5.3   Interacting Chiral Metals

In this section, we review the chiral WZW theory and then show how the free chiral metal can be written as a WZW theory with $U(N)$ symmetry at level

$k = 1$, before generalizing to arbitrary integer $k > 1$. We will refer to the $k > 1$ WZW theories as interacting chiral metals because they maintain the nonlocal $SU(N)$ symmetry of the $k = 1$ theory, but are not equivalent free fermions.

Chiral WZW Models

The chiral WZW theory in two spacetime dimensions is a nonlinear sigma model with Wess-Zumino topological term [79, 58, 66, 67] (for pedagogical reviews, see [30, 19]). The WZW fixed point action for a matrix boson $g = g_{IJ}(x, t)$ taking values in a compact group G is

$$S_k[g] = k\big(I[g] + \Gamma[g]\big), \tag{5.21}$$

where the level $k \geq 1$. For right-moving excitations, the nonlinear sigma model term is

$$I[g] = \frac{1}{4\pi} \int dt dx \, \mathrm{Tr}\Big((\partial_x g^{-1})(\partial_+ g)\Big), \tag{5.22}$$

where $\partial_+ = v\partial_x + \partial_t$. (For left-movers, substitute $\partial_+ \to \partial_- = v\partial_x - \partial_t$.) The Wess-Zumino topological term is

$$\Gamma[g] = \frac{1}{12\pi} \int dt dx dz \, \epsilon^{\mu\nu\rho} \mathrm{Tr}\Big((g^{-1}\partial_\mu g)(g^{-1}\partial_\nu g)(g^{-1}\partial_\rho g)\Big), \tag{5.23}$$

where $\mu, \nu, \rho \in \{t, x, z\}$ and the totally-antisymmetric symbol $\epsilon^{txz} = +1$. In this paper, we are interested in $G = U(N)$ and the trace is taken in the fundamental representation. The Wess-Zumino term is defined on a three-dimensional hemisphere with boundary equal to the two-dimensional spacetime. This term is independent of the extension of g to three dimensions modulo 2π, provided k is an integer.

Under the replacement $g \to g_1 g_2$, the chiral WZW action (5.21) satisfies the Polyakov-Wiegmann identity [57]:

$$S_k[g_1 g_2] = S_k[g_1] + S_k[g_2] - \frac{k}{2\pi} \int dt dx \mathrm{Tr}\Big(g_1^{-1}(\partial_+ g_1)(\partial_x g_2)g_2^{-1}\Big). \tag{5.24}$$

This identity, which is of central importance in what follows, arises from the individual multiplication rules obeyed by the nonlinear sigma model and Wess-Zumino terms:

$$I[g_1 g_2] = I[g_1] + I[g_2] - \frac{1}{4\pi} \int dt dx \mathrm{Tr}\Big(g_1^{-1}(\partial_x g_1)(\partial_+ g_2)g_2^{-1} + g_1^{-1}(\partial_+ g_1)(\partial_x g_2)g_2^{-1}\Big)$$

$$\tag{5.25}$$

and

$$\Gamma[g_1 g_2] = \Gamma[g_1] + \Gamma[g_2] + \frac{1}{4\pi} \int dt dx \mathrm{Tr}\Big(g_1^{-1}(\partial_x g_1)(\partial_t g_2)g_2^{-1} - g_1^{-1}(\partial_t g_1)(\partial_x g_2)g_2^{-1}\Big).$$
(5.26)

The Polyakov-Wiegmann identity can be used to show that the chiral WZW theory has symmetry:

$$g \to V(x_-)gW(t),$$
(5.27)

where $x_\pm = \frac{1}{2v}(x \pm vt)$ and $V(x_-), W(t)$ are matrices in $U(N)$. Invariance under right multiplication of g by the x-independent matrix $W(t)$ corresponds to the fact that $g = g_R(x_-)W(t)$, with $g_R(x_-) \in U(N)$, is the general solution to the equations of motion of $S_k[g]$ that arise upon varying $g \to g+\delta g = g(1+g^{-1}\delta g)$:

$$\partial_x\big(g^{-1}\partial_+ g\big) = 0.$$
(5.28)

This means that g should be thought of as a right-moving element of the coset $LU(N)/U(N)$, i.e., the loop group of $U(N)$ modulo arbitrary x-independent matrices $W(t)$ [67]. (Strictly speaking, the x direction should be a circle, rather than the real line, for this to be the usual loop group.) Invariance under left multiplication of g by $V(x_-)$ corresponds to a right-moving $U(N)$ Kac-Moody symmetry [21]. Conservation of the Kac-Moody currents,

$$J^a = \frac{ik}{2\pi}\mathrm{Tr}\Big(T^a(\partial_x g)g^{-1}\Big),$$
(5.29)

i.e., $\partial_+ J^a = 0$, follows upon applying (5.24) to the variation, $g \to g + \delta g = \big(1 + (\delta g)g^{-1}\big)g$. Note that $T^0_{IJ} = \delta_{IJ}$ and T^a for $a = 1, \ldots N^2 - 1$ are the same $SU(N)$ generators appearing in (5.13). These Kac-Moody currents obey the usual equal-time commutation relations:

$$\big[J^0(x,t), J^0(x',t)\big] = -\frac{ikN}{2\pi}\partial_x\delta(x - x'),$$
(5.30)

$$\big[J^a(x,t), J^b(x',t)\big] = if^{abc}J^c\delta(x - x') - \frac{ik\delta^{ab}}{4\pi}\partial_x\delta(x - x'),$$
(5.31)

for $a, b = 1, \ldots N^2 - 1$.

When the level $k = 1$, $S_k[g]$ is equivalent to N right-moving fermions with action,

$$S_{k=1}[g] \leftrightarrow i \int dt dx \sum_{I=1}^{N} \psi_I^\dagger \partial_+ \psi_I,$$
(5.32)

where "↔" indicates "equivalent to." This equivalence is the chiral version of Witten's non-Abelian bosonization [79, 58, 66, 67]. The Kac-Moody currents correspond to the fermion bilinears,

$$J^a \leftrightarrow \sum_{I,J} \psi_I^\dagger T_{IJ}^a \psi_J. \tag{5.33}$$

The level $k > 1$ theories are interacting generalizations of the $k = 1$ theory, in which the $U(N)$ symmetry is maintained. One way to think about them goes as follows [70]. Consider the theory of kN nonchiral free Dirac fermions. Similar to the free chiral metal, this theory may be viewed as arising in the low-energy limit at the surface of a stack of kN integer spin-quantum Hall states. Factorizing $U(kN)_1 \approx U(1)_{kN} \times SU(N)_k \times SU(k)_N$ for each chirality, we may couple right-moving and left-moving $SU(k)_N$ currents $I_{R,L}^a$ [2] through the marginally-relevant interaction,

$$S' = -c \int dtdx \sum_{a=1}^{k^2-1} I_R^a I_L^a. \tag{5.34}$$

For $c > 0$, the interaction (5.34) drives the free fermion system to the nonchiral $U(N)_k$ WZW model [71]. The fixed point theory, i.e., the $U(N)_k$ WZW model with $k > 1$, has the same symmetry as the $k = 1$ theory. $S_k[g]$ in (5.21) is the chiral version of this fixed point in which there are only right-moving excitations.

Perturbed WZW Models

To make contact with the free chiral metal, we need to add nearest-neighbor hopping, i.e., the H_1 term (5.2), to the $k = 1$ WZW model in (5.21). Using the identification of $U(N)$ currents in (5.33), we see that the free chiral metal is equivalent to

$$S_{k=1}[g] - \frac{h}{2\pi} \int dtdx \text{Tr}\Big(A_1(\partial_x g)g^{-1}\Big), \tag{5.35}$$

where A_1 is the linear combination of $SU(N)$ generators given in (5.15). The second term in (5.35) corresponds to minimal coupling to a constant vector potential polarized in the A_1 direction of the $SU(N)$ group. As in the free

---

[2]These currents are defined in terms of fermion bilinears as follows: $I_{R,L}^a = \sum_{I,J}(\psi_{R,L}^\dagger)_I\big(T^a \otimes \mathbb{I}\big)_{IJ}(\psi_{R,L})_J$, where T^a generate an $SU(k)$ subgroup of $SU(kN)$ and $\mathbb{I}$ is the identity matrix in the complementary $SU(N)$ subgroup.

fermion representation of this fixed point, we can gauge away the hopping term to keep the $U(N)$ Kac-Moody symmetry manifest. If we replace $g \to Mg$ with M given in (5.9), the Polyakov-Wiegmann identity (5.24) gives

$$S_{k=1}[Mg] - S_{k=1}[M] = S_{k=1}[g] - \frac{h}{2\pi} \int dt dx \text{Tr}\Big(A_1(\partial_x g)g^{-1}\Big). \qquad (5.36)$$

Because M is a gauge transformation parameter, i.e., nondynamical, we can absorb $\exp(-iS_{k=1}[M])$ into the overall normalization of the path integral for the WZW model. The final step is to define the gauge-transformed bosons as $\tilde{g} = Mg$. The path integration measure is invariant with respect to $g \to Mg$.

All of these manipulations carry over for general integer $k > 1$. The resulting interacting chiral metals will have the same symmetries as the free chiral metal. In analogy with the $k = 1$ theory, we take the $k > 1$ chiral metals to be perturbed WZW models:

$$\mathcal{S}_k[g] = S_k[g] - \frac{hk}{2\pi} \int d^2x \text{Tr}\Big(A_1(\partial_x g)g^{-1}\Big). \qquad (5.37)$$

The manifestly $U(N)$-invariant form obtains by taking $\tilde{g} = Mg$ with action, $S_k[\tilde{g}]$, and M given in (5.9). The $U(N)$ symmetry currents in this "tilded basis" are

$$\tilde{J}^a = \frac{ik}{2\pi}\text{Tr}\Big(T^a(\partial\tilde{g})\tilde{g}^{-1}\Big). \qquad (5.38)$$

These currents obey the Kac-Moody algebra (5.30) and (5.31). This algebra (at $k = 1$) is different from the commutation algebra of density operators of the free chiral metal (see Appendix 5.A). In the next section, we will make use of the standard equal-time two-point correlation functions of these currents:

$$\langle \tilde{J}^0(x)\tilde{J}^0(x')\rangle_k = \Big(\frac{i}{2\pi}\Big)^2 \frac{Nk}{(x - x')^2}, \qquad (5.39)$$

$$\langle \tilde{J}^a(x)\tilde{J}^b(x')\rangle_k = \Big(\frac{i}{2\pi}\Big)^2 \frac{k}{(x - x')^2}\frac{\delta^{ab}}{2}, \quad a, b \in \{1, \ldots N^2 - 1\}, \qquad (5.40)$$

with all other two-point correlation functions equal to zero, where $\tilde{J}^0 = J^0$ is the overall $U(1)$ number current associated with the generator $T^0_{IJ} = \delta_{IJ}$.

5.4 Two-Point Correlation Functions

In this section, we determine the two-point correlation functions of the single-particle fermion operator, the $U(1)$ number density, and the $U(1)$ current in the interacting chiral metals. We find that interactions ($k > 1$) produce $1/N$ corrections to scaling of the single-particle fermion operator as $N \to \infty$ and renormalize the amplitudes of the density and current two-point functions.

Fermion Two-Point Function

We would like to understand whether interactions ($k > 1$) give the single-particle operator $\psi_I(x)$ an anomalous dimension by computing its two-point correlation function,

$$\langle \psi_I(x) \psi_J^\dagger(0) \rangle \sim \frac{1}{x^{2\Delta}}, \tag{5.41}$$

for fixed I, J. Unfortunately, it is unknown how to write $\psi_I(x)$ in the language of non-Abelian bosonization. Nevertheless, there is an indirect approach [2] for inferring this scaling dimension Δ using a nonchiral WZW theory.

Similar to the construction of the $U(N)_k$ WZW model reviewed at the end of §5.3, we consider the theory of kN nonchiral free Dirac fermions. For each chirality, we decompose $U(kN)_1 = U(1)_{kN} \times U(N)_k \times U(k)_N$ and write the Dirac fermion in terms of its right $R_{I,a}(z)$ and left $L_{J,b}(\bar{z})$ chiral fermion components. Here the complex coordinates $z = x + iv\tau$ and $\bar{z} = x - iv\tau$. We view $I, J \in \{1, \ldots, N\}$ as wire indices and $a, b \in \{1, \ldots, k\}$ as internal flavor indices. Within each chirality sector, we allow identical nearest-neighbor hopping using the operators $R_{I,a}^\dagger (A_1)_{IJ} R_{J,a}$ and $L_{I,a}^\dagger (A_1)_{IJ} L_{J,a}$, where the $SU(N)$ matrix A_1 is defined in (5.15). Notice these hopping terms are $SU(k)$ singlets. As before, we can gauge away these hopping terms to restore manifest $SU(N)$ symmetry through the transformations,

$$R_{I,a} = \sum_J M_{IJ} \tilde{R}_{J,a}, \quad L_{I,a} = \sum_J M_{IJ}^\dagger \tilde{L}_{J,a}, \tag{5.42}$$

with M_{IJ} given in (5.9). The reason for the relative Hermitian conjugation of M_{IJ} is that the right and left movers have opposite velocities along the x direction.

In the free theory, the two-point function,

$$\langle R_{I,a}(z) R_{J,b}^\dagger(0) \rangle = \sum_{I',J'} \langle \tilde{R}_{I',a}(z) \tilde{R}_{J',b}^\dagger(0) \rangle M_{II'}(x) M_{J'J}^\dagger(0) = \frac{i}{2\pi} \frac{\delta_{ab}}{|z|} \left(M(x) M^\dagger(0) \right)_{IJ}. \tag{5.43}$$

Since the hopping matrix $M(x)M^\dagger(0)$ is an oscillatory function of x, it does not contribute to the scaling of the two-point function for large $|x|$. For $|I-J| \to \infty$ (with $N \to \infty$), $\left(M(x)M^\dagger(0) \right)_{IJ} \sim 1/|I-J|$.

Next we consider the decomposition [2],

$$\tilde{R}_{I,a}(z) \tilde{L}_{J,b}^\dagger(\bar{z}) \sim e^{i\sqrt{\frac{4\pi}{kN}} \phi(z,\bar{z})} g_{IJ}^\dagger(z, \bar{z}) h_{ab}^\dagger(z, \bar{z}), \tag{5.44}$$

where ϕ, g_{IJ}, h_{ab} are nonchiral bosons that parameterize fluctuations in the $U(1)$, $SU(N)$, and $SU(k)$ sectors. The neglected proportionality constant does not affect the scaling. Using (5.44) and the 4-point function,

$$\langle \tilde{R}_{I,a}(z)\tilde{L}^\dagger_{J,b}(\bar{z})\tilde{L}_{K,c}(z)\tilde{R}^\dagger_{L,d}(\bar{z})\rangle \sim \frac{1}{|z\bar{z}|^{\frac{1}{kN}}} \cdot \frac{\delta_{IL}\delta_{JK}}{|z\bar{z}|^{\Delta_g}} \cdot \frac{\delta_{ad}\delta_{bc}}{|z\bar{z}|^{\Delta_h}}, \qquad (5.45)$$

where $\Delta_g = \frac{N^2-1}{N(N+k)}$ and $\Delta_h = \frac{k^2-1}{k(k+N)}$, we reproduce the free field scaling dimensions $\Delta_R = \Delta_L = \frac{1}{2}\left(\frac{1}{kN} + \Delta_g + \Delta_h\right) = 1/2$ of $\tilde{R}(z)$ and $\tilde{L}(\bar{z})$ from the scalings of (5.45) with $|z|$ and $|\bar{z}|$. (A check of this decomposition in the $U(2)_1$ WZW theory is given in Appendix 5.B.)

Now we imagine gapping out the $SU(k)$ sector with an interaction of the form (5.34) to obtain the $U(N)_k = U(1)_{kN} \times SU(N)_k$ theory. Removing the contribution of h_{ab} to (5.45), we infer the scaling dimensions

$$\Delta_R^{U(N)_k} = \Delta_L^{U(N)_k} = \frac{1}{2} \cdot \frac{1+kN}{k^2+kN} = \frac{1}{2}\left(1 - \frac{k-\frac{1}{k}}{N}\right) + \mathcal{O}(1/N^2). \qquad (5.46)$$

We identify Δ in (5.41) with $\Delta_R^{U(N)_k}$. We recover free fermion scaling at $k = 1$ for any N. For $N \to \infty$, there are $1/N$ corrections to free fermion scaling that depend on k.

The Density Correlation Function

In a free Fermi gas, the equal-time $U(1)$ number density two-point function (a.k.a. the pair correlation function) gives the relative probability of finding two particles at $\mathbf{r}$ and $\mathbf{r}'$ [7]. The vanishing of this correlation function at $\mathbf{r} = \mathbf{r}'$ is a reflection of the Pauli exclusion principle. The finite, nonzero fermion density produces a nonzero asymptote as $|\mathbf{r} - \mathbf{r}'| \to \infty$. Oscillations in the correlation function are determined by the Fermi wave vector.

We are interested in computing the analog of this correlation function in the chiral metals with action $\mathcal{S}_k[g]$ for general $k \geq 1$. We focus on the long-distance, connected part of this two-point correlation function. This means that we will not directly probe the quantum statistics of the underlying interacting particles (since the insertion points will never be coincident) and that the correlator will vanish as $|\mathbf{r} - \mathbf{r}'| \to \infty$. As may be anticipated from the expression (5.29) for the symmetry currents, we will find that the density correlation function for $k > 1$ coincides with the $k = 1$ result, up to an overall factor of k. Thus, the "rate" or amplitude at which this correlation function

vanishes as $|\mathbf{r} - \mathbf{r}'| \to \infty$ gives a measure of the interaction parameterized by k. A similar conclusion obtains from the current two-point function studied in the next section.

To begin, we define the local $U(1)$ number density at $\mathbf{r} = (x, I)$ as

$$\rho_I(x) = \sum_a c_a J^a(x) = \frac{ik}{2\pi} \text{Tr}\Big(\sum_a^I c_a T^a \big(\partial_x g(x)\big) g^{-1}(x) \Big). \qquad (5.47)$$

In this and future expressions, the time dependence is left implicit with all operators evaluated at the same time; the coefficients $\{c_a\}$ in the above sum of $U(N)$ generators are chosen so that $\sum_a^I c_a T_{KL}^a = \delta_{IK}\delta_{IL}$ (no sum over I) [3]. When $k = 1$, $\rho_I(x)$ is the bosonized expression for the fermion bilinear $\psi_I^\dagger \psi_I(x)$ (no sum over I). We are interested in computing the two-point density correlation function,

$$\langle \rho_I(x)\rho_K(x') \rangle_k \qquad (5.48)$$

for nonzero hopping h at $k \geq 1$. (When $h = 0$, the $\langle \rho_I(x)\rho_K(x') \rangle_k \propto \delta_{IK}/|x - x'|^2$.)

We first factor out the k dependence in order to relate the $k > 1$ correlation functions to the $k = 1$ correlation function:

$$\langle \rho_I(x)\rho_K(x') \rangle_k = k\langle \rho_I(x)\rho_K(x') \rangle_{k=1}. \qquad (5.49)$$

To do this, we switch to the "tilded basis," $\tilde{g} = Mg$ with M given in (5.9). Up to an overall additive constant (that we ignore), the density becomes

$$\rho_I(x) = \frac{ik}{2\pi} \text{Tr}\Big(\sum_a^I c_a M T^a M^\dagger \tilde{g} \partial_x \tilde{g} \Big). \qquad (5.50)$$

We may decompose $MT^a M^\dagger$ in terms of the $U(N)$ generators as

$$M(x)T^a M^\dagger(x) = \sum_b \beta_b^a(x)T^b, \qquad (5.51)$$

for some expansion "coefficients" $\{\beta_a(x)\}$. The density correlation function becomes

$$\langle \rho_I(x)\rho_K(x') \rangle_k = \sum_a^I \sum_b^K \sum_m \sum_n c_a c_b \beta_m^a(x)\beta_n^b(x')\big\langle \tilde{J}^m(x)\tilde{J}^n(x') \big\rangle_k. \qquad (5.52)$$

---

[3]For example, when $N = 2$, $\delta_{1K}\delta_{1L} = \frac{1}{2}\mathbb{I}_{KL} + \frac{1}{2}(\sigma_3)_{KL}$ and $\delta_{2K}\delta_{2L} = \frac{1}{2}\mathbb{I}_{KL} - \frac{1}{2}(\sigma_3)_{KL}$, where $\mathbb{I}$ is the 2×2 identity matrix and σ_3 is the usual Pauli matrix.

Notice that the only dependence on k occurs in the current two-point functions. Replacing $\langle \tilde{J}^m(x)\tilde{J}^n(x')\rangle_k \to k\langle \tilde{J}^m(x)\tilde{J}^n(x')\rangle_{k=1}$ using (5.39) and (5.40), we may invert the above relations in the $k=1$ theory to obtain the desired result in (5.49).

We now compute the $k=1$ density two-point function directly using the free fermion representation of the theory:

$$\langle \rho_I(x)\rho_K(x')\rangle_{k=1} = \langle : \psi_I^\dagger \psi_I(x) :: \psi_K^\dagger \psi_K(x') :\rangle. \tag{5.53}$$

The colons denote normal ordering, which here means that we compute the connected part of this fermion four-point function. Notice that we do not need to determine the explicit form of the expansion coefficients $\{c_a\}$ or $\{\beta_b^a\}$ that occur above. Going to the "tilded basis" (5.8), we encounter

$$\langle \rho_I(x)\rho_K(x')\rangle_{k=1} = -\frac{1}{4\pi^2}\Big(M(x)M^\dagger(x')\Big)_{IK} \times \Big(M(x')M^\dagger(x)\Big)_{KI}\frac{1}{(x-x')^2}, \tag{5.54}$$

where we used the "tilded basis" fermion two-point functions,

$$\langle \tilde{\psi}_I(x)\tilde{\psi}_K^\dagger(x')\rangle = \frac{i}{2\pi}\frac{\delta_{IK}}{x-x'}. \tag{5.55}$$

We evaluate the product of matrix elements by diagonalizing the matrix A_1, which occurs in $M(x)$ (see (5.9) and (5.15)):

$$A_1 = U\Lambda U^\dagger \equiv \begin{pmatrix} u_1 & u_2 & \ldots u_N \end{pmatrix}\begin{pmatrix} \lambda_1 & 0 & 0.. \\ 0 & \lambda_2 & 0.. \\ 0 & 0 & \lambda_{3}.. \\ .. \end{pmatrix}\begin{pmatrix} u_1 & u_2 & \ldots u_N \end{pmatrix}^\dagger, \tag{5.56}$$

where

$$u_l = \sqrt{\frac{2}{N}}\begin{pmatrix} \sin\left(\frac{2\pi l\times 1}{N}-\frac{\pi}{4}\right) \\ \sin\left(\frac{2\pi l\times 2}{N}-\frac{\pi}{4}\right) \\ \vdots \\ \sin\left(\frac{2\pi l\times N}{N}-\frac{\pi}{4}\right) \end{pmatrix}, \quad \lambda_l = 2\cos\left(\frac{2\pi l}{N}\right), \ l=1,2,\ldots,N, \tag{5.57}$$

and substitute into (5.54). The product of matrix elements takes a functional form that allows us to evaluate $|I-K|$ for noninteger values. We plot the density two-point functions when $N=40$ in Figs. 5.4.1 and 5.4.2. This value
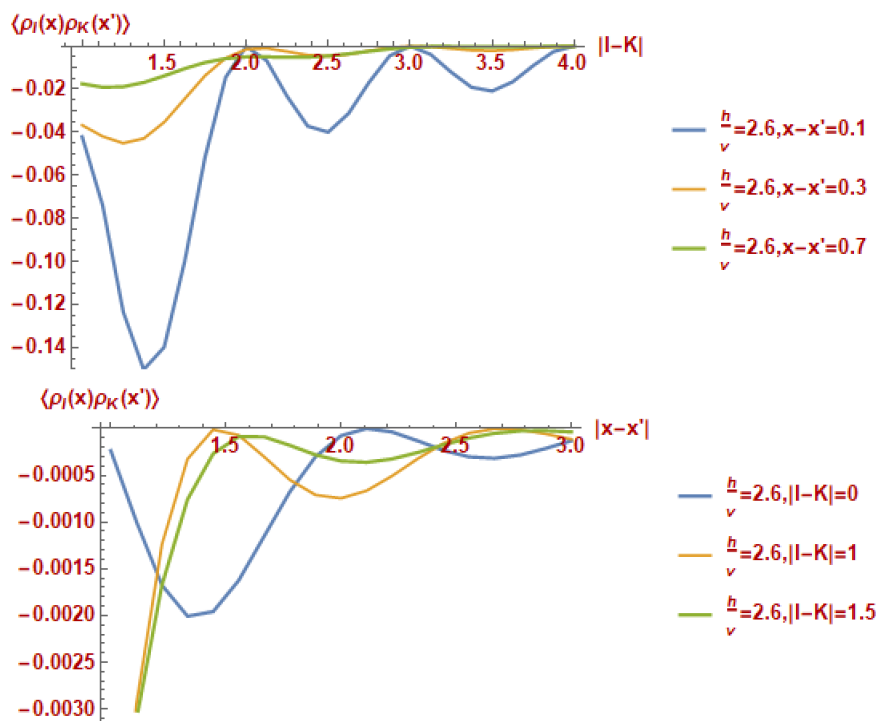
Figure 5.4.1: Density two-point functions, normalized by k, as a function of $|I - J|$ at fixed $|x - x'|$ (top) and $|x - x'|$ at fixed $|I - K|$ (bottom).
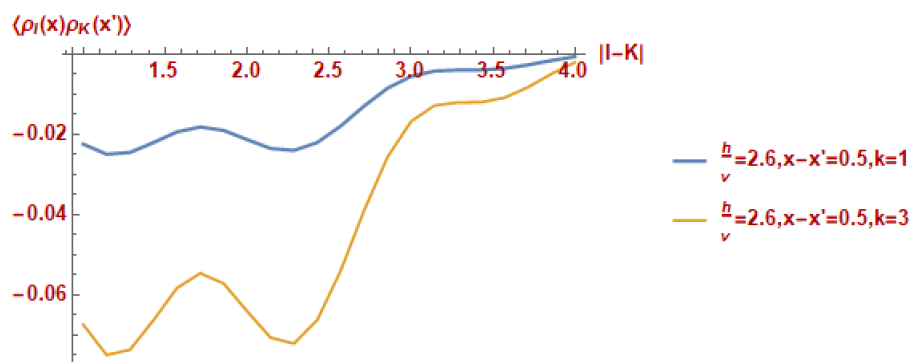

Figure 5.4.2: Comparison of the density two-point functions at $k = 1$ and $k = 3$ as a function of $|I - J|$ at fixed $|x - x'|$.

of N appears to be sufficiently large to accurately capture the $N \to \infty$ limit. The oscillations in these curves are due to the Fermi surface. We comment that jth-neighbor hopping may be included similarly, since the various A_j and $B_{j'}$ matrices (appearing in (5.15) and (5.16)) matrices commute with one another.

The Current Correlation Function

The $U(1)$ current density along the x direction is equal to the (charge) density $\rho_I(x)$. Its two-point function therefore coincides with the $\rho_I(x)$ two-point function studied in the previous section. In this section, we therefore focus on the two-point correlation function of the $U(1)$ current along the y direction.

It is simplest to define the $U(1)$ current by way of the free fermion representation of the $k = 1$ WZW theory. To this end, we use the Peierls substitution to introduce a gauge field A^y polarized along the y direction into the hopping term H_1 in (5.2):

$$H_1[A^y] = \frac{h}{2} \int dx \sum_{I,J} \delta_{J,I+1} \psi_I^\dagger e^{iA^y_{IJ}(x)} \psi_J + \text{h.c.} \tag{5.58}$$

To linear approximation in A^y, the corresponding current (density) along the y direction is

$$J_I^y(x) \equiv \left(\frac{\delta H_1}{\delta A^y_{I,I+1}} + \frac{\delta H_1}{\delta A^y_{I-1,I}} \right)\Big|_{A^y=0}$$

$$= h \sum_{K,L} \psi_K^\dagger P^I_{KL} \psi_L, \tag{5.59}$$

where the matrix,

$$P^I_{KL} = \frac{1}{2i} \left(\delta_{K,I-1}\delta_{L,I} - \delta_{K,I}\delta_{L,I-1} + \delta_{K,I}\delta_{L,I+1} - \delta_{K,I+1}\delta_{L,I} \right). \tag{5.60}$$

P^I coincides with a linear combination of the $U(N)$ generators $Y^{(I,I+1)}$ and $Y^{(I-1,I)}$ defined below (5.16). For general $k \geq 1$, we therefore take the $U(1)$ current density along the y direction to be

$$J_I^y(x) = \frac{ik}{2\pi} \text{Tr} \left(P^I \left(\partial_x g(x) \right) g^{-1}(x) \right). \tag{5.61}$$

Having defined the y current $J_I^y(x)$, we set $A^y = 0$ in the remainder.

We are interested in computing the two-point correlation function,
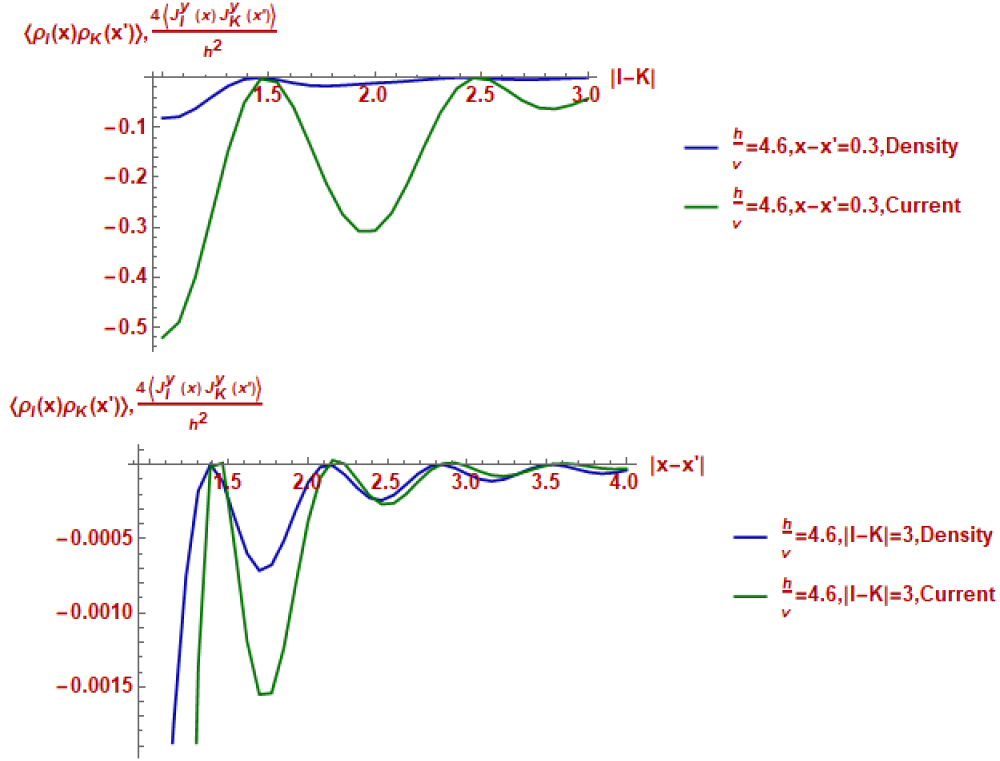
$$\langle J_I^y(x) J_K^y(x') \rangle_k. \tag{5.62}$$

Figure 5.4.3: Comparison of the $U(1)$ density and y current two-point functions, normalized by k, as a function of $|I - J|$ at fixed $|x - x'|$ (top) and $|x - x'|$ at fixed $|I - K|$ (bottom).

As before, the $k > 1$ correlation functions are proportional to the $k = 1$ result:

$$\langle J_I^y(x) J_K^y(x') \rangle_k = k \langle J_I^y(x) J_K^y(x') \rangle_{k=1}. \tag{5.63}$$

$\langle J_I^y(x) J_K^y(x') \rangle_{k=1}$ can be computed using the free fermion representation of the $k = 1$ theory. Mirroring the computation in the previous section, we find

$$\langle J_I^y(x) J_K^y(x') \rangle_{k=1} = -\frac{h^2}{4\pi^2} \mathrm{Tr}\Big(M^\dagger(x) P^I M(x) \, M^\dagger(x') P^K M(x') \Big) \times \frac{1}{(x - x')^2}. \tag{5.64}$$

Comparisons of this $U(1)$ y-current two-point function—evaluated using the same method as in the previous section—and the density two-point function are shown in Fig. 5.4.3 when $N = 40$.

5.5 Discussion

In this paper, we proposed Wess-Zumino-Witten (WZW) theories with $U(N)$ symmetry at level $k \geq 1$ in two spacetime dimensions to be interacting chiral

metals in two spatial dimensions. The extra spatial dimension arises from the $U(N)$ flavor degrees of freedom of the WZW model. The parameter $N \to \infty$ counts the number of points on the Fermi surface. The $k = 1$ theory is equivalent to Balents and Fisher's free 2d chiral metal. The $k > 1$ theories are interacting generalizations, in which the symmetries of the $k = 1$ theory are maintained. This construction provides a simple illustration of the ersatz Fermi liquid proposal of Else, Thorgren, and Senthil [14]. Specifically, that there are interacting Fermi systems that maintain the same symmetry as the Fermi liquid. Here, it is the $U(N)$ symmetry (which includes $U(1)$ number conservation and discrete translation invariance along the y direction) and continuous translation invariance along the x direction of the free 2d chiral metal that are preserved at nonzero interaction $k > 1$. We determined the two-point function of the single-particle fermion operator at $k > 1$. We found corrections to its anomalous dimension that depend on k; these corrections are organized in an expansion in $1/N$. We also computed the two-point function of the $U(1)$ number density and current operators for general $k \geq 1$. The level k results in an overall multiplicative rescaling of the amplitude of decay of these local correlation functions [4].

There are a number of directions of future research.

• The most straightforward generalization is to non-chiral metals with an open Fermi surface, which would arise from 2d arrays of non-chiral Luttinger liquids. It would be interesting to consider the Lifshitz transition to a closed Fermi surface and/or potential instabilities of the non-chiral theories. Another possibility is to gauge some of the $U(N)$ symmetry. This symmetry is anomalous in the chiral metals considered here; the non-chiral generalizations admit anomaly-free subgroups (see, e.g., [11]).

• The nonlocal $SU(N)$ symmetry can be maintained in the presence of nonuniform hopping and/or random scalar potential quenched disorder [5]. (This fact is essential to the theory of neutral modes in quantum Hall edge-state theories [60, 33, 32].) A direct study of the free fermion description of the $k = 1$ theory shows that the metal avoids localization because of its nonzero chirality

---

[4]The absence of non-Fermi liquid behavior in the $U(1)$ density and current two-point functions is similar to what occurs in the spinon-gauge problem [35].

[5]Nonuniform hopping h_I and/or scalar potential disorder $V_I(x)$ can be gauged away using $M(x) = \mathcal{T}_x \exp\left(-i \int_{x_0}^{x} dy \left(\sum_{m=1}^{N} V_m(y)\mathbb{I}^{(m)} - \frac{h_m}{v} X^{(m,m+1)}\right)\right)$, where $\mathcal{T}_x$ is an x-ordering operator, x_0 is an arbitrary basepoint, and $\mathbb{I}_{IJ}^{(m)} = \delta_{m,I}\delta_{m,J}$.

and the asymmetry in its dispersion along the x and y directions [5, 6]. We expect the chiral models we considered with $k > 1$ to also be stable against localization.

• It is important to find a microscopic realization for how k may be varied. We reviewed one construction in §5.3, which relied on nonlocal interactions from the point of view of the underlying fermions. Whether this deformation can be achieved via coupling to a local field is an open question.

APPENDIX

5.A   The Free Chiral Metal Current Algebra

In this appendix, we derive the commutation algebra of the Fourier modes of the density operator of the chiral metal. This algebra is similar to the algebra of density operators in a system with a closed Fermi surface in the presence of a weak magnetic fields [22, 8, 28, 14]; this algebra is different than the Kac-Moody algebra (5.30) and (5.31) at $k = 1$.

To derive this algebra, we use the point-splitting trick, familiar from $(1 + 1)$-dimensional theories with Kac-Moody algebra, following Chapter 5 of [19]. For convenience, we choose a slightly different nearest-neighbor hopping term than used in the main text ("σ_y" as opposed to "σ_x" hopping), with hopping amplitude w, and denote the fermion field as $R_I(x, t)$. The action is

$$S = \int dt dx \sum_I R_I^\dagger(x,t)\, i(\partial_t + v_x\, \partial_x\,)R_I(x,t) + i\,w \sum_I (R_I^\dagger R_{I+1} - R_{I+1}^\dagger R_I) \tag{5.65}$$

$$= \int dt dx \sum_{k_y} R_{k_y}^\dagger(x,t)\, i(\partial_t + v_x\, \partial_x\,)R_{k_y}(x,t) - 2\,w \sum_{k_y} \sin(k_y a)R_{k_y}^\dagger R_{k_y} \tag{5.66}$$

In the second equality, we introduced the Fourier transformed fields,

$$R_I = \frac{1}{\sqrt{N}} \sum_{k_y} R_{k_y}\, e^{i\,k_y\, Ia}, \tag{5.67}$$

where N is the number of wires and we are here denoting the spacing between wires as a. The dispersion relation is

$$\epsilon_{\boldsymbol{k}} = v_x\, k_x + 2w \sin(k_y a). \tag{5.68}$$

The Fermi surface is the locus in (k_x, k_y)-space for which $\epsilon_{\boldsymbol{k}} = 0$. The ground state $|G\rangle$ is the manybody state in which, for a given k_y, all single-particle states with negative $v_x\, k_x + 2w \sin(k_y a)$ are occupied

We take the x direction to have size L and view k_y as a flavor index. Defining $R_{k_x; k_y}$ and $k_x = \frac{2\pi}{L} n_{k_x}$ by

$$R_{k_y}(x) = \frac{1}{L} \sum_{n_{k_x} \in \mathbb{Z}} e^{i\frac{2\pi}{L} n_{k_x} x} R_{k_x; k_y}, \tag{5.69}$$

the two-point function of single-particle operators $R_{k_x; k_y}$ is

$$\langle R_{p_x; p_y}^\dagger R_{k_x; k_y}\rangle = \delta_{p_x k_x}\, \delta_{p_y k_y}\, \theta\big(-v_x\, k_x - 2w \sin(k_y a)\big), \tag{5.70}$$

where $\theta(x)$ is the step function. Correlation functions here and below are computed in the ground state $|G\rangle$. The maximal index $n_{k_x}^{\max}$ labeling the highest k_x wave vector occupied, for a given k_y, is obtained from

$$v_x\, k_x + 2w \sin[k_y a] = 0 \;\Rightarrow\; n_{k_x} = \frac{-2w \sin[k_y a]}{v_x} \times \frac{L}{2\pi}. \qquad (5.71)$$

Thus, we find

$$
\begin{aligned}
\langle R_{p_y}^\dagger(x) R_{k_y}(x')\rangle &= \frac{\delta_{p_y k_y}}{L} \sum_{n_{k_x}=-\infty}^{n_{k_x}^{\max}} e^{-i\frac{2\pi}{L} n_{k_x}(x-x')}\\
&= \frac{\delta_{p_y k_y}}{L} \frac{1}{1 - e^{i\frac{2\pi}{L}(x-x'+i\alpha)}} \times e^{i\frac{2\pi}{L}(x-x'+i\alpha)\times\frac{2w\sin[k_y a]}{v_x}\times\frac{L}{2\pi}}\\
&= \delta_{p_y k_y} \frac{i}{2\pi} \frac{1}{x-x'+i\alpha} \times e^{i(x-x'+i\alpha)\times\frac{2w\sin[k_y a]}{v_x}}, \qquad (5.72)
\end{aligned}
$$

where α is a short-distance cutoff.

We define the following operators:

$$J_{R,k_y}^{q_y}(x) = \; : R_{k_y}^\dagger(x)\, R_{k_y+q_y}(x) : \; + \lim_{\epsilon\to0}\langle R_{k_y}^\dagger(x+\epsilon)\, R_{k_y+q_y}(x-\epsilon)\rangle, \qquad (5.73)$$

where k_y labels a point on the Fermi surface and q_y is a small deviation about k_y. The operators $J_{R,k_y}^{q_y}(x)$ are the Fourier modes of the density operator.

Using Eq. (5.72), we find the equal-time commutator,

$$
\begin{aligned}
[J_{R,k_y}^{q_y}(x), J_{R,k_y'}^{q_y'}(x')] = \delta_{k_y-k_y',-q_y}\delta_{-q_y,q_y'}&\left(\frac{i}{2\pi}\frac{\delta(x-\epsilon,x'+\epsilon')}{(x+\epsilon)-(x'-\epsilon')}e^{i(x-x'+i\alpha)\frac{2w\sin[k_y a]}{v}}\right.\\
&\left.-\frac{i}{2\pi}\frac{\delta(x+\epsilon,x'-\epsilon')}{(x'+\epsilon')-(x-\epsilon)}e^{i(x'-x+i\alpha)\frac{2w\sin[k_y' a]}{v_x}}\right), \quad (5.74)
\end{aligned}
$$

where ϵ and ϵ' are the point-splitting distances used to define $J_{R,k_y}^{q_y}(x)$ and $J_{R,k_y'}^{q_y'}(x')$. We approximate

$$
\begin{aligned}
e^{+i(x-x'+i\alpha)\frac{2w\sin[k_y a]}{v_x}} &\approx 1 + i(x-x'+i\alpha)\frac{2w\sin[k_y a]}{v_x}\\
&\approx 1 + i(x-x')\frac{2w\,k_y a}{v_x}. \qquad (5.75)
\end{aligned}
$$

Inserting this approximation into the above commutator, we find

$$
\begin{aligned}
[J_{R,k_y}^{q_y}(x), J_{R,k_y'}^{q_y'}(x')] \approx \delta_{k_y-k_y',-q_y}\delta_{q_y+q_y',0}&\left(\frac{i}{2\pi}\frac{\delta(x-\epsilon,x'+\epsilon')}{(x+\epsilon)-(x'-\epsilon')} - \frac{i}{2\pi}\frac{\delta(x+\epsilon,x'-\epsilon')}{(x'+\epsilon')-(x-\epsilon)}\right)\\
+\delta_{k_y-k_y',-q_y}\delta_{q_y+q_y',0}&\left(\frac{i}{2\pi}\frac{\delta(x-\epsilon,x'+\epsilon')}{1}\times i\,\frac{2w\,k_y a}{v_x} - \frac{i}{2\pi}\frac{\delta(x+\epsilon,x'-\epsilon')}{1}\times i\,\frac{2w\,(k_y+q_y)a}{v_x}\right.
\end{aligned}
$$

$$= \delta_{k_y - k'_y, -q_y} \left(\delta_{q_y + q'_y, 0} \frac{-i}{2\pi} \partial_x \delta(x - x') + q_y \, \delta_{q_y + q'_y, 0} \, \delta(x - x') \frac{1}{2\pi} \frac{2wa}{v_x} \right).$$

This is similar to the commutation algebra of density operators for a system with a Fermi surface in the presence of a weak, uniform magnetic field [22, 8, 28, 14]. To make this comparison, we identify x as the Fourier transform of the momentum space direction normal to the Fermi surface, y as a label of a point on the Fermi surface, and the magnetic field $B \sim wa/v_x$. One remark about Eq. (5.76) is that the model we consider here is nonchiral along y direction: the commutation algebra for operators near $k_y a = 0$ obtained in Eq. (5.76) comes in pair with the commutation algebra near $k_y a = \pi$. Therefore, unlike in [22, 8, 28, 14], there is no t'Hooft anomaly along the y direction when we gauge our model.

5.B   Chiral Decomposition in the $U(2)_1$ WZW Model

In this appendix, we provide an explicit demonstration for how the nonchiral matrix boson of the $U(2)_1$ WZW model factorizes in terms of its chiral components. This indicates how the scaling dimension of a nonchiral field decomposes in terms of left and right scaling dimensions. This decomposition supports the inferred scaling dimension of the fermion operator obtained in §5.4.

Witten's formula [79] says $R_i \, L_j^\dagger \sim (g^\dagger)_{ij} \, e^{i\sqrt{\frac{4\pi}{N}} \, \phi_C}$, with $N = 2$ and $i, j \in \{\uparrow, \downarrow\}$. We will show how the matrix boson $g_{ij} \in SU(2)$ factorizes in terms of its chiral components. We write g as

$$g = \frac{1}{\sqrt{2}} \begin{pmatrix} e^{i\sqrt{2\pi} \, \phi_S} & -e^{-i\sqrt{2\pi} \theta_S} \\ e^{+i\sqrt{2\pi} \theta_S} & e^{-i\sqrt{2\pi} \, \phi_S} \end{pmatrix}. \tag{5.77}$$

Here and below exponential operators are assumed to be normal ordered. We adopt the definitions:

$$\phi_C = \phi_{R,C} + \phi_{L,C}, \quad \theta_C = -\phi_{R,C} + \phi_{L,C}, \tag{5.78}$$

$$\phi_S = \phi_{R,S} + \phi_{L,S}, \quad \theta_S = -\phi_{R,S} + \phi_{L,S}. \tag{5.79}$$

The charge and spin bosons $\{\phi_C, \phi_S\}$ are related to the up and down bosons $\{\phi_\uparrow, \phi_\downarrow\}$ used in Abelian bosonization of a spin-1/2 fermion by $\phi_C = \frac{1}{\sqrt{2}} (\phi_\uparrow + \phi_\downarrow)$ and $\phi_S = \frac{1}{\sqrt{2}} (\phi_\uparrow - \phi_\downarrow)$.

The right $SU(2)$ currents are

$$J_R^a(z) = \lim_{w \to z} \frac{i}{2\pi} \text{Tr}[\frac{\sigma^a}{2} g^\dagger(w) \, \partial_- g(z)], \tag{5.80}$$

for $a = x, y, z$ and $\partial_- = -2\frac{\partial}{\partial z} = (\frac{\partial}{\partial v t} - \frac{\partial}{\partial x})$. Inserting (5.77) into (5.80), we find

$$2J_R^x(z) = \frac{-i}{2\pi}\frac{1}{w-z} : 2\cos[2\sqrt{2\pi}\phi_{R,S}(z)] : \tag{5.81}$$

$$2J_R^y(z) = \frac{-1}{2\pi}\frac{1}{w-z} : 2i\sin[2\sqrt{2\pi}\phi_{R,S}(z)] : \tag{5.82}$$

$$2J_R^z(z) = \frac{+1}{\sqrt{2\pi}}4\,\partial_z\phi_{R,S}(z). \tag{5.83}$$

Here $w - z = \alpha$ is understood to equal a short-distance cutoff. It's easy to check that this result is consistent with Abelian bosonization using

$$\psi_{R\uparrow} = \frac{\kappa_{R\uparrow}}{\sqrt{2\pi\alpha}}e^{i\sqrt{2\pi}[\phi_{R,C}+\phi_{R,S}]}, \ \psi_{R\downarrow} = \frac{\kappa_{R\downarrow}}{\sqrt{2\pi\alpha}}e^{i\sqrt{2\pi}[\phi_{R,C}-\phi_{R,S}]}, \tag{5.84}$$

$$\psi_{L\uparrow} = \frac{\kappa_{L\uparrow}}{\sqrt{2\pi\alpha}}e^{-i\sqrt{2\pi}[\phi_{L,C}+\phi_{L,S}]}, \ \psi_{L\downarrow} = \frac{\kappa_{L\downarrow}}{\sqrt{2\pi\alpha}}e^{-i\sqrt{2\pi}[\phi_{L,C}-\phi_{L,S}]}, \tag{5.85}$$

for Klein fields $\kappa_{R,L}$.

Next, following [68], we factorize the matrix field g in Eq. (5.77) as

$$g(x,t) = g_R(x,t)\, g_L^\dagger(x,t) = \Big(g_1(x-t)\, h(t)\Big)\Big(g_2(x+t)\, h(t)\Big)^\dagger$$

$$= g_1(x-t)\, g_2^\dagger(x+t), \tag{5.86}$$

where $h(t)$ is an arbitrary x-independent $SU(2)$ group element. This x-independent factor was mentioned in §5.3. The presence of $h(t)$ means that $g(x,t)$ does not factorize in terms of a product of holomorphic and antiholomorphic fields when written in terms of g_R and g_L. The factorization (5.86) should be consistent with (5.77). This requires

$$\frac{1}{\sqrt{2}}\begin{pmatrix} e^{i\beta\,\phi_S} & -e^{-i\beta\theta_S} \\ e^{+i\beta\theta_S} & e^{-i\beta\,\phi_S} \end{pmatrix} = \frac{1}{\sqrt{2}}\begin{pmatrix} e^{i\beta\,(\phi_{R,S}+\phi_{L,S})} & -e^{-i\beta(-\phi_{R,S}+\phi_{L,S})} \\ e^{+i\beta(-\phi_{R,S}+\phi_{L,S})} & e^{-i\beta\,(\phi_{R,S}+\phi_{L,S})} \end{pmatrix}$$

$$= \frac{1}{\sqrt{2}}\begin{pmatrix} C\,e^{i\beta\phi_{R,S}} & -D\,e^{i\beta\phi_{R,S}} \\ D^*\,e^{-i\beta\phi_{R,S}} & C^*\,e^{-i\beta\phi_{R,S}} \end{pmatrix}\frac{1}{\sqrt{2}}\begin{pmatrix} A\,e^{i\beta\phi_{L,S}} & -B\,e^{-i\beta\phi_{L,S}} \\ B^*\,e^{+i\beta\phi_{L,S}} & A^*\,e^{-i\beta\phi_{L,S}} \end{pmatrix}$$

$$\equiv g_1(x-t)\, g_2^\dagger(x+t), \tag{5.87}$$

where $\beta \equiv \sqrt{2\pi}$. There is not a unique solution for the complex numbers A, B, C, D. We take

$$(A, B, C, D) = \big(\sqrt{2}\cos[\frac{\pi}{8}], \sqrt{2}\sin[\frac{\pi}{8}], \sqrt{2}\cos[\frac{\pi}{8}], \sqrt{2}\sin[\frac{\pi}{8}]\big). \tag{5.88}$$

We thereby identify

$$g_R(x,t) = \begin{pmatrix} \cos[\frac{\pi}{8}] e^{i\beta\phi_{R,S}(z)} & -\sin[\frac{\pi}{8}] e^{i\beta\phi_{R,S}(z)} \\ \sin[\frac{\pi}{8}] e^{-i\beta\phi_{R,S}(z)} & \cos[\frac{\pi}{8}] e^{-i\beta\phi_{R,S}(z)} \end{pmatrix}.h(t), \qquad z = x - t, \quad (5.89)$$

We can check that, based on (5.29), $J_R^a(x) = \frac{i}{2\pi}\text{Tr}[\frac{\sigma^a}{2}(\partial_x g_R) g_R^\dagger]$ equals the result we obtain via the nonchiral matrix g in Eq. 5.83. Writing ∂_x instead of ∂_z ensures that the differential operator only acts on $g_1(x-t)$ and not on $h(t)$.

Finally, we can check the fermion scaling dimension is consistent with (5.89). Using (5.84), we have

$$\langle R_I(z) R_J^\dagger(0,0) \rangle \sim e^{\frac{2\pi}{4\pi}\langle \phi_{R,C}(z)\phi_{R,C}(0)\rangle} \times e^{\frac{2\pi}{4\pi}\langle \phi_{R,S}(z)\phi_{R,S}(0)\rangle} \sim \frac{1}{z}. \qquad (5.90)$$

This implies the scaling dimension of the right-moving fermion is determined by

$$2\Delta_{R_I} = 1 = \left(\frac{1}{N} + \frac{N^2 - 1}{N(N+1)}\right)_{N=2} \Rightarrow \Delta_{R_I} = \frac{1}{4} + \frac{1}{4} = \Delta_{\phi_C} + \Delta_{g_R}, \quad (5.91)$$

where I, J are $SU(2)$ indices.

BIBLIOGRAPHY

[1]   Ar. Abanov and A. Chubukov. "Anomalous Scaling at the Quantum Critical Point in Itinerant Antiferromagnets". In: *Phys. Rev. Lett.* 93 (2004), p. 255702.

[2]   Ian Affleck. "Exact critical exponents for quantum spin chains, non-linear σ-models at $\theta = \pi$ and the quantum hall effect". In: *Nuclear Physics B* 265.3 (1986), pp. 409–447. ISSN: 0550-3213. URL: https://www.sciencedirect.com/science/article/pii/0550321386901677.

[3]   B. L. Altshuler, L. B. Ioffe, and A. J. Millis. "Low-energy properties of fermions with singular interactions". In: *Phys. Rev. B* 50 (1994), p. 14048.

[4]   Natan Andrei, Michael R. Douglas, and Andrés Jerez. "Chiral liquids in one dimension: A non-Fermi-liquid class of fixed points". In: *Phys. Rev. B* 58 (12 Sept. 1998), pp. 7619–7625. URL: https://link.aps.org/doi/10.1103/PhysRevB.58.7619.

[5]   Leon Balents and Matthew P. A. Fisher. "Chiral Surface States in the Bulk Quantum Hall Effect". In: *Phys. Rev. Lett.* 76 (1996), p. 2782.

[6]   Leon Balents, Matthew P. A. Fisher, and Martin R. Zirnbauer. "Chiral metal as a ferromagnetic super spin chain". In: *Nucl. Phys. B* 483 (1997), p. 601.

[7]   Gordon Baym. *Lectures on quantum mechanics*. CRC Press, 2018.

[8]   A. H. Castro Neto and Eduardo Fradkin. "Bosonization of Fermi liquids". In: *Phys. Rev. B* 49 (16 Apr. 1994), pp. 10877–10892. URL: https://link.aps.org/doi/10.1103/PhysRevB.49.10877.

[9]   Sudip Chakravarty, Richard E. Norton, and Olav F. Syljuåsen. "Transverse Gauge Interactions and the Vanquished Fermi Liquid". In: *Phys. Rev. Lett.* 74 (1995), p. 1423.

[10]   J. T. Chalker and A. Dohmen. "Three-Dimensional Disordered Conductors in a Strong Magnetic Field: Surface States and Quantum Hall Plateaus". In: *Phys. Rev. Lett.* 75 (1995), p. 4496.

[11]   Stephen-wei Chung and S. -H. Henry Tye. "Chiral gauged Wess-Zumino-Witten theories and coset models in conformal field theory". In: *Phys. Rev. D* 47 (10 May 1993), pp. 4546–4566. URL: https://link.aps.org/doi/10.1103/PhysRevD.47.4546.

[12]   Jeremias Aguilera Damia et al. "Two-Dimensional Non-Fermi-Liquid Metals: A Solvable Large-N Limit". In: *Phys. Rev. Lett.* 123 (9 Aug. 2019), p. 096402. URL: https://link.aps.org/doi/10.1103/PhysRevLett.123.096402.

[13] Luca V. Delacretaz et al. "Nonlinear Bosonization of Fermi Surfaces: The Method of Coadjoint Orbits". In: *arXiv e-prints*, arXiv:2203.05004 (Mar. 2022), arXiv:2203.05004. arXiv: 2203.05004 [cond-mat.str-el].

[14] Dominic V. Else, Ryan Thorngren, and T. Senthil. "Non-Fermi Liquids as Ersatz Fermi Liquids: General Constraints on Compressible Metals". In: *Phys. Rev. X* 11 (2 Apr. 2021), p. 021005. URL: https://link.aps.org/doi/10.1103/PhysRevX.11.021005.

[15] V. J. Emery et al. "Quantum Theory of the Smectic Metal State in Stripe Phases". In: *Phys. Rev. Lett.* 85 (10 Sept. 2000), pp. 2160–2163. URL: https://link.aps.org/doi/10.1103/PhysRevLett.85.2160.

[16] Ilya Esterlis et al. "Large-N theory of critical Fermi surfaces". In: *Phys. Rev. B* 103 (23 June 2021), p. 235129. URL: https://link.aps.org/doi/10.1103/PhysRevB.103.235129.

[17] A. Liam Fitzpatrick et al. "Non-Fermi-liquid behavior of large-N_B quantum critical metals". In: *Phys. Rev. B* 89 (2014), p. 165114.

[18] A. Liam Fitzpatrick et al. "Non-Fermi-liquid fixed point in a Wilsonian theory of quantum critical metals". In: *Phys. Rev. B* 88 (2013), p. 125116.

[19] Eduardo Fradkin. *Field Theories of Condensed Matter Physics*. Cambridge University Press, 2013.

[20] Thierry Giamarchi. *Quantum Physics in One Dimension*. International Series of Monographs on Physics (Book 121). Oxford University Press, 2004.

[21] Peter Goddard and David Olive. "Kac-Moody and Virasoro algebras in relation to quantum physics". In: *International Journal of Modern Physics A* 1.02 (1986), pp. 303–414.

[22] F. D. M. Haldane. "Luttinger's Theorem and Bosonization of the Fermi Surface". In: *Proceedings of the International School of Physics "Enrico Fermi," Course CXXI: "Perspectives in Many-Particle Physics,"* (). Ed. by R. Broglia and J. R. Schrieffer. arXiv: cond-mat/0505529 [cond-mat.str-el].

[23] B. I. Halperin, Patrick A. Lee, and Nicholas Read. "Theory of the half-filled Landau level". In: *Phys. Rev. B* 47 (12 Mar. 1993), pp. 7312–7343. URL: http://link.aps.org/doi/10.1103/PhysRevB.47.7312.

[24] SangEun Han and Yong Baek Kim. "Non-Landau Fermi Liquid induced by Bose Metal". In: *arXiv e-prints*, arXiv:2102.05052 (Feb. 2021), arXiv:2102.05052. arXiv: 2102.05052 [cond-mat.str-el].

[25] Sean A. Hartnoll et al. "Transport near the Ising-nematic quantum critical point of metals in two dimensions". In: *Phys. Rev. B* 89 (2014), p. 155130.

[26] Tobias Holder and Walter Metzner. "Anomalous dynamical scaling from nematic and U(1) gauge field fluctuations in two-dimensional metals". In: *Phys. Rev. B* 92 (4 July 2015), p. 041112. URL: https://link.aps.org/doi/10.1103/PhysRevB.92.041112.

[27] Tobias Holder and Walter Metzner. "Fermion loops and improved power-counting in two-dimensional critical metals with singular forward scattering". In: *Phys. Rev. B* 92 (24 Dec. 2015), p. 245128. URL: https://link.aps.org/doi/10.1103/PhysRevB.92.245128.

[28] A. Houghton and J. B. Marston. "Bosonization and fermion liquids in dimensions greater than one". In: *Phys. Rev. B* 48 (11 Sept. 1993), pp. 7790–7808. URL: https://link.aps.org/doi/10.1103/PhysRevB.48.7790.

[29] Yen-Ta Huang and Dung-Hai Lee. "Non-abelian bosonization in two and three spatial dimensions and applications". In: *Nuclear Physics B* 972 (2021), p. 115565. ISSN: 0550-3213. URL: https://www.sciencedirect.com/science/article/pii/S0550321321002625.

[30] Andrew J. A. James et al. "Non-perturbative methodologies for low-dimensional strongly-correlated systems: From non-Abelian bosonization to truncated spectrum methods". In: *Reports on Progress in Physics* 81.4, 046002 (Apr. 2018), p. 046002. arXiv: 1703.08421 [cond-mat.str-el].

[31] Shamit Kachru et al. "Mirror symmetry and the half-filled Landau level". In: *Phys. Rev. B* 92 (23 2015), p. 235105. URL: http://link.aps.org/doi/10.1103/PhysRevB.92.235105.

[32] C. L. Kane and Matthew P. A. Fisher. "Impurity scattering and transport of fractional quantum Hall edge states". In: *Phys. Rev. B* 51 (19 May 1995), pp. 13449–13466. URL: https://link.aps.org/doi/10.1103/PhysRevB.51.13449.

[33] C. L. Kane, Matthew P. A. Fisher, and J. Polchinski. "Randomness at the edge: Theory of quantum Hall transport at filling $\nu=2/3$". In: *Phys. Rev. Lett.* 72 (26 June 1994), pp. 4129–4132. URL: https://link.aps.org/doi/10.1103/PhysRevLett.72.4129.

[34] D. V. Khveshchenko. "Geometrical approach to bosonization of $D > 1$ dimensional (non)-Fermi liquids". In: *Phys. Rev. B* 52 (7 Aug. 1995), pp. 4833–4841. URL: https://link.aps.org/doi/10.1103/PhysRevB.52.4833.

[35] Yong Baek Kim et al. "Gauge-invariant response functions of fermions coupled to a gauge field". In: *Phys. Rev. B* 50 (1994), p. 17917.

[36] Ethan Lake, T. Senthil, and Ashvin Vishwanath. "Bose-Luttinger liquids". In: *Phys. Rev. B* 104 (1 July 2021), p. 014517. URL: https://link.aps.org/doi/10.1103/PhysRevB.104.014517.

[37] Michael J. Lawler and Eduardo Fradkin. "Local quantum criticality at the nematic quantum phase transition". In: *Phys. Rev. B* 75 (2007), p. 033304.

[38] Patrick A. Lee. "Gauge field, Aharonov-Bohm flux, and high-T_c superconductivity". In: *Phys. Rev. Lett.* 63 (6 Aug. 1989), pp. 680–683. URL: https://link.aps.org/doi/10.1103/PhysRevLett.63.680.

[39] Sung-Sik Lee. "Low-energy effective theory of Fermi surface coupled with U(1) gauge field in $2 + 1$ dimensions". In: *Phys. Rev. B* 80 (2009), p. 165102.

[40] Sung-Sik Lee. "Recent Developments in Non-Fermi Liquid Theory". In: *Annual Review of Condensed Matter Physics* 9 (Mar. 2018), pp. 227–244. arXiv: 1703.08172 [cond-mat.str-el].

[41] A. Luther. "Tomonaga Fermions and the Dirac Equation in Three-Dimensions". In: *Phys. Rev. B* 19.1 (1979), p. 320.

[42] Ruochen Ma and Chong Wang. "Emergent anomaly of Fermi surfaces: a simple derivation from Weyl fermions". In: *arXiv e-prints*, arXiv:2110.09492 (Oct. 2021), arXiv:2110.09492. arXiv: 2110.09492 [cond-mat.str-el].

[43] Max A. Metlitski and Subir Sachdev. "Quantum phase transitions of metals in two spatial dimensions. I. Ising-nematic order". In: *Phys. Rev. B* 82 (2010), p. 075127.

[44] Max A. Metlitski and Subir Sachdev. "Quantum phase transitions of metals in two spatial dimensions. II. Spin density wave order". In: *Phys. Rev. B* 82 (2010), p. 075128.

[45] W. Metzner, D. Rohe, and S. Andergassen. "Soft Fermi Surfaces and Breakdown of Fermi-Liquid Behavior". In: *Phys. Rev. Lett.* 91 (2003), p. 066402.

[46] Olexei I. Motrunich. "Variational study of triangular lattice spin- $1/2$ model with ring exchanges and spin liquid state in κ- $(ET)_2$ Cu_2 $(CN)_3$". In: *Phys. Rev. B* 72 (4 July 2005), p. 045105. URL: https://link.aps.org/doi/10.1103/PhysRevB.72.045105.

[47] Olexei I. Motrunich and Matthew P. A. Fisher. "d-wave correlated critical Bose liquids in two dimensions". In: *Phys. Rev. B* 75 (23 June 2007), p. 235116. URL: https://link.aps.org/doi/10.1103/PhysRevB.75.235116.

[48] David F. Mross et al. "Controlled expansion for certain non-Fermi-liquid metals". In: *Phys. Rev. B* 82 (2010), p. 045121.

[49] Ranjan Mukhopadhyay, C. L. Kane, and T. C. Lubensky. "Sliding Luttinger liquid phases". In: *Phys. Rev. B* 64 (4 July 2001), p. 045120. URL: https://link.aps.org/doi/10.1103/PhysRevB.64.045120.

[50] Chaitanya Murthy and Chetan Nayak. "Almost Perfect Metals in One Dimension". In: *Phys. Rev. Lett.* 124 (13 Mar. 2020), p. 136801. URL: https://link.aps.org/doi/10.1103/PhysRevLett.124.136801.

[51] Chetan Nayak and Frank Wilczek. "Non-Fermi liquid fixed point in 2 + 1 dimensions". In: *Nucl. Phys. B* 417 (1994), p. 359.

[52] Vadim Oganesyan, Steven A. Kivelson, and Eduardo Fradkin. "Quantum theory of a nematic Fermi fluid". In: *Phys. Rev. B* 64 (2001), p. 195109.

[53] Aavishkar A. Patel and Subir Sachdev. "Critical strange metal from fluctuating gauge fields in a solvable random model". In: *Phys. Rev. B* 98 (12 Sept. 2018), p. 125134. URL: https://link.aps.org/doi/10.1103/PhysRevB.98.125134.

[54] Eugeniu Plamadeala, Michael Mulligan, and Chetan Nayak. "Perfect metal phases of one-dimensional and anisotropic higher-dimensional systems". In: *Phys. Rev. B* 90 (2014), p. 241101.

[55] Joseph Polchinski. "Effective field theory and the Fermi surface". In: (1992). arXiv: hep-th/9210046 [hep-th].

[56] Joseph Polchinski. "Low-energy dynamics of the spinon-gauge system". In: *Nucl. Phys. B* 422 (1994), p. 617.

[57] Alexander M. Polyakov and P. B. Wiegmann. "Goldstone Fields in Two-Dimensions with Multivalued Actions". In: *Phys. Lett. B* 141 (1984), pp. 223–228.

[58] Alexander M. Polyakov and P. B. Wiegmann. "Theory of Nonabelian Goldstone Bosons". In: *Phys. Lett. B* 131 (1983). Ed. by M. Stone, pp. 121–126.

[59] S. Raghu, Gonzalo Torroba, and Huajia Wang. "Metallic quantum critical points with finite BCS couplings". In: *Phys. Rev. B* 92 (20 Nov. 2015), p. 205104. URL: https://link.aps.org/doi/10.1103/PhysRevB.92.205104.

[60] N. Read. "Excitation structure of the hierarchy scheme in the fractional quantum Hall effect". In: *Phys. Rev. Lett.* 65 (12 Sept. 1990), pp. 1502–1505. URL: https://link.aps.org/doi/10.1103/PhysRevLett.65.1502.

[61] Sam P. Ridgway and Chris A. Hooley. "Non-Fermi-Liquid Behavior and Anomalous Suppression of Landau Damping in Layered Metals Close to Ferromagnetism". In: *Phys. Rev. Lett.* 114 (22 June 2015), p. 226404. URL: https://link.aps.org/doi/10.1103/PhysRevLett.114.226404.

[62] T. Senthil. "Theory of a continuous Mott transition in two dimensions". In: *Phys. Rev. B* 78 (4 July 2008), p. 045109. URL: https://link.aps.org/doi/10.1103/PhysRevB.78.045109.

[63] R. Shankar. "Renormalization group approach to interacting fermions". In: *Rev.Mod.Phys.* 66 (1994), p. 129.

[64] S. L. Sondhi and Kun Yang. "Sliding phases via magnetic fields". In: *Phys. Rev. B* 63 (5 Jan. 2001), p. 054430. URL: https://link.aps.org/doi/10.1103/PhysRevB.63.054430.

[65] Xue-Yang Song et al. "Electric polarization as a nonquantized topological response and boundary Luttinger theorem". In: *Phys. Rev. Research* 3 (2 Apr. 2021), p. 023011. URL: https://link.aps.org/doi/10.1103/PhysRevResearch.3.023011.

[66] Jacob Sonnenschein. "Chiral Bosons". In: *Nucl. Phys. B* 309 (1988), pp. 752–770.

[67] Michael Stone. "Coherent State Path Integrals and the Bosonization of Chiral Fermions". In: *Phys. Rev. Lett.* 63 (1989), p. 731.

[68] Michael Stone. "How to make a bosonized Dirac fermion from two bosonized Weyl fermions". In: (May 1989).

[69] Shouvik Sur and Sung-Sik Lee. "Chiral non-Fermi liquids". In: *Phys. Rev. B* 90 (2014), p. 045121.

[70] Alexei M Tsvelik. *Quantum field theory in condensed matter physics*. Cambridge university press, 2007.

[71] AM Tsvelik. "$1+1$-dimensional sigma model at finite temperatures". In: *Sov. Phys. JETP* 66 (1987), p. 221.

[72] C.M. Varma, Z. Nussinov, and Wim van Saarloos. "Singular or non-Fermi liquids". In: *Physics Reports* 361.5 (2002), pp. 267–417. ISSN: 0370-1573. URL: http://www.sciencedirect.com/science/article/pii/S0370157301000606.

[73] Ashvin Vishwanath and David Carpentier. "Two-Dimensional Anisotropic Non-Fermi-Liquid Phase of Coupled Luttinger Liquids". In: *Phys. Rev. Lett.* 86 (4 Jan. 2001), pp. 676–679. URL: https://link.aps.org/doi/10.1103/PhysRevLett.86.676.

[74] Chong Wang et al. "Emergent anomalies and generalized Luttinger theorems in metals and semimetals". In: *Phys. Rev. B* 104 (23 Dec. 2021), p. 235113. URL: https://link.aps.org/doi/10.1103/PhysRevB.104.235113.

[75] Yuxuan Wang and Andrey V. Chubukov. "Quantum phase transition in the Yukawa-SYK model". In: *Phys. Rev. Research* 2 (3 July 2020), p. 033084. URL: https://link.aps.org/doi/10.1103/PhysRevResearch.2.033084.

[76] Steven Weinberg. *The quantum theory of fields. Vol. 2: Modern applications*. Cambridge University Press, 2013. ISBN: 9781139632478, 9780521670548, 9780521550024.

[77] X. G. Wen. "Metallic non-Fermi-liquid fixed point in two and higher dimensions". In: *Phys. Rev. B* 42 (10 Oct. 1990), pp. 6623–6630. URL: https://link.aps.org/doi/10.1103/PhysRevB.42.6623.

[78] Xiao-Gang Wen. "Low-energy effective field theories of fermion liquids and the mixed $U(1) \times \mathbb{R}^d$ anomaly". In: *Phys. Rev. B* 103 (16 Apr. 2021), p. 165126. URL: https://link.aps.org/doi/10.1103/PhysRevB.103.165126.

[79] Edward Witten. "Nonabelian Bosonization in Two-Dimensions". In: *Commun. Math. Phys.* 92 (1984). Ed. by M. Stone, pp. 455–472.

Chapter 6

SUMMARY OF THIS THESIS

In summary, this thesis investigates the metallic state of matter in two dimensions by studying different models which focus on different aspects in each chapter. Now we recap the key results for each chapter as follows.

In Chapter 2, we studied the influence of quenched disorder and a dissipative Coulomb interaction on two different quantum phase transitions: an integer quantum Hall transition (IQHT) and a superconductor-insulator transition (SIT). We considered both transitions using effective theories that consist of a Dirac fermion coupled to a $U(1)$ Chern-Simons gauge field at level 0 for IQHT, and $\frac{1}{2}$ for SIT. We implemented the renormalization group analysis at one-loop level for disorder fluctuation and $\frac{1}{N_f}$ level for gauge fluctuation (the number fermion flavors $N_f \gg 1$), to study the critical properties of these theories. We found both theories to be stable to the addition of a Coulomb interaction. The IQHT was stable to $\mathcal{C}$ preserving disorder and exhibited a line of diffusive fixed points with $\mathcal{CT}$ disorder. ($\mathcal{C}$ is charge-conjugation symmetry and $\mathcal{T}$ is time-reversal symmetry.) The SIT exhibited a line of fixed points parameterized by the Coulomb coupling when $\mathcal{C}$ is preserved. Other cases resulted in runaway flow.

In Chapter 3, from semi-classical approach, we revisit the integer quantum Hall transition in terms of composite fermion with impurity, under which the particle-hole symmetry is the emergent symmetry induced by disorder. We further study the stability problem when the disorder trigger particle-hole symmetry breaking. The stability condition is similar to the Landau level projection of the the half-filled Landau level problem. We then compute the electrical conductivity tensor based on self-consistent Born approximation. The values of the conductivity are the coefficients of the NLSM if we neglect its RG flow behavior. We also obtain the $\theta = \pi$ topological term from the reduction of WZW model, which was alternatively obtained from the fermionic theory via Fujikawa technique of evaluating chiral rotation measure verifiable only at zero density limit. The resulting IR theory is equivalent to the $O(3)$ NLSM. The topological term alters the renormalization group flow of the sigma model—

which in its absence flows to a massive phase—towards a gapless fixed point. Our result shows how particle-hole symmetry can emerge in the HLR composite fermion theory and gives further evidence for the possible IR equivalence of the Dirac and HLR theories.

In Chapter 4, we studied the effects of a quenched random, transverse magnetic field on a 2d Dirac fermion placed at finite density. Under the assumption that the amplitude of the disorder potential is smaller than the depth of the Fermi momentum, we showed how the effective theory reduces to an infinite collection of chiral fermions coupled by the vector potential random matrix. This simplification allows for an exact treatment of the effects of the disorder without using any conventional way of treating the impurity (replica, supersymmetry, Keldysh). The task of solving S-D equation is then transformed into the task of computing infinite series. We consider the short-range impurity and reproduce the known result of diffusive Fermi liquid; the long-range impurity can be generalized directly in the similar way as long as we can compute the higher-point of Gaussian average of random matrices. This is an exactly solvable model from real space-time coordinates. We also obtain physical observables including the spectrum function as well as the electrical transport in the collisionless $\hbar\omega/k_B T \to \infty$ limit. The finite temperature transport can also be computed numerically, which is on the opposite order of limits $\hbar\omega/k_B T \to 0$.

In Chapter 5, we present the explicit example to realize the two spatial dimensions Fermi surface with $LU(1)$ and $SU(N)$ symmetry microscopically in terms of a collections of the integer quantum Hall edge states with fermion hopping within different edges. The extra spatial dimension arises from the $SU(N)$ flavor degrees of freedom of the WZW model. We determined the two-point function of the single-particle fermion operator at $k > 1$. We found corrections to its anomalous dimension that depend on k; these corrections are organized in an expansion in $1/N$. The interacting nature of fermion is probable from the relative amplitude of current-current correlation function. This construction provides a simple illustration of the ersatz Fermi liquid. In our example, if one gauges the theory, there is t'Hooft anomaly in the $SU(N)$ sector but free for $LU(1)$ sector, which can be read out from the obtained commutation algebra.